

NINE MILE POINT I
PIPE CRACK TASK FORCE REPORT

Compiled by
D. E. Delwiche

Approved: *Gm Gordon*
G. M. Gordon, Chairman
Pipe Crack Task Force

9990999999

REGULATORY DOCKET FILE COPY

CONTRIBUTORS TO NINE MILE POINT I

PIPE CRACK TASK FORCE REPORT

TASK FORCE MEMBERS

G.M. Gordon, Chairman
(General Electric Company)

R. Oleck
(Niagara Mohawk Power Corporation)

J. Danko
(Electric Power Research Institute)

K. Schmidt
(Nuclear Energy Services)

R. Hookway
(Teledyne Engineering Services)

SUPPORTING CONTRIBUTORS

Niagara Mohawk Power Co.

F. Hawksley

Electric Power Research Institute

M. Behravesch (NDE Center)

L. Becker (NDE Center)

S. Kazuoka

G. Dau

R. Stone (NDE Center)

W. Childs

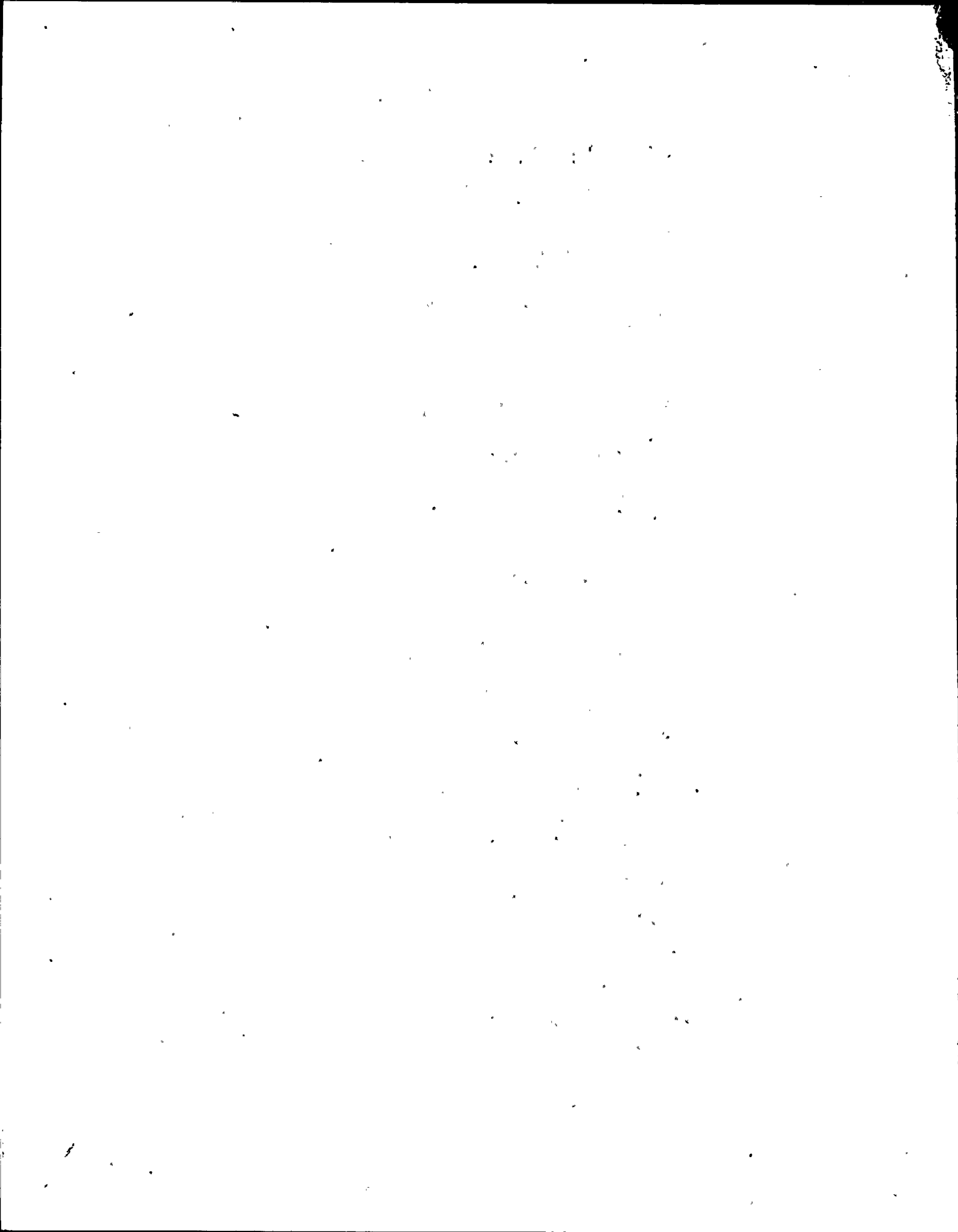
Nutech

R. Cargill

Battelle Columbus Laboratories

M. Landow

V. Pasupathi



SUPPORTING CONTRIBUTORS (Cont'd)

Nuclear Energy Services

P. Barry
M. Stamm

Teledyne Engineering Services

R. Pace

General Electric Co. - Nuclear Energy Business Operation

M. Bensch
R. Horn
J. Sundberg
B. Gordon
B. Rajala
J. Cutt
D. Delwiche
R. Carnahan
S. Ranganath
K. Ramp

Acknowledgements

Sincere appreciation is expressed to the following individuals and companies for the use of their data in the preparation of Section X: I. Hamada, Y. Mori, F. Hataya and S. Hattori of Hitachi Research Laboratory, M. Akashi of Ishikawajima - Harima Heavy Industries Co., Ltd. and M. Hishida of Toshiba Corporation.

TABLE OF CONTENTS

	Page
MAJOR CONCLUSIONS.....	i
EXECUTIVE SUMMARY.....	S-1
A. Extent of Cracking.....	S-2
B. Metallographic Examination.....	S-3
C. Stresses.....	S-4
D. Materials.....	S-5
E. Environment.....	S-7
F. Ultrasonic Examination.....	S-7
Furnace Sensitized Safe-End Procedures.....	S-8
Piping Procedures.....	S-8
Crack Growth/U.T. Detectability.....	S-10
G. Cause of Cracking.....	S-12
SECTION I. INTRODUCTION.....	1-1
SECTION II. EXTENT AND DISTRIBUTION OF CRACKING.....	2-1
Examination Results.....	2-1
Correlation of U.T. and PT Results.....	2-2
SECTION III. LABORATORY CHARACTERIZATION OF CRACKS.....	3-1
Introduction.....	3-1
Observations and Conclusions.....	3-1
Field Examination.....	3-2
Metallographic Examinations.....	3-6
A. Boat Sample "A".....	3-6
B. Boat Sample "B".....	3-8
C. Sample 3 - Piping Sections.....	3-10
D. Boat Samples "C", "D", "E", and "F".....	3-12
E. Section of Elbow-to Pipe Weld.....	3-14
Composition - Chemistry and Structure.....	3-16
Sensitization Measurements.....	3-16
A. ASTM A-262 Practice A.....	3-16
B. Electrochemical Potentiokinetic Reactivation (EPR).....	3-16
Hardness.....	3-17
Ferrite Survey.....	3-17

TABLE OF CONTENTS (Continued)

	Page
SECTION IV. STRESSES AND STRESS RULE INDEX.....	4-1
Background.....	4-1
Weight During Normal Operation.....	4-2
Thermal Expansion.....	4-3
Operational Concerns.....	4-4
A. Snubbers.....	4-4
B. Pump Vibration.....	4-5
C. Sway Braces.....	4-5
Stress Summary.....	4-6
Residual Stresses.....	4-6
Stress Rule Index.....	4-7
References.....	4-12
SECTION V. MATERIALS AND FABRICATION HISTORIES.....	5-1
Recirculation System Configuration.....	5-1
Material and Fabrication.....	5-2
A. Pipe.....	5-2
B. Elbow and Tees.....	5-3
C. Safe-Ends.....	5-4
Welding.....	5-4
SECTION VI. WATER CHEMISTRY AS POTENTIAL CONTRIBUTING FACTOR.....	6-1
Evaluation of General Electric Water Chemistry	
Data Base of NMP-1.....	6-1
A. Reactor Water Conductivity.....	6-3
B. Reactor Water Chloride.....	6-4
C. Hydrogen Ion Concentration.....	6-4
D. Reactor Water Silica.....	6-5
E. Feedwater Conductivities.....	6-5
F. Feedwater Dissolved Oxygen.....	6-6
G. Metallic Impurities.....	6-6
Evaluation of Water Chemistry Transients.....	6-6
Summary.....	6-8

TABLE OF CONTENTS (Continued)

	Page
SECTION VII. EFFECTS OF DECONTAMINATION.....	7-1
Introduction.....	7-1
Decontamination and Stress Corrosion Cracking.....	7-2
A. Laboratory Studies.....	7-2
B. Operating Experiences.....	7-6
Discussion.....	7-7
Conclusions.....	7-8
References.....	7-9
SECTION VIII. ULTRASONIC EVALUATION.....	8-1
Introduction and Background.....	8-1
A. Sequence of Events.....	8-1
B. Principle Aspects of the 1982 U.T.	
Examination at Nine Mile Point 1.....	8-3
Recirculation System ISI Examination Results.....	8-5
ISI Inspection Comparisons 1979-1982.....	8-6
A. Safe-Ends.....	8-7
B. Balance of Recirculation Pipe System.....	8-8
Evaluation of Ultrasonic Examination Performance	
Following Pipe Removal.....	8-10
A. Correlation of U.T. and PT Data.....	8-11
B. Search Unit and Procedure Correlation.....	8-11
C. Effects of Chemical Decontamination on Detection.....	8-12
D. In-Situ vs. Laboratory U.T. Examination.....	8-15
E. Crack Depth Information.....	8-16
APPENDIX A - Procedure Excerpts.....	8-31
APPENDIX B - Transducer Usage for Safe End Examination.....	8-36
SECTION IX. APPARENT CRACK GROWTH RATES - GENERIC IMPLICATIONS.....	9-1
A. Materials Data Base.....	9-1
B. Crack Growth Rates of Nine Mile Point Material.....	9-2
C. Model Qualifications and Predictions.....	9-4
1. Circumferential Flaw.....	9-5
2. Axial Crack.....	9-8

TABLE OF CONTENTS (Continued)

		Page
	D. U.T. Detectability vs. Geometry vs. Crack Growth Rate.....	9-10
	E. References.....	9-14
SECTION	X. STRESS CORROSION PERFORMANCE OF TYPE 316 NUCLEAR GRADE S/S.....	10-1
	Introduction.....	10-1
	Theoretical Analysis.....	10-2
	A. Thermodynamics.....	10-3
	B. Kinetics.....	10-5
	Sensitization and Corrosion Test Results.....	10-7
	A. Crack Initiation.....	10-7
	B. Crack Propagation.....	10-13
	Discussion.....	10-14
	Conclusions.....	10-15
	References.....	10-18
SECTION	XI. EVALUATION OF RECIRCULATION SYSTEM REPAIRS AND REPLACEMENT.....	11-1
	Safe End Replacement.....	11-1
	Pipe Replacement.....	11-2
	Expected Performance of Repairs/Replacement.....	11-2
	APPENDIX A. Mill Test Certificates and Test Reports.....	A-1

MAJOR CONCLUSIONS

1. Cracking at Nine Mile Point-1 (NMP-1) was due to weld Heat Affected Zone (HAZ) Intergranular Stress Corrosion Cracking (IGSCC) with initiation on inner surface.
2. The extent of IGSCC cracking at NMP-1 was somewhat greater than that observed at most other plants. 85% of recirculation piping welds have indications of cracking.
3. Shop and field welds were equally affected, indicating welding fabrication was not a significant variable.
4. The base material was normal (e.g., not sensitized) but weld heat affected zones (HAZ) were lightly sensitized Type 316 S/S.
5. The leaking safe-end cracks were all axially oriented, potentially making ultrasonic examination (U.T.) difficult.
6. Cracking in piping welds was not detected prior to 1982 due to limited sampling and the U.T. technique employed for the assumed non-service sensitive system.
7. The U.T. techniques employed in 1982 were highly effective.
8. A high percentage of welds have Stress Rule Indices (SRI) ≥ 1.2 . This was perhaps due to the larger percentage of welds to fittings which generally experience higher stresses. Also the pressure stress contribution to the SRI may have been slightly higher.
9. Plant steady state water chemistry was equivalent to the average U.S. BWR plant.
10. Higher than average Cl^- and conductivity transients occurred in '71 and '79 but it is unlikely those contributed to crack initiation.

11. Aside from a high incidence of $SRI \geq 1.2$, none of the contributing factors (stress, environment, sensitized material) were excessive enough to expect the degree of IGSCC which occurred. This preponderance of cracking, even for this old a plant, may be an upper bound in the IGSCC data base.
12. Pipe decontamination did not aggravate cracking but appears to have made cracking more visible to ultrasonic examination.
13. Even for those welds with the maximum extent of cracking, full structural margin existed, and would have been maintained for at least an additional 18 months.

- NMP-1 CRACKING FULLY CONSISTENT WITH OUR UNDERSTANDING
- THEREFORE, TYPE 316 NUCLEAR GRADE REPLACEMENT MATERIAL IS FULLY ADEQUATE FOR PLANT DESIGN LIFE.

EXECUTIVE SUMMARY

On March 23, 1982, during a hydrotest at Nine Mile Point-1 (NMP-1) prior to startup, inspection revealed through wall leaking cracks in two of the ten furnace sensitized recirculation safe ends. On March 26, 1982, ultrasonic examinations on these two safe ends and one other confirmed crack-like indications. In mid-April, 1982, two boat samples were obtained from one of the safe ends in the vicinity of the through wall cracks. One each of these samples was sent to General Electric and Battelle Laboratories for evaluation. The results of those evaluations in mid-May confirmed the presence of intergranular stress corrosion cracking (IGSCC). Subsequent ultrasonic examination of the 28" recirculation piping revealed crack-like indications in many of the piping weld heat affected zones examined at both shop and field welds.

Following the discovery of extensive IGSCC at NMP-1, Niagara Mohawk Power Corporation (NMPC) decided to replace the entire 28-inch recirculation system piping consisting of five loops including safe ends with Type 316 Nuclear Grade material. To provide added assurance that the 316 Nuclear Grade replacement material will not suffer similar cracking due to some unique plant specific cause, NMPC appointed an interdisciplinary Task Force on September 29, 1982. The stated objectives of the Task Force were:

1. Investigate the cause of cracking in the recirculation system piping and safe ends.
2. Determine the reasons why cracking was not seen before 1982.
3. Evaluate the adequacy of ultrasonic testing techniques.
4. Evaluate system pipe stresses, and stress rule index values.
5. Examine other relevant issues which may bear on generic concerns.
6. Evaluate the adequacy of replacement material.

The Task Force has held four meetings to fully review the NMP-1 IGSCC situation and to establish the necessary inputs needed to allow accomplishment of the stated objectives. This report documents results of relevant investigations, findings, and assessments made by the Task Force.

A. Extent of Cracking

To date, 62 of the 76 welds in the five recirculation loops have been examined using either ultrasonic (U.T.) and/or dye penetrant (PT) examination procedures. Of these, 53 (85%) were found to have indications of cracking associated with a heat affected zone (HAZ). Shop welds and field welds were approximately equally affected.

Because each weld has two heat affected zones (HAZ) adjacent to it, it is perhaps more appropriate to consider the frequency of HAZ cracking. Considering a total of 104 HAZ's examined, 75 (72%) had crack indications, with approximately equal percentages of shop and field HAZ's cracked. Figure S-1 is a layout of the cracked and uncracked weld locations in each loop.

In a number of the welds with U.T. and/or PT indications, the extent of cracking was found to be quite extensive with the cracking covering a significant fraction of the circumference. An example of such an extensively cracked weld is shown in Figure S-2. It can be seen from the map of PT indications, the cracking on the elbow side of the weld covers about 180° of circumference. The measured depth of 0.2 to 0.45" based on sensitive U.T. examination from the cut edge of the pipe are also shown. The region of maximum crack depth was further evaluated by progressive grinding and crack depth was found to be about 0.5 inches, about 50% of wall. A structural margin evaluation was performed for the most extensively cracked weld characterized and it was verified that adequate margin existed for all cases. Further, the plant could have continued to operate for another 12-18 months without dropping below code allowable structural margins.

Significant additional in-service-ultrasonic inspection on several older BWR plants has been performed subsequent to the NMP-1 examination in response to the IE Bulletin 82-03. The results to date are summarized in Figure S-3. As may be seen, for most of the plants evaluated, less than 10% of the welds inspected had reportable indications. However, in the cases of NMP-1, Hatch 2, Browns Ferry-1, and Vermont Yankee, a significant fraction of the welds did have reportable indications.

B. Metallographic Examination

Boat samples and piping segments containing cracks were removed from the recirculation piping system of NMP-1 and sent to laboratories for metallographic evaluation and failure analysis. The boat samples and piping segments contained representative examples of axially oriented and circumferentially oriented cracks removed from furnace sensitized RPV safe ends as well as from shop and field welds of the recirculation loops.

Optical metallographic and scanning electron fractographic examinations have resulted in the following conclusions:

- o The through wall safe end cracking was due to IGSCC of a furnace sensitized high carbon Type 316 stainless steel.
- o Although trace elements were found on the fracture faces of one of the boat samples, the origin of the containments could not be determined from the examinations performed, nor can the presence of the containments be associated with the presence of cracking.
- o The through wall leakage was, in each case examined, due to axially oriented cracks.
- o All shop and field weld heat affected zone (HAZ) pipe cracking was intergranular stress corrosion cracking, with inner surface initiation.
- o Electrochemical potentiokinetic reactivation (EPR) measurements and other sensitization studies showed that pipe and elbow base metal was nonsensitized (annealed) material, while the weld heat affected zones (HAZ's) were found to be lightly sensitized in a typically narrow zone. Cracking was associated with the weld HAZ's.
- o Some crack propagation into weld metal had occurred; however, arrest would occur as the crack propagated towards weld regions of higher ferrite content.

C. Stresses

A detailed investigation of the NMP-1 recirculation system stresses was made to determine whether the extensive cracking that took place was attributable to unduly high stress levels. As part of this evaluation, investigations were made to assure that there were no outside influences on the stress in the system that would contribute to an increased frequency of cracks.

The details are presented in Section IV of this report.

The conclusions are:

1. All weight, thermal and vibratory stresses are low for both normal and abnormal operating modes and in no way contribute to cracking here more than in any other plant.
2. The pressure stress contribution to the SRI is somewhat higher than that for more recent BWR recirculation loop designs. The pipe wall thickness in more recent BWR is higher, mainly to provide greater seismic margins. Nevertheless, the pressure stresses are still within the appropriate design code allowables.

The Stress Rule Index (SRI) was computed by Teledyne Engineering Services for a typical NMP-1 recirculation loop (loop 15). The values are presented in Table S-1 for reference. These values were based on stresses developed by Teledyne in the re-analysis for this task forced in which the minimum thickness for stress computation was used instead of nominal values. The SRI values calculated here by TES compare closely with those values calculated by General Electric and presented to the NRC in October 1982. The differences which do exist are due primarily to the treatment of a branched (Sweep-o-let) type of connection. The number used by TES for this type of connection was higher (2.1 vs. 1.7) than that used by GE, reflecting a greater level of conservatism in the TES results. For the NMP-1 case, the main contributors to the SRI are pressure stress and weld residual stress. As can be seen, the SRI values exceed the field threshold cracking value of 1.1 for all welds evaluated. This is unusual and may be

Table S-1
SRI Values for NMP-1 - Loop 15
(Developed by Teledyne Engineering Services)

<u>Node</u>	<u>Location</u>	<u>As Designed SRI</u>
101	Elbow	1.2
105	Tee	2.2
115	Tee	2.1
135	Valve	1.2
155	Elbow	1.2
156	Pump	1.3
200	Pump	1.2
205	Elbow	1.2
225	Valve	1.2
270	Elbow	1.4

due to somewhat higher pressure stress plus the absence of a significant number of pipe/pipe butt welds in the NMP recirculation system. Pipe/pipe butt welds have lower code stress intensification factors and are generally below the threshold SRI value in other BWR plants.

D. Materials

The five 28-inch recirculation loops were constructed of Type 316 stainless steel pipes, elbows, and fittings. The straight sections of pipe were fabricated by the National Annealing Box Company of rolled and welded plate. The elbows and reducing tees were fabricated by the Crane Company of wrought plate. All wrought pipes, elbows, and reducing tees were solution annealed and water quenched. Shop welded subassemblies were fabricated by the Grinnell Company. Shop welds were not given a subsequent heat treatment.

The National Annealing Box spool pieces were formed from four heats of material with carbon contents ranging from 0.042% to 0.055%. The elbows and tees were fabricated from 19 heats of material with carbon contents ranging from 0.050 to 0.075%. In most cases, the heats from which the specific piping segments were fabricated is not documented.

The ten 28-inch recirculation safe ends were fabricated from the same heat of 0.054% carbon Type 316 stainless steel forgings per ASTM A336. Although the safe end forgings were solution heat treated following fabrication, the safe ends were subsequently post-weld heat treated with the reactor pressure vessel resulting in a furnace sensitized condition.

The GE purchase specification for the recirculation system required all welded joints to be made by the inert-gas tungsten-arc process with internal gas purging for at least the root pass and the second layer. Shielded metal arc was allowed for the remainder of the weld. The weld filler metal was required to meet ASTM A298 or A371. The acceptance criteria also called for a 5% minimum ferrite, as measured on undiluted weld deposit, and a Cr to Ni ratio minimum of 1.9.

Estimates for typical heat input values during welding are 26 to 88 K.joules/inch for the shop welds, and 25 to 44 K.joules/inch for the field welds.

The replacement piping for the NMP-1 recirculation system piping is fabricated from a Type 316 Nuclear Grade material. This material choice, with controlled fabrication procedures, is anticipated to be fully resistant to IGSCC, and will preclude this BWR from any additional IGSCC concerns in the recirculation piping system.

Prior to the bulk of the in-service U.T. inspection performed in March 1982 at NMP-1, the five recirculation loops were decontaminated to reduce personnel Man-Rem exposure. A review of the relevant laboratory data, and the operating experience of reactor systems decontaminated by the same proprietary CAN-DECON process indicates that decontamination, per se, had no impact on the observed occurrence of intergranular stress corrosion cracking (IGSCC) of the large diameter Type 316 stainless steel piping at Nine Mile Point Unit 1. The only contribution that the CAN-DECON cleaning process appears to have had on the piping IGSCC is that it increased the detectability of the cracks during ultrasonic examination. A similar effect of decontamination on U.T. crack detectability may have occurred at Vermont Yankee recently, where U.T. examination subsequent to decontamination resulted in 58% of the

welds exhibiting reportable indications (up to 360° around the HAZ in several cases).

E. Environment

With respect to the NMP-1 coolant environment, the steady state long term conductivity values have been equivalent to that of a typical domestic U.S. BWR, while the weekly maximum chloride levels have been somewhat higher than average although still well within specification. In addition to these steady state values, two significant off-chemistry transients occurred and these were evaluated. As a result it is concluded that there is no obvious basis for believing that water chemistry played a significant role in accelerating IGSCC at NMP-1.

F. Evaluation of Ultrasonic Effectiveness

Following the discovery of the visually detected leakage of two of the ten furnace-sensitized recirculation system safe ends, U.T. examinations of the two affected safe ends, and one other safe end, as well as a significant portion of the balance of the recirculation piping system performed. As described previously, these added examinations revealed indications in the heat affected zones of recirculation system welds at the inner surface. A large number of indications, in the five recirculation loops were identified, and by subsequent penetrant examination and metallographic laboratory examinations were confirmed to be cracks caused by a stress corrosion mechanism.

Since the plant contained extensive IGSCC, including leaking axial safe end cracks in 1982, the question arises as to why no reportable indications were found by U.T. in earlier examinations including the one nine-months earlier in 1981. To evaluate this question, a detailed assessment was performed for the U.T. procedures employed over the 1979-82 period for the furnace sensitized safe ends and also for the balance of the recirculation piping welds which were examined by a less sensitive procedure prior to 1982.

FURNACE SENSITIZED SAFE END PROCEDURES

A review of the ISI records of the 1979-82 period compares the inspection parameters of the safe ends in loops 11-15. In reviewing these and other supporting records, the following conclusions have been reached relative to the comparison of the 1981 and 1982 NMP-1 safe end inspections.

1. A higher sensitivity was used for the scanning in 1982.

In 1982, more gain was added to the calibration sensitivity for scanning than in 1981 (typically 10dB versus 6dB).

2. The time devoted to some of the safe end examinations in 1981 appears to be too short for optimum detection of IGSCC.
3. The 1981 inspection took place after the presence of IGSCC had been confirmed by leakage, creating a psychology of inspection contributing to more careful examination and more willingness to call cracks.
4. The through wall leaking safe end cracks are axial and thus were probably somewhat shielded from effective U.T. examination by the unground weld crowns.

PIPING PROCEDURES

A similar review of the piping inspections derived from the ISI records of 1981 and 1982 for the common joints inspected in both years was also performed.

The following conclusions are considered to relate to the difference between the 1981 and 1982 inspection results on the balance of the recirculation system, and may explain why the cracking condition was not detected in earlier inspections:

1. Only two joints were inspected during the 1981 ISI, namely 32-FW-10-W and 32-FW-36-W. Comparison of ISI results in 1981 and 1982 is hence limited to these two welds.
2. The procedure used in 1981 (a procedure acceptable to Section XI, Appendix III) is ineffective for detection of IGSCC because of the 50% DAC reporting level.

Indications were found in both joints in 1982 with amplitudes less than 50% DAC (10% notch) using 1/2" diameter 1.5 MHz transducers.

3. The transducers used in 1982 resulted in effectively a more sensitive examination compared to 1981.

The 0.5"x1.0" 2.25 MHz transducer used in 1981 will have a lower sensitivity to small defects (due to its large size) than the transducers used in 1982. It is expected that these indications would have been on the order of 20% DAC or less in 1981. The 1981 procedure required a 50% DAC reporting level.

4. Unground crowns may interfere (often do) with detection of cracks, in particular axially oriented ones.

PT of 32-FW-36-W revealed a substantial axial crack. This crack is not easily detectable ultrasonically due to interference from unground crown.

5. In 1982, more gain was added to the calibration sensitivity for scanning than 1981 (both 10 dB and 20 dB versus 6 dB).
6. The time spent on scanning and recording is considerably lower for 1981 than 1982, and may be too short for optimum inspection for IGSCC.
7. The same psychology of inspection after confirmation of IGSCC was present in 1982 as in the case of the safe end inspection.

8. IGSCC experience of inspection personnel was higher in 1982 than 1981 (availability of IGSCC samples and participation in EPRI NDE Center workshops).
9. Chemical decontamination appears to have increased detectability of cracks. A high frequency of 360° intermittent cracking was found in pipe segments which had been examined subsequent to chemical decontamination.

CRACK GROWTH/U.T. DETECTABILITY

The above discussion leads to the conclusion that the 1982 examination was more sensitive than the 1981 examination, such that axially oriented cracks of some depth, on the order of 20% wall thickness, might not have been detected in 1981. However, if assuming a 20% wall crack was present in 1981, a higher than expected residual stress and an abnormally high crack growth rate would be required to drive the crack through-wall in the time between the 1981 and 1982 exam dates. To help resolve this disparity, analytically and experimentally determined stress profiles were developed to establish a residual stress estimate for axial cracks in the furnace sensitized NMP safe-end welds. In addition, a section of a cracked NMP safe-end was characterized by U.T. examination, and select cracks were removed for a three dimensional profiling.

The analytical residual stress analysis, with supportive experimentally determined through-wall residual stresses from similar large diameter piping configurations, predicts that a flaw of 10% wall will grow to a length of ~0.50" in 9 months of operation. And it would require an additional 12 months to propagate the crack through-wall. With these levels of residual stress, the crack would have to have been at least 45 to 50% through-wall 10 months prior to leakage.

A correlation between the crack size prediction and a U.T. characterization was then accomplished by duplicating the 1981, and improved 1982 ISI examination techniques on a segment of a cracked NMP pipe to safe end weld. Following U.T. evaluation, the pipe segment was sectioned, and four cracks were selected for a three dimensional profiling. The first crack would have

been called a reportable indication using the 1981 techniques. The second crack would be marginally detectable with the 1981 technique, and the third and fourth would not have been called reportable indications. Through the use of the more sensitive 1982 ISI methods all except one are reportable indications, with estimated crack depths by U.T. from 0.12 inches to 0.20 inches.

The three dimensional crack profiling has shown the axial cracks to be on the order of 40 to 60% wall, rather than the 12 to 20% as U.T. examination would indicate. The results are tabulated below:

<u>Crack</u>	<u>Detectable* by 1981 ISI Methods</u>	<u>Detectable* by 1982 Improved Techniques</u>	<u>Crack Depth</u>
6	Yes	Yes	0.52 in. (50% wall and 0.20 in. deep secondary crack)
4	Marginally	Yes	0.610 in. (48% wall)
1	No	Yes	0.620 in. (59% wall)
7	No	Marginally	0.400 in. (38% wall)

*With unground weld crown.

The table suggests the limit of detectability for the 1981 examination without ground weld crowns was approximately 45% to 60% thru-wall. (Visibility of crack No. 6 was enhanced by the secondary crack.) With the improved technique, the detectability is significantly improved. However, further study would be required to establish the actual lower limit of detectability of an axial crack in the configurations observed at NMP-1. It can be concluded from this study that because of the U.T. methods employed and the presence of unground extended weld crowns at the safe end to pipe/elbow welds, axial cracks up to 45 percent thru-wall, were probably present at the time of the 1981 ISI examination, but not detected. With the improved methods used in

the 1982 ISI examination, the axial cracking of this depth would have been detected.

G. Cause of Cracking

The pattern of intergranular cracking observed at NMP-1 was somewhat greater than that observed at most other BWR plants. The cracking covers a significant fraction of the circumference of a large percentage of the weld heat affected zones (HAZ), in the 28-inch diameter recirculation system piping. Based on the observed pattern of extensive U.T. and P.T. indications, it is important to establish any plant unique causative factors that might influence the long term performance of the Type 316 Nuclear Grade replacement material.

In the present NMP-1 Task Force investigation of causative and potentially aggravating factors, each of the three concurrent necessary conditions associated with IGSCC of welded stainless steel in BWR environment was examined in great detail. These factors are (1) a sensitized microstructure, i.e., chromium depleted grain boundaries, (2) high temperature, high purity water containing dissolved oxygen (and possible contaminants), and (3) total sustained applied plus residual stresses exceeding a threshold value, i.e., resulting in microstrains capable of continuously rupturing the passive grain boundary film normally formed at the metal/water interface (surface).

Figure S-4 lists some of the potential aggravating factors explored by the Task Force and describes the situation existing for each factor at NMP-1. Slightly higher pressure stress level and the absence of pipe/pipe butt welds may have been aggravating factors. These resulted in a very high percentage of welds with SRI ≥ 1.2 . This may have contributed to the large number of cracked welds observed. Although the pressure stresses were fully compliant with all relevant codes, on the average they are higher than those present at recent BWR plants. Thus, the presence of higher SRI values at NMP-1 would explain the higher incidence of intergranular crack initiation since the SRI is a measure of the probability of crack initiation at a given weld HAZ. The SRI has not, however, been correlated with the total number of multiple nucleated cracks at any given HAZ or with the depth of cracking (which is a function of the through-wall stress distribution).

In addition to the high percentage of SRI ≥ 1.2 welds, the implementation of decontamination prior to most of the U.T. examination appears to have resulted in the reporting of a significantly higher percentage of welds with 360° intermittent indications than for other plants examined without decontamination.

The Task Force considered the relevance of the previously observed NMP-1 piping materials performance on the long term performance of the Type 316 Nuclear Grade replacement material. It is concluded, based on a review of the Type 316 Nuclear Grade literature and available test results that no IGSCC is to be expected over the remaining NMP-1 operating lifetime since one of the three necessary conditions, i.e., sensitization, is not present with the low carbon ($\leq 0.02\%$) material. Thus, regardless of SRI value, IGSCC will not initiate. Further, the Type 316 Nuclear Grade material has added resistance against potential off-chemistry transients that might inadvertently occur over the remaining plant lifetime.

Suction

	Loop Number				
	11	12	13	14	15
SE/Elbow	PT (LOF)	PT ^{UT} (LOF)	PT, UT	PT	PT, Leak In SE, UT
Elbow/Spool	PT (LOF)	PT	PT, UT Max. Depth = 0.5 in.	PT	PT, UT Max. Depth by UT = 0.55 in., GE Met Exam
Spool/Pipe	PT	No Spool	UT, PT	UT-NO Ind.	UT (2 Spools)
Pipe/Valve	UT	UT	UT	UT	UT
Valve/Pipe	UT	UT	UT	UT	UT
Pipe/Elbow	PT, UT	PT, UT	PT, UT	PT, UT 0.250 in. Depth by Met	UT, PT
Elbow/Elbow	PT, UT	PT, UT	PT, UT	PT, UT	UT, PT

PT = PT Indications UT = UT Indications NI = Not Inspected

S-14

Figure S-1. Status of Pipe Crack Evaluation at Nine Mile Point.

Discharge

	Loop Number				
	11	12	13	14	15
Pump/Elbow	PT, UT	PT, UT	PT, UT	PT, UT	PT, UT
Elbow/Spool	PT-No Ind. UT	PT, UT	PT	PT, UT	PT
Spool/Valve	NI	NI	NI	NI	NI
Valve/Pipe	NI	NI	NI	NI	NI
Pipe/Spool	UT Spots PT-No Ind	UT, PT 0.320 in. Depth by Met		PT, UT	NI (2 Spools)
Spool/Elbow	PT	PT	PT-No Ind.	PT	PT-No Ind.
Elbow/Spool	PT	NI	PT	PT-No Ind.	PT-No Ind.
Spool/SE	UT Leaks in SE	NI	PT, UT	PT-No Ind.	PT-No Ind.

PT = PT Indications UT = UT Indications NI = Not Inspected

30131-34

Figure S-1. Status of Pipe Crack Evaluation at Nine Mile Point (continued)

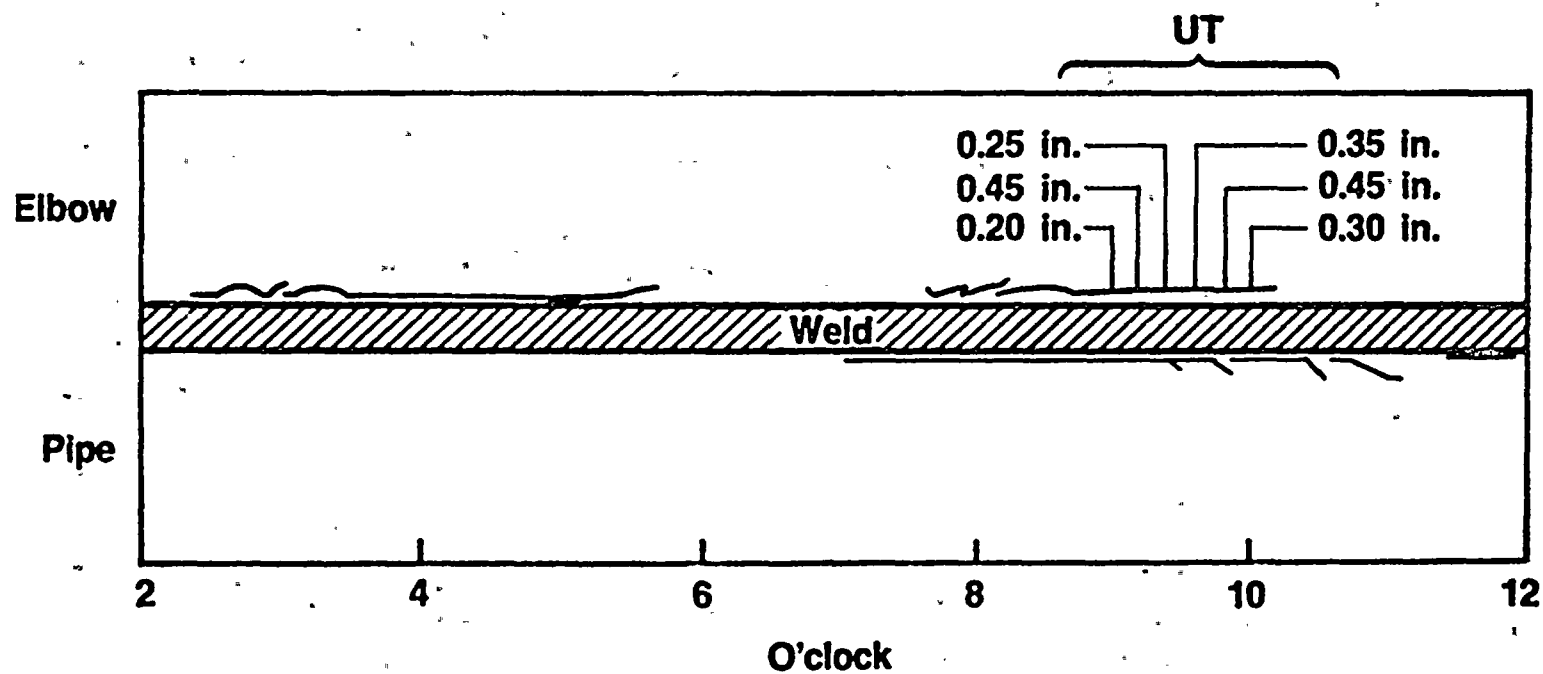


Figure S-2. Sketch of PT Indications in Loop 13 Suction Elbow/Pipe Weld

<u>Plant</u>	<u>Approximate No. Welds Inspected</u>	<u>Approximate No. of Welds With Crack Indications</u>	<u>Percent of Pipe Welds With Reportable Indications</u>
Nine Mile Point 1	62	53	85
Monticello	135	6	4
Browns Ferry Unit 2	49	2*	4*
Quad Cities Unit 1	9	0	0
Dresden Unit 2	54 ⁺	10**	20
Millstone Unit 1	13	0	0
Hatch Unit 1	63	6	9
Hatch Unit 2	117	38***	32
Brunswick Unit 1	36	3	8
Oyster Creek	31	2	6
Duane Arnold	63	0	0
Peach Bottom 2	3	1	33
Peach Bottom 3	97 (ongoing)	15	15
Vermont Yankee	59 (ongoing)	34	58
Browns Ferry Unit 1	33 (ongoing)	22	67
Cooper	116 (ongoing)	15	13

*Presumed to be due to fatigue.

**Includes one indication for 28" furnace sensitized safe end.

***Includes one 360° circumferential indication in manifold end cap 20-30% of wall confirmed to date.

+1 of 2 indications still under evaluation

⁺includes 2 FSSE

Figure S-3. ISI of Large S/S Piping Welds per NRC IE Bulletins 82-03 and 83-02 for Domestic Operating Plants Who Have Inspected (as of 6/83).

POTENTIAL AGGRAVATING FACTORS

o DEGREE OF SENSITIZATION

- Possibility of furnace sensitization due to fabrication procedures.
- Presence of localized and/or uniform cold work.
- Excessive weld repairs.

o STRESS LEVEL

- Potential for excessive stresses/cyclic loadings.
 - . Pressure stresses.
 - . Stress intensification factors due to the presence of fittings.
 - . Plant run with some loops valved out.
 - . Hangup at supports.

o ENVIRONMENT

- Steady state water quality.
- Water chemistry transients.
- Pipe decontamination prior to U.T.

SITUATION AT NMP-1

- Evaluation of fabrication records plus metallography indicates no furnace sensitization present.
- Evaluation of metallography indicates no undue cold work was present.
- Metallographic evaluation of cracked welds indicates that weld repair is not a significant factor.
- Somewhat higher than in recent BWR's but still well within relevant 1968 B 31.1 code allowables. But it is not clear whether this is unique to the NMP-1 design. Therefore, no definitive conclusions can be made on the role of pressure stress.
- More pipe/fitting welds and fewer resultant pipe/pipe butt welds than for most other BWR recirculation systems resulting in high stress intensification factor welds.
- Added stresses were minor.
- Added stresses were minor.
- Avg. conductivity/slightly higher than avg. Cl^- .
- 1971 & 1979 conductivity and chloride transients are unlikely to have accelerated crack initiation.
- Did not aggravate cracking but made cracking more visible to U.T.

Figure S-4. Potential NMP-1 Aggravating Factors

SECTION I INTRODUCTION

The Nine Mile Point-1 (NMP-1) nuclear power plant is a Model 2 Boiling Water Reactor (BWR) owned and operated by Niagara Mohawk Power Corporation (NMPC). The nuclear steam supply system (NSSS) was designed by the General Electric Company. The architect-engineer function was performed by Niagara Mohawk who in turn contracted Stone and Webster Company to construct the power plant. The construction permit was issued in April 1965, with first synchronization achieved four and one-half years later in November 1969. Commercial operation began in December 1969, and full power was achieved two months later in January, 1970.

Nine Mile Point-1 was originally designed to generate 500 MWe at full power. This was later increased to 610 MWe. The plant has five separate recirculation loops which are constructed of 28" diameter, Type 316 stainless steel piping. Through March, 1982, the NMP-1 plant was in operation for approximately 12 years, (78,000 on-line hours). On March 20 1982, the reactor was shut down to repair a recirculation pump seal. Following this repair, a hydrotest of the primary system was performed on March 23 to check the repair. During this check leakage was visually detected at two of the ten recirculation system safe-ends. These safe-ends, constructed of T-316 stainless steel, had been furnace sensitized during the initial manufacture of the reactor pressure vessel. With this discovery, further visual inspection revealed three pinhole indications and a single 1/2" long indication oriented parallel to the axis of the safe-end(s). All the indications were located in the heat-affected zone (HAZ) on the safe-end side of the weld joining the piping to the safe-ends. Ultra-sonic inspections were then performed on the two leaking safe-ends plus one additional safe-end, and intermittent crack indications were confirmed and verified by a boat sample to be IGSCC. Based upon these events, Niagara Mohawk decided to replace all the recirculation system safe-ends.

An NRC meeting was held in Bethesda, Md., on April 22, 1982, to review these IGSCC incidents and to obtain NRC approval for the proposed safe-end replacement program.

Following the initial series of inspections, the non-destructive examination effort was expanded. Ultrasonic examination was performed on the HAZ's of the recirculation pump discharge casting to riser elbow welds. Code reportable indications were found in two of the five elbow welds and non-reportable U.T. indications were found in the other three. The indication orientation was circumferential. Examination by dye penetrant on the inside diameter of the pipe confirmed the presence of cracks, and replication techniques substantiated the intergranular nature of the cracks. Finally, a boat sample was removed from one discharge weld and destructively examined revealing intergranular stress corrosion cracking (IGSCC). Once again the examination effort was expanded. Ultrasonic inspection was performed on all remaining welds where radiation fields were acceptable. Cracking was indicated in a large number of welds.

In a letter dated August 6, 1982, NMPC notified the NRC of this extensive additional apparent cracking and indicated the intention to replace all the 28-inch recirculation system piping.

The presence of IGSCC in large diameter piping was not new. In early 1978, cracks were found at the KRB plant in West Germany. A total of six welds were found cracked in the HAZ on the pipe side of the pipe-to-safe-end welds. These circumferential cracks, found in 24" diameter T-304 stainless steel piping, initiated very close to the fusion line and propagated up to 0.2" into the pipe wall. This plant had also operated for a substantial time, approximately 68,000 hours. The discovery of cracks in large diameter recirculation piping was not unexpected after the earlier IGSCC incidents in small diameter piping. The necessary conditions for IGSCC: sensitized material, high stresses, and oxygenated coolant, exist regardless of pipe diameter. The NRC also concluded that there was no safety concern for cracking in large piping as stated in NUREG-0531.

In early 1981, additional cracks were detected in the 22" diameter recirculation ring header at the Fukushima Unit 3 nuclear power plant. These cracks, were located adjacent to the sweepolet which joined the header to the riser piping. Indications were found in a total of three tee joints using ultrasonic examination and later confirmed using dye penetrant. The header had been constructed of Type 304 stainless steel. Following detection, the joints were given an induction heating stress improvement to mitigate IGSCC, temporarily, and replaced one year later with T-304LC stainless steel as a permanent fix.

Based on extensive NRC review of the cracking in the NMP-1 recirculation piping and its generic implications, in Bethesda, Md., on September 20, and October 15, 1982, the NRC issued IE Bulletin 82-03, Rev. 1, (dated Oct. 20, 1982) which established specific recommendations to be taken by eight licensees who owned plants that were to have an outage prior to January 31, 1983. The recommendations required inspection of the recirculation piping. These inspections led to the discovery of cracking in large diameter T-304 stainless piping in six other plants to date, Monticello, Hatch-1, Brunswick Unit-1, Dresden-2, Vermont Yankee, and Hatch Unit-2.

Following the discovery of extensive IGSCC at NMP, NMPC decided to replace the entire 28-inch recirculation system piping with Type 316 Nuclear Grade material. To provide added assurance that the 316 Nuclear Grade replacement material will not suffer similar cracking due to some unique plant specific cause, NMPC appointed an interdisciplinary Task Force on Sept. 29, 1982. The stated objectives of the Task Force were:

1. Investigate the cause of cracking in the recirculation system piping and safe-ends.
2. Determine the reasons why cracking was not seen before 1982.
3. Evaluate the adequacy of ultrasonic testing techniques.
4. Evaluate system pipe stresses and stress rule index values.
5. Examine other relevant issues which may bear on generic concerns.
6. Evaluate the adequacy of the replacement recirculation piping material.

The Task Force held four meetings to fully review the NMP-1 IGSCC situation and to establish the necessary inputs needed to allow accomplishment of the stated objectives. This report documents results of relevant investigations, findings and assessments made by the Task Force.

SECTION II

EXTENT AND DISTRIBUTION OF CRACKING

Of the 76 welds in the five recirculation loops, 62 have been examined by ultrasonic testing (U.T.) or liquid penetrant (PT). Boat samples of leaking safe ends and cracked weld heat affected zones (HAZs) have been sent to General Electric in San Jose and J.G. Sylvester Associates, Inc., for metallographic examination. Full-circumference samples containing the weld and, in most cases, several inches of pipe on either side have been distributed to a variety of testing labs through the coordinative efforts of the Electric Power Research Institute (EPRI).

EXAMINATION RESULTS

The ultrasonic and liquid penetrant examination results are recorded on the recirculation system loop welding diagrams shown in Figures 1-5. Forty-four welds have been examined by U.T., with indications reported in forty-three. The indications ranged from barely perceptible spots to lengths of six inches or longer. Not all of the U.T. indications were reportable in accordance with Section XI of the ASME code. The distribution of crack lengths as determined by U.T. is shown in Figure 6, which illustrates that the majority of the recorded indications are one inch or less in length.

Forty-nine of the 76 recirculation system welds were liquid penetrant examined in order to obtain additional data as to the extent of cracking, and to corroborate the U.T. data. Most of this work was performed at Battelle Labs under contract with EPRI. Several welds were examined at Nine Mile Point by Niagara Mohawk and General Electric personnel. Indications were found in 37 of the 49 welds examined by PT. Weld rollout diagrams with sketches of the PT indications are attached (Figures 7 through 11). Photographs of selected PT indications are presented with the metallographic examination results in the next section.

CORRELATION OF U.T. AND PT RESULTS

Because indications were detected in nearly all (43 of 44) of the welds examined by U.T., but only about three-fourths (38 of 49) of those examined by PT, it is apparent that there are other effects producing U.T. indications or tight cracking not detected by PT. A comparison of the U.T. and PT results for the weld HAZs examined by both techniques is provided in Table 1. Of 51 weld HAZs examined by both U.T. and PT, there are 40 in which agreement (cracking or no cracking) exists. Two of the HAZs have PT but not U.T. indications, and nine have U.T. but not PT indications.

The latter result, U.T. but not PT indications, could result from oxide buildup within a crack, preventing the penetrant from entering, or from U.T. signals caused by geometric reflectors. Conversely, U.T. non-detection could result from an inability to properly position the U.T. probe due to geometric constraints of the pipe surface, or from IGSCC related attenuation resulting from extensive grain boundary deterioration.

Tables 2 through 4 summarize the U.T. and PT data. Table 2 lists the number of welds with U.T. or PT indications in either of the adjacent HAZs, and Table 3 is a comparison of the frequency and extent of cracking in the suction and discharge sides of the loop. Table 2 shows that 53 of the 62 welds examined (85%) have crack indications associated with them. Thirty-four of the 62 examined welds are field welds, of which 29 (85%) have indications. Twenty-eight are shop welds, of which 24 (86%) have indications. And as can be seen in Table 3, the frequency of cracking is about equal for the suction and discharge side.

Table 4 shows that 75 of 104 (72%) HAZs examined have indications. This is less than the percentage of welds with indications because several welds have indications in only one of two HAZs. As is the case for shop and field welds, the incidence of cracking of shop and field weld HAZs is nearly identical (indications in 75% of shop weld HAZs, 71% of field weld HAZs). Table 4 also compares the incidence of cracking among the HAZs of pipes, elbows, reducing tees, and safe ends. Pipe and elbow HAZs, which comprise the majority of the population, also have nearly identical rates of cracking: 80% vs 74-77% for pipes and elbows respectively. Because it is not clear whether the indications next to Loop 14 SW-9 are on the elbow or the tee side, 0 of 7, or 1 of 7 reducing tee HAZs may have indications.

In either case, this is substantially lower than the incidence of cracking of the other fittings. Since the carbon content of the tees is between 0.054% and 0.075% (see Section V), and the stress rule index is greater than 2.0* (Section IV), there is no obvious explanation for this, other than the fact that tee HAZs comprise a small percentage of the total population of HAZs and thus have a higher probability of deviating from the mean.

For the HAZs with PT indications, the fraction of the circumference that is cracked has been estimated. The results are listed in Figures 1-5 and summarized in Tables 5 and 6. A size distribution of the PT indications is shown in Figure 12. Table 5 lists the average percent of circumference cracked for each type of HAZ. For the HAZs of shop welds, field welds, pipes and elbows the average circumferential extent of cracking is 15-16%. This, and the fact that there was little variation in the incidence of cracking (% of HAZs cracked), illustrates that the HAZs of shop and field welds, and of pipes and elbows were equally susceptible to cracking in the environment to which they were exposed.

The average circumferential extent of cracking of furnace sensitized safe ends is slightly higher than that of pipe and elbows, with much of the safe end cracking axial and, in two cases, through-wall.

The extent of cracking in each of the five recirculation loops is compared in Table 6. The incidence of cracking ranges from 59% in loop 15 to 94% in loop 12, and the average circumferential extent ranges from 6.3% in loop 11 to 22% in loop 13. It appears that the most extensive cracking occurred in loops 12 and 13, but the leaking safe ends were in loops 11 and 15. On an absolute scale the incidence of cracking in each loop is quite high. It should be noted, however, that the degree of inspection performed on the Nine Mile Point-1 recirculation system was unusually high, and that Nine Mile Point-1 is one of the oldest operating BWR plants. Other plants, until recently, have not inspected to the degree of Nine Mile Point-1.

*These fittings can be treated as "branch connections" rather than reducing Tee's. As branch connections the stress rule index value is 1.7 rather than 2.1.

TABLE 1

COMPARISON OF ULTRASONIC AND LIQUID PENETRANT EXAMINATION RESULTS

<u>Recirculation Loop</u>	<u>No. of HAZs: PT'd and UT'd</u>	<u>No. of HAZs With Agreement Between PT & UT</u>	<u>No. of HAZs With UT, But Not PT Ind.</u>	<u>No. of HAZs With PT, But Not UT Ind.</u>
11	12	7	5	0
12	10	8	2	0
13	13	10	1	2
14	8	8	0	0
15	8	7	1	0
	<u>51</u>	<u>40</u>	<u>9</u>	<u>2</u>

TABLE 2
COMPARISON OF SHOP AND FIELD WELDS

<u>Loop</u>	<u>Type of Weld</u>	<u>No. Welds</u>	<u>No. Welds Examined</u>	<u>No. Welds With UT/or PT Indications</u>
11	Field	9	7	6
	Shop	6	6	5
12	Field	9	5	5
	Shop	5	5	5
13	Field	9	7	7
	Shop	6	6	5
14	Field	9	7	5
	Shop	6	6	5
15	Field	10	8	6
	Shop	7	5	4
<hr/>				
	Field	46	34	29 = 85%*
	Shop	30	28	24 = 86%*
<hr/>				
	Total	76	62	53 =85%*

*Fraction of examined welds.

TABLE 3.

Comparison of Suction and Discharge Piping Welds

<u>Loop</u>	No. HAZ's With Indications/ No. Examined	
	<u>Suction</u>	<u>Discharge</u>
11	6/11	9/11
12	8/9	7/7
13	10/11	8/11
14	7/11	7/11
15	10/13	3/9
	<u>41/55 (75%)</u>	<u>34/49 (69%)</u>

<u>Loop</u>	Ave. % Circ. by PT (HAZ's w/PT Ind.)	
	<u>Suction</u>	<u>Discharge</u>
11	5.0%	6.7%
12	11%	20%
13	40%	9.1%
14	18%	8.9%
15	13%	29%
	<u>20%*</u>	<u>13%*</u>

*Note that this is not simply the average of the above averages.

TABLE 4

EXAMINATION RESULTS BY HAZ

No. HAZs With Indications/No. Examined

<u>HAZ Type</u>	<u>Loop 11</u>	<u>Loop 12</u>	<u>Loop 13</u>	<u>Loop 14</u>	<u>Loop 15</u>	<u>Total</u>
Shop Weld	7/12	9/10	9/12	9/12	7/10	41/56 (73%)
Field Weld	8/10	6/6	9/10	5/10	6/12	34/48 (71%)
Pipe	9/10	7/8	9/12	7/10	7/9	39/49 (80%)
Elbow	5/8	7/7	7/8	5-6/8	5/8	29-30/39 (74-77%)
Tee	0/2	0/0	0/0	0-1/2	0/3	0-1/7 (0-14%)
Safe End	<u>1/2</u>	<u>1/1</u>	<u>2/2</u>	<u>1/2</u>	<u>1/2</u>	<u>6/9 (67%)</u>
	15/22 (68%)	15/16 (94%)	18/22 (82%)	14/22 (64%)	13/22 (59%)	75/104 (72%)

TABLE 5

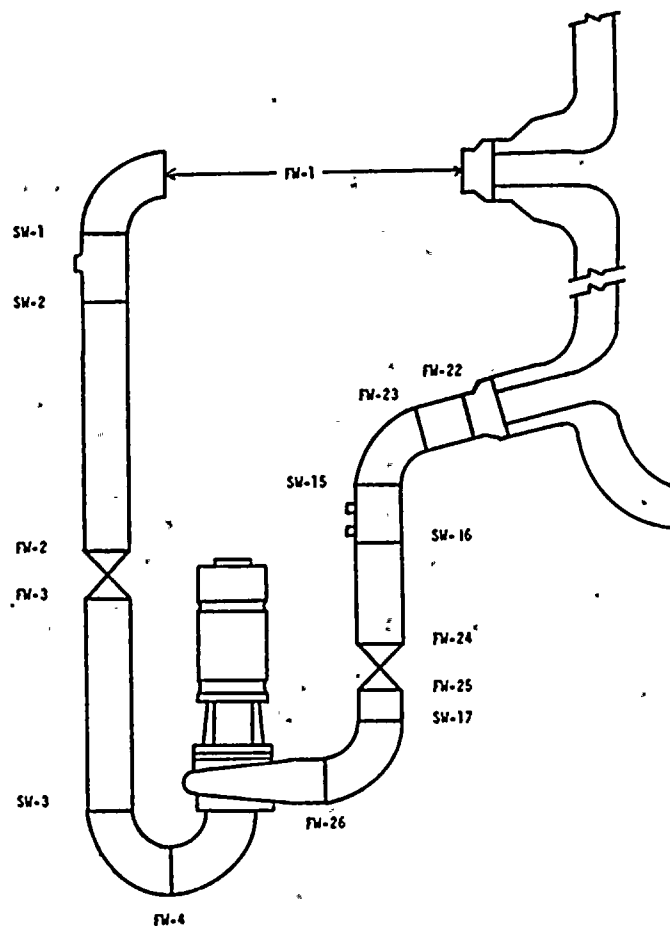
Average Fraction of Circumference Cracked by PT

<u>HAZ Type</u>	<u>Ave. % Circ. by PT</u>
Shop Weld	16%
Field Weld	16%
Pipe	15%
Elbow	15%
Tee	0% or 13%
Safe End	23%

TABLE 6

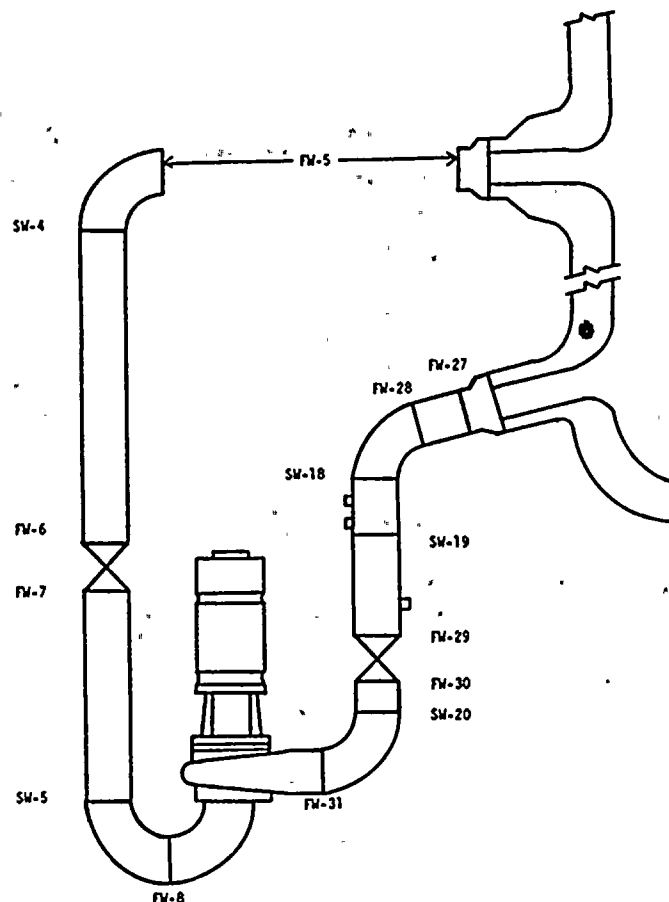
Extent of Cracking by Recirc. Loop

<u>Loop</u>	<u>% Circ. by Pt (HAZs with PT Indications)</u>
11	6.3
12	17
13	22
14	13
15	19



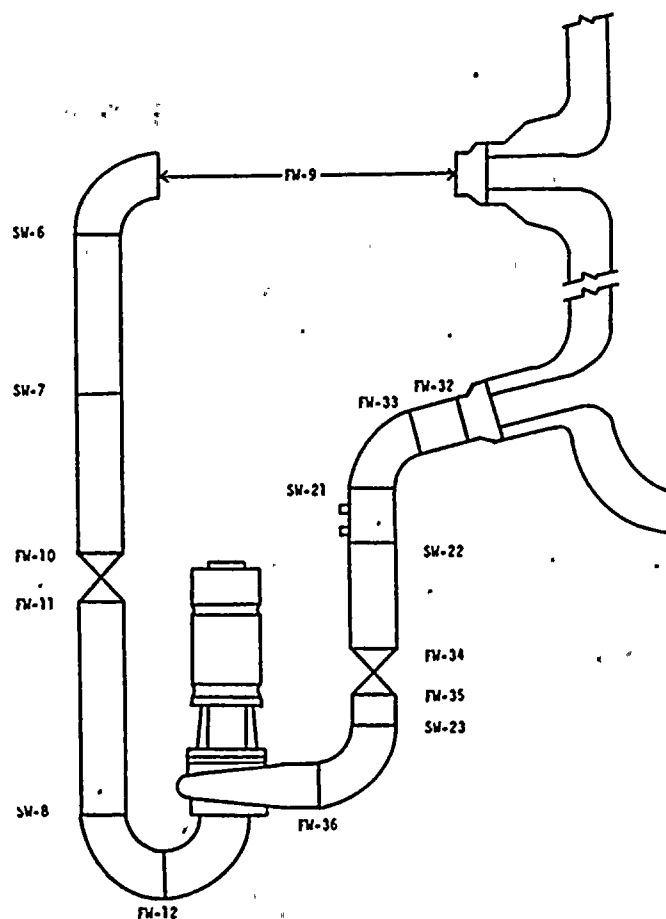
<u>Weld</u>	<u>HAZ</u>	<u>UT Results</u>	<u>PT Results</u>	<u>% Circ. by PT</u>
FW-1	Safe-End	---	No Indications	0
	Elbow	---	No Indications	0
SW-1	Elbow	---	No Indications	0
	Tee	---	No Indications	0
SW-2	Tee	No Indications	No Indications	0
	Pipe	Indications	No Indications	0
FW-2	Pipe	Indications	---	-
FW-3	Pipe	Indications	---	-
SW-3	Pipe	Indications	No Indications	0
	Elbow	Indications	Circ. Indications	0-5
FW-4	Elbow (Upstream)	Indications	Circ. Indications	5-10
FW-26	Elbow	Indications	Circ. Indications	0-5
SW-17	Elbow	Indications	No Indications	0
	Pipe	No Indications	No Indications	0
SW-16	Upstream Pipe	Indications	No Indications	0
	Downstream Pipe	Indications	No Indications	0
SW-15	Pipe	---	Circ. & Axial Indications	5-10
	Elbow	---	No Indications	0
FW-23	Elbow	---	Axial Indications	0-5
	Pipe	---	Circ. & Axial Indications	5-10
FW-22	Pipe	Indications	Circ. & Axial Indications	0-5
	Safe End	Indications	Circ. & Axial Indications, Leak	10-15

Figure 1. Recirculation Loop No. 11 Examination Results.



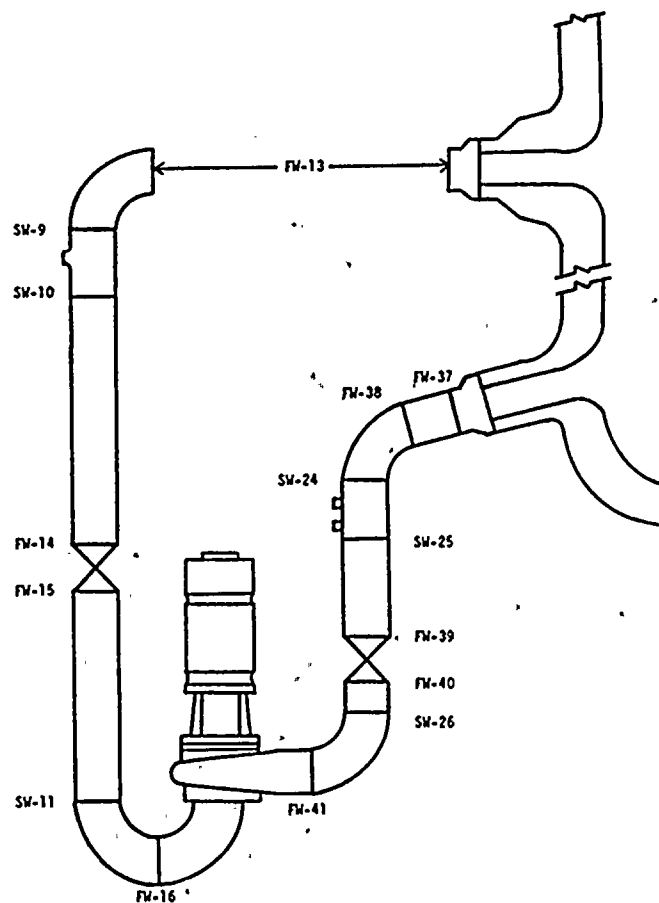
<u>Weld</u>	<u>HAZ</u>	<u>UT Results</u>	<u>PT Results</u>	<u>% Circ. by PT</u>
FW-5	Safe End	Indications	No Indications	0
	Elbow	Indications	No Indications	0
SW-4	Elbow	---	1 Axial Indication	0-5
	Pipe	---	No Indications	0
FW-6	Pipe	Indications	---	-
FW-7	Pipe	Indications	---	-
SW-5	Pipe	Indications	2 Axial Indications	0-5
	Elbow	Indications	Circ. Indications	0-5
FW-8	Upstream Elbow	Indications	Branched Circ. Indications	35-40
FW-31	Elbow	Indications	Branched Circ. Indications	25-30
SW-20	Elbow	Indications	Circ. Indications	0-5
	Pipe	Indications	Circ. Indications	10-15
SW-19	Upstream Pipe	Indications	Branched Circ. Indications	55-60
	Downstream Pipe	Indications	Branched Circ. Indications	25-30
SW-18	Pipe	---	Circ. & Axial Indications	5-10
	Elbow	---	Circ. Indications	5-10

Figure 2. Recirculation Loop No. 12 Examination Results.



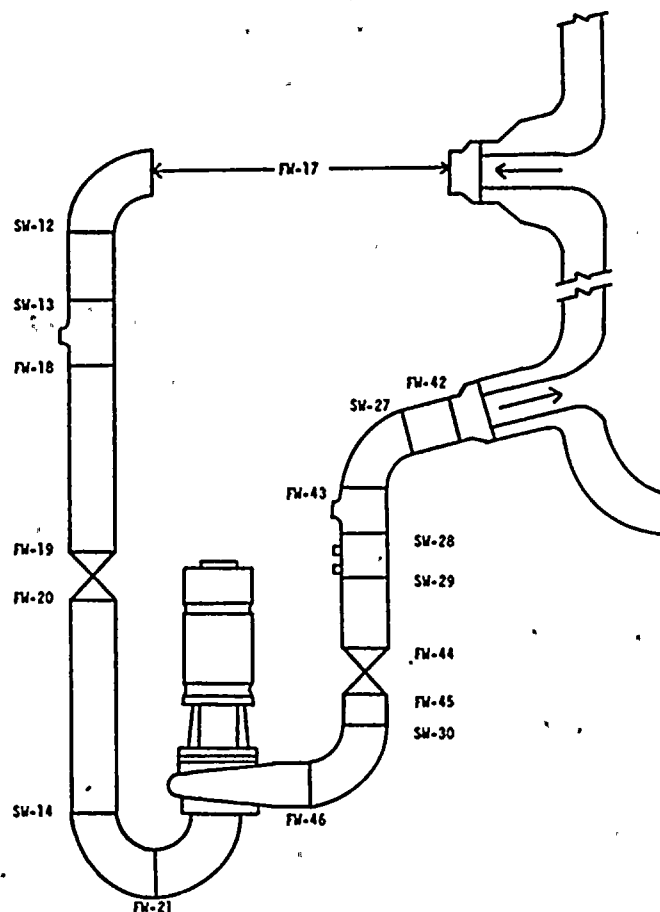
<u>Weld</u>	<u>HAZ</u>	<u>UT Results</u>	<u>PT Results</u>	<u>% Circ. by PT</u>
FW-9	Safe End	Indications	Circ. & Axial Indications	> 50%
	Elbow	Indications	No Indications	0
SW-6	Elbow	Indications	Branched Circ. Indications	45-50
	Pipe	Indications	Branched Circ. Indications	35-40
SW-7	Upstream Pipe	Indications	Indications	
	Downstream Pipe	---	No Indications	
FW-10	Pipe	Indications	---	-
FW-11	Pipe	Indications	---	-
SW-8	Pipe	Indications	Circ. & Axial Indications	40-45
	Elbow	Indications	Circ. & Axial Indications	15-20
FW-12	Upstream Elbow	Indications	Branched Circ. Indications	40-45
FW-36	Elbow	Indications	Circ. & Axial Indications	0-5
SW-23	Elbow	Indications	Branched Circ. Indications	20-25
	Pipe	No Indications	Branched Circ. Indications	30-35
SW-22	Upstream Pipe	---	Circ. & Axial Indications	5-10
	Downstream Pipe	---	Circ. Indications	0-5
SW-21	Pipe	---	No Indications	0
	Elbow	---	No Indications	0
FW-33	Elbow	---	Circ. Indications	0-5
	Pipe	---	No Indications	0
FW-32	Pipe	No Indications	Circ. & Axial Indications	5-10
	Safe End	Indications	Circ. Indications	0-5

Figure 3. Recirculation Loop No. 13 Examination Results.



Weld	HAZ	UT Results	PT Results	% Circ. by PT
FW-13	Safe End	---	Circ. & Axial Indications	30-35
	Elbow	---	No Indications	0
SW-9	Elbow or Tee	---	Circ. Indications	10-15
	Elbow or Tee	---	No Indications	0
SW-10	Tee	No Indications	---	-
	Pipe	No Indications	---	-
FW-14	Pipe	Indications	---	-
FW-15	Pipe	Indications	---	-
SW-11	Pipe	Indications	Circ. & Axial Indications	15-20
	Elbow	Indications	Circ. & Axial Indications	15-20
FW-16	Upstream Elbow	Indications	Branched Circ. Indications	15-20
FW-41	Elbow	Indications	Circ. & Axial Indications	0-5
SW-26	Elbow	Indications	Branched Circ. Indications	20-25
	Pipe	Indications	Circ. Indications	5-10
SW-25	Upstream Pipe	Indications	Circ. Indications	0-5
	Downstream Pipe	Indications	Branched Circ. Indications	0-5
SW-24	Pipe	---	Circ. Indications	0-5
	Elbow	---	Circ. Indications	20-25
FW-38	Elbow	---	No Indications	0
	Pipe	---	No Indications	0
FW-37	Pipe	---	No Indications	0
	Safe End	---	No Indications	0

Figure 4. Recirculation Loop No. 14 Examination Results.



Weld	HAZ	UT Results	PT Results	% Circ. by PT
FW-17	Safe End	Indications	Circ. Indications, Leak	20-25
	Elbow	No Indications	No Indications	0
SW-12	Elbow	Indications	Circ. Indications	10-15
	Pipe	Indications	Circ. Indications	15-20
SW-13	Pipe	Indications	---	-
	Tee	No Indications	---	-
FW-18	Tee	No Indications	---	-
	Pipe	Indications	---	-
FW-19	Pipe	Indications	---	-
FW-20	Pipe	Indications	---	-
SW-14	Pipe	Indications	Circ. Indications	5-10
	Elbow	Indications	No Indications	-
FW-21	Upstream Elbow	Indications	Circ. Indications	0-5
FW-46	Elbow	Indications	Circ. Indications	20-25
SW-30	Elbow	---	Branched Circ. Indications	40-45
	Pipe	---	Branched Circ. Indications	20-25
FW-43	Tee	---	No Indications	0
	Elbow	---	No Indications	0
SW-27	Elbow	---	No Indications	0
	Pipe	---	No Indications	0
FW-42	Pipe	---	No Indications	0
	Safe End	---	No Indications	0

Figure 5. Recirculation Loop No. 15 Examination Results.

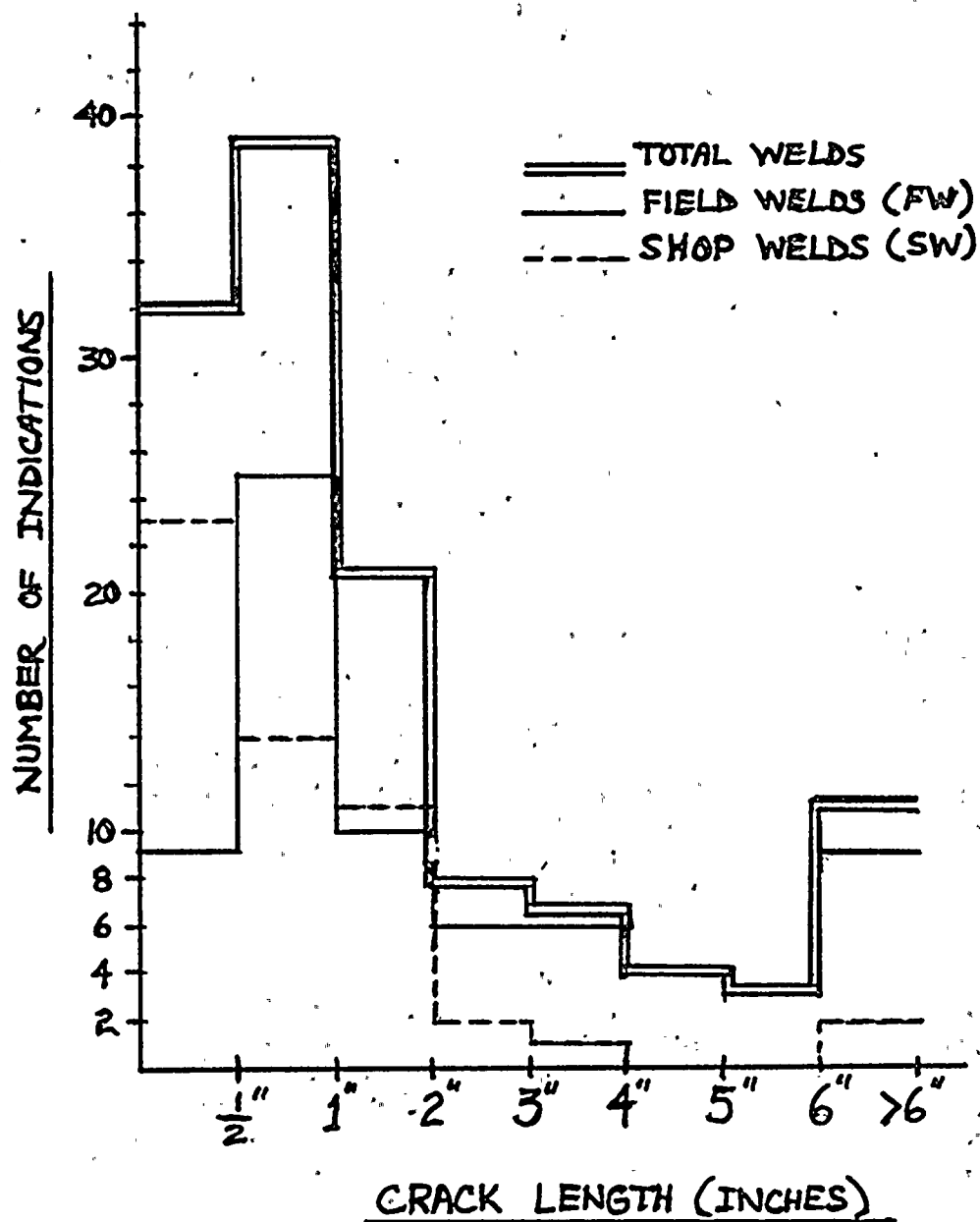


Figure 6. Frequency Distribution of Crack Lengths

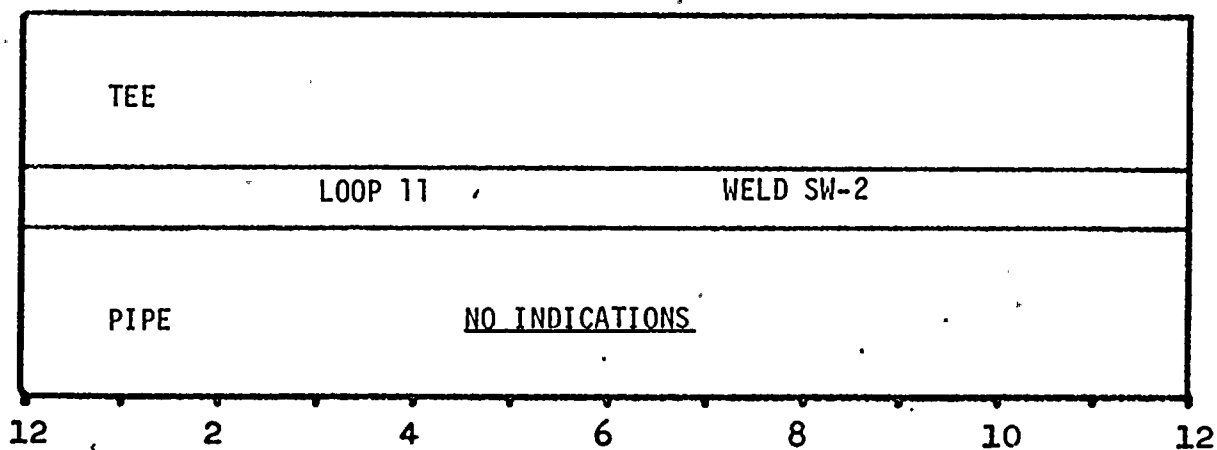
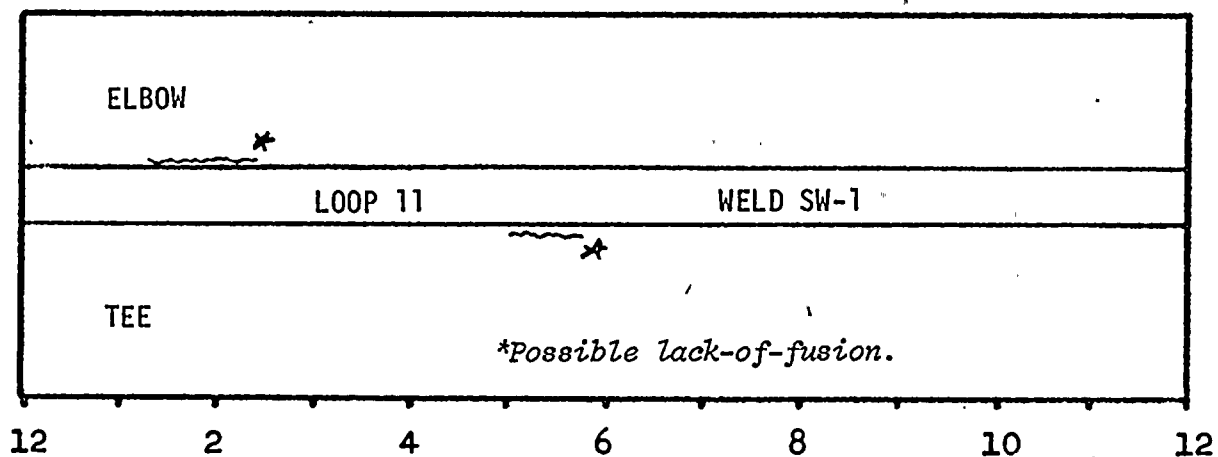
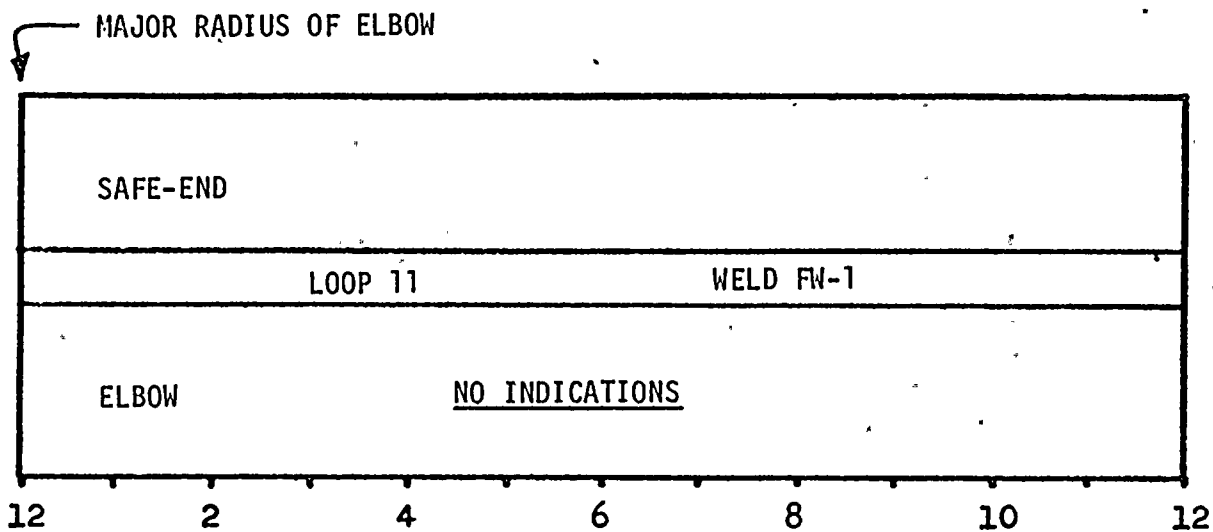


FIGURE 7: Dye Penetrant inspection results, welds of Loop 11.
(Refer to Figure 1 for weld locations.)

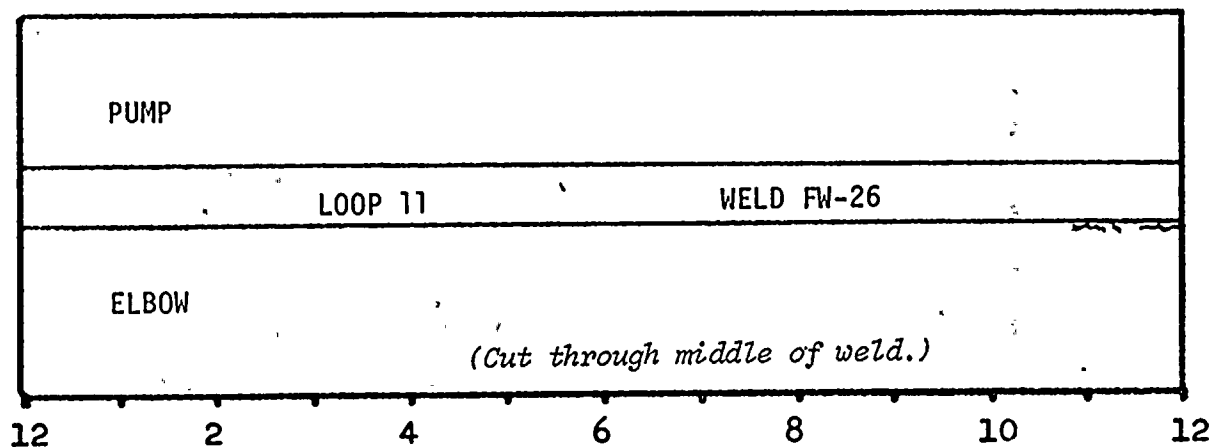
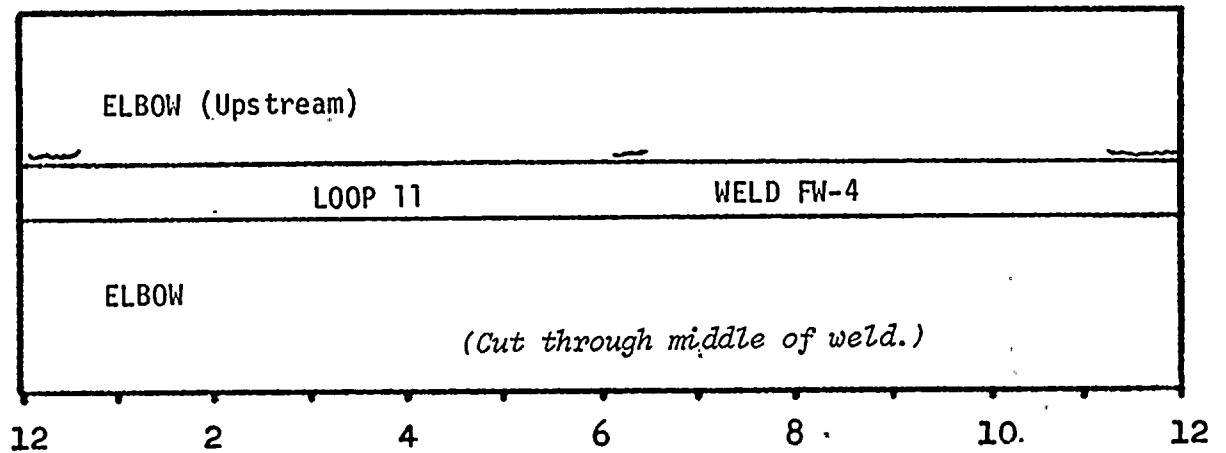
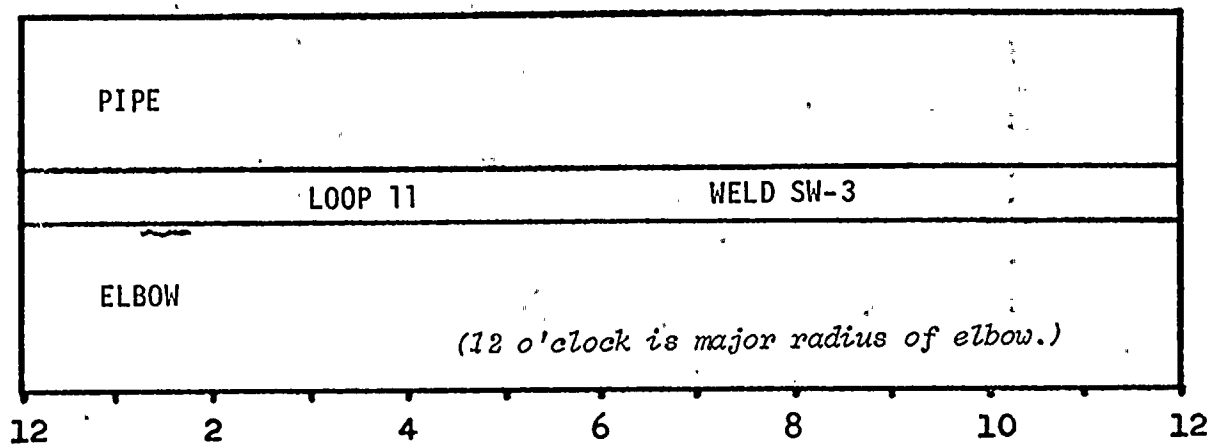


FIGURE 7. (continued) Dye Penetrant inspection results. Welds of Loop 11. (Refer to Figure 1 for weld locations.)

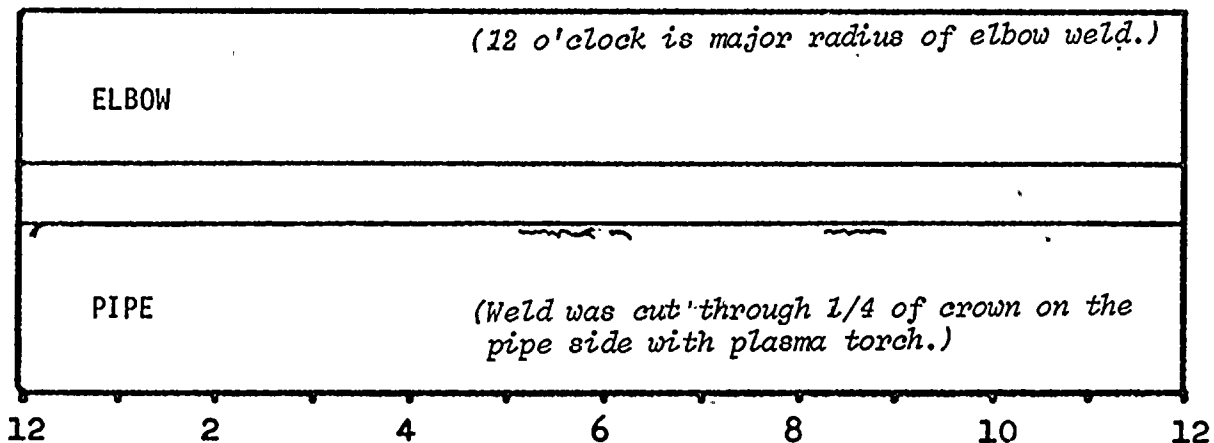
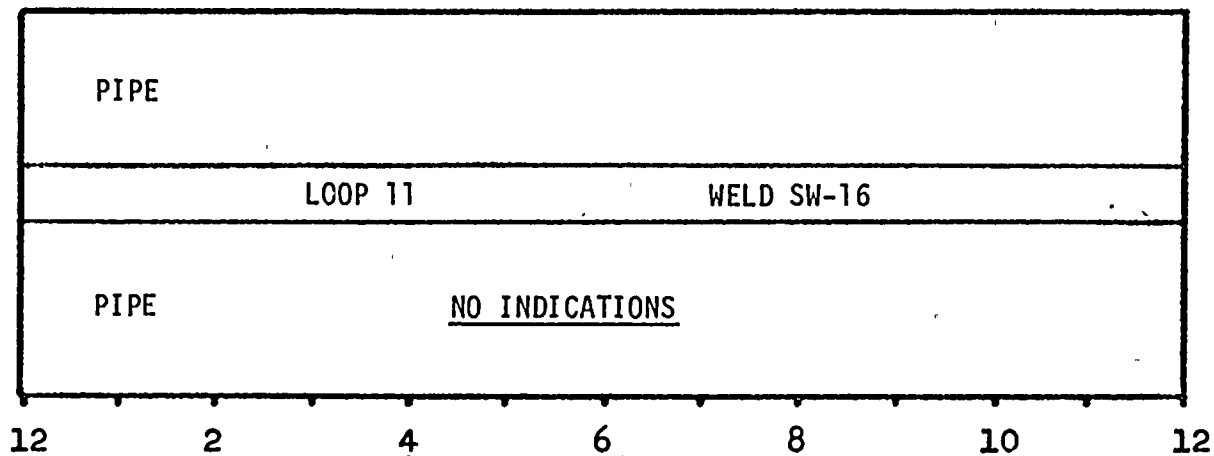
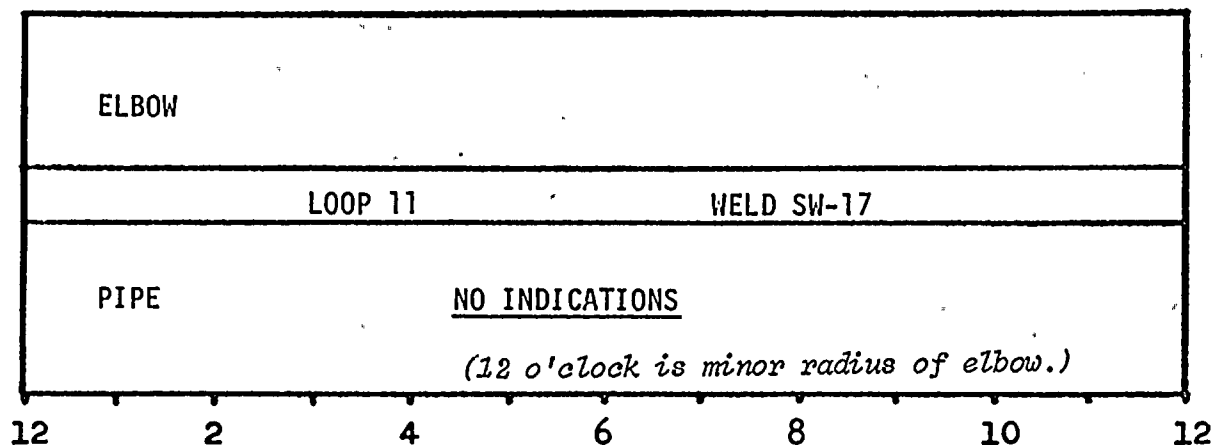


FIGURE 7. (Continued) Dye Penetrant results, welds of Loop 11.
 (Refer to Figure 1 for weld locations.)

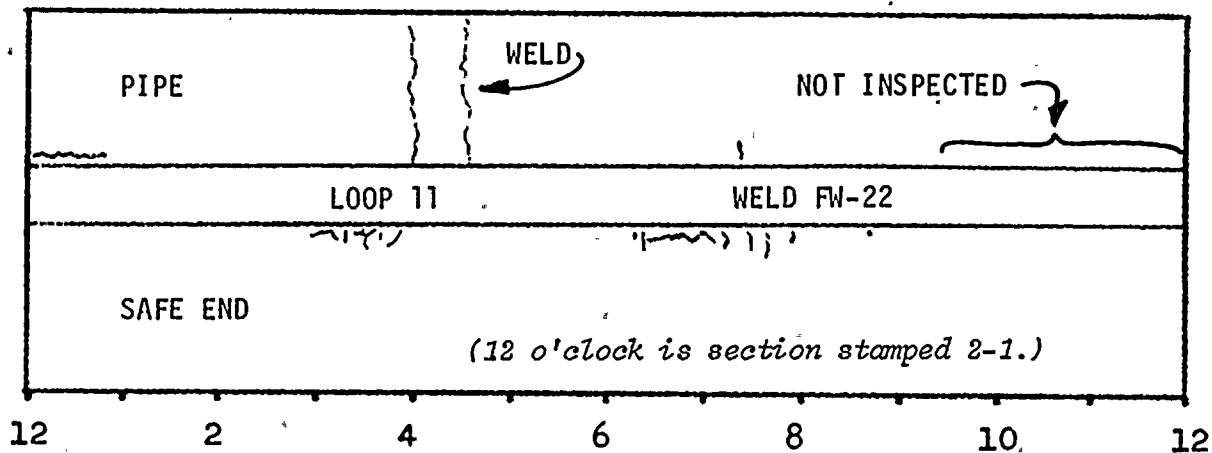
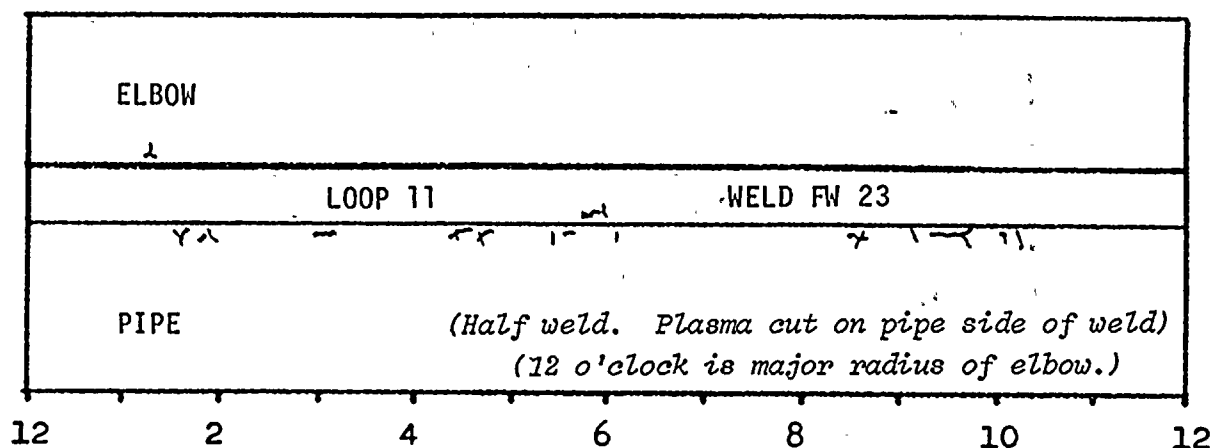


FIGURE 7. (Continued) Dye Penetrant inspection results, welds of Loop 11. (Refer to Figure 1 for weld locations.)

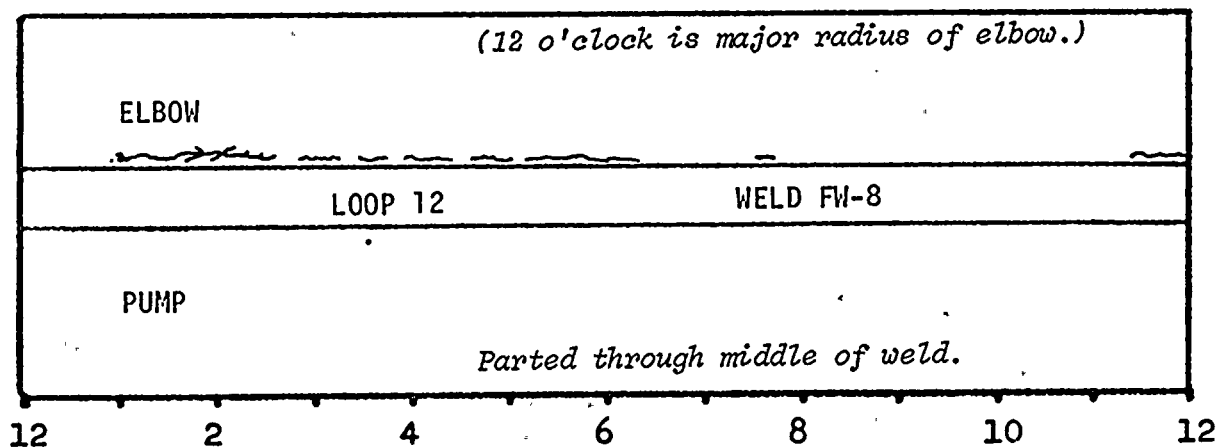
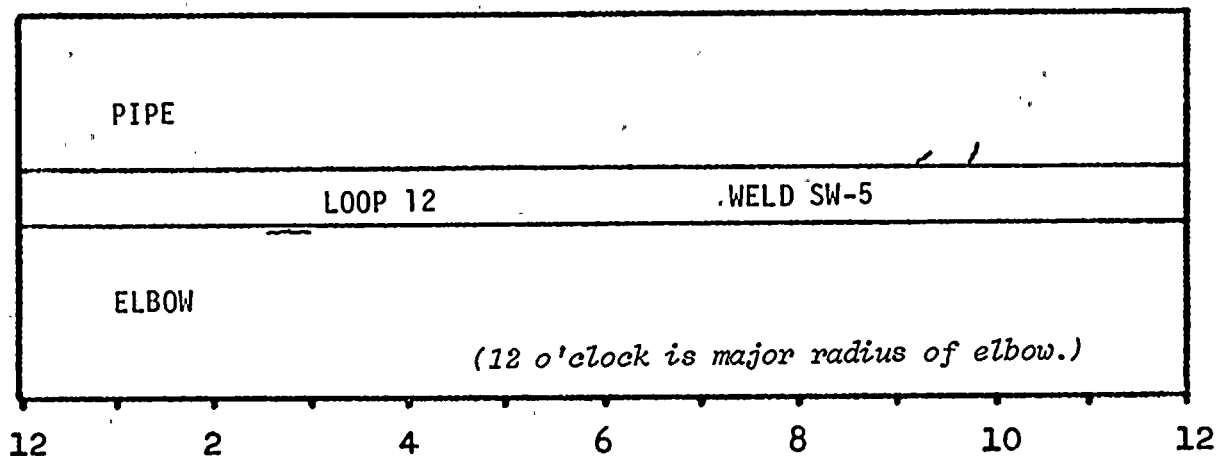
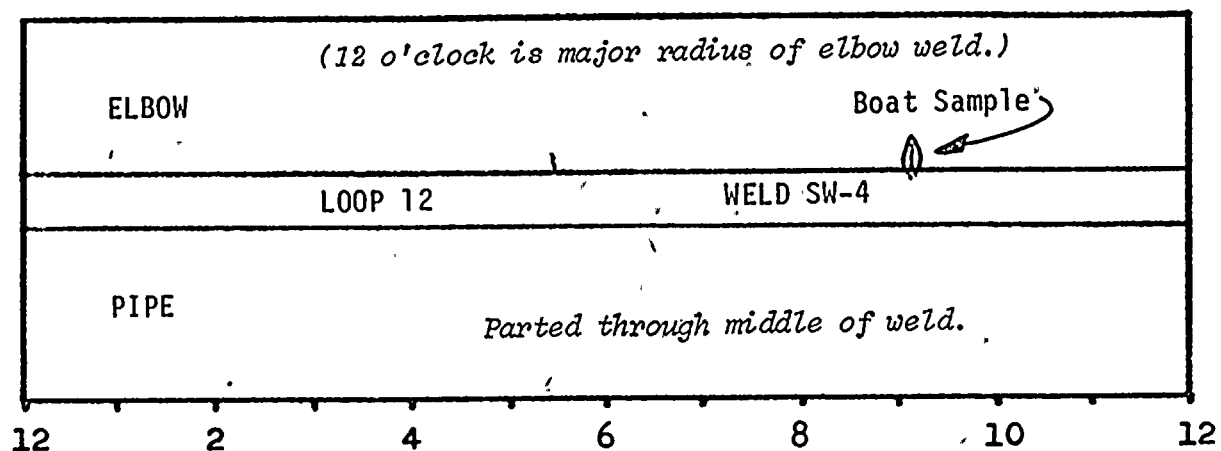


FIGURE 8. Dye Penetrant inspection results, Loop 12 welds.
(Refer to Figure 2 for weld locations.)

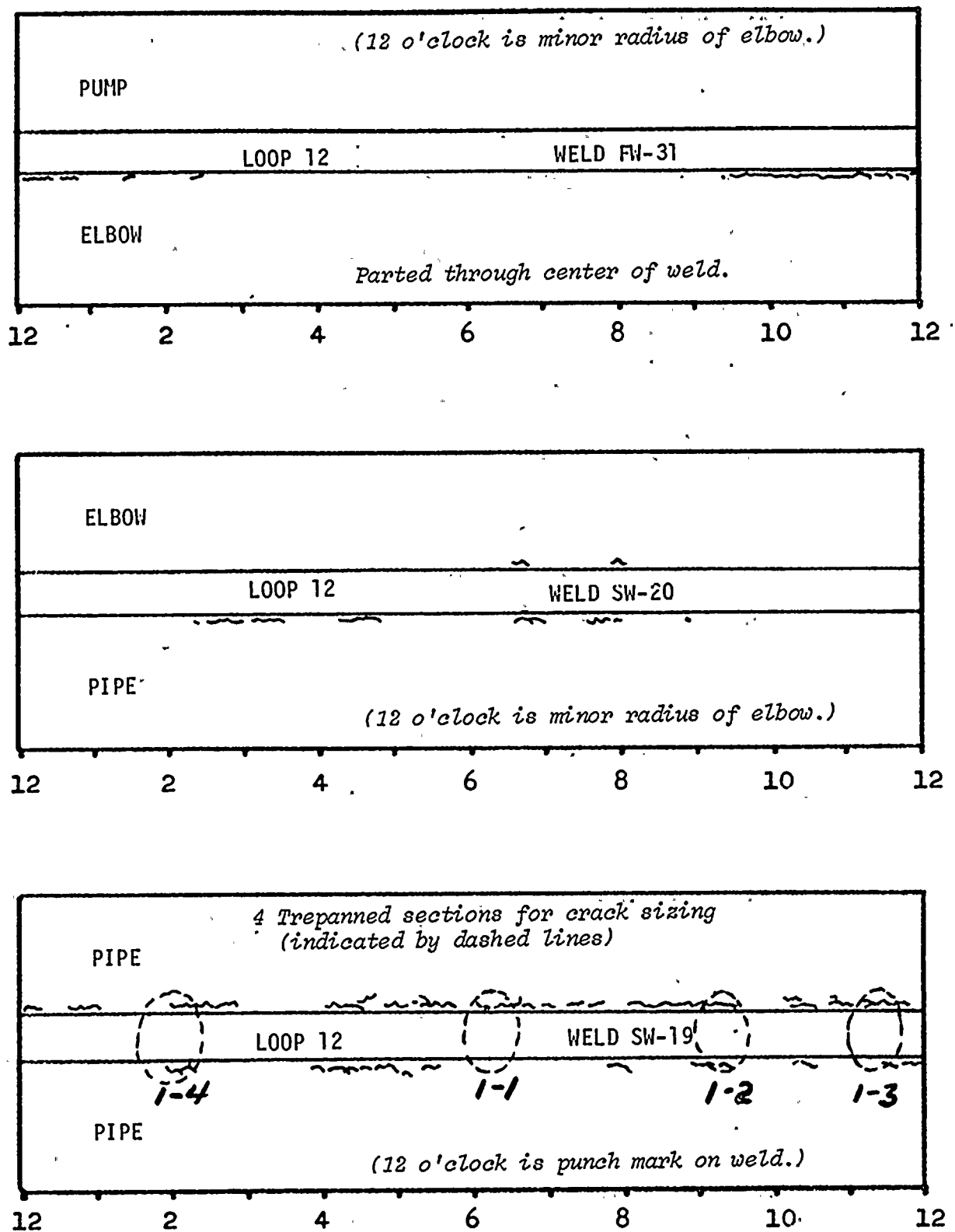


FIGURE 8. (Continued) Dye Penetrant inspection results, Loop 12 welds.
(Refer to Figure 2 for weld locations.)

PIPE	Plasma cut through edge of crown on pipe side of weld.	
	LOOP 12	WELD SW-18
ELBOW	(12 o'clock is major radius of elbow.)	

FIGURE 8. (Continued) Dye Penetrant inspection results, Loop 12 welds.
(Refer to Figure 2 for weld locations.)

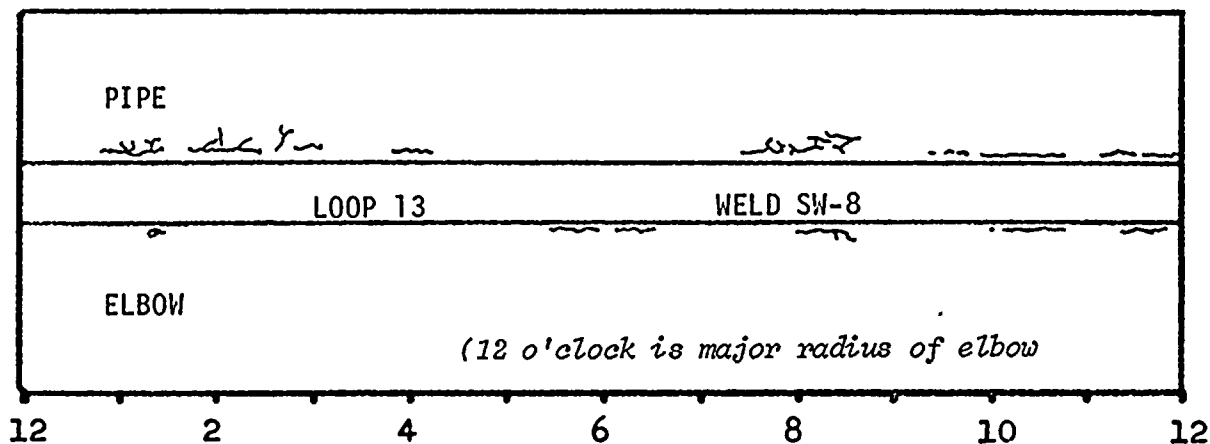
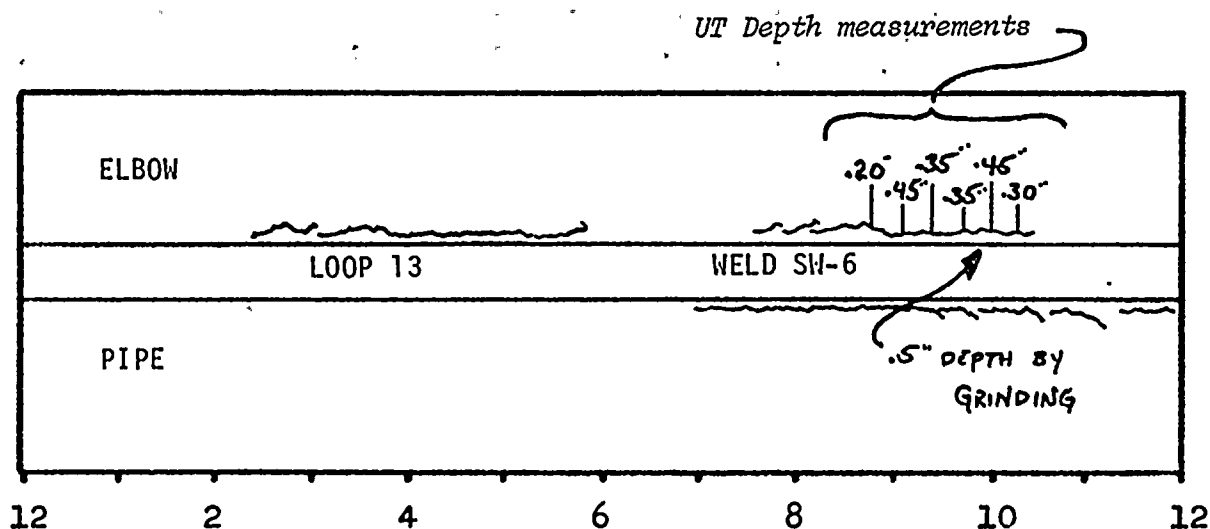
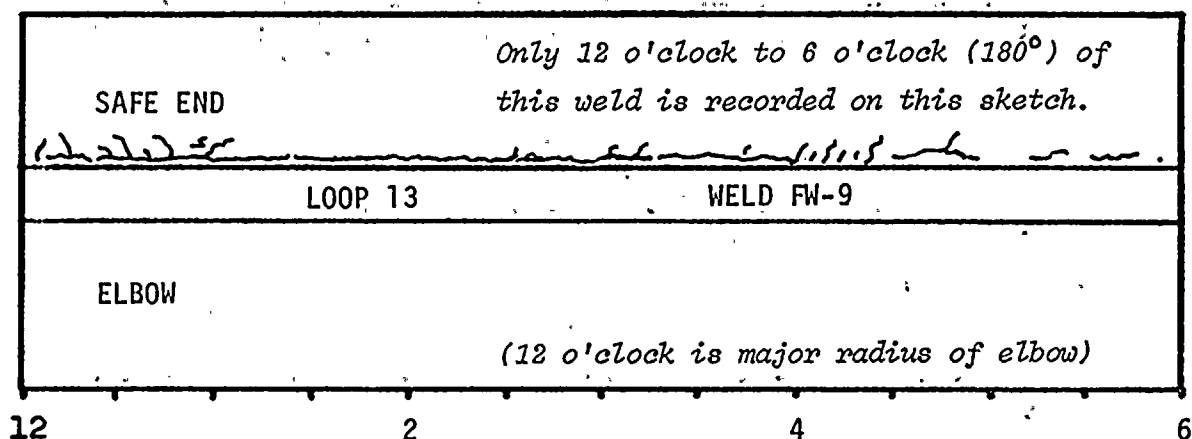


FIGURE 9. Dye Penetrant inspection results, Loop 13 welds.
(See Figure 3 for weld locations.)

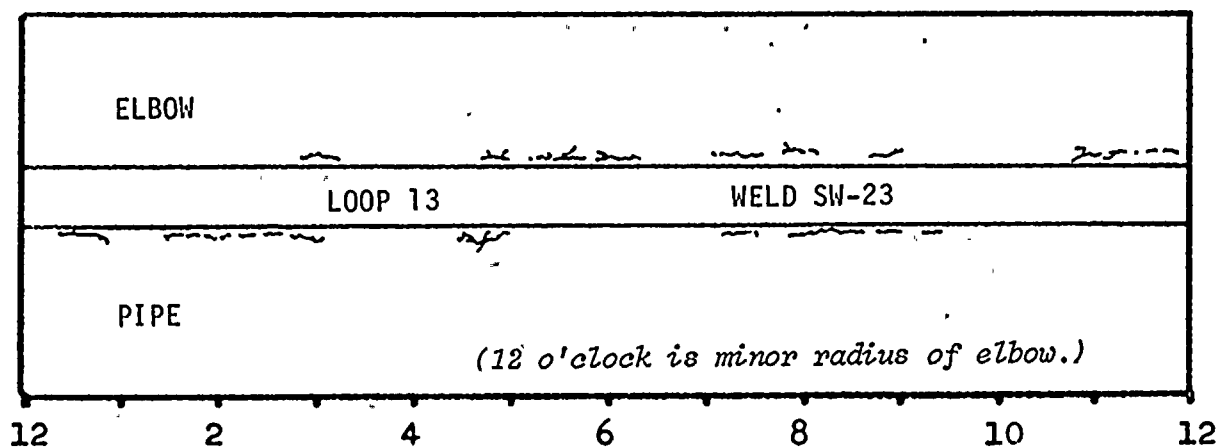
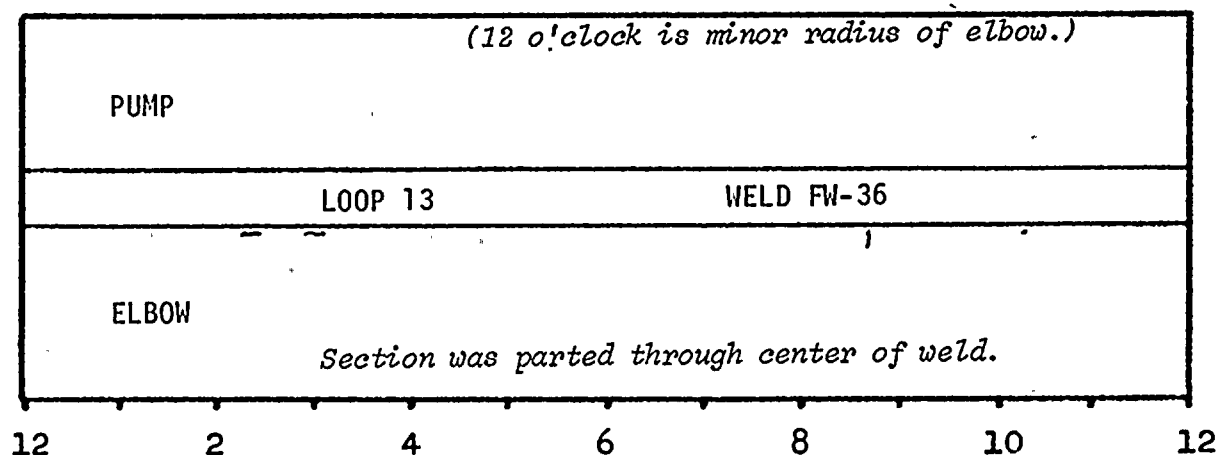
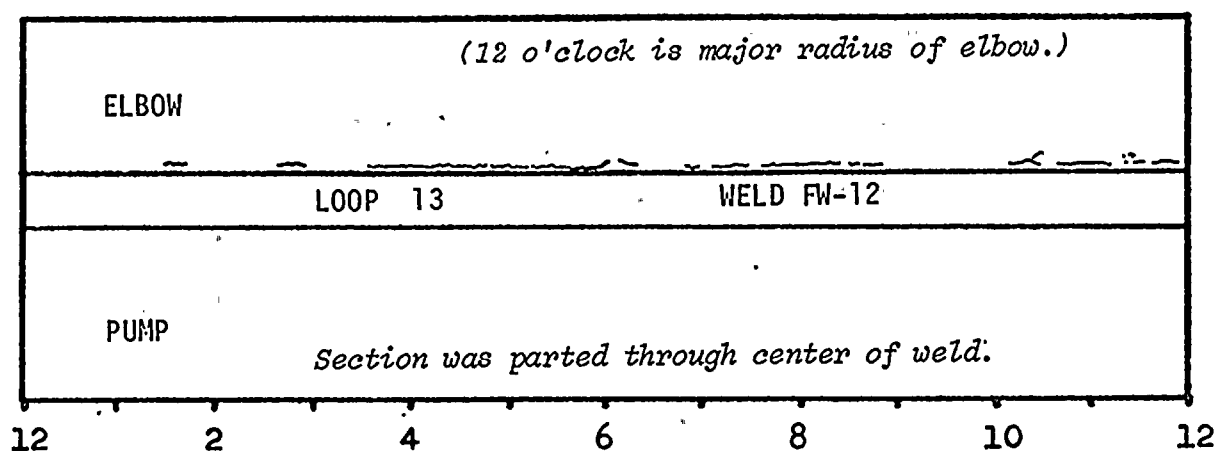


FIGURE 9. (Continued) Dye Penetrant inspection results, Loop 13 welds. (Refer to Figure 3 for weld locations.)

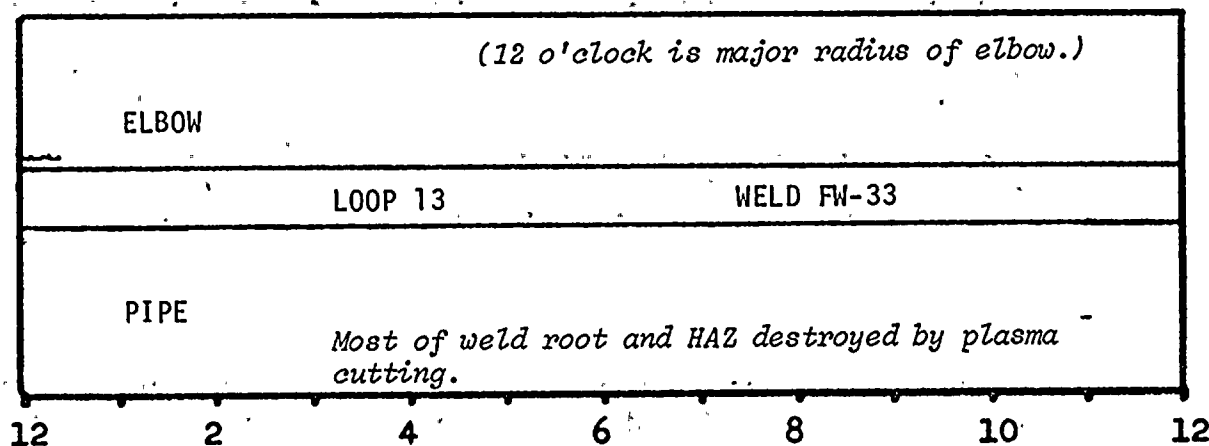
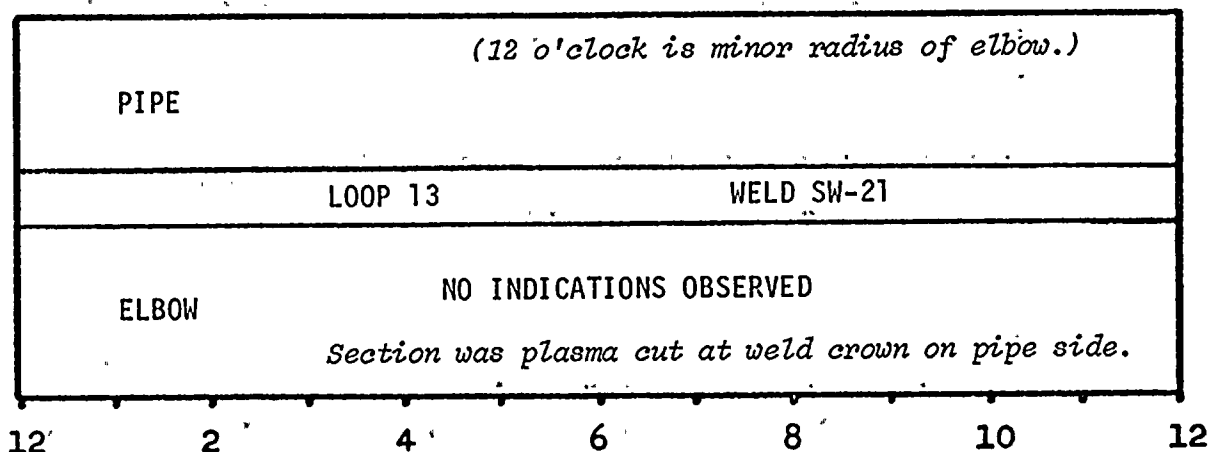
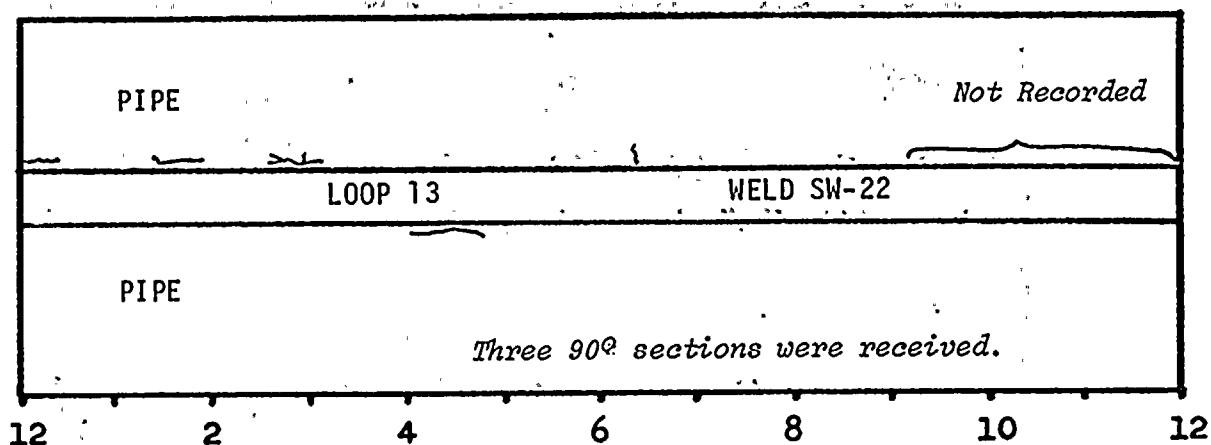


FIGURE 9. (Continued) Dye Penetrant inspection results, Loop 13 welds. (See Figure 3 for weld locations.)

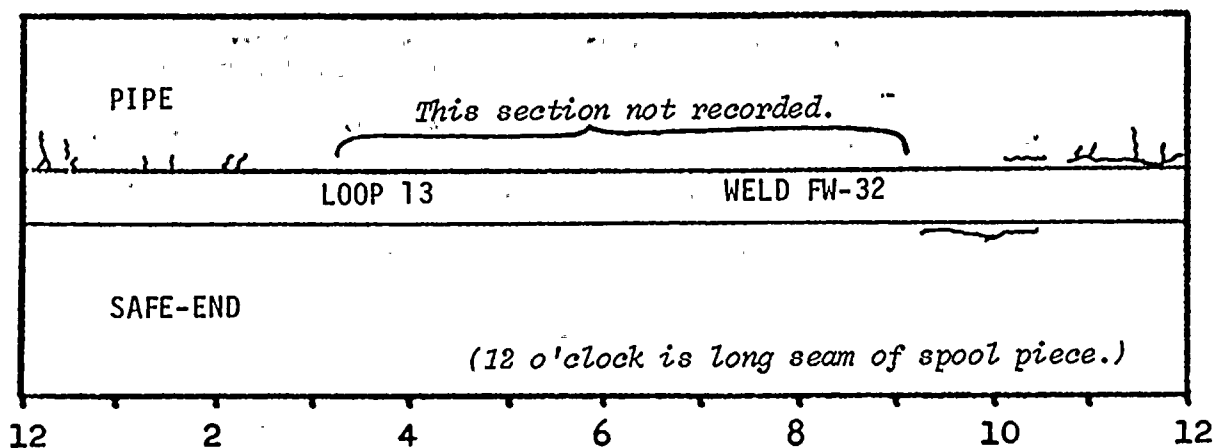


FIGURE 9. (Continued) Dye Penetrant inspection results, Loop 13 welds. (See Figure 3 for weld locations.)

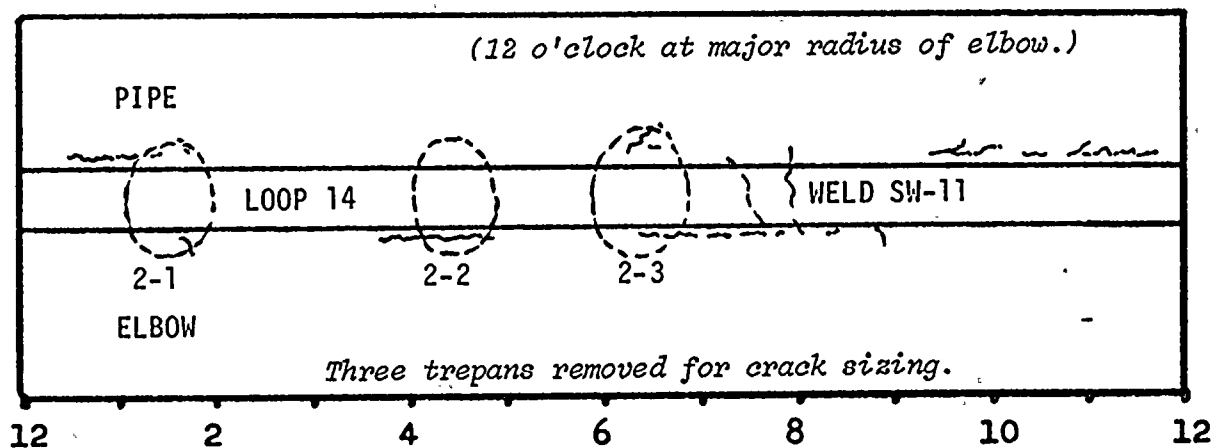
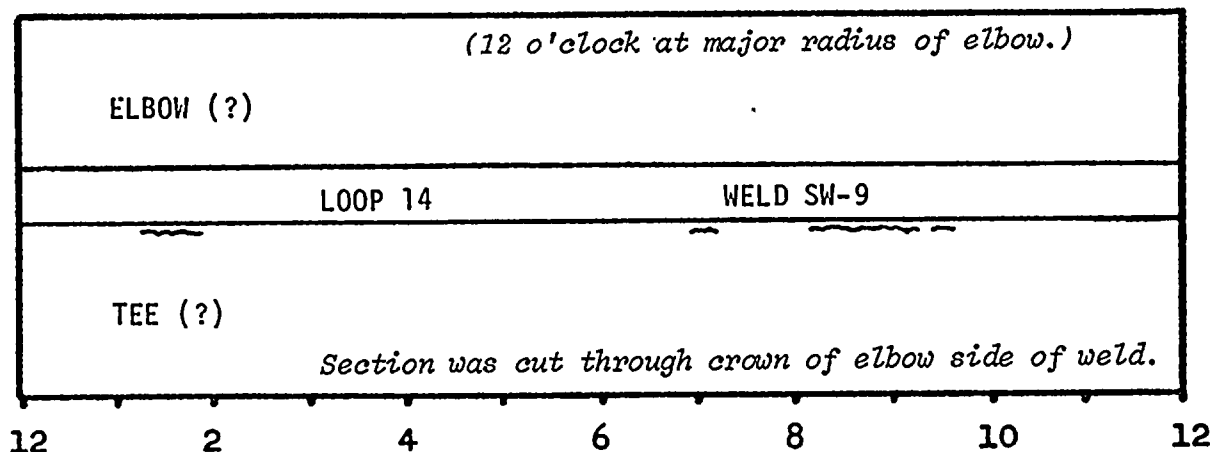
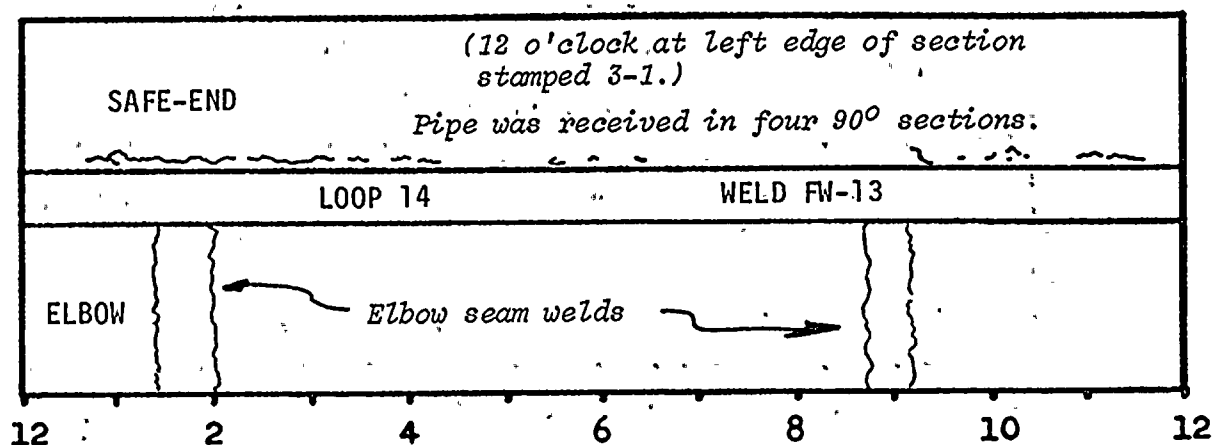


FIGURE 10. Dye Penetrant inspection results, Loop 14 welds.
(Refer to Figure 4 for weld locations.)

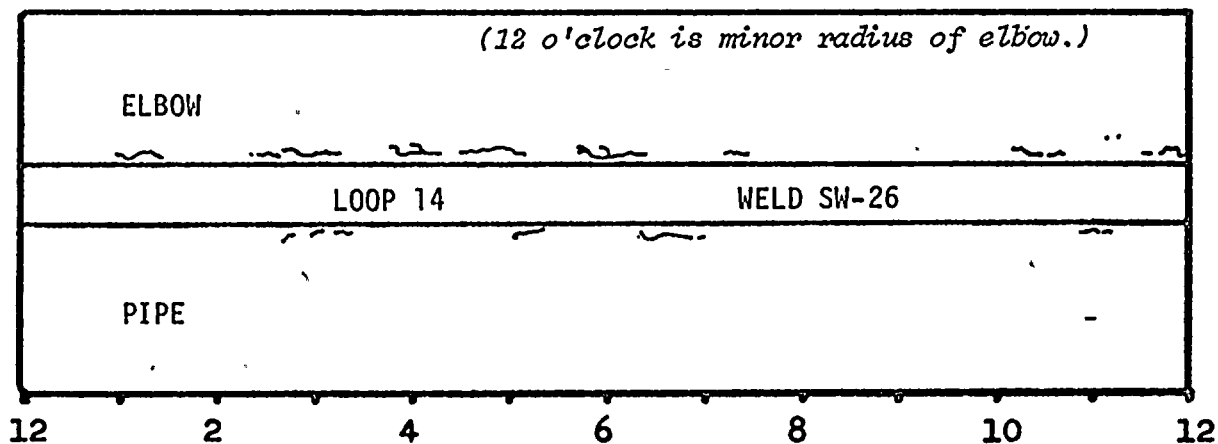
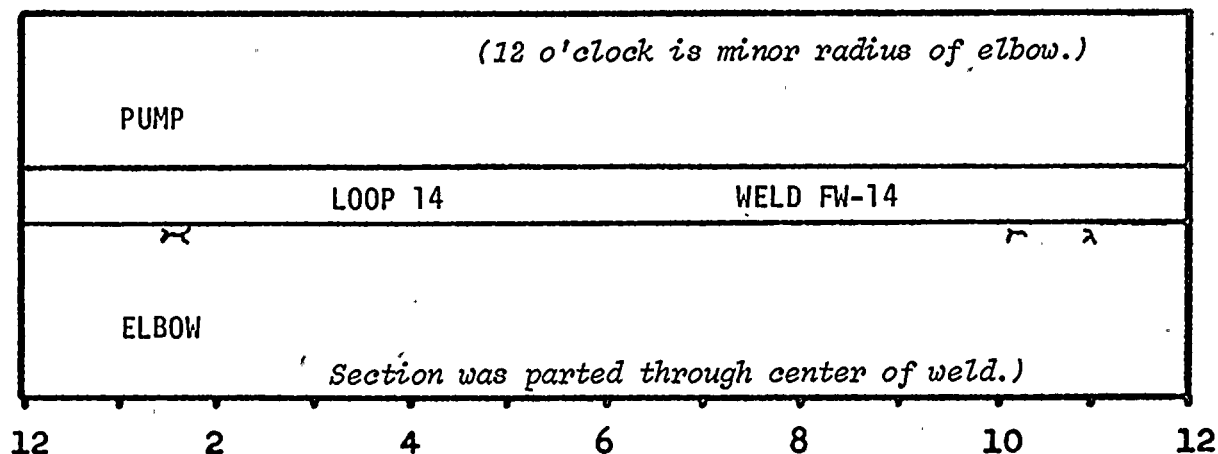
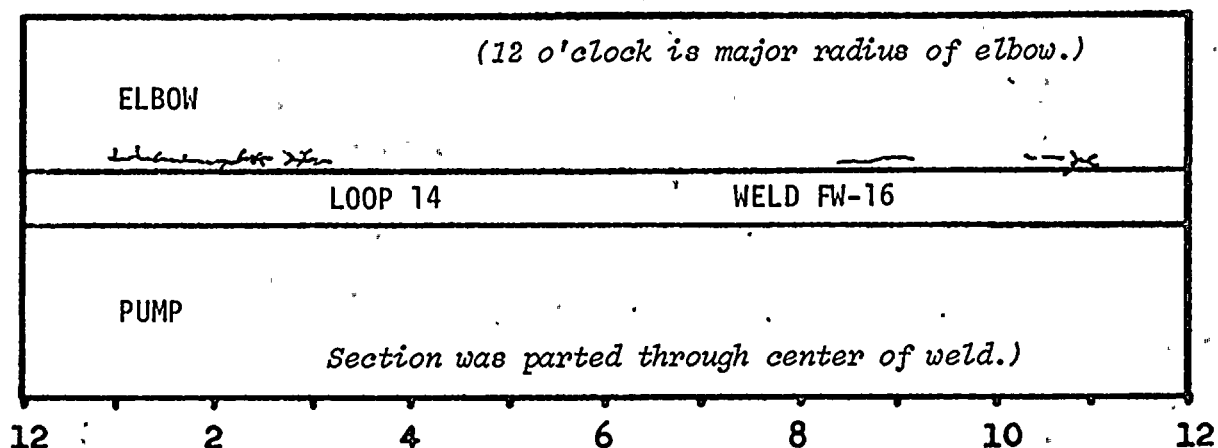


FIGURE 10. (Continued) Dye Penetrant inspection results, Loop 14 welds. (Refer to Figure 4 for weld locations.)

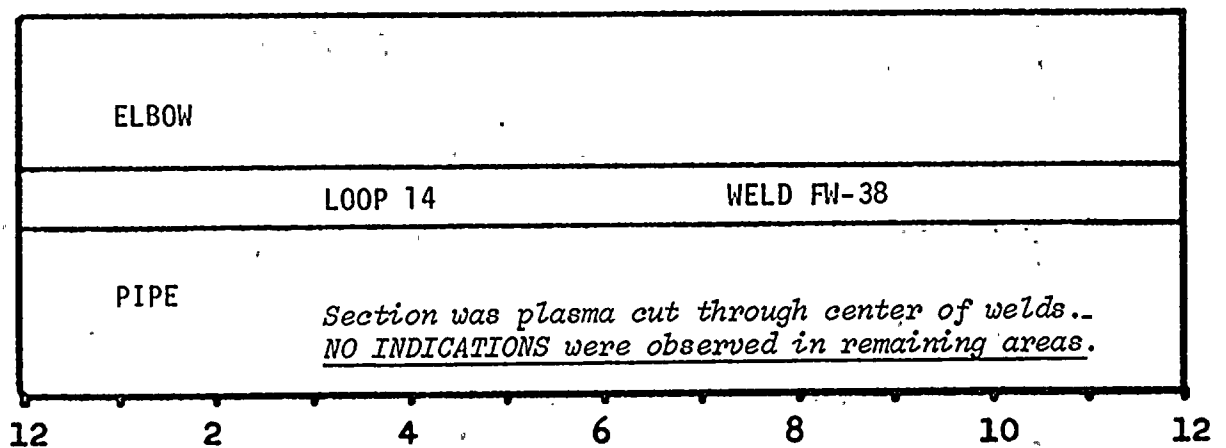
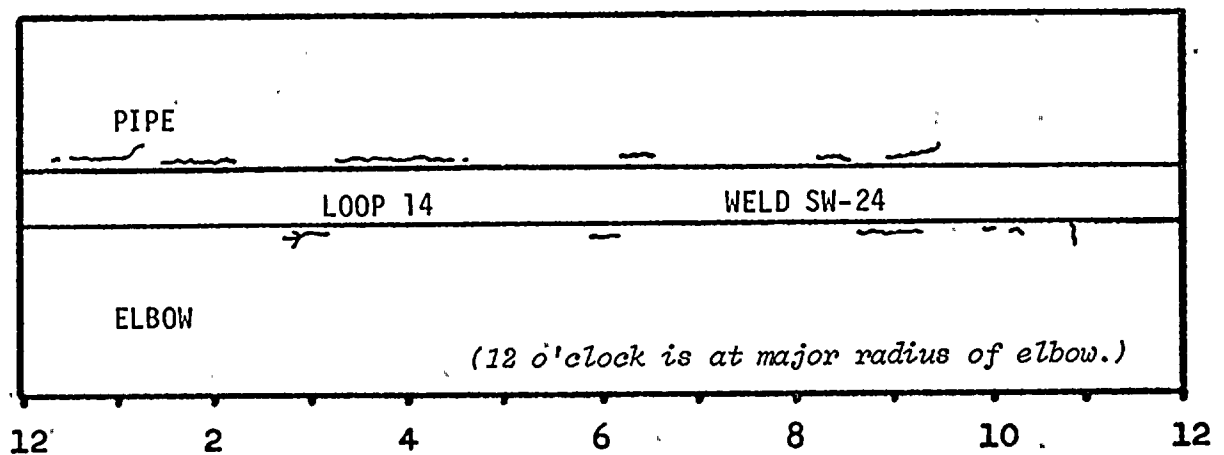
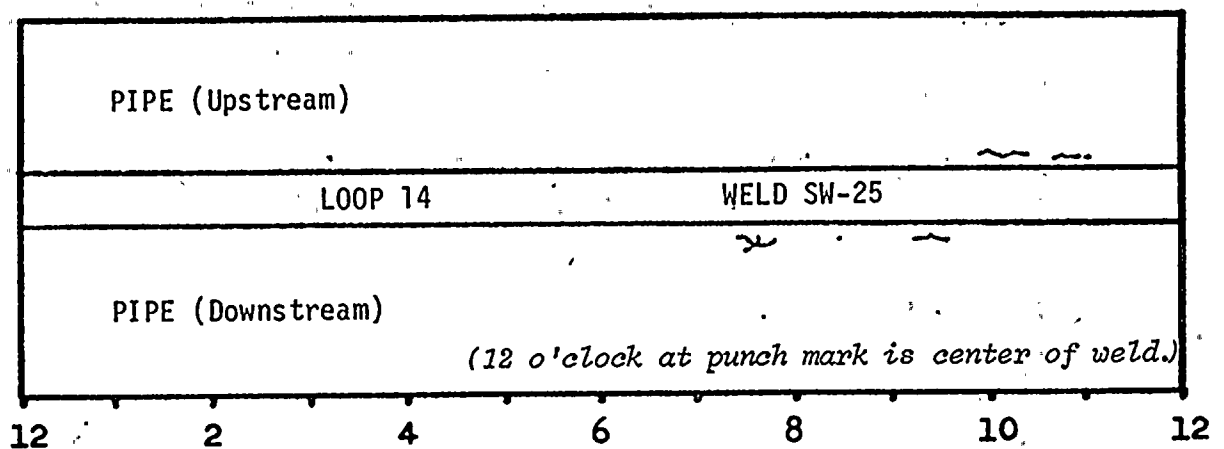


FIGURE 10. (Continued). Dye Penetrant inspection results, Loop 14 welds. (Refer to Figure 4 for weld locations.)

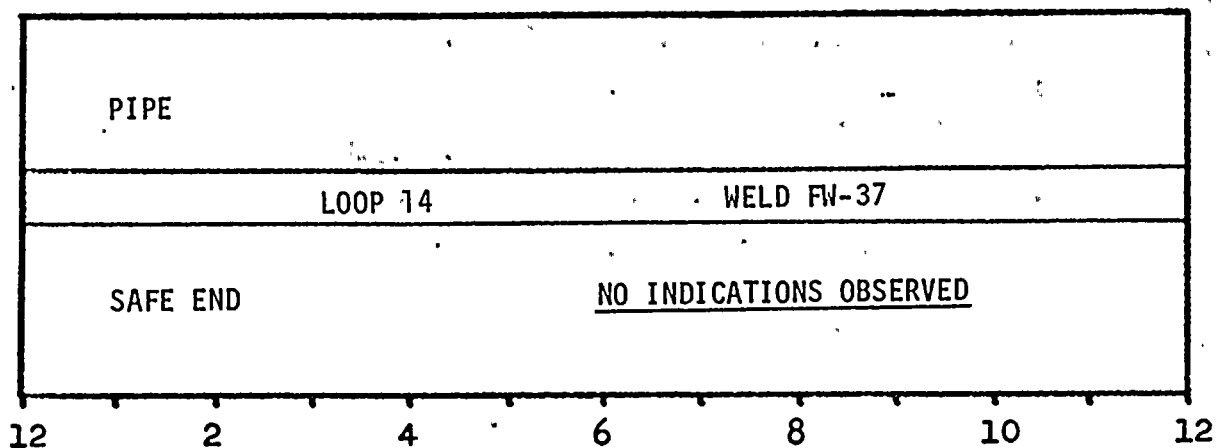


FIGURE 10. (Continued) Dye Penetrant inspection results, Loop 14 welds. (Refer to Figure 4 for weld locations.)

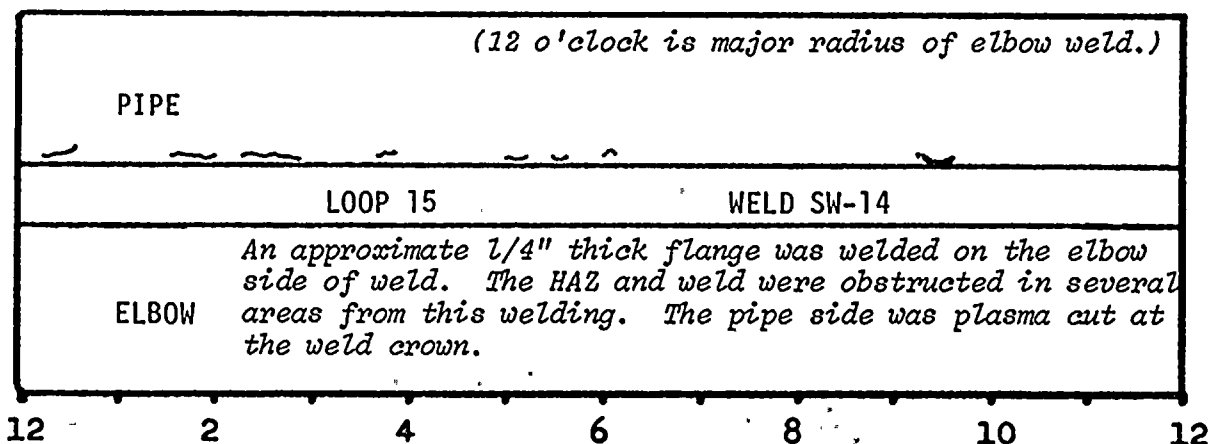
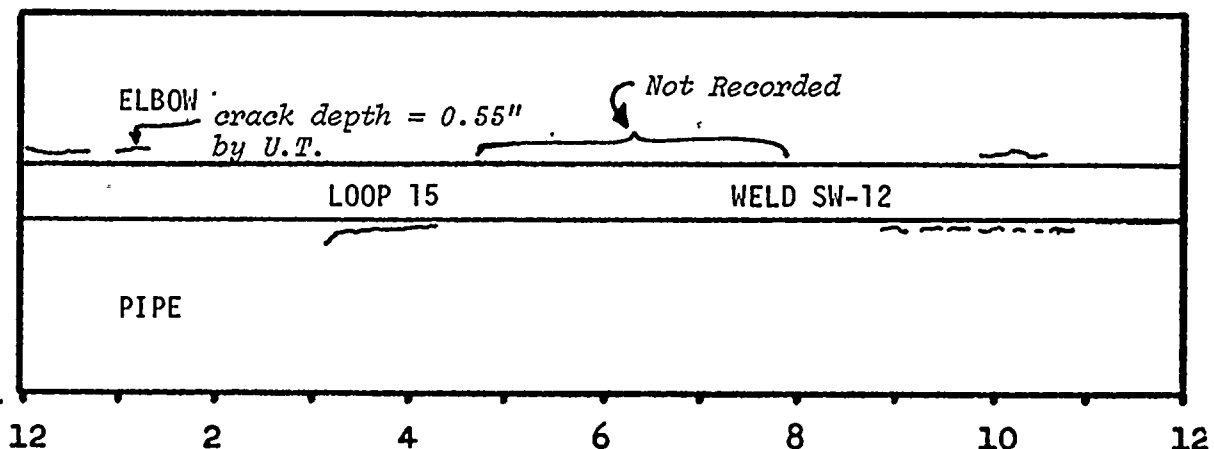
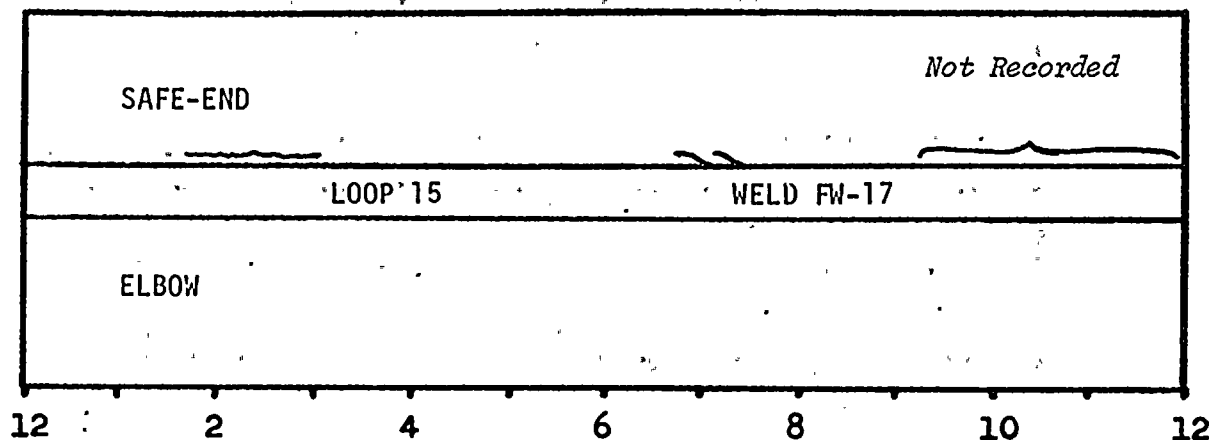


FIGURE 11. Dye Penetrant inspection results, Loop 15 welds.
(Refer to Figure 5 for weld locations.)

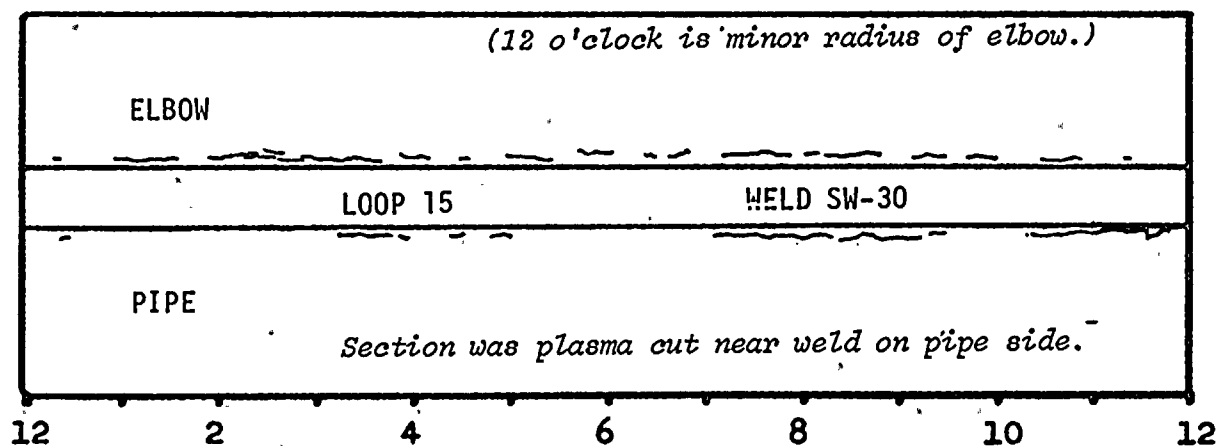
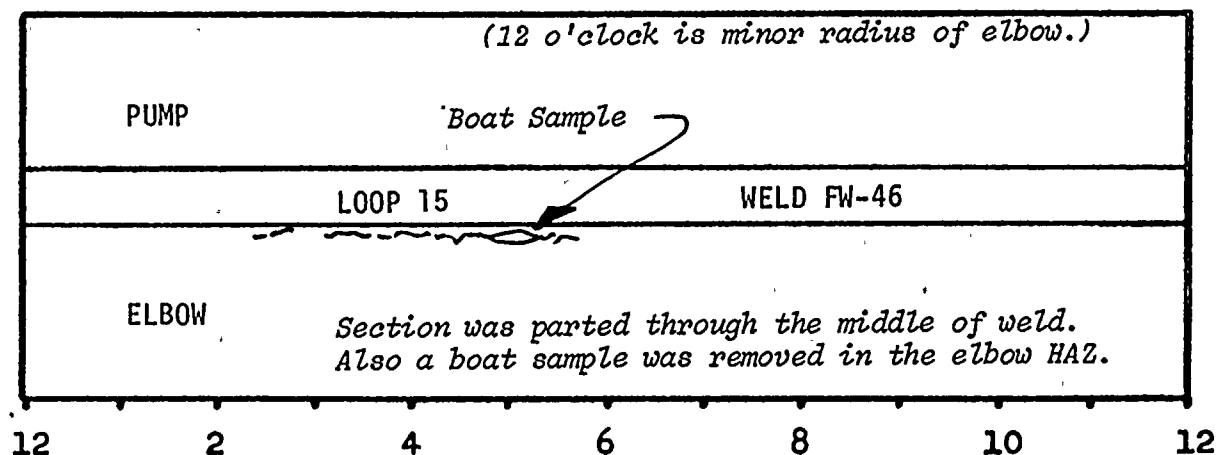
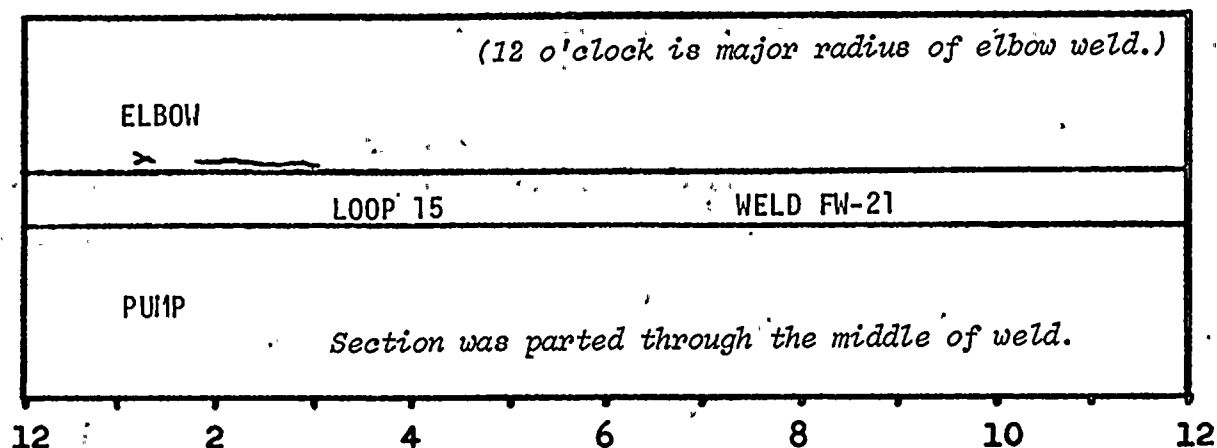


FIGURE 11. (Continued) Dye Penetrant inspection results, Loop 15 welds. (Refer to Figure 5 for weld locations.)

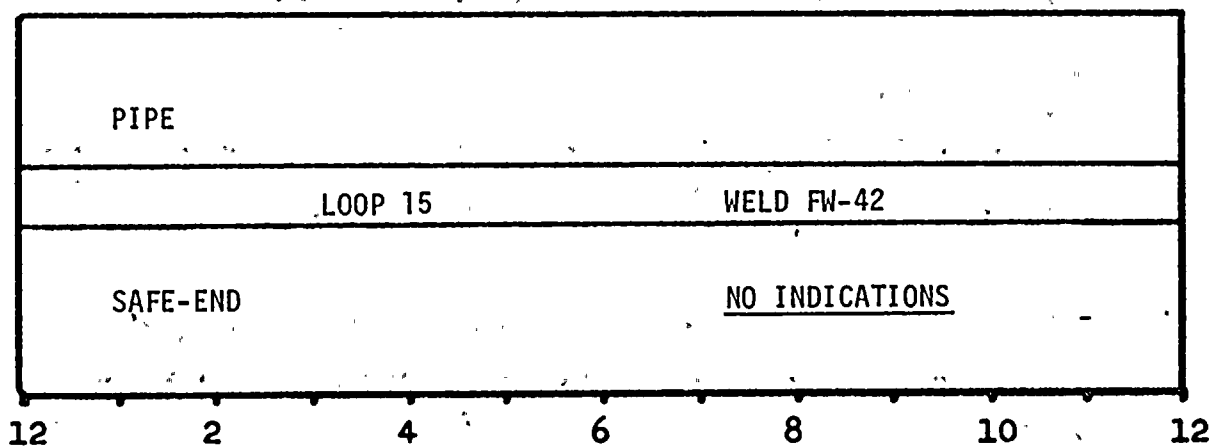
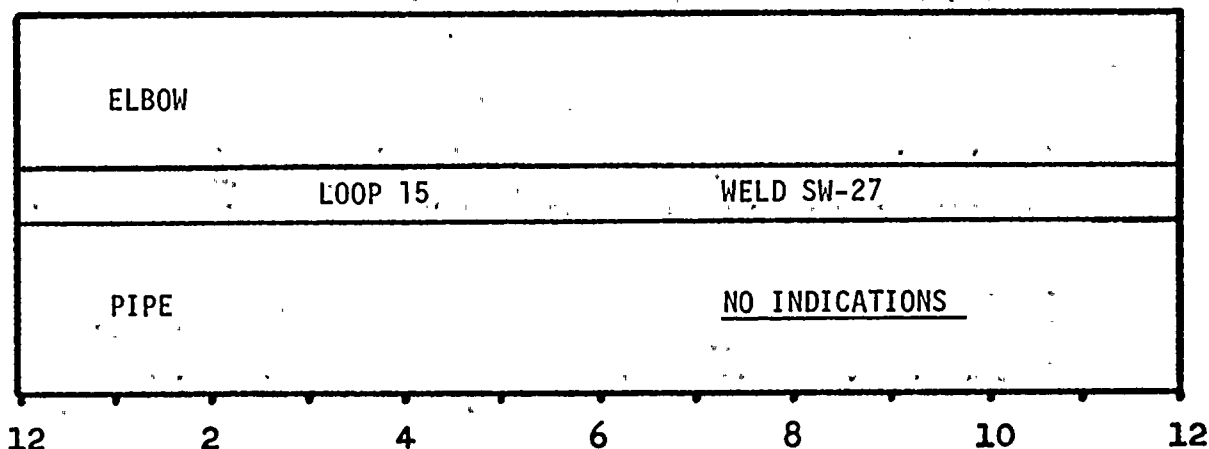
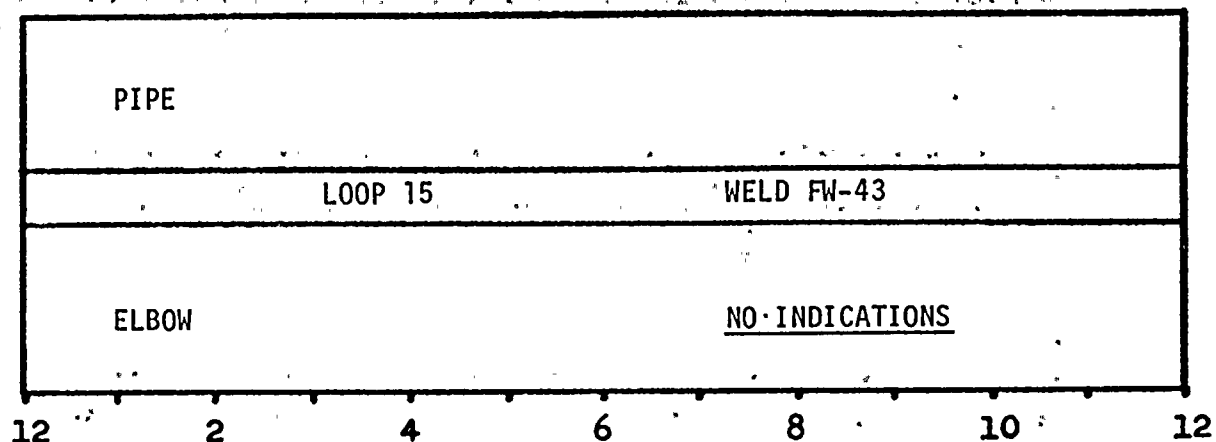
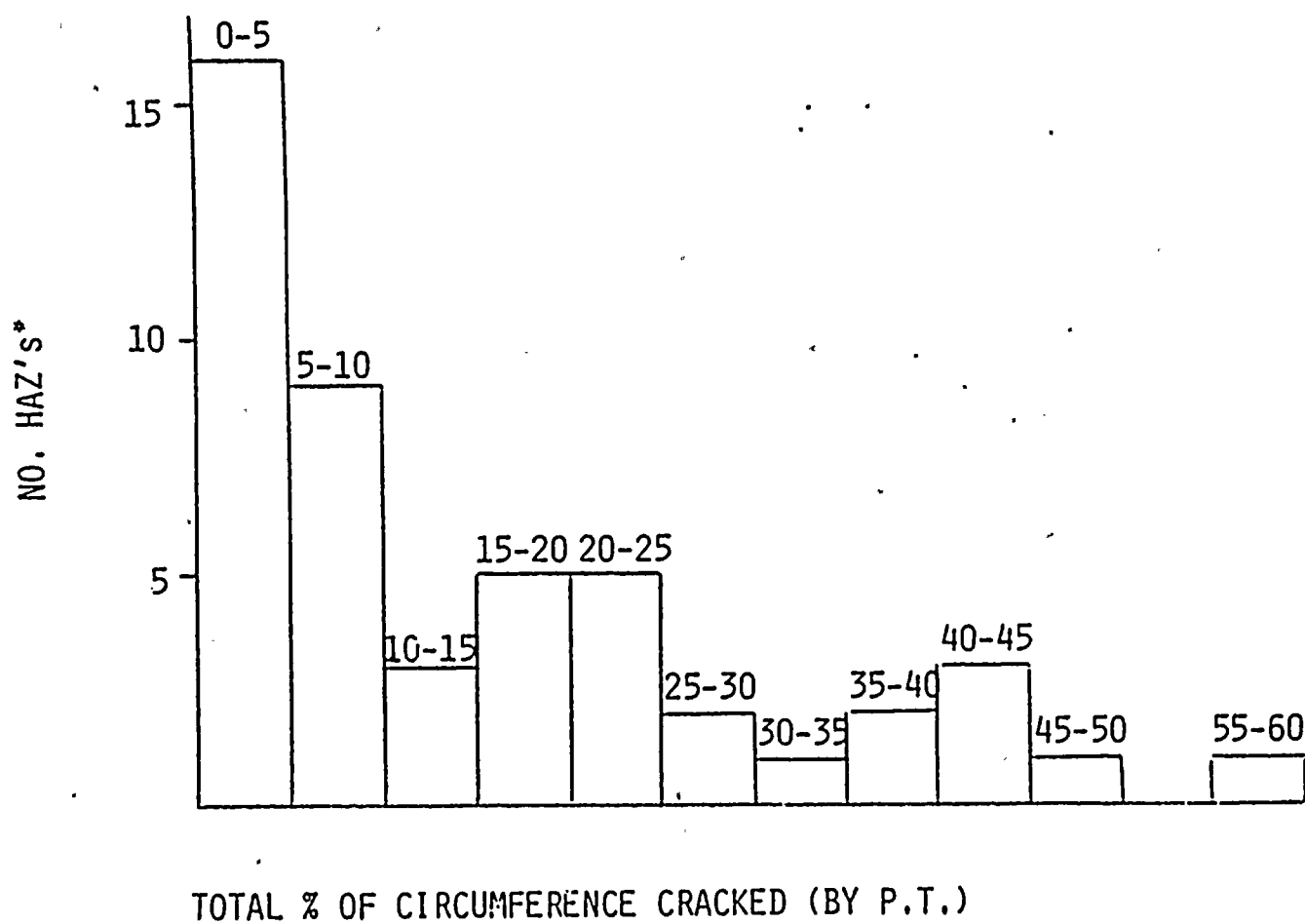


FIGURE 11. (Continued). Dye Penetrant inspection results, Loop 15 welds. (Refer to Figure 5 for weld locations.)



*ONLY INCLUDES HAZ's W/P.T. INDICATIONS

Figure 12. Extent of Cracking/Frequency Histogram.

SECTION III

LABORATORY CHARACTERIZATION OF CRACKS

INTRODUCTION

To characterize the extent and morphology of cracking, boat samples were removed from four weld areas for laboratory examination, and one quarter circumference of pipe to elbow weld (loop 15, shop weld 12) was shipped to GE Vallecitos Nuclear Center for a comprehensive evaluation and failure analysis. An additional boat sample, containing a cracked region of a safe-end was cut out and shipped to Battelle Columbus Laboratories for detailed examination. The examinations included visual examination, metallography, and scanning electron microscopy, with the objective of characterizing the mechanism of cracking.

OBSERVATIONS AND CONCLUSIONS

1. The mechanism of the through-wall cracking, which caused the safe-end to leak, is IGSCC of furnace sensitized Type 316 stainless steel. The mechanism of the pipe heat affected zone cracking was IGSCC of weld sensitized Type 316 stainless steel.
2. Shallow transgranular cracking, incidental to the IGSCC, was found on the O.D. surface of Boat Sample "A" from weld FW-22 of Loop 11 leaking safe-end.
3. The cracks of Boat Sample "B" from the same Loop 11 safe-end were found to contain contaminants. Analysis of the material showed the presence of sulphur and chlorine and a number of other elements.

The origin of contaminants cannot be determined from the examinations performed. It's possible they could have been introduced subsequent to the cracking of the piping. No contaminants were found on the fracture surfaces of Boat Sample "A".

4. All safe-end thru-wall cracking, which resulted in leakage, was observed to be associated with axially (Transverse) oriented cracking.
5. All cracks examined were intergranular, with an inside surface initiation, in the weld heat affected zones of both field and shop welds.
6. Electrochemical potentiokinetic reactivation (EPR) measurements on several areas of pipe and elbow base metal gave readings near zero, verifying the base material is in a solution annealed condition. The weld heat affected zones have low values indicating a narrow sensitized region. This was also verified by metallography.
7. Carbide precipitation was evident (by metallographic examination) at crack initiations.
8. Some cracks propagated into the weld metal to a maximum distance of .050".
9. Some cracks had propagated across the longitudinal previously solution annealed pipe seam welds in the heat affected zone region of the butt weld.

FIELD EXAMINATION

Introduction

In April, 1982 ultrasonic (U.T.) indications were discovered in a 28-inch Type 316 stainless steel elbow, welded in the field to the discharge side of the No. 15 recirculation pump. (Weld FW 46 in Fig. 5 of Section 2.) Cracking was confirmed by subsequent visual and dye penetrant examination of the pipe I.D. In-situ metallography was performed to determine the cause of cracking. Replicas of a visible crack in the HAZ were examined by the General Electric Co. in San José and confirmed IGSCC.

Results and Discussion

The affected elbow is located in the pump discharge portion of the No. 15 recirculation loop and connects the recirculation pump outlet to a vertical run of piping. It is welded directly to the cast stainless steel recirculation pump. The weld was made during field fabrication of the recirculation loop.

Access to the elbow was gained via the recirculation pump, as sketched in Figure 1. Circumferential cracks were visible approximately 0.125 - 0.250 in. from the weld fusion line at 7:00 and 9:00.* A third visible crack, reported to be located at 12:00, was not investigated.

In-situ metallography was performed by a Niagara Mohawk Power Co. employee working with a General Electric Company engineer and consisted of:

1. Polishing the surface to a 600-grit finish.
2. Etching electrolytically with oxalic acid.
3. Reproducing the surface structure with cellulose acetate replicating tape.

The visible crack at 9:00 was chosen for examination.

A composite photograph of the replica is shown in Figure 2. The cracking is oriented horizontally across the top. Grain boundaries are not visible, but the angular, branched appearance indicates that the crack is intergranular. Areas of interest are indicated by the arrows marked A, B, and C. At location A, branches of the main crack appear to have surrounded several grains. At B and C it appears to zig-zag around the grains. Short penetrations into the adjacent grain boundaries are visible at location B. The intergranular crack morphology combined with its location in the presumably weld sensitized HAZ leads to the conclusion that the mechanism of cracking is IGSCC.

Subsequent U.T. examination of other welds in the recirculation systems, resulted in the identification of a large number of indications considered to be cracks. All original recirculation system piping, between safe-ends and pump nozzles, for both suction and discharge sides of all five loops was removed for replacement. As will be discussed in a later section, the original piping is being replaced with a Type 316 Nuclear Grade stainless steel with a much lower susceptibility to intergranular stress corrosion cracking (IGSCC) than the originally used material.

*This reference system is defined by looking into the pump outlet (against the flow direction) with 12:00 at the top.

Twelve sections of welded piping which had been cut from the recirculation system and taken out of the drywell were examined visually and by liquid penetrant. Each section consisted of a 10-15 inch ring, containing a circumferential weld, which had been removed from one end of either: 1) the 90° pump suction elbow (reactor vessel outlet) which connects the outlet safe-end to the downcomer or, 2) the 76° pump discharge elbow which connects the riser to a spool piece. (The spool piece is welded to the inlet safe-end.) The position of the elbows is shown in Fig. 1, Section 2, a sketch of recirc. loop No. 11. In loop 15 the positions of the shop and field welds of the 76° discharge elbow are the reverse of loop 11.

The results of visual and liquid penetrant examination are given in Table 1. A total of 20 heat affected zones (HAZ's), not including safe-ends, were examined. Visible cracks or crack-like PT indications were found in 11. Three HAZ's exhibited cracking over more than 30% of the circumference. Figure 3 photographs show circumferential PT indications on the elbow side of the loop 13 discharge elbow to riser weld. Approximately 30% of the circumference is cracked. Figure 4 shows indications on both sides of the elbow to riser weld from the pump discharge side of loop 12. Note the short axial indications in the HAZ on the pipe side of the weld.

The most extensive PT indications were found in the loop 13 suction elbow-to-downcomer weld (Figures 5 and 6). Approximately 50% of the elbow HAZ and 40% of the pipe HAZ were found to contain circumferential cracks. Several cracks were visible without liquid penetrant. Boat samples were removed near the 9:00* and 10:00 locations using a hand held cutting tool. The excavations that resulted were 1/4-3/8 in. in depth. Figures 7 and 8 show circumferential PT indications running continuously through the excavations, indicating that the cracks are at least 1/4 in. deep. A larger grinding tool equipped with a strawberry burr was used to chase the cracks further into the pipe wall. It was found (Figure 9) that the crack near 10:00 on the elbow side of the weld penetrated nearly 0.50 in. into the pipe wall. Note that the crack turned to follow the weld fusion line after propagating radially for about .30-.35 in.

*The Longitudinal weld seams of the elbow were designated as 6:00 and 12:00.

Ultrasonic crack depth measurements were made between the two excavations by a GE Test Engineer. The transducer was placed on the end of the pipe about 0.50 in. from the weld root. This technique was made possible because the rough plasma-arc cut surface had been machined flat. Measurements at six locations from 9:00 to 10:00 ranged from 0.20 in. to 0.45 in. (see Figure 10). Good agreement between U.T. and grinding was obtained at the 10:00 location where the crack depth measured 0.45 in. by U.T. and 0.50 in. by grinding. The deepest crack measured by U.T. was 0.55 in., in the loop 15 suction elbow/pipe ring, on the elbow side. The corresponding PT indication was light compared to an adjacent indication which measured 0.30 in. in depth by U.T.

Many of the twelve examined weldments were found to contain fairly dark circumferential PT indications which hugged the edge of the weld root. An example is shown in Figure 11. Boat samples removed from two such locations revealed that the indications were caused by a superficial lack of fusion between the weld root and adjacent base material. In most cases it was not difficult to distinguish indications of this type from crack-like indications.

To determine whether the base material of the recirc. piping was sensitized due to the possibility of an inadequate solution heat treatment, EPR measurements were conducted on the loop 13 suction elbow. Measurements on both the inner and outer surfaces, well away from all circumferential and longitudinal welds, resulted in Pa values less than 10^{-3}c/cm^2 , indicating that the base material is in the solution annealed condition. This finding is consistent with documents stating that elbows fabricated by the Crane Company were heated to $2,000^\circ\text{F} \pm 25^\circ\text{F}$ for one hour per inch of thickness and water quenched.

METALLOGRAPHIC EXAMINATIONS

Boat samples and piping segments containing cracks were removed from the recirculation piping system and sent to laboratories for metallographic evaluation and failure analyses. Listed in Table 2 is a description of the samples removed for examination and an identification of the investigating laboratory.

The results of the metallographic examinations performed on the boat samples are described in detail in the following sections. Table 3 is a summary of metallographic examinations.

A. BOAT SAMPLE "A"

Boat sample "A" is one of two samples removed from the outside surface of the leaking regions of the safe-end of recirculation loop safe-end weld No. FW-22 of the Nine Mile Point recirculation loop Number 11. Each sample contained the outer surface portion of the visible cracks at the 12:00 location. The orientation of each crack was nearly transverse (axial). Figure 12 is a schematic showing the location of the safe-end weld samples examined at Battelle Columbus Laboratories (BCL) and at General Electric Companies Vallecitos Nuclear Center (GE-VNC). Sample "A" included part of the safe-end-to-pipe weld.

The loop 11 recirculation loop discharge safe-end is one of two 28-inch safe ends found to have had through wall leakage. The safe-ends were fabricated from Type 316 stainless steel (0.054%C) and were used in a furnace sensitized condition due to the RPV post weld heat treatment.

Visual Examination

A low magnification photograph of sample "A" is shown in Figure 13. The thick (left) end was cut partially into the safe-end-to-pipe weld. The thin end points toward the reactor vessel. The visible crack had not quite propagated through-wall in the plane of the cut surface, but there was not much material holding the specimen together, making it easy to break apart.

Metallography

The sample was broken into two pieces, identified as A-1 and A-2. Section A-1, the thick end, was mounted on its O.D. surface to enable examination of the surface cracking. Section A-2 was mounted on its side to reveal surface and sub-surface cracking. Low magnification photographs of sections A-1 and A-2 after

BOAT SAMPLE "A" (Continued)

polishing and etching are shown in Figures 14 and 15 respectively. The safe-end to pipe weld can be seen in Figure 14. Figure 15 shows another weld approximately 0.25 in. away, which is probably the result of a repair weld or weld metal build up during original fabrication.

A high magnification photograph of the fracture end of section A-2 is shown in Figure 16. This is the lower left portion of Figure 20, 0.06-0.08 in. below the O.D. Surface. The primary fracture and the secondary cracks behind it are intergranular, and the clearly visible grain boundaries show that the microstructure is sensitized. It is apparent that the intergranular stress corrosion (IGSCC) cracking initiated on the I.D. surface, and Figures 14 and 15 provide corroborating evidence. This cracking occurred as a result of the combination of sensitization, high temperature oxygenated water, and a tensile stress (residual and applied).

The upper left region of Figure 15 is shown at high magnification in Figure 22. The top of Figure 17 is the safe-end O.D. surface. Two transgranular cracks can be seen propagating in from the O.D. The one on the left, marked A, is 0.005 in. deep in the plane of polish. These cracks are incidental to the leaking cracks and may have resulted from a chloride containing substance being in contact with the outside of the safe-end. It is possible that they initiated when hot reactor water began leaking from the through-wall cracks and interacted with the piping insulation.

Figure 18 reveals that the tip of the crack in section A-1 penetrates approximately 0.006 in. into the safe-end to pipe weld. IGSCC will occasionally penetrate a short distance into a weld before crack arrest occurs because dilution of the outermost portion of the weld results in a local region low in delta ferrite. This phenomenon occurs during welding due to the mixing at the weld-base metal interface. Hence depletion of the outermost weld metal of ferrite forming elements can occur.

Scanning Electron Microscopy (SEM)

SEM was used to examine the O.D. surface, and the fracture surface after the specimen was broken open. A composite 50X photograph of the axially oriented crack on the O.D. surface is shown in Figure 19. The crack length is about 0.22 in., but this figure is an approximation because the crack becomes very thin, making the tip difficult to locate.

BOAT SAMPLE "A" (Continued)

A typical area of the fracture surface is shown in Figure 30. The fracture is intergranular and covered by scaly oxide deposits. Energy dispersive X-ray analysis shows that the scale deposit is Cr rich, as would be expected of the oxide layer. No contaminants were found on the fracture surface.

B. BOAT SAMPLE "B"

Boat sample "B" is the second of two samples removed from the outside of the leaking regions of the safe-end of recirculation loop safe-end weld No. FW-22 of recirculation loop Number 11. This sample was examined at the Battelle Columbus Laboratories (BCL).

Visual Examination

The boat sample shipped to Battelle was a small wedge shaped piece approximately 1 inch long and 1/4 inch thick. Figure 12 shows the schematic sketch of the safe-end and location of sample "B" which was examined at Battelle Columbus Laboratories. The sample was visually examined with a stereomicroscope. One crack approximately 1/2" long was observed on the outer surface. In addition, crusty crystalline-like deposits were observed on the outer surface, along with some rust colored stains. Figure 21 shows the appearance of the specimen in the as-received condition.

Scanning Electron Microscopy

The as-received sample was examined with the scanning electron microscope. The primary purpose of this examination was to analyze the deposits on the surface using the energy dispersive X-ray analyzer. Figures 22 and 23 show the appearance of deposits observed on the outer surface of the piping along with the X-ray analysis obtained on the deposits. It can be seen that the deposits are very high in silicon along with iron and chromium and nickel. In addition, trace concentrations of sulphur, phosphorous and chlorine were observed. Semiquantitative analysis obtained on one area of the deposit is shown below:

Si	37.2%
P	0.625
S	0.55
Cl	0.47
Ca	0.064
Cr	35.57
Fe	23.38
Ni	2.04
Cu	0.4

BOAT SAMPLE "B" (Continued)

Metallography

Subsequent to scanning electron microscopy examination, a small piece was cut from the end containing the crack. This piece was mounted in a metallographic mount and prepared for examination of the transverse cross section. The examination revealed one long thru-wall crack with significant branching. Figure 24 shows the appearance of the crack in the etched condition. It can be seen that the crack is entirely intergranular.

Analysis of Material Trapped Within Crack

Examination of the metallographic specimen in the as-polished condition showed the presence of a significant amount of corrosion products or contaminants in the crack. In order to determine the nature of the material, the specimen was examined with an energy dispersive X-ray analyzer associated with the scanning electron-microscope. A number of areas in the crack were examined. In all cases varying amounts of chlorine and sulphur were observed along with a number of other elements. Figures 25, 26, 27, and 28 show the appearance of the contaminant and the results of the X-ray analyses obtained on the material. Also shown are the semiquantitative elemental analyses obtained. These two areas shown were found to contain the highest amount of chlorine and sulphur. The origin of the material cannot be determined from the examinations performed. It is possible they could have been introduced subsequent to the cracking of the piping.

SEM Examination of the Fracture Surface

The fracture surface of a portion of the specimen was examined with the SEM, after the fracture surfaces had been separated by a saw cutting through the unbroken ligament. Figure 29 shows a typical area on the fracture surface. The intergranular fracture morphology is clearly apparent. This fracture morphology is typical of that observed in the intergranular stress corrosion cracking mode in boiling water reactor stainless steel pipe.

C. SAMPLE 3 - PIPING SECTIONS - SUCTION

SAFE-END AND ELBOW WELDS

Sample 3 are piping sections containing a part of the suction safe-end to elbow weld FW-17 of loop 15 and a part elbow-to-pipe weld, SW-12, just downstream from FW-17. As described earlier, leaking was found at the 8:00 o'clock position on the safe-end, and numerous U.T. and P.T. indications were observed about the circumference of the weld on both the safe-end, and the pipe sides. U.T. and P.T. indications were found on the pipe-to-elbow weld SW-12.

The portions of the loop 15 suction safe-end-to elbow weld were removed and shipped to Battelle Columbus Laboratories for examination. The section was located near 7:00 o'clock, (Figure 30). The second sample, also sent to Battelle for examination was removed from the 12:00 o'clock position of weld No. SW-12 of loop 15 (one weld down-stream from FW-17). The piping section is shown in Figure 36.

Several metallographic samples were removed from the two piping sections for optical metallographic examination. The cutting diagram of the portion from the 7:00 o'clock position is given in Figure 30. The arrows indicate the surfaces that were examined. Figure 31 is the cutting diagram for the portion of the pipe-to-elbow weld removed from the 12:00 o'clock position.

Figure 32 is a 4X view of sample "A-4" showing the crack in the safe-end. This etched view was prepared by grinding through the pipe wall thickness beginning on the pipe I.D. surface. This is the inner surface view of the axially oriented through wall leaking crack in the safe-end. The O.D surface view of the same crack can be seen in Figure 30, on that sample marked "A-4".

Figure 33 is a cross-section etched view of the same sample of Figure 32. No cracks were observed in this sample of the safe-end-to-elbow weld.

Figure 34 is a sectional view of sample "B-1", removed from the portion of the loop 15 suction elbow-to-pipe weld SW-12. A short crack can be seen near the weld fusion line on the pipe side of the weld. Sample "B-2", shown in Figure 35, is a

sample removed from a location just adjacent to sample "B-1" of Figure 31. This polished and etched view reveals a crack near the fusion line on the elbow side of the weld.

Sample "B-3", shown polished and etched in a 4X view in Figure 36 is a cross sectional view of the elbow seam weld. No evidence of cracking was found in this view.

D. BOAT SAMPLES "C", "D", "E", AND "F"

Boat Sample "C"

This section was cut across the weld SW-6 between an elbow and pipe on loop 13, (see Fig. 3 of Section 2).

Figure 37 after penetrant examination. The large indication at the left is the elbow side, and a smaller indication on the right is in the pipe side. Details of the crack on the elbow side are shown in Figures 38 and 39. Figure 38 shows the crack location with respect to the weld. The cracking is completely intergranular, and carbides can be seen outlining the grain boundaries, indicative of light sensitization. Figure 39 shows enlarged detail of the center and bottom of the section. The carbides at the grain boundaries are more evident at higher magnification. This crack went through the entire section, about 200". Figure 40 shows the crack on the pipe side. It is ~.120" deep, and stops immediately at the circumferential weld. The crack is in the longitudinal seam weld of the rolled and welded pipe. Since this weld has been solution annealed (prior to welding), the ferrite content is extremely low and the material behaves similarly to wrought material. Figure 41 shows the end of the crack, and it has arrested almost on contact with the higher ferrite circumferential weld.

Boat Sample "D"

This section was cut from the same weld as sample "C", but at a different circumferential location. The as-received sample is shown in Figure 42, with a large crack visible on the elbow side. During handling, this section separated. Figure 43 shows a portion of the fracture, and a second adjacent crack. Figures 44 and 45 show more detailed views at the beginning and end of the crack. Grain boundary carbide precipitates are readily visible. The grain size of the elbow material is larger than normally encountered. The crack mode is intergranular. The section which separated during handling was examined by scanning electron microscopy (SEM). The entire fracture surface was intergranular. The presence of heavy oxide obliterated any other fracture features which may have been present.

Boat Sample "E"

This section was removed from loop 12, shop weld SW-4, shown in the sketch of Section 2. A penetrant indication was present on the elbow side of the weld, as shown in Figure 46. The indication was not a crack, but a very small lack of fusion area which acted as a crevice and retained the penetrant. Figure 47 illustrates this condition.

Boat Sample "F"

This sample was removed from loop 12, field weld FW-5, between the safe-end and elbow, on the suction side of the pump. An indication was present on the elbow side, as shown in Figure 48. This indication proved to be slight lack of fusion between two weld passes as shown in Figure 49. No propagation had occurred.

Section of Elbow to Pipe Weld

A 90° section of elbow to pipe weld from shop weld SW-12, loop 15, was examined in great detail. (See Figure 5 of Section 2.) The section had been cut through the edge of the weld on the pipe side, and again about 10" into the elbow. Looking at the inside surface, the entire section was 22" long (circumferentially) and 10" axially. It consisted of 5/8" of pipe, the weld, and ~9 1/2" of elbow material. The inside had been decontaminated electrolytically, so the surface was clean and bright except for large areas where slag from the plasma cutting operation had adhered. To simplify handling, a circumferential cut was made about 1" on the elbow side of the weld, resulting in a ring section 22" long and 1 3/4" wide, containing 5/8" of pipe, plus weld, and 1 1/8" of elbow material. This section was cleaned of slag, and examined by dye penetrant. Masking tape marked at 1" intervals was fastened to the inside to map indication locations. Seven indications, varying from 5/16" to 1 1/4" in length, were found on the pipe side, for a total length of 5 1/4" or 24% of the total circumference. One indication 7/8" long was present on the elbow side, 4% of total length. Typical indications are shown in Figures 50 and 51. Assuming that the center of each indication should be the deepest part of the crack, sections from the center of each indication were polished, and the crack depth measured by microscope. The cracks on the pipe side ranged in depth from .100" to .275". The crack on the elbow side was .137". These measurements are in good agreement with the depths estimated previously by ultrasonic examination of .1 to .2".

Metallographic sections were prepared from one crack on each side of the weld. The entire crack on the elbow side is shown at low magnification in Figure 52. Crack depth at this plane was .110". It was intergranular, and penetrated into the weld about .015". More detailed views of the beginning and end are shown in Figure 53. Significant grain boundary carbide precipitates are evident in the vicinity of the crack. The section was repolished and etched with Kahlings reagent to emphasize ferrite in the weld. Figure 54 shows the crack arresting when it reaches an area of the weld containing significant ferrite. Figure 55 shows the pipe side of this section. No cracking is present, although grains are outlined by carbides, which is caused by weld sensitization.

The crack on the pipe side is shown in Figure 56. The crack is intergranular, and has propagated into the weld ~ 0.050 ". The beginning and end of the crack are shown in Figures 57 and 58. There were very few carbide precipitates at this location. Most of the propagation into the weld has been in a low ferrite zone. Because of the apparent lack of visible carbides at this section, further work was done using SEM and also dark field illumination. Figure 59 shows the pipe heat affected zone at 800x by SEM. Figure 60 shows a similar area at 800x by dark field illumination. Almost continuous carbides are present in both photos.

COMPOSITION

Chemistry & Structure

Since the heat numbers are unknown, chemical analysis of the elbow and pipe side of loop 15 shop weld 32-SW-12-W was performed and the results are given in Table 4. The compositions including carbon contents of both the elbow and pipe materials (.065 and .049%, respectively) are within the normal range for regular grade Type 316 stainless steel.

SENSITIZATION MEASUREMENTS

A. ASTM A-262-Practice A

In order to determine the degree of sensitization in the safe-end material, boat sample "B" was repolished and subjected to the ASTM A 262 Practice A Sensitization test. Figures 61 and 62 show the structure observed on the specimen. The evaluation of the etched structure revealed that the sample was primarily a dual structure. Closer examination revealed that several grains were completely surrounded by ditches. Hence, according to Practice A the sample has to be evaluated as having a ditch (sensitized) structure.

B. Electrochemical Potentiokinetic Reactivation (EPR)

EPR measurements, a method for determining the degree of carbide precipitation in stainless steels, were made on pipe and elbow base metal and heat affected zones. All base metal measurements resulted in readings of ~zero, indicating a lack of sensitization. The values for the weld HAZs were low, indicating a narrow sensitized region existed. The low EPR values compare with the metallographic examination, where carbides were evident only in a narrow region of the weld heat affected zones. Although most experience with EPR has been on Type 304 stainless, with some procedural changes, the technique is also applicable for use with Type 316 stainless steel. The EPR values of welded Type 316 S/S are lower than for an equivalent carbon content welded Type 304 S/S (see Section X.). The EPR tests verify that the base material is in the solution annealed condition.

HARDNESS

A hardness survey was made on the weld, SW-12, pipe and elbow weld removed from loop 15, with the following results:

<u>Location</u>	<u>Hardness R_B</u>
Weld	90-92
Fusion line, pipe side	90-92
Fusion line, elbow side	88-91
Pipe, base metal	85-88
Elbow, base metal	84-88

The hardness appears normal.

FERRITE SURVEY

Measurements by Ferrite Scope were made on various portions of a weld section (SW-12 of loop 15).

<u>Location</u>	<u>Ferrite %</u>
Main weld, center	10.5-11.5
Consumable insert	1
Fusion line	3-6

These numbers appear reasonable except for the consumable insert (root). Since none of the cracks appear to have involved the root pass, the low ferrite has not been associated with the cracking problem.

TABLE 1

Results of Visual and Liquid Penetrant ExaminationSuction

<u>Loop</u>	<u>Weld</u>	<u>Results</u>
11	Elbow/Safe-End FW-1	PT indications attributed to lack of fusion at weld root.
11	Elbow/Pipe SW-1	PT indications attributed to lack of fusion at weld root.
12	Elbow/Safe-End FW-5	Superficial lack of fusion at weld root verified by boat sample. Elbow carbon content=0.045%
12	Elbow/Pipe SW-4	Axial PT indication in elbow HAZ, superficial lack of fusion at weld root verified by boat sample.
13	Elbow/Pipe SW-6	Extensive cracking in both HAZ's: Approx. 50% of circumference in elbow and 40% in pipe. Max. measured crack depth=0.5 in., by grinding. Base material not sensitized by EPR.
15	Elbow/Safe-End FW-17	PT indications in safe-end only.
15	Elbow/Pipe SW-12	PT indications in both HAZ's. Max. depth by U.T.=0.55 in. Quarter ring sent to Vallecitos revealed cracking over 24% of circumference of pipe and 4% of elbow.

TABLE 1 (Continued)

Discharge

<u>Loop</u>	<u>Weld</u>	<u>Results</u>
11	Elbow/Spool Piece FW-23	Short circumferential PT indication in elbow. Most of pipe HAZ obliterated by plasma-arc cut.
12	Elbow/Riser SW-18	PT indications in both HAZ's. Carbon content of elbow = 0.063%.
13	Elbow/Riser SW-21	Circumferential PT indications over approx. 30% of elbow. Elbow carbon content = 0.063%.
14	Elbow/Riser SW-24	PT indications in both HAZ's. Elbow carbon content - 0.054%.
15	Elbow/Riser FW-43	No PT indications.

TABLE 2

SAMPLE DESCRIPTION

<u>SAMPLE</u>	<u>IDENTIFICATION</u>	<u>LABORATORY</u>
1. Boat Sample "A"	Axially oriented leaking crack - safe-end side of weld FW-22 of loop 11.	General Electric Vallecitos Nuclear Center
2. Boat Sample "B"	Axially oriented leaking crack - safe-end side of weld FW-22 of loop 11.	Battelle Columbus Laboratories
3. Piping Sections	Sections containing axial cracking - suction safe-end to elbow weld FW-17 of loop 15, and SW-12, elbow to pipe weld of loop 15.	Battelle Columbus Laboratories
4. Boat Sample "C"	Cracked - both sides of elbow-to-pipe weld SW-6 of loop 13.	General Electric Vallecitos Nuclear Center
5. Boat Sample "D"	Same as Boat Sample "C".	General Electric Vallecitos Nuclear Center
6. Boat Sample "E"	Penetrant indication - elbow side of SW-4 of loop 12.	General Electric Vallecitos Nuclear Center
7. Boat Sample "F"	Penetrant indication - elbow side of FW-5 of loop 12.	General Electric Vallecitos Nuclear Center
8. Section of Elbow - To-Pipe	90° section of elbow-to-pipe weld from SW-12 of loop 15.	General Electric Vallecitos Nuclear Center

TABLE 3

SUMMARY OF METALLOGRAPHIC EXAMINATIONS

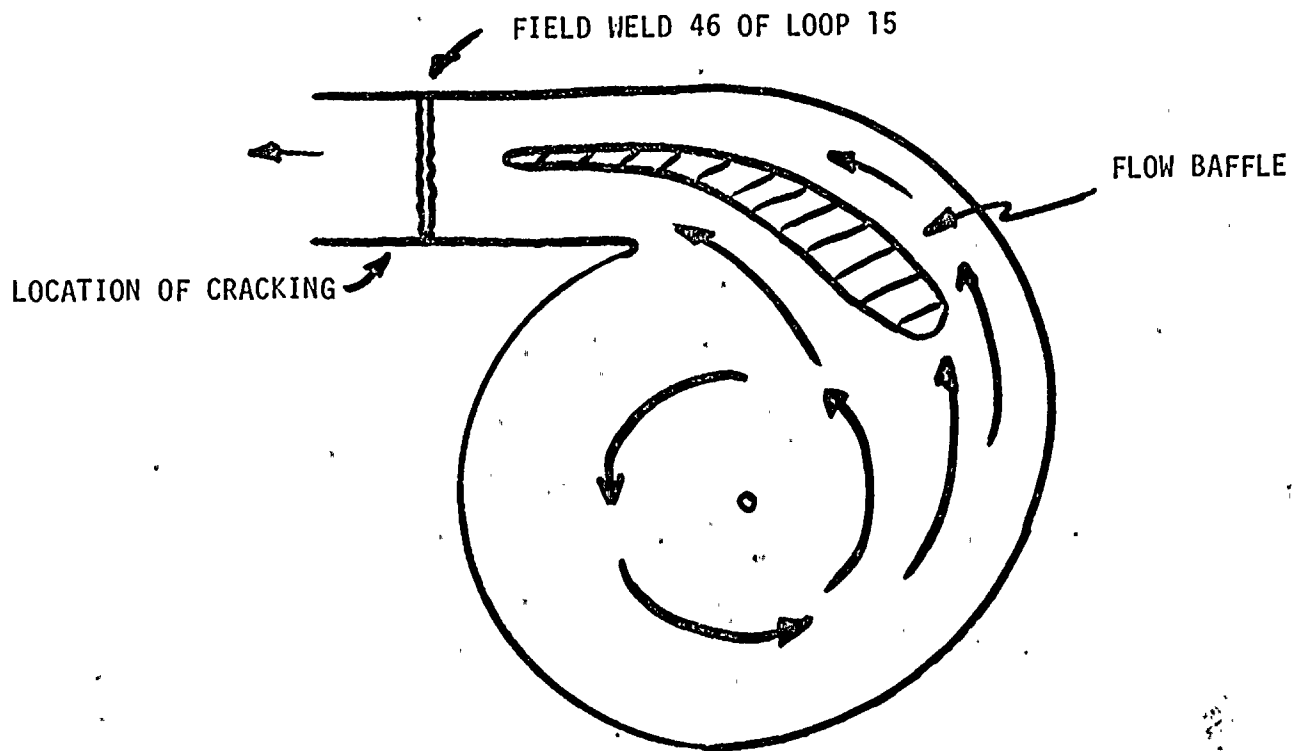
<u>MATERIAL</u>	<u>SAMPLE(S)</u>	<u>RESULTS</u>
Safe-end-field weld HAZ	<ul style="list-style-type: none"> ● Boat sample A & B from FW-22 of loop 11 ● Sample FW-17 of loop 15 	<ul style="list-style-type: none"> ● Thru wall crack is axial on both I.D. & O.D. of safe-end. ● Material sensitized (by PWHT of RPV). ● IGSCC present. ● Trace contaminants of S.P. and Cl found.
Pipe & Elbow Shop Welds	<ul style="list-style-type: none"> ● Sample SW-12 of loop 15 ● Sample SW-6 of loop 13 ● Sample SW-4 of loop 12 	<ul style="list-style-type: none"> ● IGSCC contained in weld HAZ's of elbow material and pipe material. ● Many P.T. indications are due to lack of fusion.
Spool piece - seam weld	<ul style="list-style-type: none"> ● Sample SW-12 of loop 15 ● Sample SW-6 of loop 13 	<ul style="list-style-type: none"> ● Solution annealed condition. ● Cracking by IGSCC <u>only</u> if weld material is in HAZ of circumferential weld.
Pipe & elbow field welds	<ul style="list-style-type: none"> ● Sample FW-5 of loop 12 ● P.T. of FW-23 of loop 11, and FW-31 of loop 12 	<ul style="list-style-type: none"> ● Some P.T. indications due to lack of fusion @ fusion line. ● Other P.T. indications due to IGSCC.*

*Note: This not confirmed by Met. work.

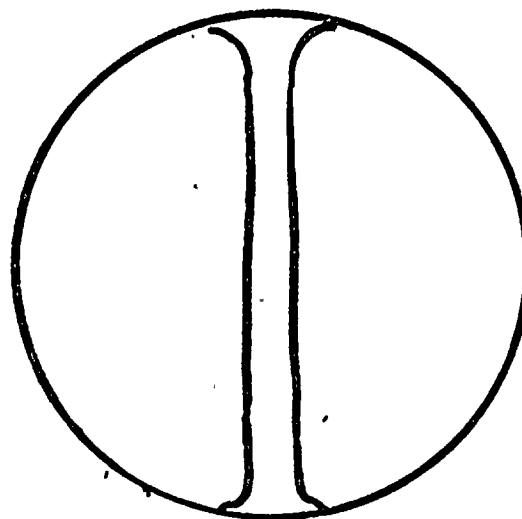
TABLE 4
CHEMICAL ANALYSIS OF LOOP 15 (32-SW-12-W)
SUCTION ELBOW/PIPE MATERIALS

	<u>Pipe</u>	<u>Elbow</u>	<u>Weld</u>
Al	<.005%	.006%	<.005%
B	.003	.001	--
C*	.049	.065	.050
Co	0.14	0.23	--
Cr	17.36	16.64	18.90
Cb	0.05	0.05	0.04
Cu	0.15	0.23	0.08
Mn	1.64	1.68	2.00
Mo	2.70	2.49	2.42
Ni	13.67	13.01	11.04
P	.033	.027	.024
S	.017	.014	.020
Si	0.46	0.65	0.92
Ti	.006	.020	<.005
V	.06	.04	.03

*Determined by LECO carbon analyzer



RECIRCULATION PUMP - TOP VIEW



28"

FLOW BAFFLE - END VIEW

Figure 1. Sketch of Loop 15 recirculation pump showing location of HAZ crack indications.

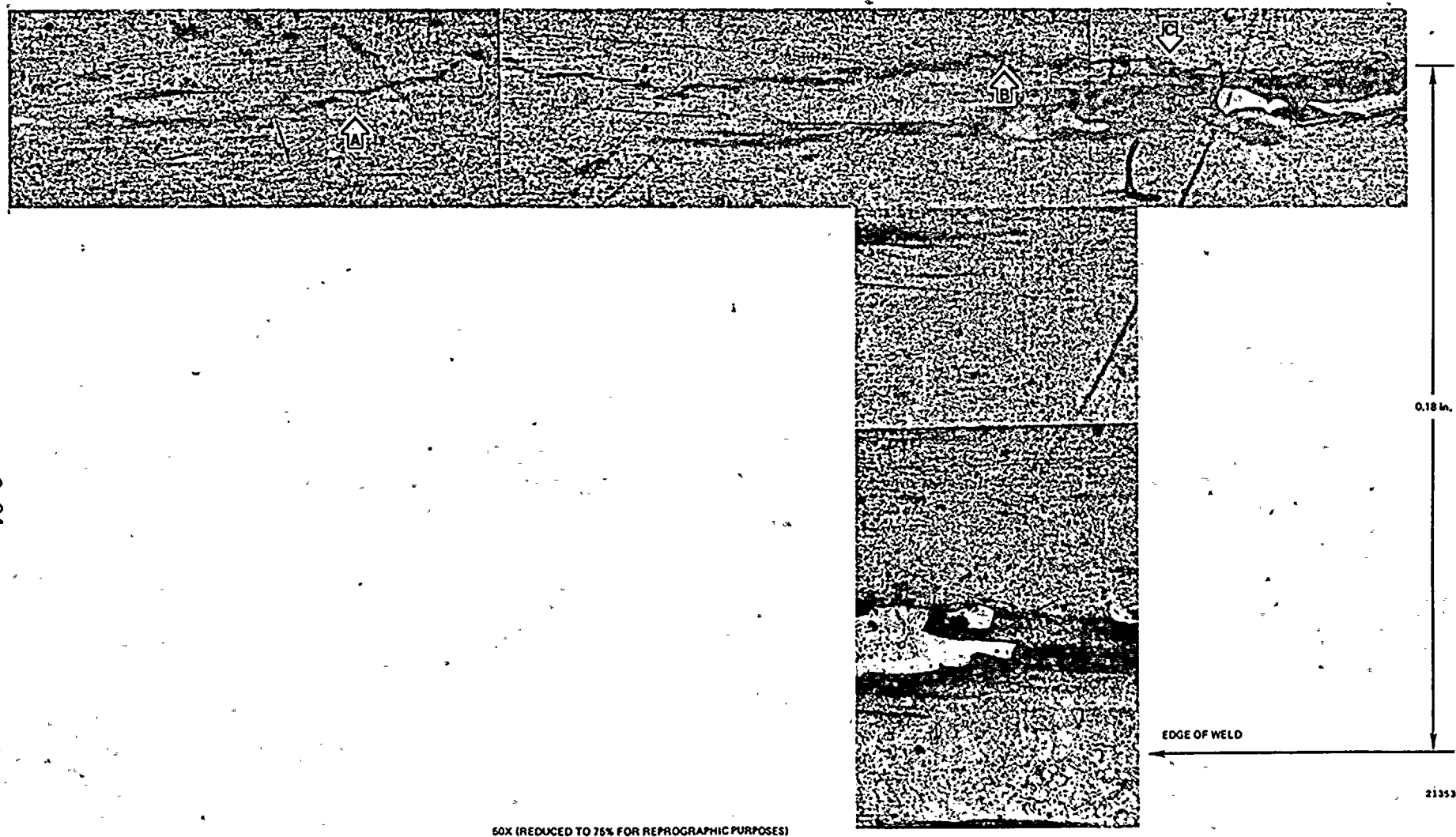


Figure 2. Composite Photograph of Intergranular Crack in Weld Heat Affected Zone (HAZ) at 9:00 Azimuth.

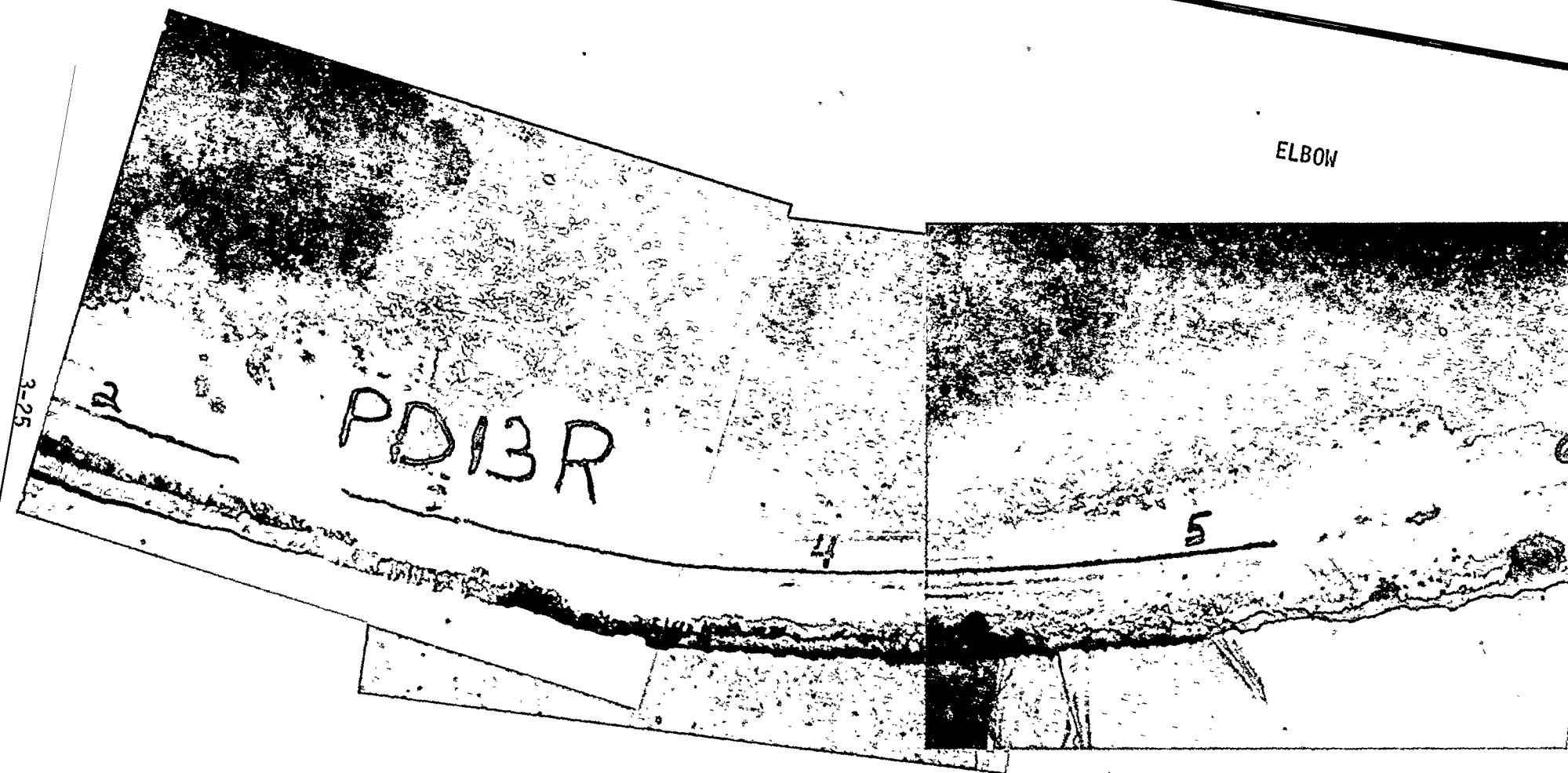


Figure 3. Loop 13 Pump Discharge Weld No. P32-SW-21-W.
Note all indications are on elbow side of weld.

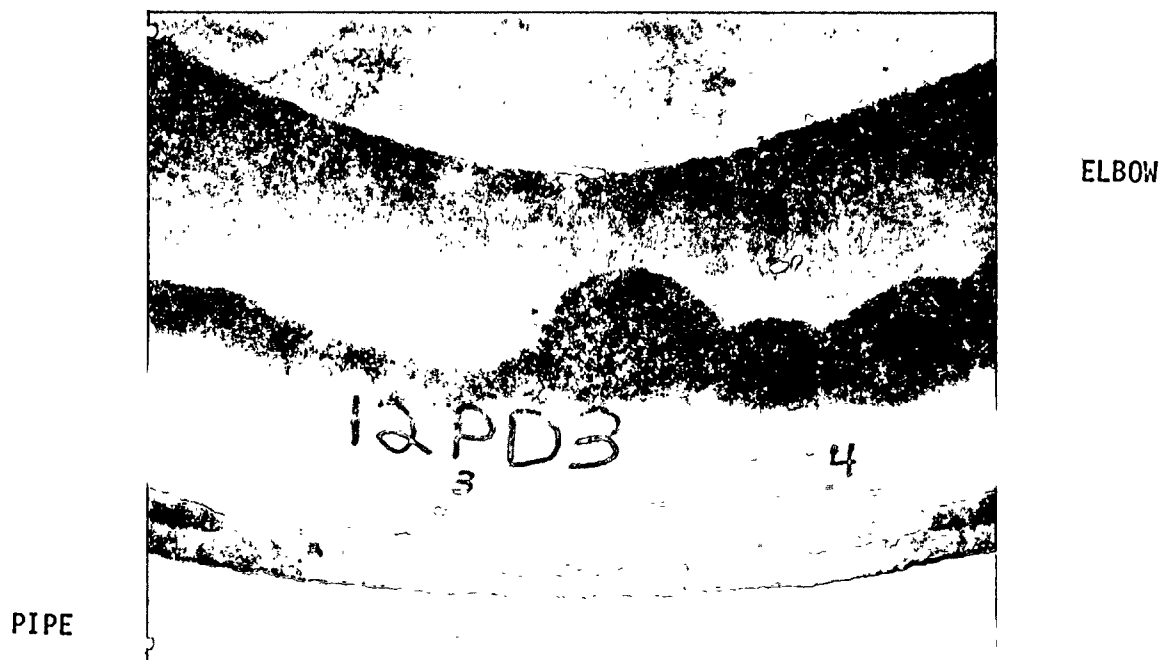


Figure 4. Loop 12 Pump Discharge Weld No. FW-31. Weld HAZ indications on side surface of pipe and elbow.



Figure 5. Photo of Indications in Loop 13 Suction Elbow/Pipe Weld (Weld SW-6).

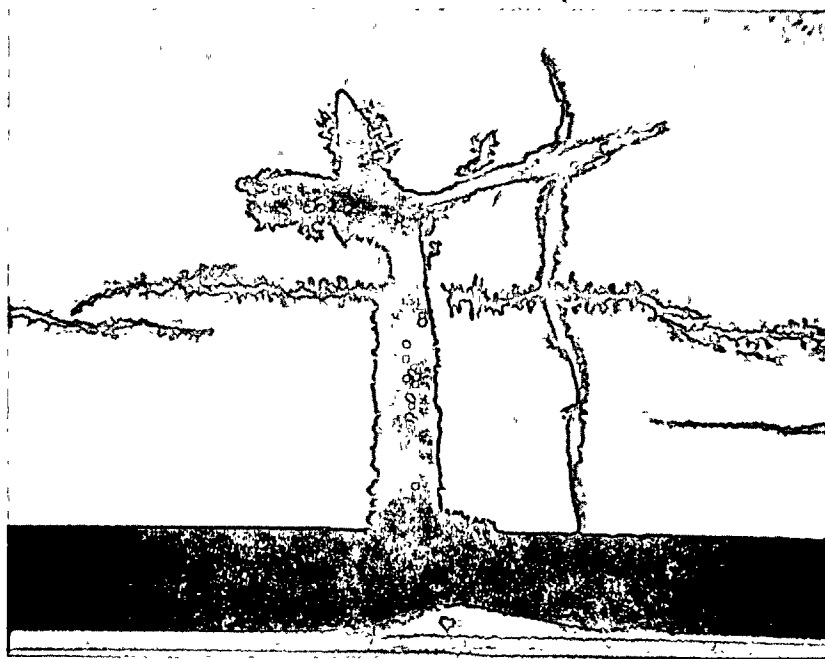


Figure 6. Photo of PT Indications in Loop 13
Suction Elbow/Pipe Weld. (Weld SW-6)



Figure 7. Excavation Remaining After Boat Sample
Removal at 9:00.

WELD



ELBOW

PIPE

Figure 8. Excavation at 10:00.

PIPE



ELBOW

Figure 9. PT Pattern of Crack in Loop 13, Weld SW-6, After Grinding.

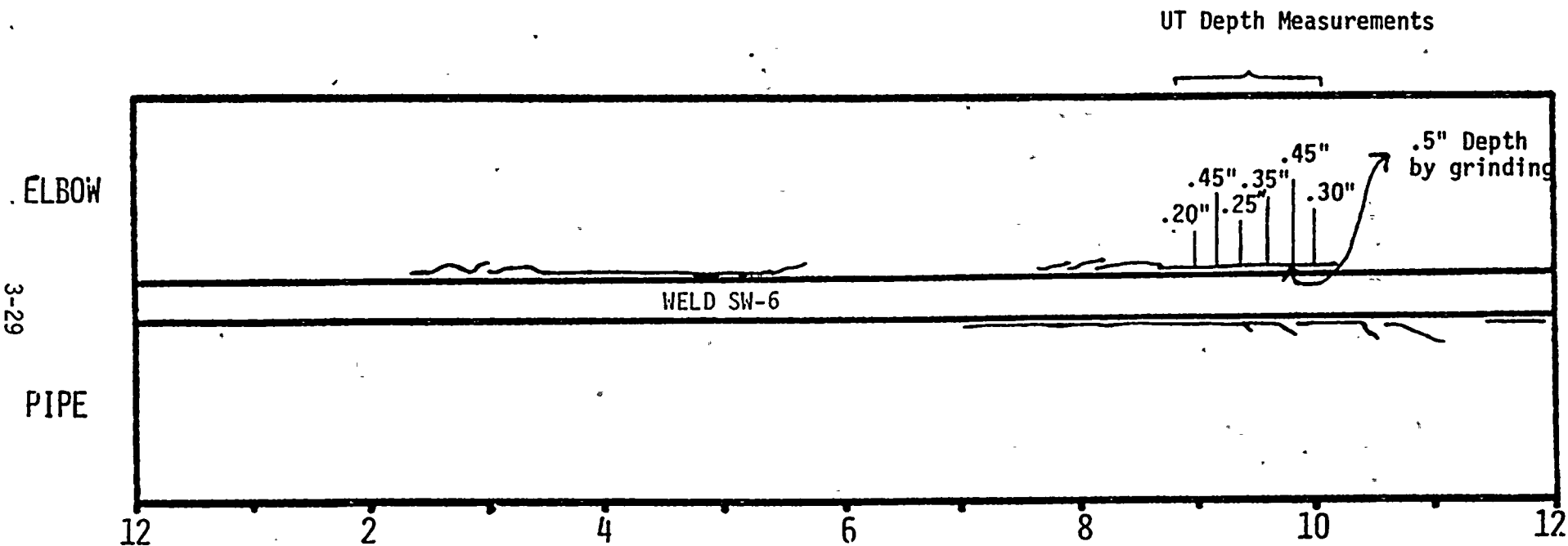


Figure 10. Loop 13 Suction Elbow/Pipe Weld, Showing Results of U.T. Depth Measurements.



ELBOW

SAFE-END

Figure 11. PT indication due to superficial lack of fusion at weld root.

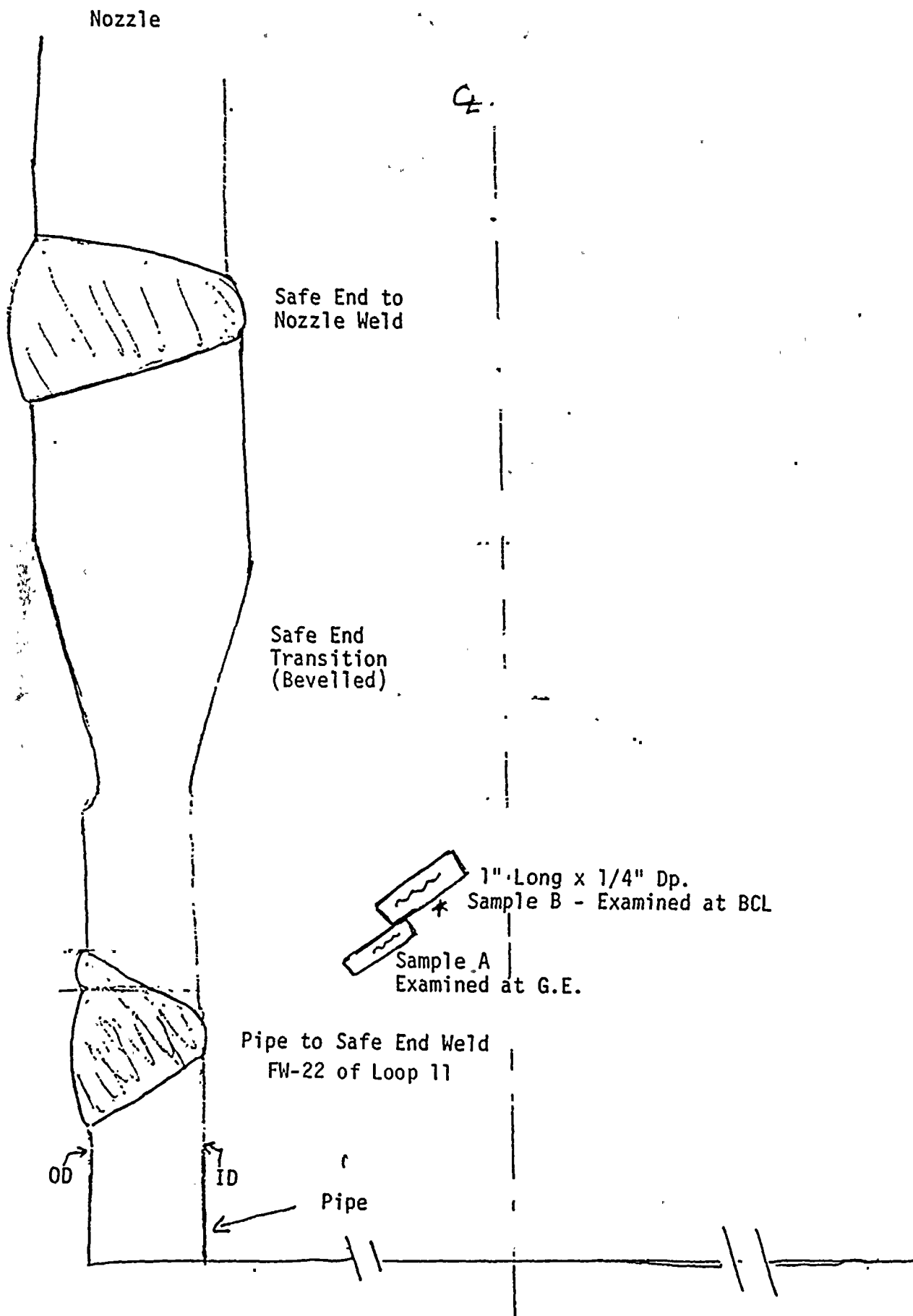


Figure 12. Schematic Showing the Location of the Safe End Weld Samples Examined at BCL (Section View), and GE - VNC.

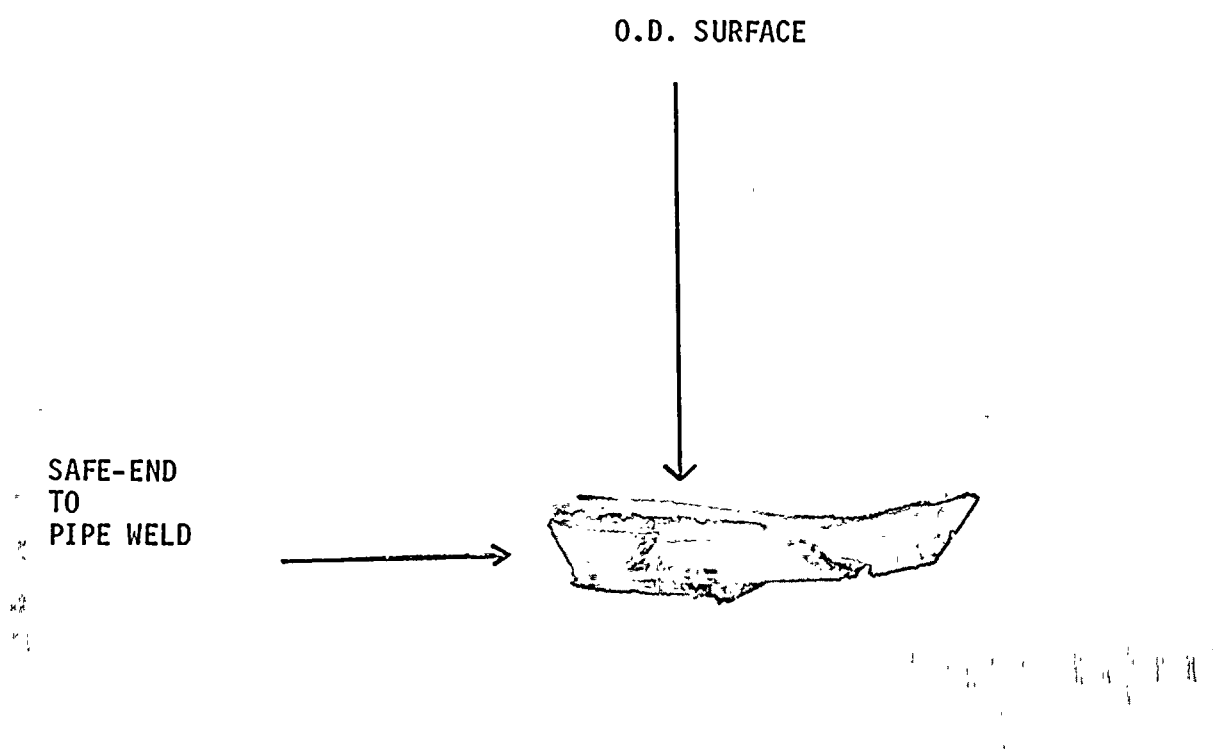


Figure 13. Photograph of Boat Sample showing partially opened crack, 3.5%.

SAFE-END
TO PIPE
WELD

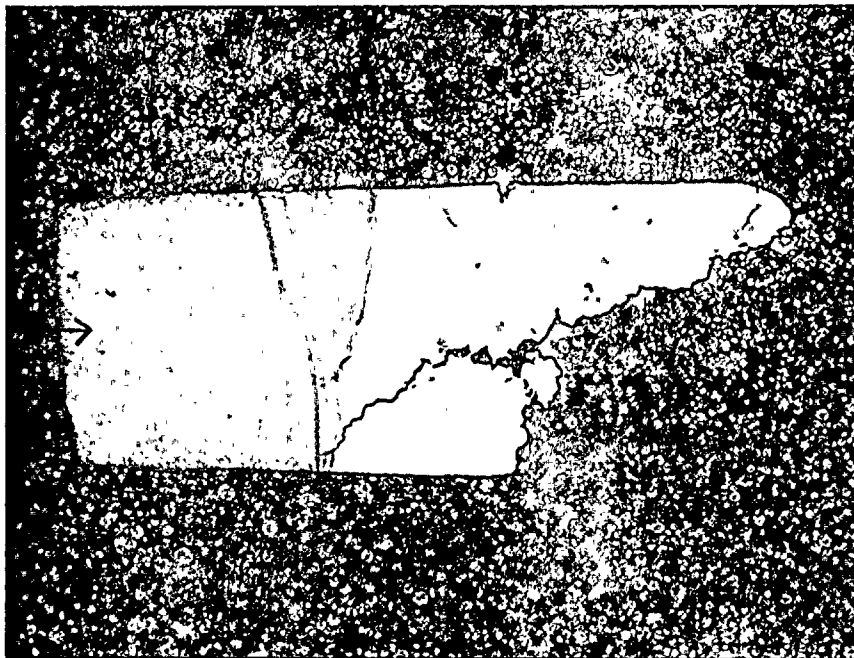
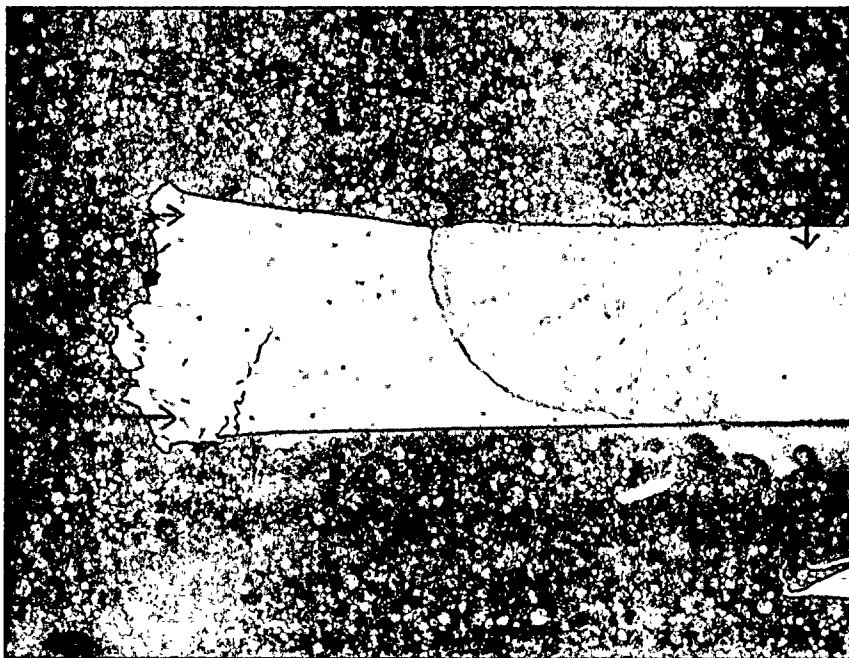


Figure 14. O.D. surface of Section A-1 after breaking open to reveal fracture surface, Oxalic Acid Etch. 15X

Location of
Fig. 17

Location of
Fig. 16



O.D.

Figure 15. Section A-2, Oxalic Acid Etch, 15X.

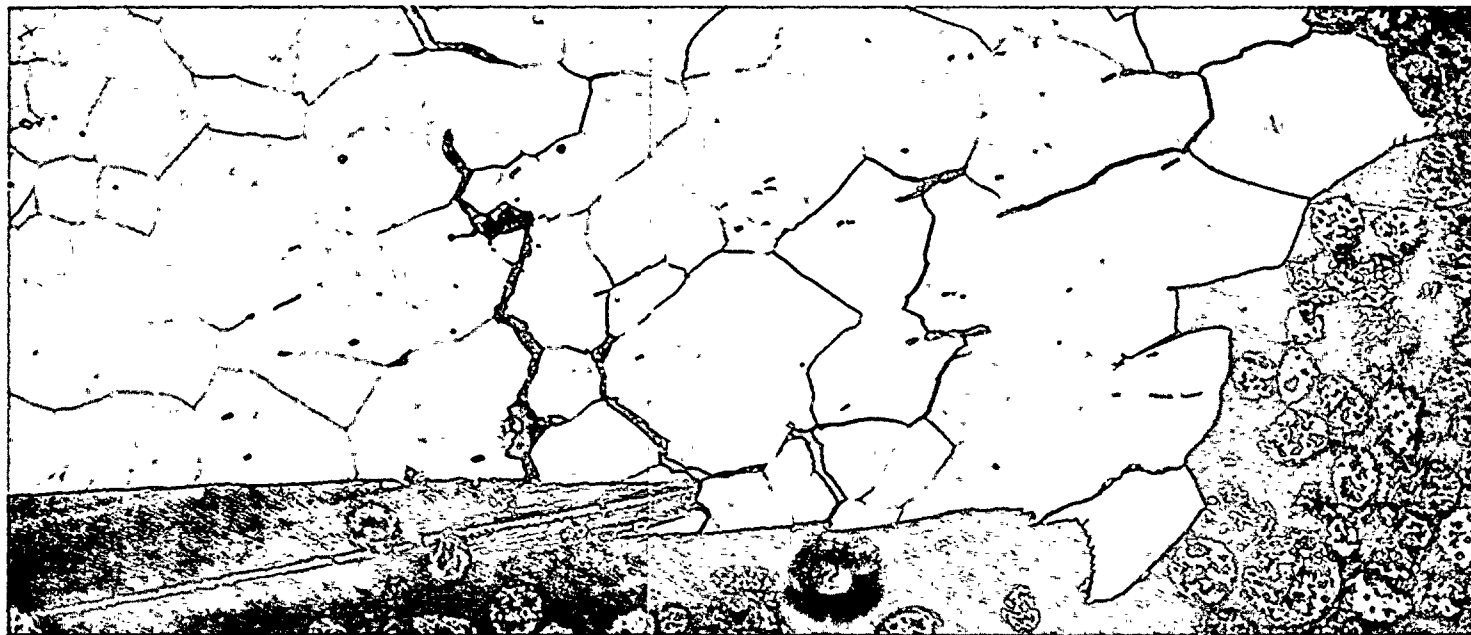


Figure 16. Lower left region of Fig. 15, showing intergranular cracking.
Oxalic Acid Etch, 125X.

O.D. Surface

"A"

"B"



Figure 17. Outside-initiated transgranular cracking on upper left region of Figure 15, Oxalic Acid Etch, 125X.

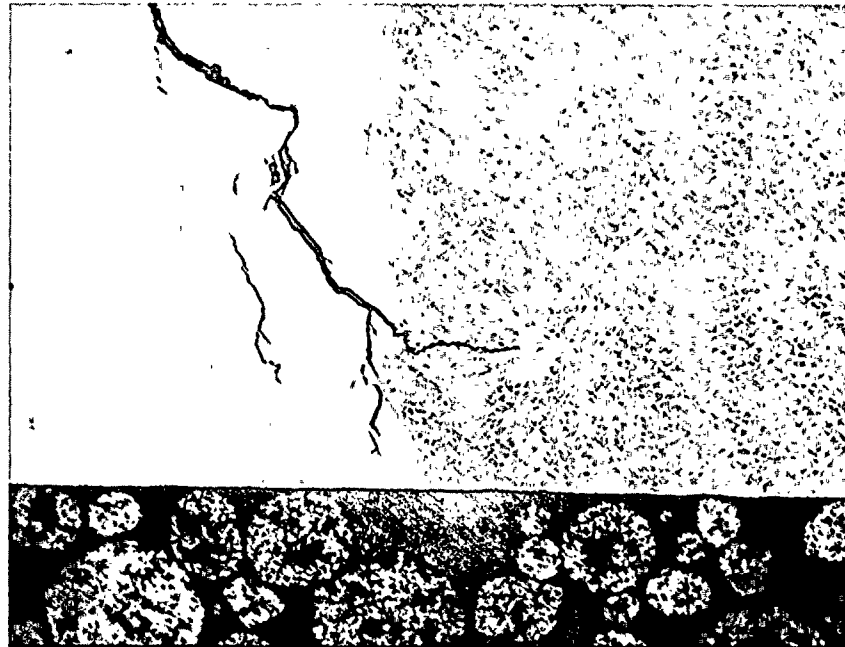


Figure 18. Crack arrest in weld materia, 125X
Oxalic Acid Etch.

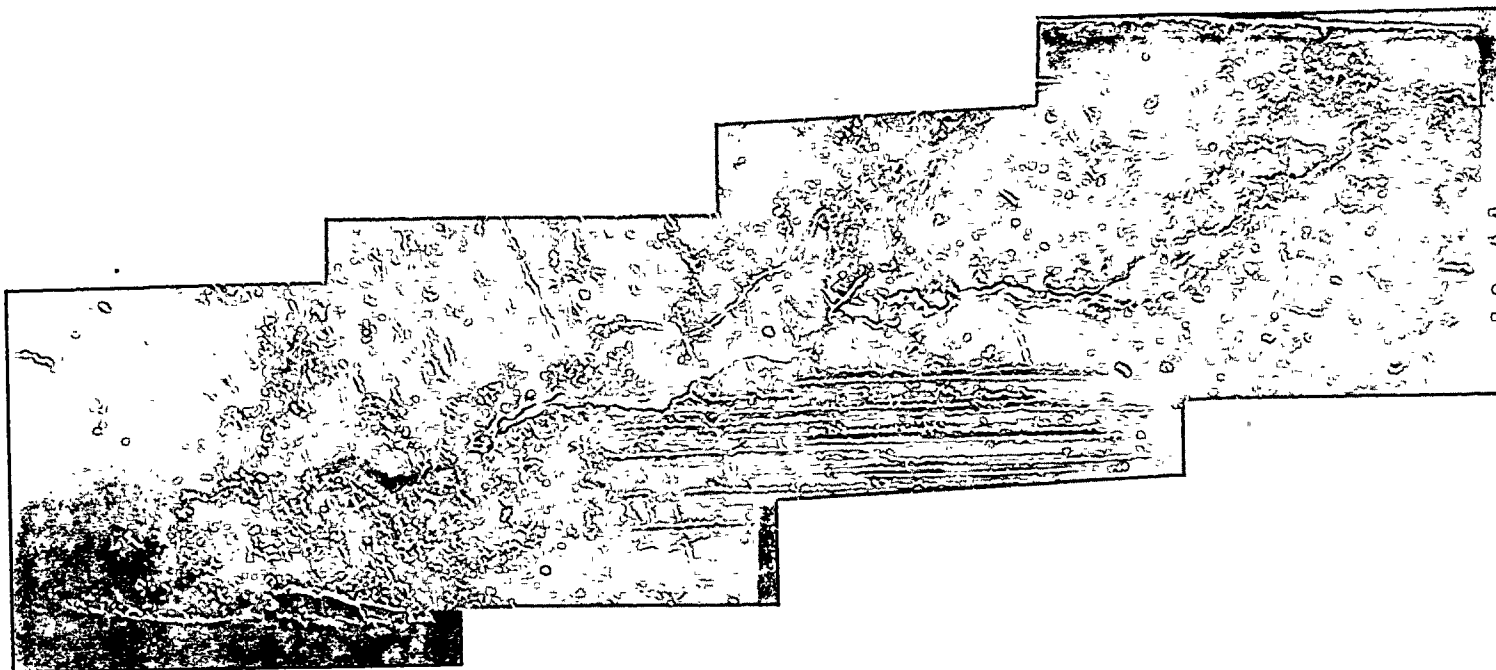
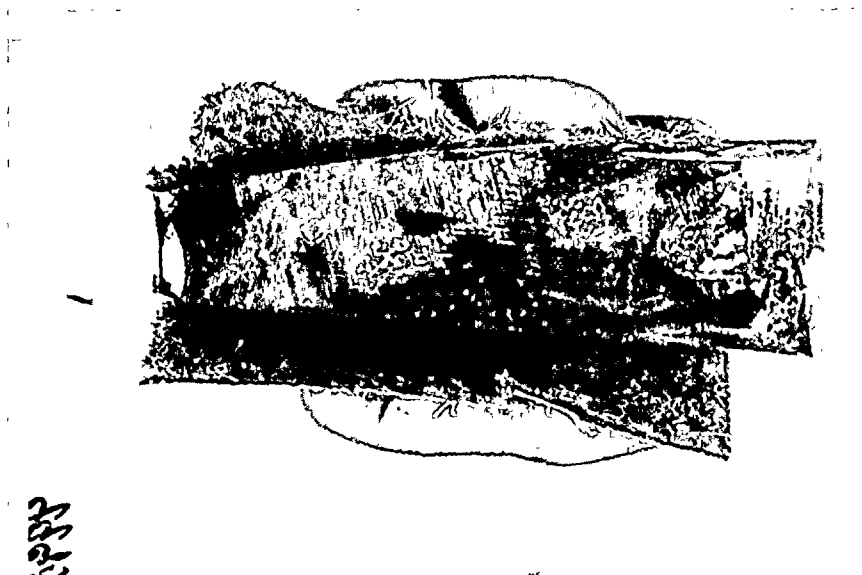


Figure 19. SEM photograph of O.D. surface crack, 50X.



Figure 20. SEM Photograph Showing Intergranular Fracture and Scaly Oxide Layer 300X.



C9990

~2.5X

Figure 21. Appearance of the Piping Sample from Nine Mile Point Reactor in the As-Received Condition.



SEM1023

20X

FIGURE 22. APPEARANCE OF THE SURFACE DEPOSIT FROM THE NINE MILE POINT PIPING SAMPLE IN THE AS-RECEIVED CONDITION.

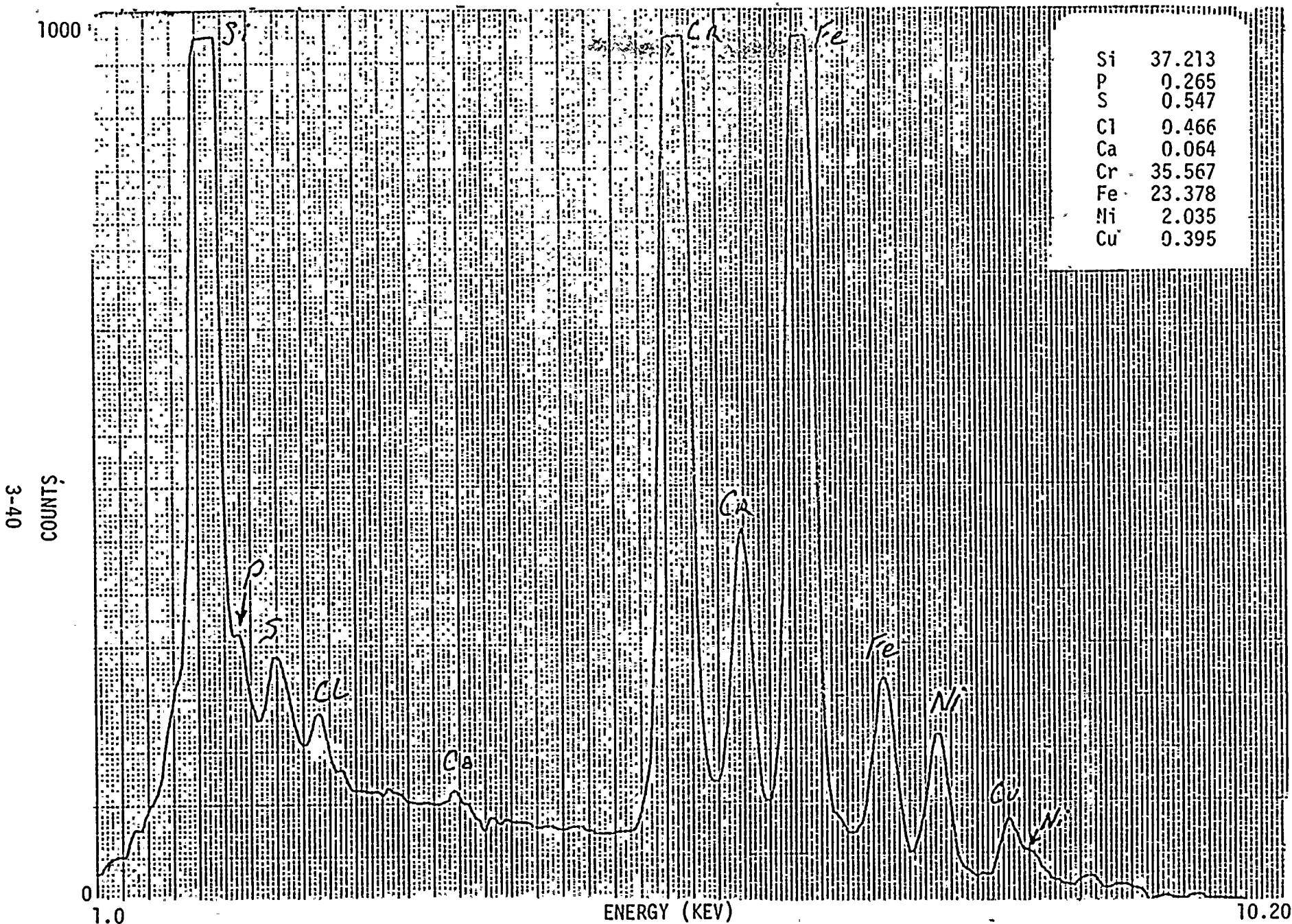
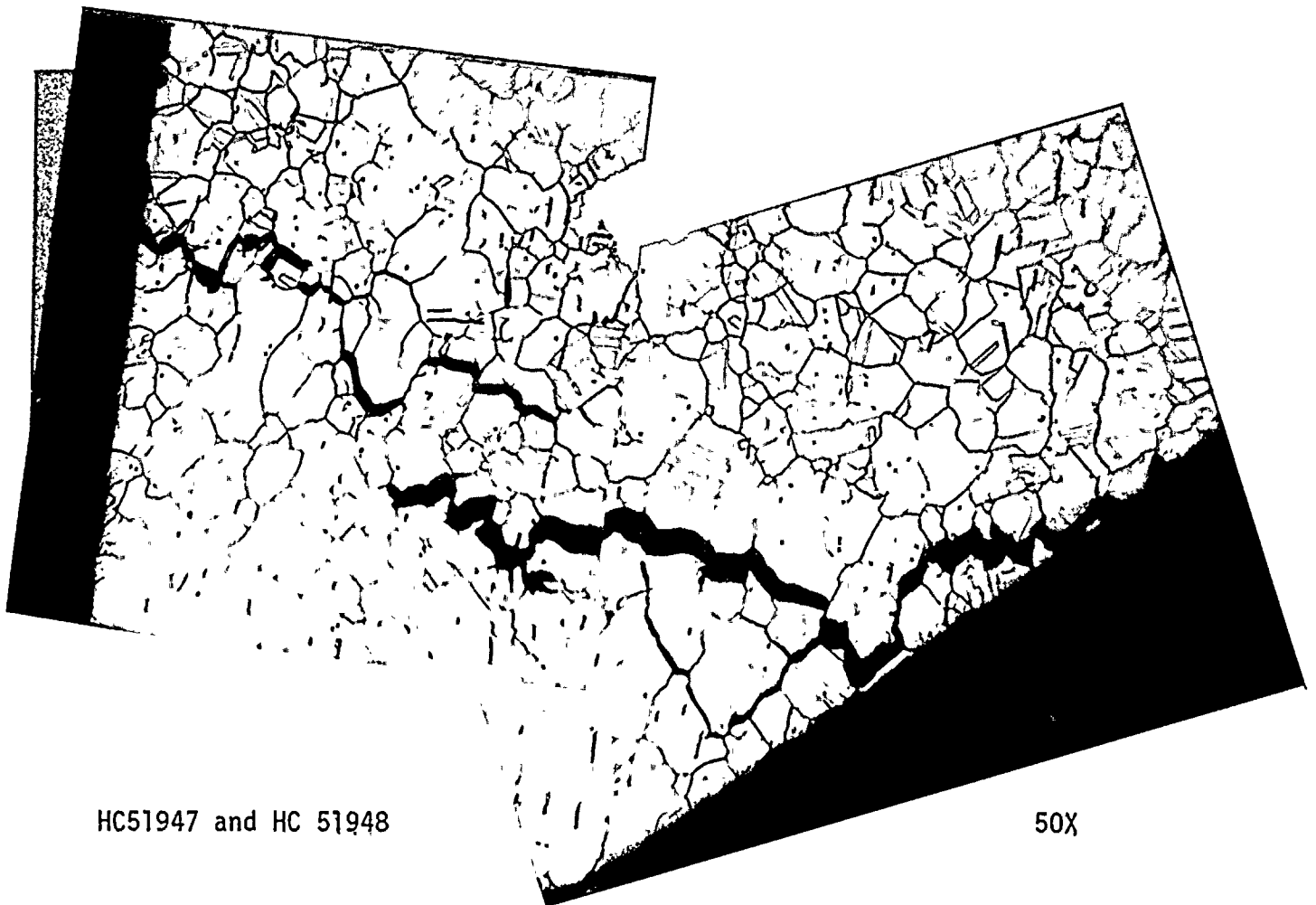


FIGURE 23. ANALYSIS OF DEPOSITS ON THE OUTER SURFACE OF THE NINE MILE POINT REACTOR PIPE SAMPLE SHOWN IN FIGURE 22.



HC51947 and HC 51948

50X

FIGURE 24. APPEARANCE OF THE CRACK IN THE ETCHED CONDITION.



SEM1034

600X

FIGURE 25. APPEARANCE OF THE CORROSION PRODUCT OBSERVED
INSIDE THE CRACK.

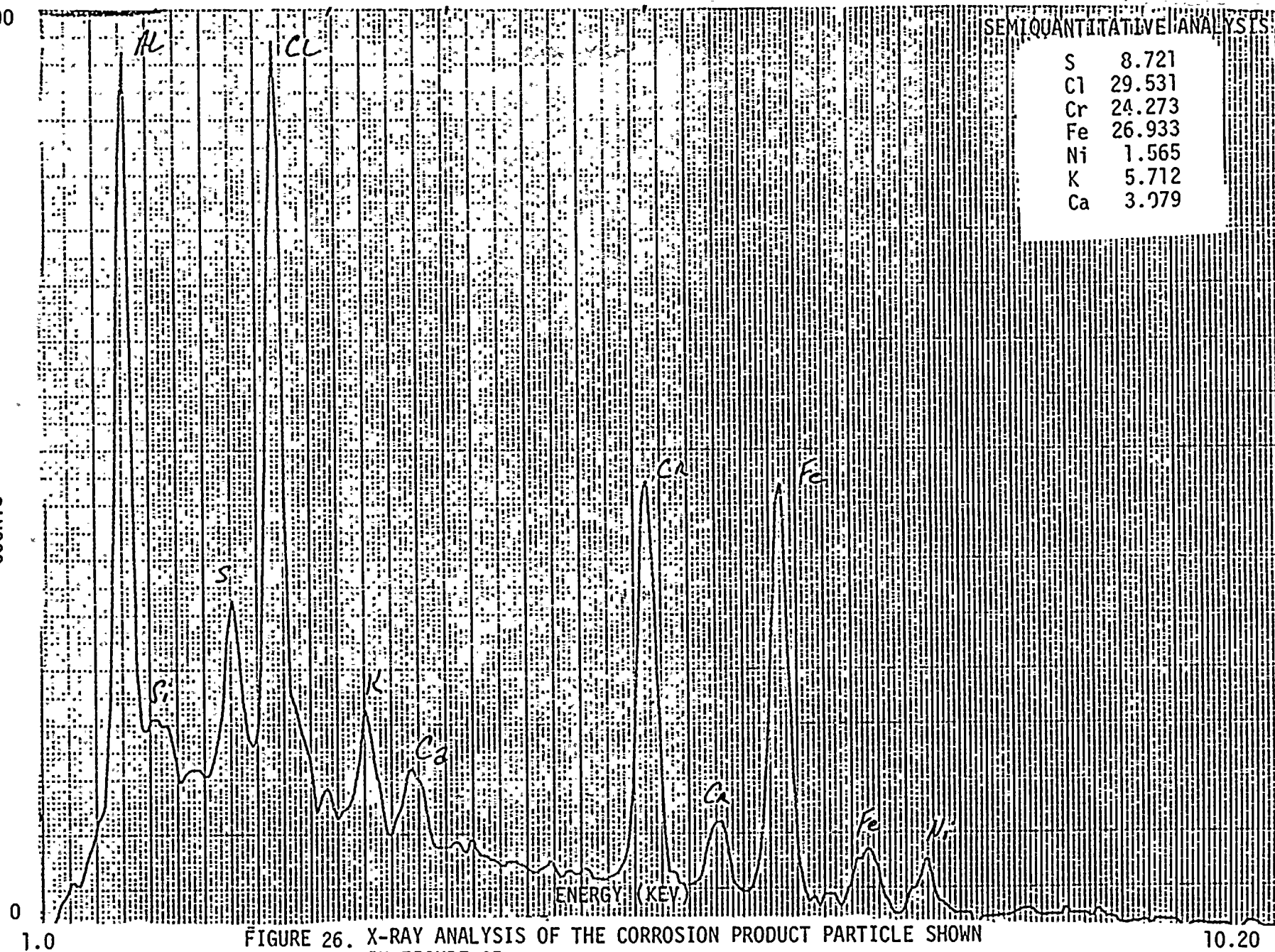


FIGURE 26. X-RAY ANALYSIS OF THE CORROSION PRODUCT PARTICLE SHOWN
IN FIGURE 25.



420X

FIGURE 27. APPEARANCE OF THE CORROSION PRODUCT OBSERVED
INSIDE THE CRACK.

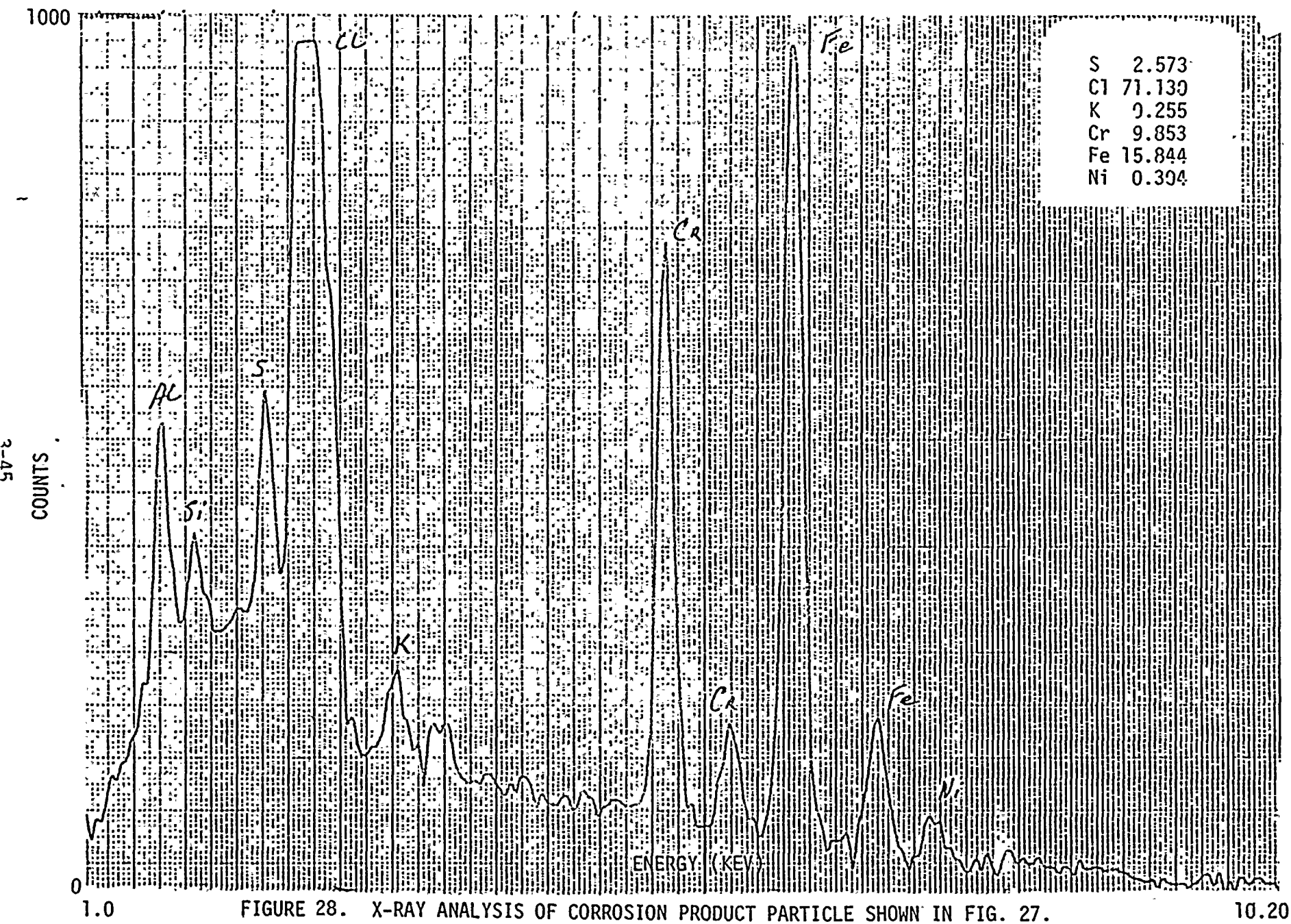
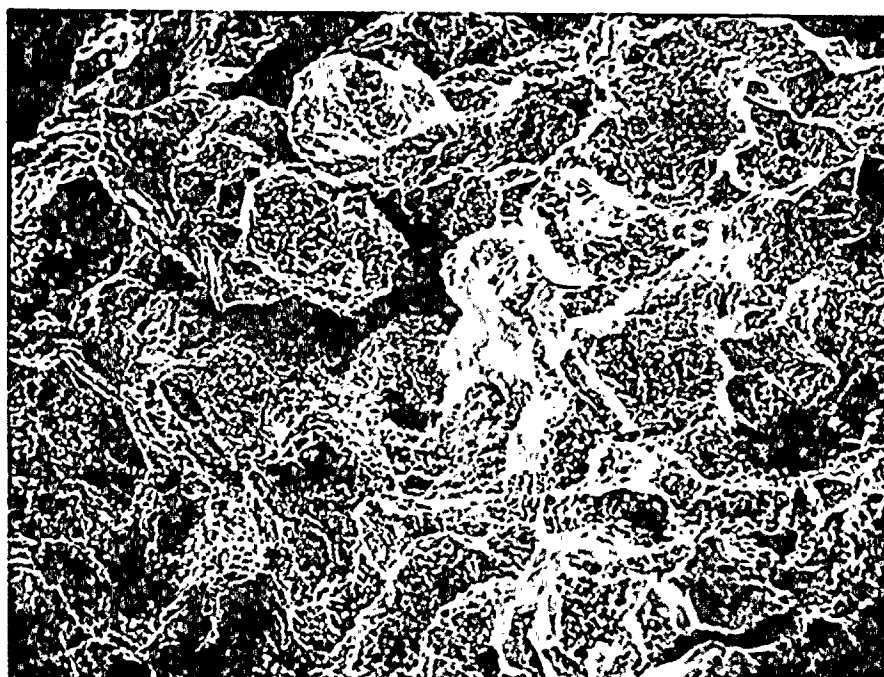
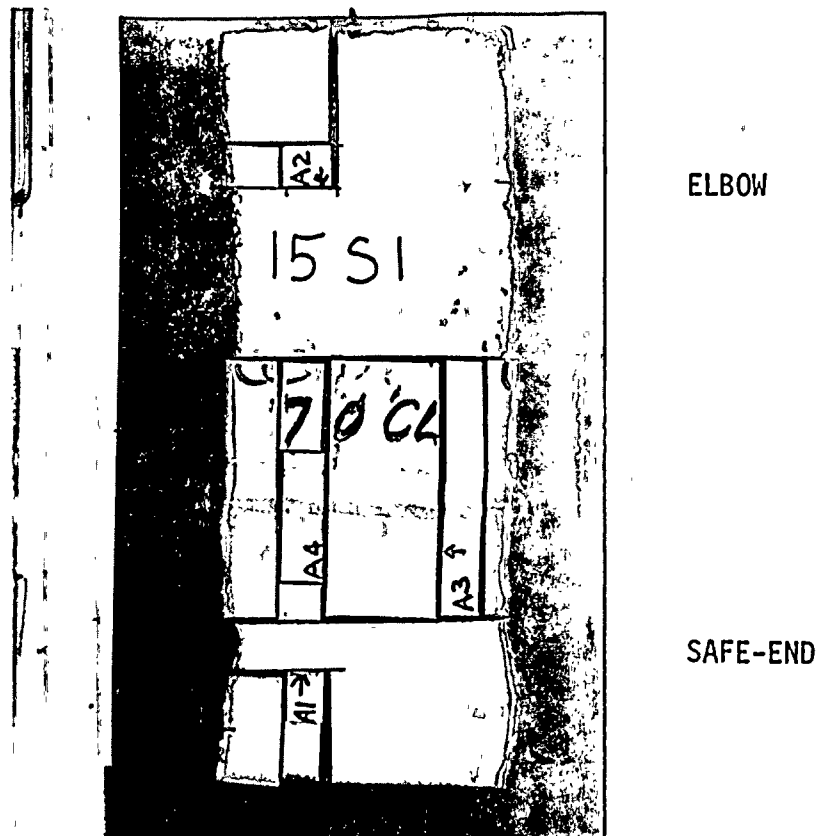


FIGURE 28. X-RAY ANALYSIS OF CORROSION PRODUCT PARTICLE SHOWN IN FIG. 27.



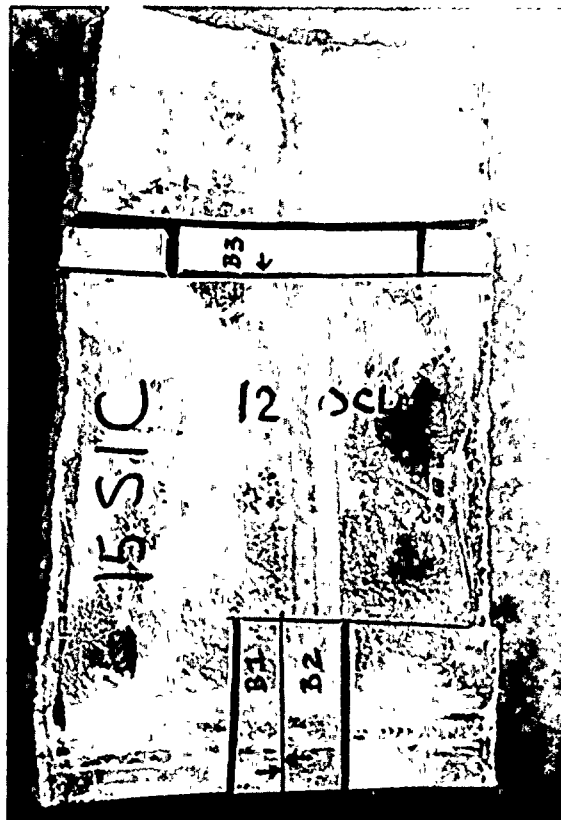
85X

FIGURE 29. SEM FRACTOGRAPH OF THE NINE MILE POINT SAFE-END SAMPLE SHOWING THE INTERGRANULAR FRACTURE MORPHOLOGY.



A423

FIGURE 30. CUTTING DIAGRAM OF A PORTION OF THE LOOP 15 SUCTION SAFE-END-to-ELBOW WELD. SECTION WAS LOCATED NEAR 7 O'CLOCK. ARROWS INDICATE SURFACE THAT WAS EXAMINED.



ELBOW

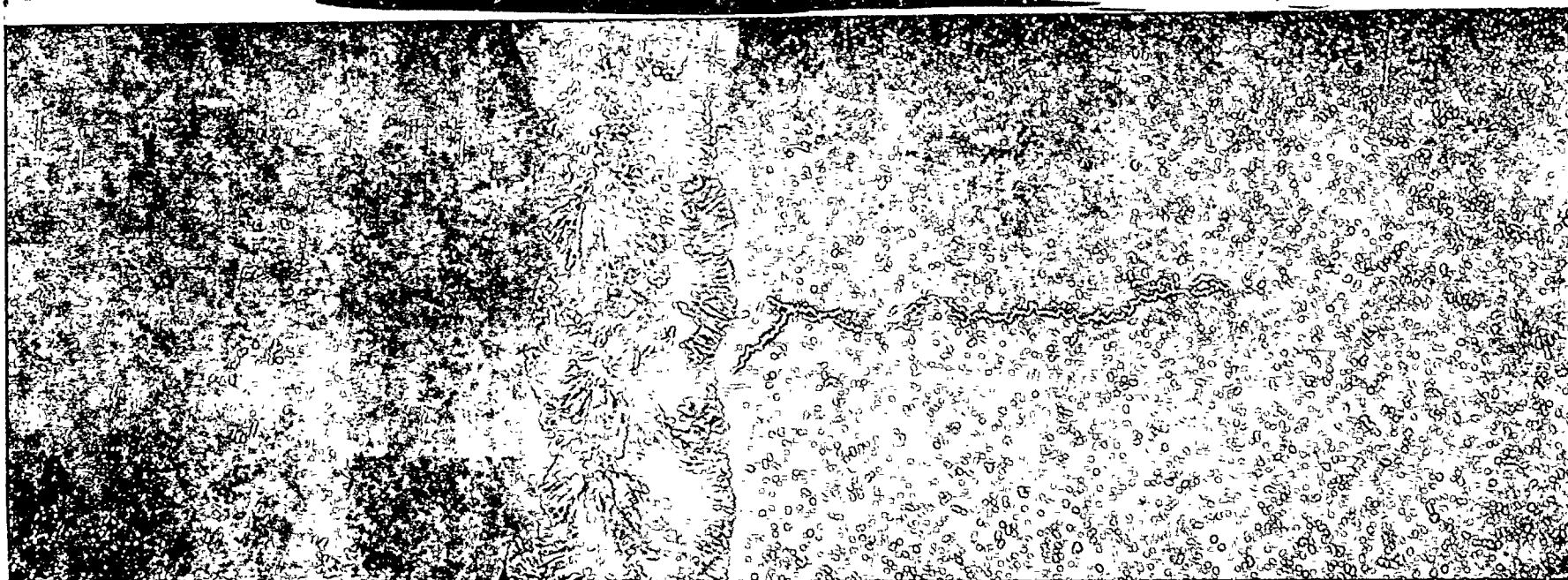
PIPE

A424

FIGURE 31. CUTTING DIAGRAM OF A PORTION OF THE
LOOP 15 SUCTION SAFE-END-ELBOW-TO-PIPE
WELD. SECTION WAS LOCATED AT 12 O'CLOCK.
ARROWS INDICATE SURFACE THAT WAS EXAMINED.

ELBOW

SAFE-END



9K371

4X

FIGURE 32. SAMPLE A4 SHOWING THE CRACK IN THE SAFE-END. THE SAMPLE WAS GROUND THROUGH THE PIPE WALL THICKNESS.

ELBOW

SAFE-END



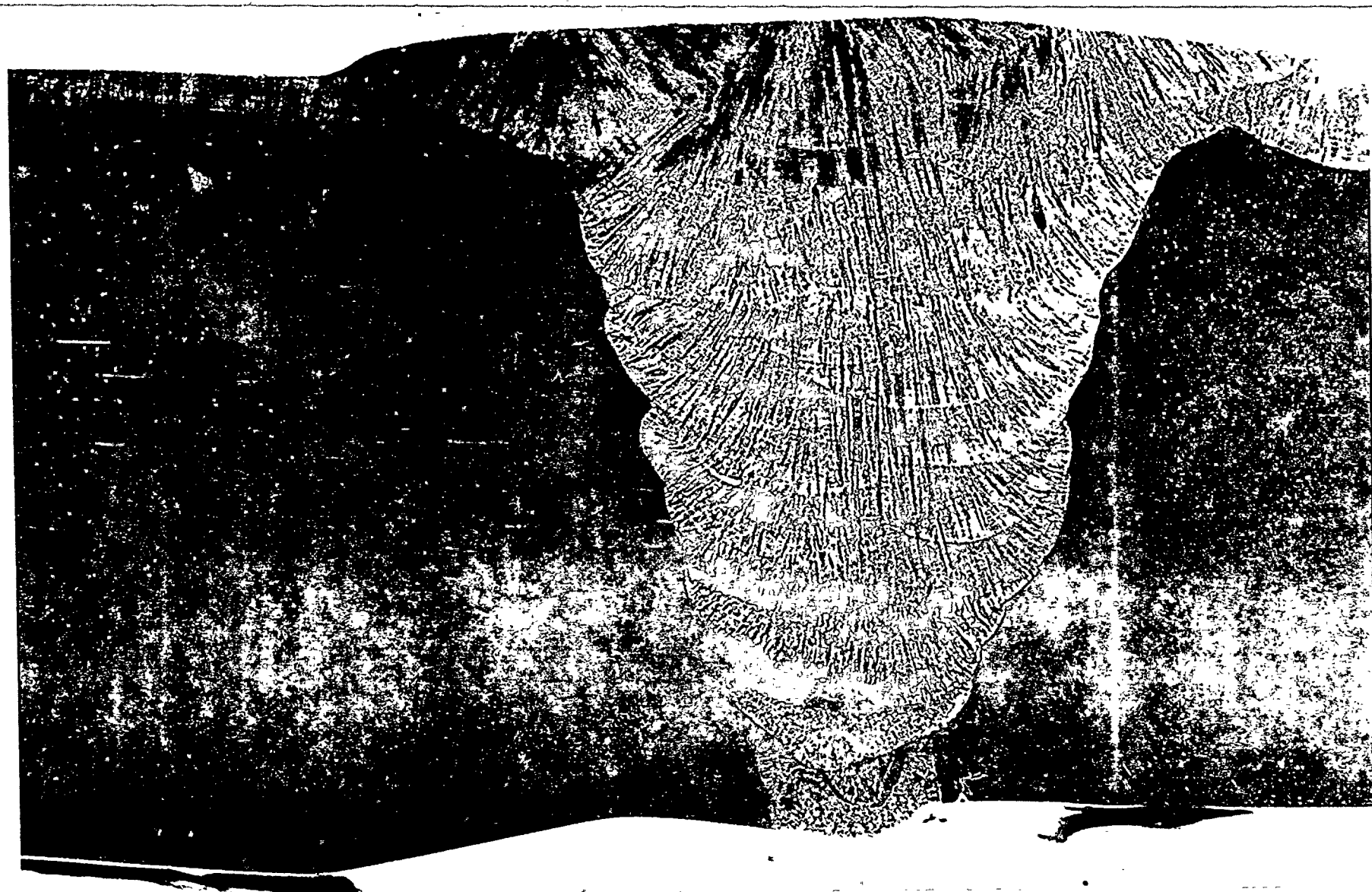
FIGURE 33. SAMPLE A4 SHOWING A CROSS-SECTION THROUGH THE SAFE-END-TO-ELBOW WELD. NO CRACKS WERE OBSERVED IN THIS SAMPLE.

9K369

4X

3-50

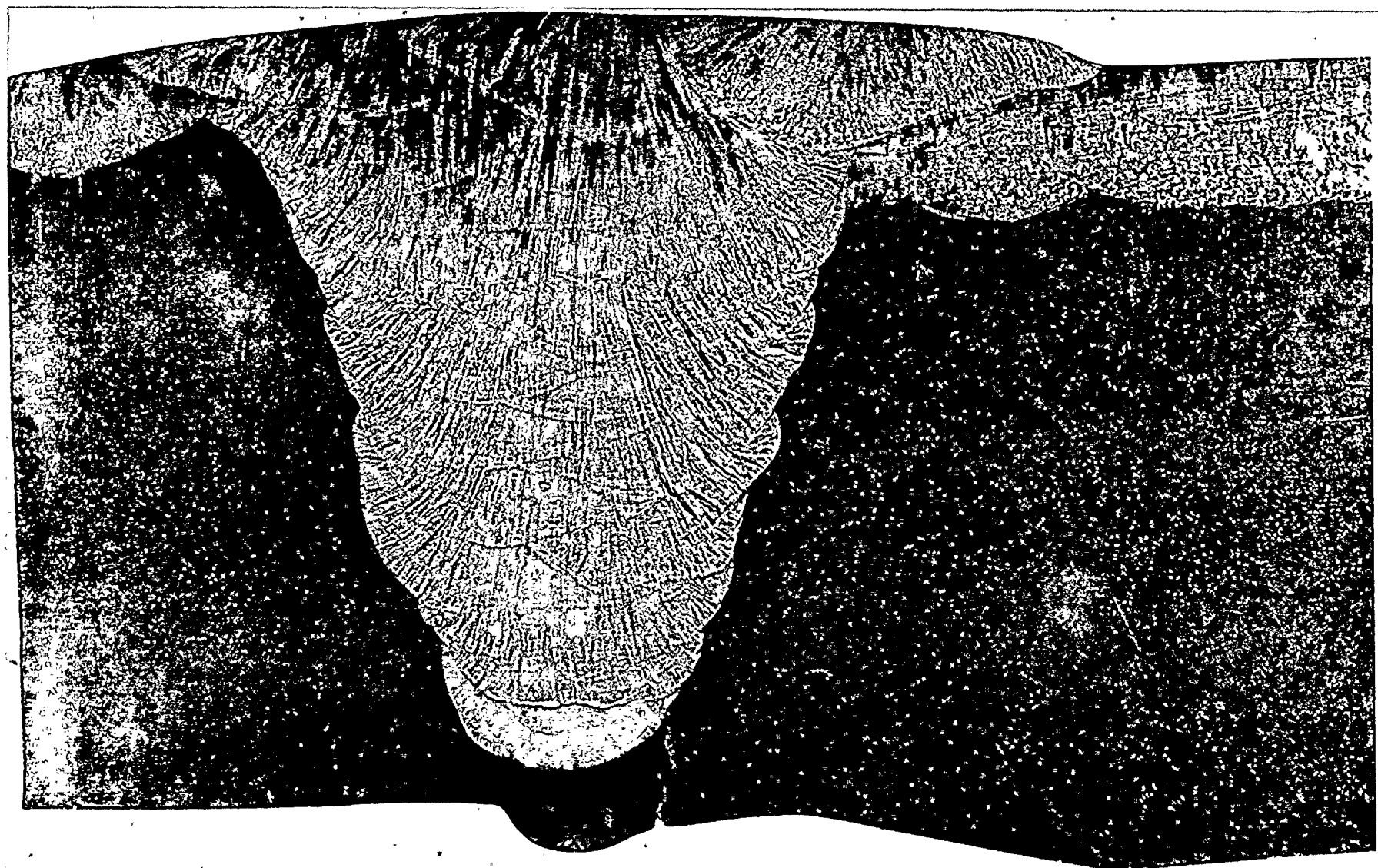
3-51



9K372

4X

FIGURE 34. SAMPLE B1 SHOWING A SHORT CRACK NEAR THE WELD ROOT ON THE PIPE SIDE OF THE WELD.



3-52

9K373

4X

FIGURE 35. SAMPLE B2 SHOWING A CRACK NEAR THE FUSION LINE ON THE ELBOW SIDE TO THE WELD.



9K374

4X

FIGURE 36. SAMPLE B-3 SHOWING A CROSS SECTION OF THE ELBOW SEAM WELD.

ELBOW

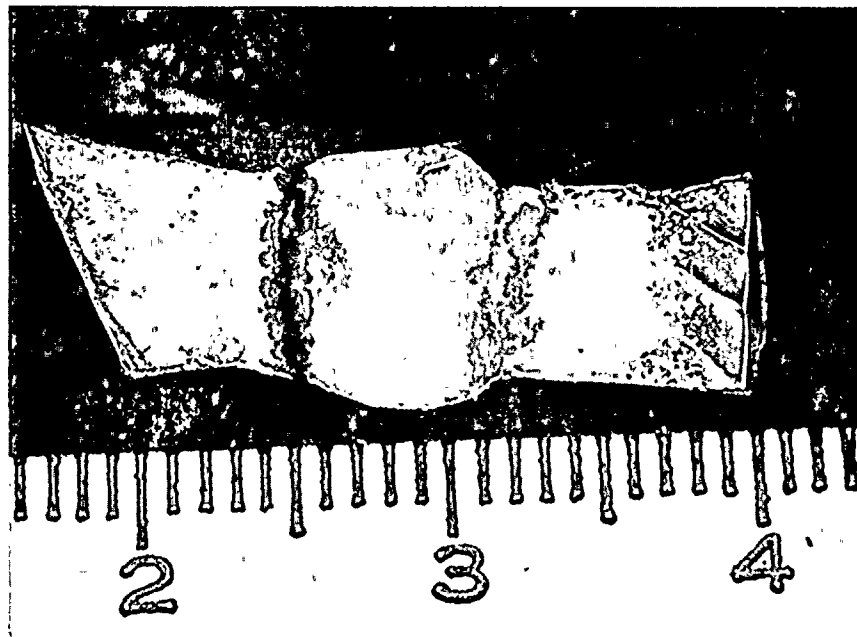
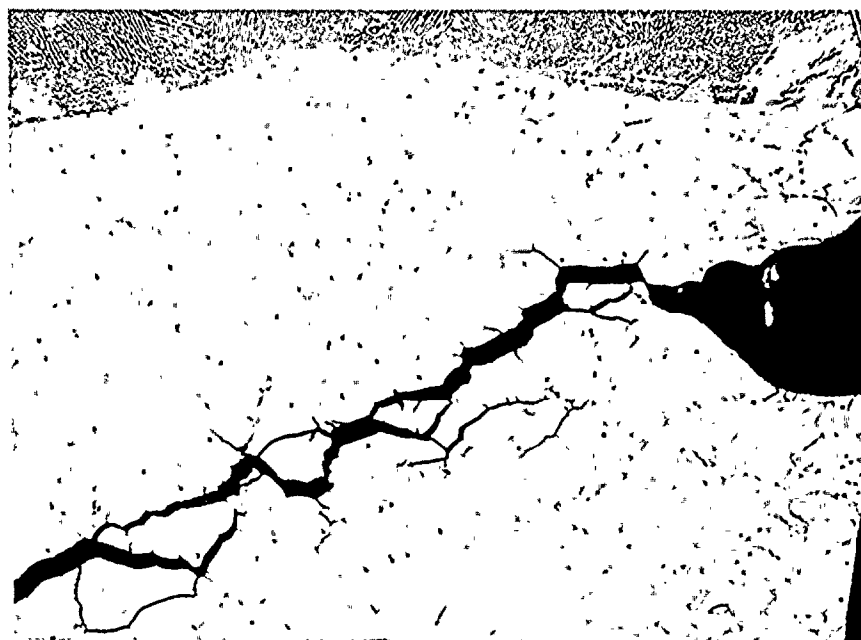


Figure 37. Penetrant examined - Boat Sample C, removed from weld SW-6 of Loop 13



50X

Figure 38. Etched
Crack on elbow side - Boat Sample C.

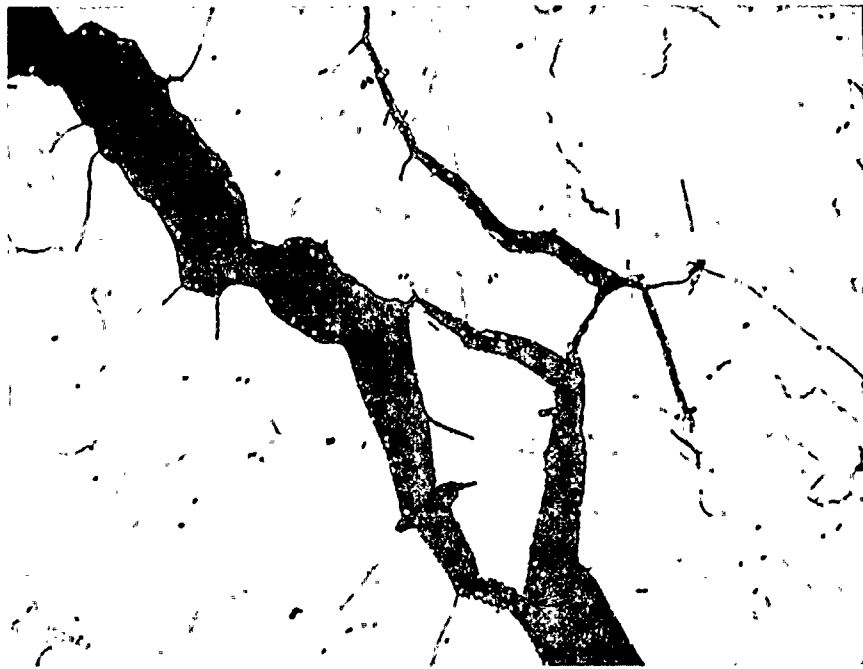


Figure 39. Etched - Boat Sample C
Detailed view, center portion.

128X

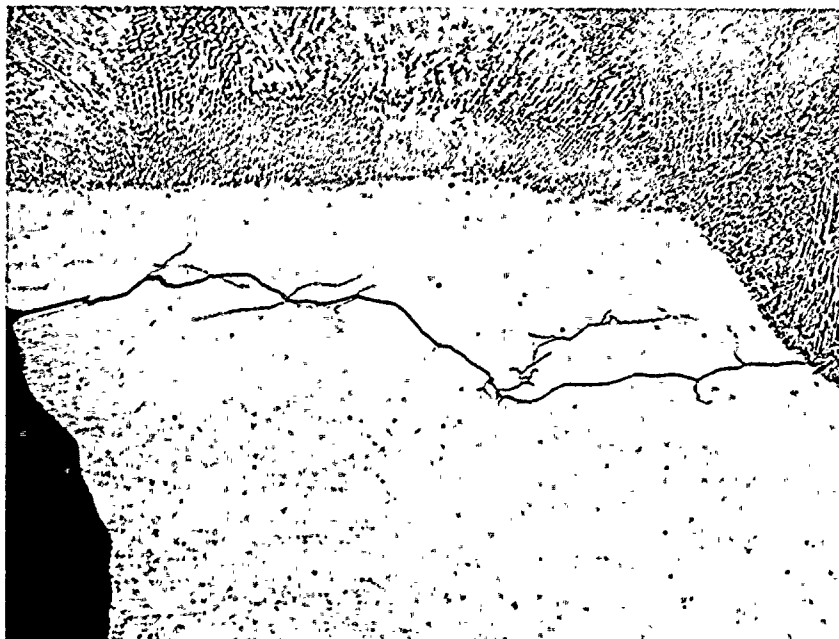


Figure 40. Etched view of crack on pipe side. 33X

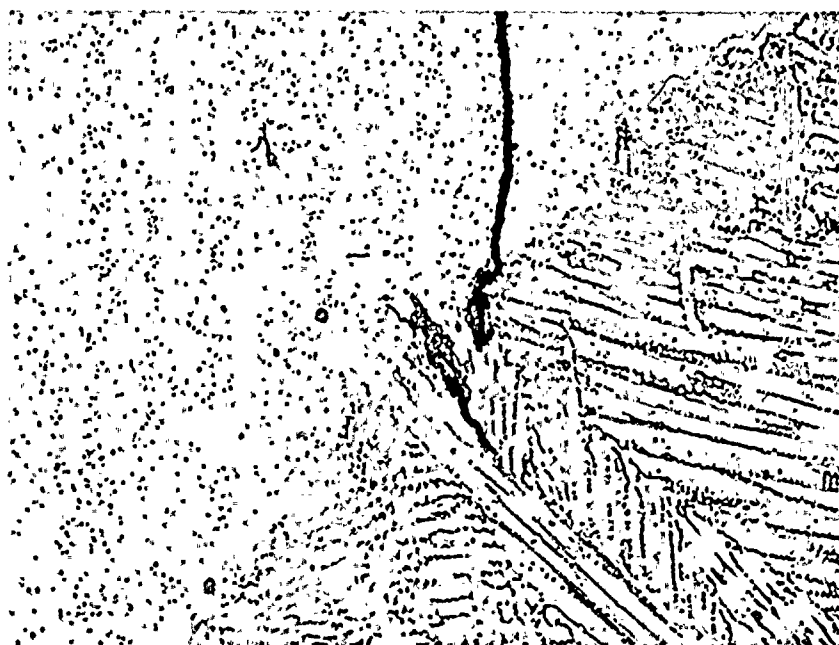


Figure 41. Etched detail at bottom of crack. 250X

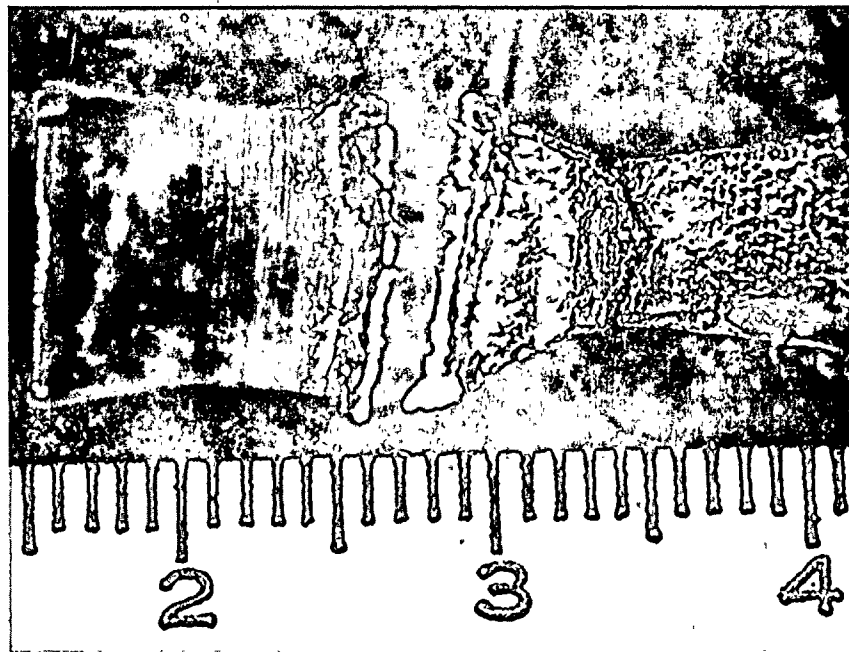


Figure 42. Boat Sample D removed from SW-6 of Loop 13.

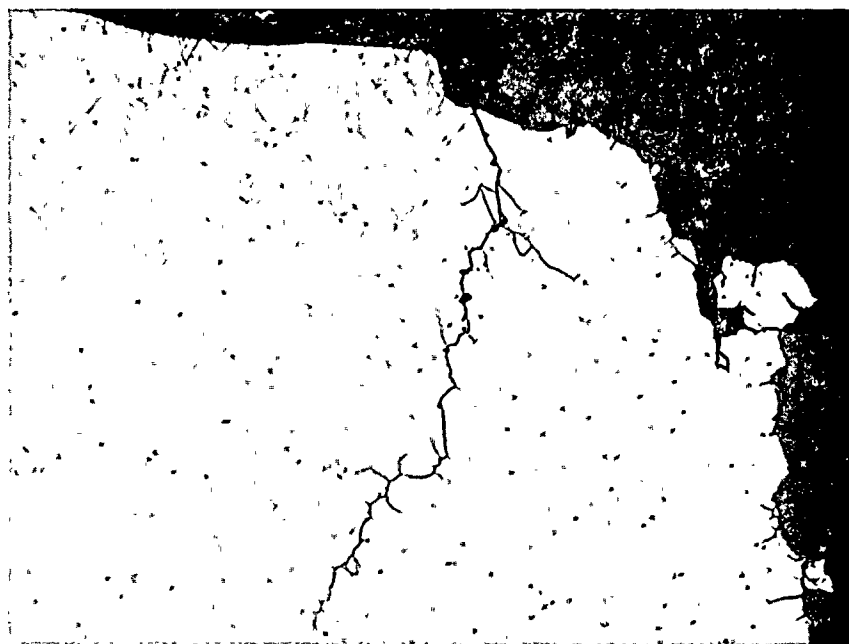


Figure 43. Etched view of Sample D, containing portion of fracture, and adjacent crack. 33X

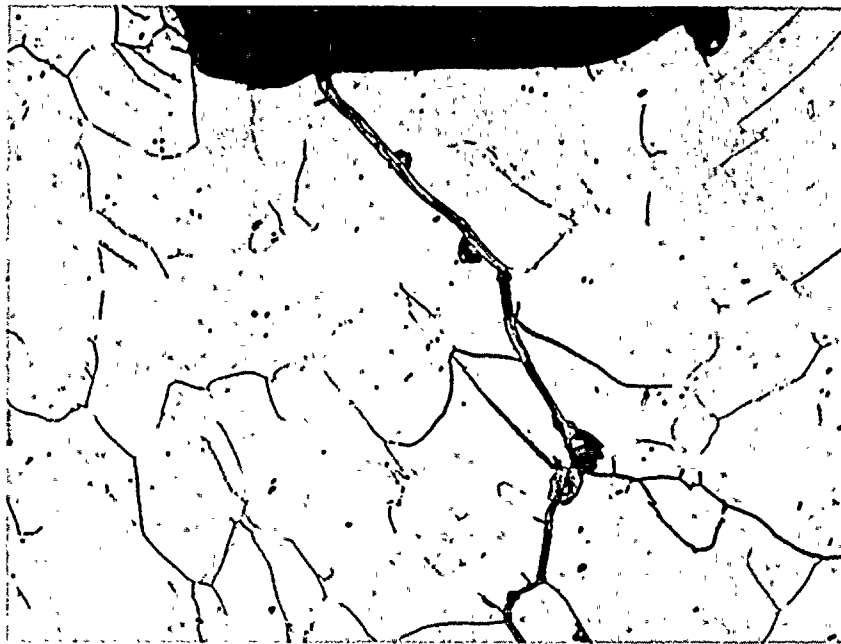


Figure 44. Etched view of Sample D containing
beginning of crack in Figure 43.

128X



Figure 45. Etched view of end of crack
in Figure 43.

128X

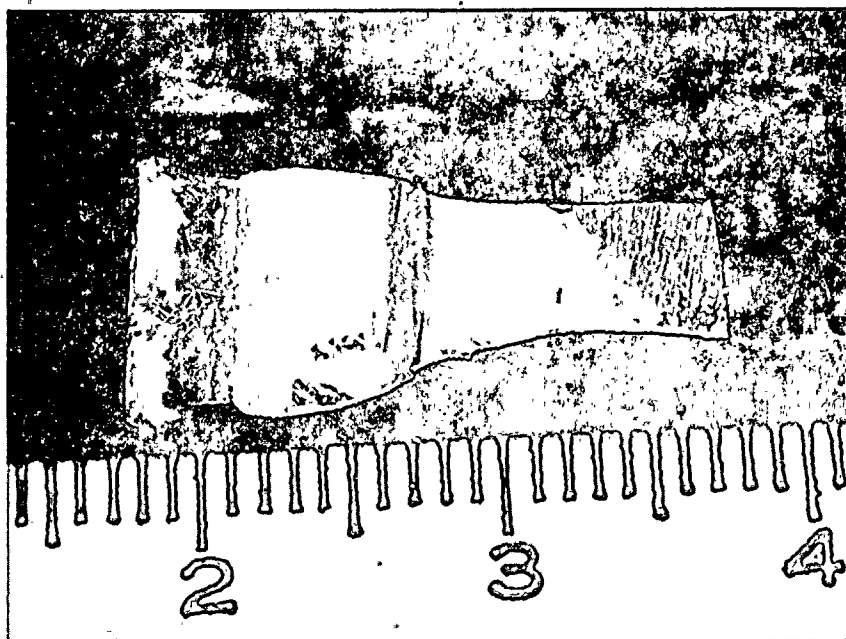


Figure 46. Penetrant examined view of Boat Sample E removed from SW-4 of Loop 12.

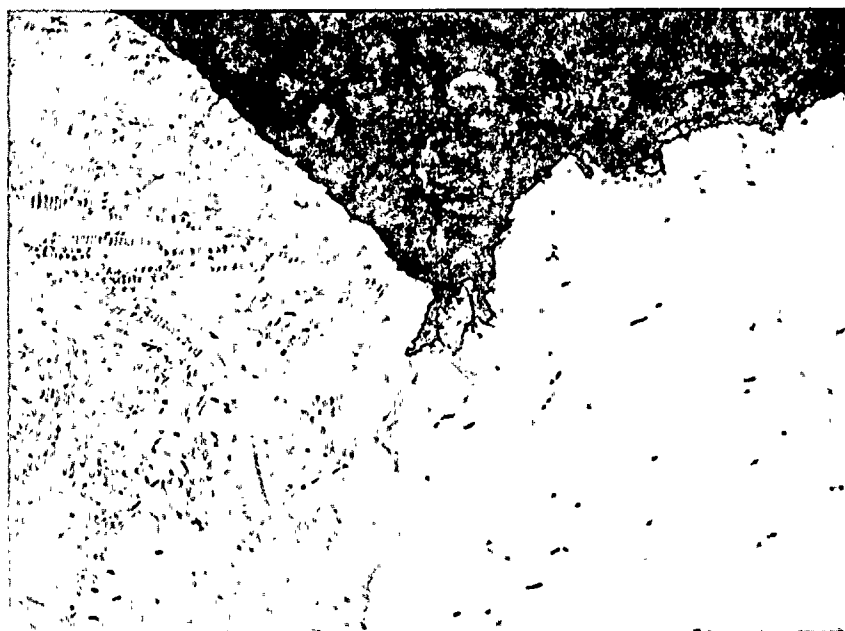


Figure 47. Etched view of indication at elbow side of Boat Sample E.

128X

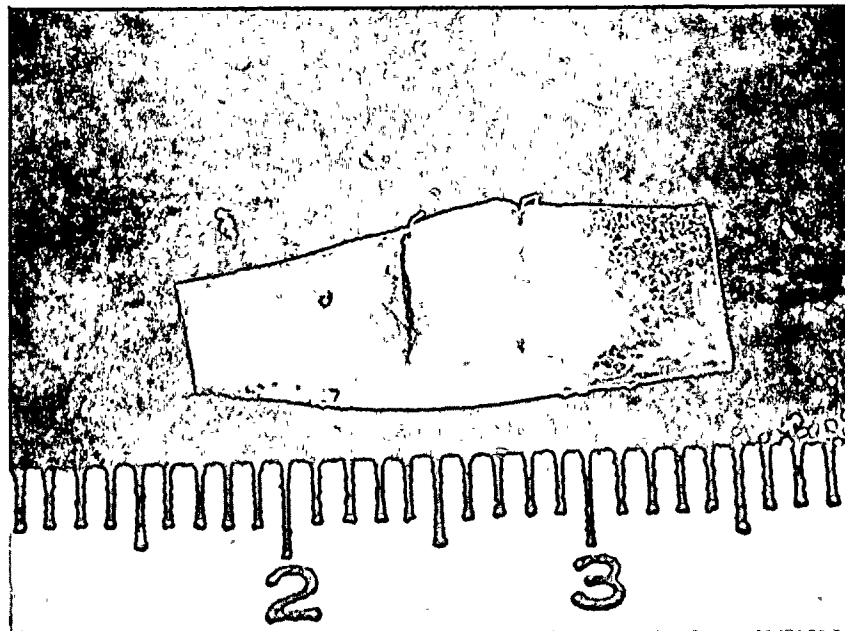


Figure 48. Penetrant examined view of Boat Sample F removed from field weld FW-5 of Loop 12.



Figure 49. Etched indication of Figure 48.

50X

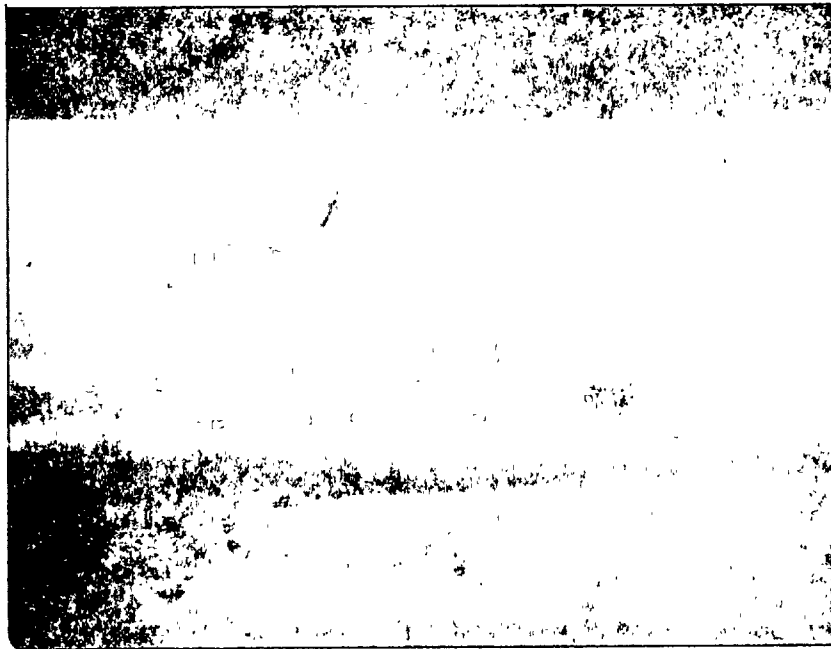


Figure 50. Penetrant examined view of indication on elbow side. Section was removed from SW-12 of Loop 15. ~2X

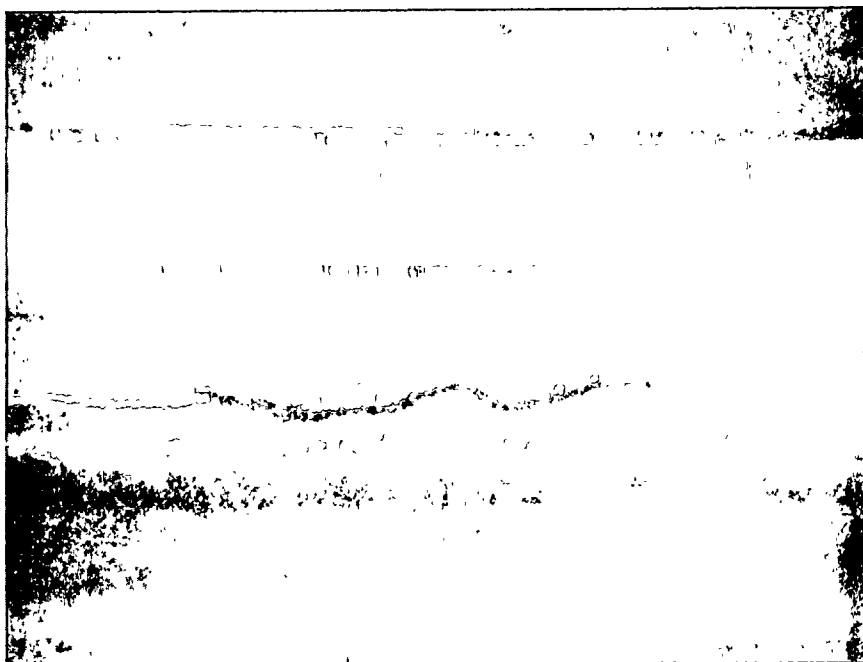


Figure 51. Penetrant examined view of longest indication, pipe side of pipe-to-elbow weld SW-12 removed from Loop 15. ~2X



Figure 52. Etched view of entire crack, elbow side of SW-12 of Loop 15.

33X



128X

Figure 53. Etched view of beginning of crack in Figure 50.

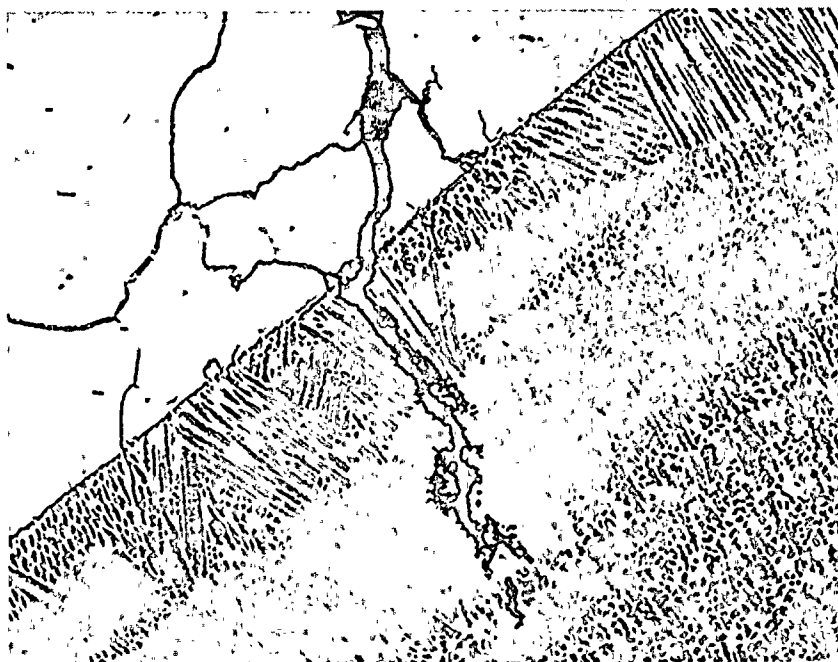


Figure 54. Kahling etched view of crack extending into weld. This view shows crack arrest in weld metal containing significant ferrite.

128X

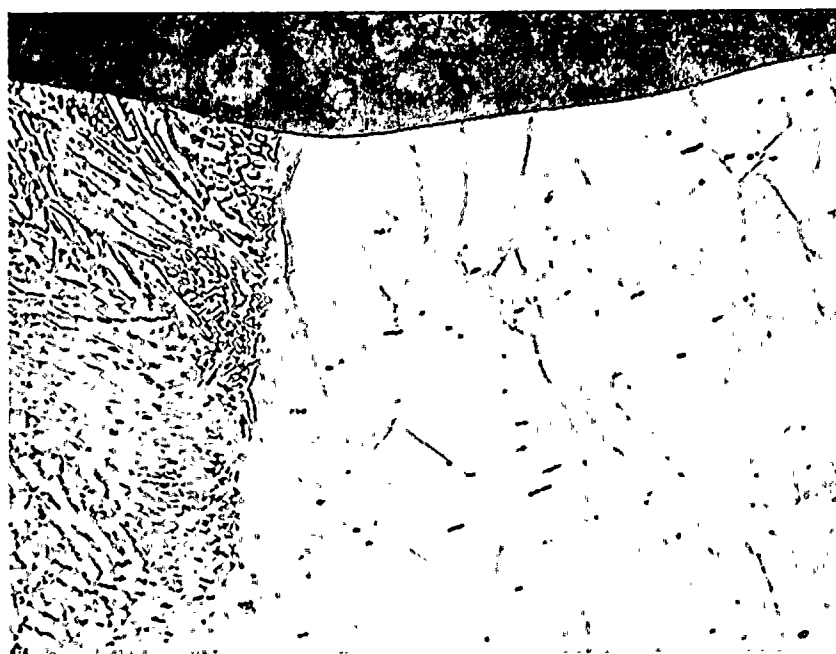


Figure 55. Etched view pipe side, same section as seen in Figure 50.

128X



33X

Figure 56. Etched view crack in pipe side. Sample was removed from shop weld SW-12 of Loop 15.

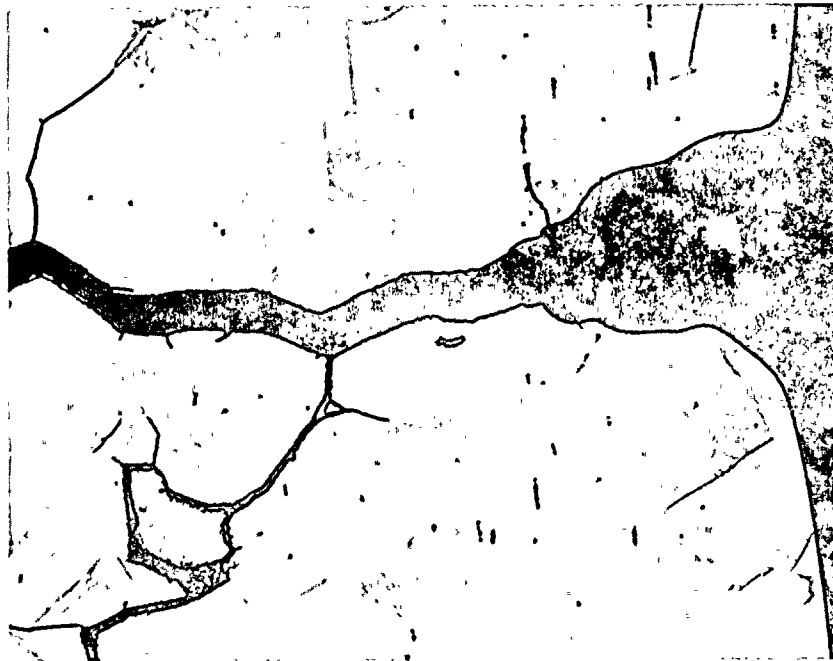


Figure 57. Etched view, beginning of crack
of Figure 56.

128X

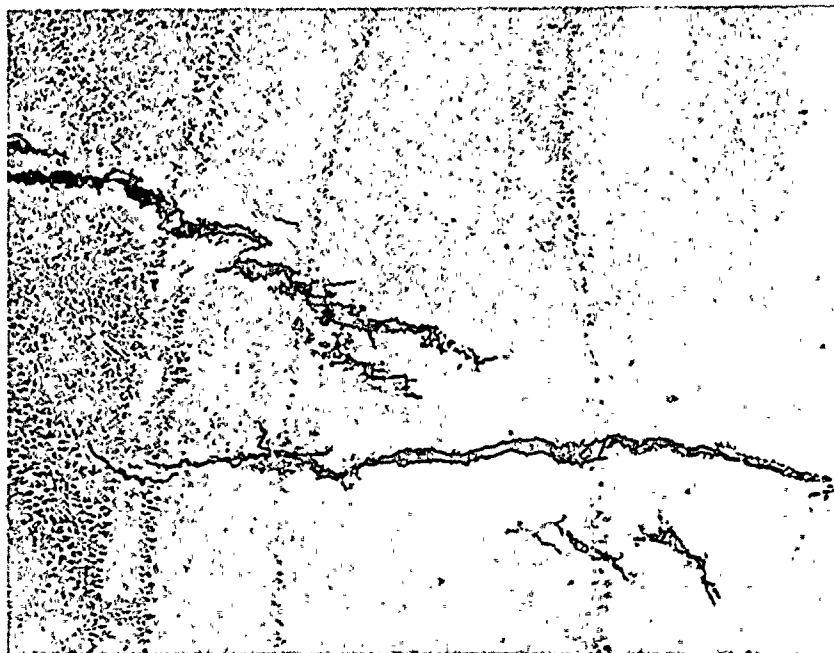
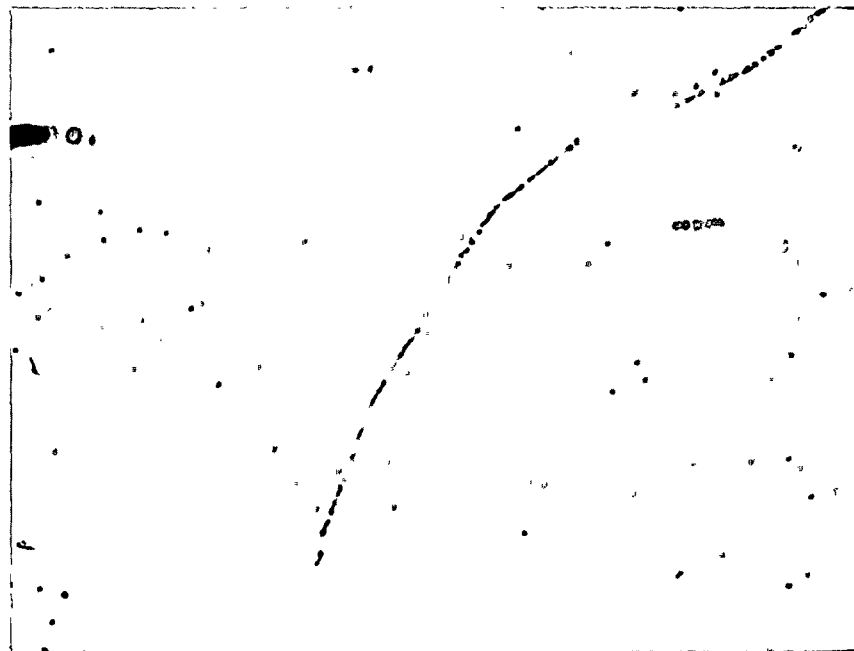


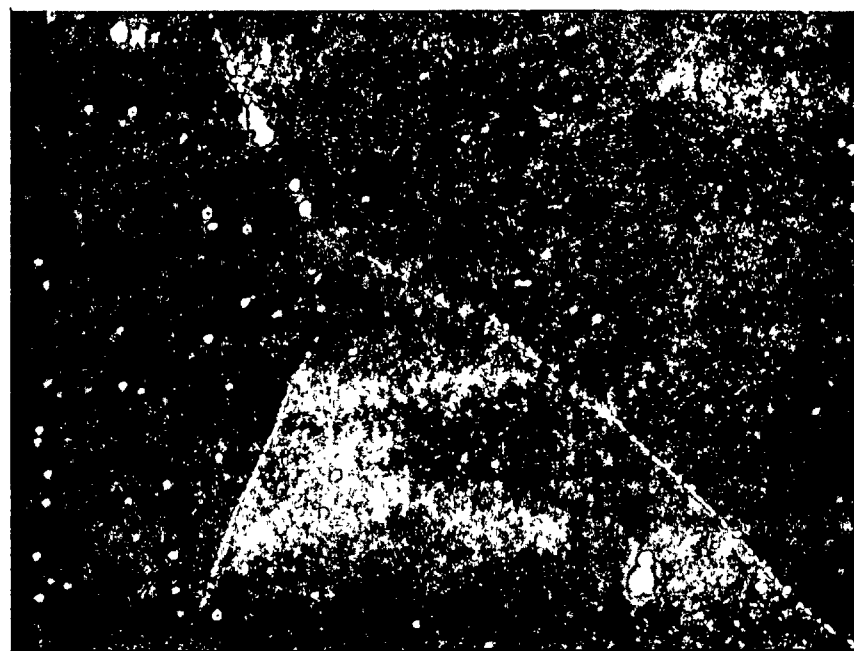
Figure 58. Kahling etched view of end of crack
of Figure 56.

128X



800X

Figure 59. SEM view of pipe side HAZ, showing carbides.



800X

Figure 60. Dark field view of pipe side HAZ, showing carbides precipitated at grain boundaries.



200X

FIGURE 61. APPEARANCE OF SPECIMEN MICROSTRUCTURE AFTER THE DEGREE OF SENSITIZATION TEST (ASTM-A-262 PRACTICE A).



500X

FIGURE 62. APPEARANCE OF SPECIMEN MICROSTRUCTURE AFTER THE DEGREE OF SENSITIZATION TEST (ASTM A-262 PRACTICE A)

SECTION IV

STRESSES AND STRESS RULE INDEX

Based upon the investigation as described below, stresses in the system are of nominal magnitude with the pressure stresses somewhat higher than more recent BWR designs, and there is nothing with respect to operation, support of the piping, or restraint of thermal expansion that have contributed abnormally to the apparent extent of cracking discovered.

BACKGROUND

In an attempt to pinpoint the cause of the extensive cracking, a detailed investigation of the pipe stresses in the system has been performed comparing the as-designed condition with the as-installed including any variations from the originally expected operating modes for the system.

The piping of concern here was reviewed to investigate pipe stress due to pressure, weight during normal operation, thermal expansion for all operating modes, and residual stresses. The stress rule index was also computed. In addition, the as-installed support system was reviewed to assure proper operation for all components. The components included here are the snubbers, spring sway braces, and constant support spring hangers.

Teledyne Engineering Services analyzed three of the five recirculation loops with their associated branch piping.² All recirculation loops are similar in geometry with the exception of the branch piping. The range

of operational stress level of the recirculation piping was bounded by analyzing the geometries of recirculation loop 12, which contains no branch piping and loop 15 which contains the largest (14-inches diameter) diameter branch. In addition, the two loops which were found to have through wall indications were modelled. The two loops are loop 11 and loop 15.

Stress levels were consistently well below allowable for the three loops. The effects of the branch piping on the recirculation piping were as anticipated (i.e., marginally larger stresses than the non-branch loop). Therefore, the stresses reported within this document are mainly for loop 15 which contains shutdown cooling branch piping.

WEIGHT DURING NORMAL OPERATION

These include stresses due to the weight of the piping components, insulation, and contents with the support system in the as-designed condition and in the as-installed condition. Investigation of the as-installed condition by NMPC personnel indicated a possible discrepancy in the spring hanger settings for the as-installed versus the as-designed condition. These discrepancies are tabulated below.

<u>Hanger No.</u>	<u>Load No. As-Designed</u>	<u>Load No. As-Installed</u>
H-3 Loop 11	20000 lbs	17900 lbs
H-3 Loop 12		
H-3 Loop 13		
H-3 Loop 14		
H-3 Loop 15		
Loads are per hanger. Two hangers exist at each support		

NOTE: The above hanger load information has been verified by NMPC personnel by calibration testing. See reference letters: R. Pavlik-ITT-Grinnell Corp. to Niagara Mohawk Pwr. Corp. dated Jan. 25, 1982, and February 7, 1983.

The maximum as installed weight stress for the recirculation piping is approximately 375 psi at node 270 (see Figure 1). This is the same as the as-designed weight case (i.e., the spring hanger load reductions cause only an insignificant change in stress on the recirculation loop piping).

To assure proper (exact) weight distribution on the new system, new constant support springs will be installed.

An additional non-operational deadweight case was investigated which includes a dewatered pump. This represents a condition that may exist during plant shutdown while maintenance is performed on the pump or pump motor. The pump motor was also assumed to be removed. The constant support springs are not pinned. The weight stress from this case is approximately 1200 psi at node 270. These stresses are low and will not be a problem for the recirculation system.

THERMAL EXPANSION

During normal operation of the plant, the recirculation loops are at the same temperature as the reactor due to the high flow rates through the loops. That is, with the reactor at 550°F, the loops are isothermal at 550°F. This represents the as-designed normal operating condition.

There have been times during operation of the plant when a loop (or loops) have been "valved-out". In this event the pump is not operating and the valves (upstream and downstream) are closed leaving a stagnant leg of water below the valves. The stagnant water in the loops cools off to approximately containment ambient (100°F) away from the reactor. In addition, a case may be postulated where the branch piping would flow into the "valved out" recirculation loop riser and into the reactor pressure vessel. The results would be a totally hot leg from the recirculation pump isolation valve to the reactor. The stresses

resulting from the "valved out" temperature distribution with branch flow into a loop have been investigated and found to be generally higher than the normal operating condition stresses. The maximum intensified thermal expansion stresses during normal operation are approximately 3000 psi at the branch tee. For the "valved out" branch flow case maximum intensified thermal stress levels occur at the same location and are approximately 9200 psi.

According to operating records at the site, the following loops were "valved-out":

Loop 11	66 days	9/20/72 (32 days) and 8/27/79 (34 days)
Loop 12	32 days	8/17/73
Loop 13	31 days	2/7/82.
Loop 15	720 days	6/21/79 to 7/3/81

The "valved out" stress level increase (see Table 1) does not represent a significant increase in the SRI values which are in the range of 1.2 (except at the tee welds, see Table 1). Further, Table 2 does not demonstrate any significant difference in crack location or the number of cracks for the piping systems which have been "valved out" for different durations of time (including no "valve out"). It therefore appears that the "valved out" case does not contribute to the recirculation pipe cracking.

OPERATIONAL CONCERNS

A. Snubbers: The recirculation pump is on a "floating" base. The base is supported by spring and snubber type supports only. A portion of the thermal expansion of the piping is accommodated by the floating pump base. During the past (1979) outage the snubber configuration of the pump base was changed. Also, the hydraulic snubbers throughout the recirculation piping were replaced with mechanical type snubbers. To assure that binding of the mechanical snubbers from displacements due to thermal expansion were not a

problem the vertical pump base snubbers were instrumented with LVDT's. The plant operational LVDT displacement data measured at the recirculation pump bases indicates that the snubbers were functioning properly under thermal load. The measured snubber deflections were comparable to the thermal expansion analysis deflections.

To further verify proper operability of the snubbers, a representative sample of the snubbers were tested by Teledyne Engineering Services. These tests indicated proper operation during normal plant conditions as well as during dynamic loading events. This testing is reported in Teledyne Engineering Services' test report number TR-5923-1.

B. Pump Vibration: Pump vibration was not considered to be a problem for the recirculation piping. Nine Mile Point internal correspondence 55-01-013 indicated that the worst case impeller mass imbalance would result in a maximum stress of 313 psi with a maximum deflection of 0.0074 inches. Nine Mile Point has tested the pump vibration instrumentation (3-23-82). The test data indicates that the maximum pump deflection is 0.9 mils (0.0009 inches) and the pumps vibration sensors are set slightly above the maximum tested deflection. The tested deflection is significantly less than the maximum deflection obtained from analysis, indicating that no vibrational stress problems exist from pump operation.

C. Sway Braces: The vibrational sway braces existing on the recirculation piping risers if properly installed and operating are designed to have no effect on the operational deadweight and thermal stress levels. A representative sample of sway braces have been tested by Teledyne Engineering Services to assure proper operation both in the past and for the future. (See Teledyne Engineering Services' test report number TR-5923-1.)

STRESS SUMMARY

The recirculation piping was reanalyzed for the operating conditions discussed in Sections I and II only. The resultant maximum stress summary is listed for recirculation loop 15. The additional information for loops 11 and 12 are listed for the same point to compare relative stress magnitude between loops.

Recirculation Loop 15

Node 265 pump discharge riser tee

Operational weight and pressure stress = 8220 psi*

Thermal expansion stress range = 9138 psi

Recirculation Loop 11

Node 265 pump discharge riser tee

Operational weight and pressure stress = 8054 psi*

Thermal expansion stress range = 1676 psi

Recirculation Loop 12

Node 265 pump discharge (no branch line or tee)

Operational weight and pressure stress = 8014 psi*

Thermal expansion stress range = 947 psi

*Axial component of pressure stress.

The pressure stresses may be somewhat higher than other more recent BWR recirc. loop designs, due to the pipe wall thickness. The pressure stresses are still within the appropriate design code allowables.

RESIDUAL STRESSES

Residual stresses present in the weld heat affected zone contribute significantly to stress corrosion cracking and are therefore, accounted for in the General Electric stress rule index (SRI).

A residual stress value of 27,000 psi for the 28-inch diameter run piping was used in calculating the SRI numbers. This value is an extrapolation of data based on the envelope of maximum axial values measured by GE and others on schedule 80 pipe sizes ranging from 4-inches to 26-inches.

For RESID = 27,000 the approximate contribution to the SRI is 0.374.

STRESS RULE INDEX

The stress rule index was computed for the recirculation loop using loads and stresses for the as-designed cases in addition to the as-installed (including "valved-out" conditions) case.

The stress rule index has been computed as follows:

$$SRI = \frac{P_m + P_b}{S_y} + \frac{Q + F + R}{S_y + .002E}$$

where: $P_m = \frac{P_o D_o}{2t}$

P_o = operating pressure (psi)
 D_o = outside diameter (inches)
 t = wall thickness (inches)

$$P_b = B_2 \frac{D_o}{2I} M_a$$

M_a = resultant deadweight moment (in/lb)
 I = moment of inertia (in⁴)
 B_2 = primary loop stress index

$$Q + F = (K_1 C_1 - 1) \frac{P_o D_o}{2t} + C_2 K_2 \frac{D_o}{2I} M_i + K_3 C_3 EAB (\alpha_A T_A - \alpha_B T_B)$$

or

$$SRI = \frac{\frac{P_o D_o}{2t} + B_2 \frac{D_o}{2I} M_A}{S_y} + \frac{(K_1 C_1 - 1) \frac{P_o D_o}{2t} + C_2 K_2 \frac{D_o}{2I} M_i + K_3 C_3 E_{AB} (\alpha_A T_A - \alpha_B T_B) + R}{S_y + .002E}$$

K_1, K_2, K_3 = local stress indices (NB-3680, Reference 3)

C_1, C_2, C_3 = secondary stress indices (NB-3680, Reference 3)

M_i = thermal (operating) resultant moment (in/lb)

E_{AB} = Young's modulus (average for dissimilar materials)

α_A, α_B = thermal expansion (in/in/°F)

T_A, T_B = operating temperature (°F)

R = residual stress (Reference 4) (psi)

S_y = yield stress (Reference 3, Table I-2.2) (psi)

E = Young's modulus (Reference 3, Table I-5.0) (psi)

The Stress Rule Index was computed for recirculation loop 15 and is presented in Table 1. The primary contributors to the Stress Rule Index are pressure stress and residual stress. The higher pressure stresses here appear to drive the SRI values somewhat higher, since the residual stresses are assumed constant for a given pipe diameter. This may account for a higher incidence to cracking.

Table 1

<u>Node</u>	<u>Description</u>	<u>SRI As-Designed</u> ⁽¹⁾	<u>Max SRI As-Installed</u> ⁽²⁾
101	Elbow	1.239	1.391
105 ⁽³⁾	Tee	2.155	2.291
115 ⁽³⁾	Tee	2.132	2.283
135	Valve	1.181	1.262
155	Elbow	1.188	1.287
156	Pump	1.262	1.397
200	Pump	1.182	1.260
205	Elbow	1.179	1.339
225	Valve	1.185	1.282
270	Elbow	1.429	1.444

- NOTE: (1) As-designed - including normal deadweight + 550°F thermal case effects.
 (2) As-installed - including normal deadweight + "valved out" pump with branch flow + "valved out" pump no branch flow thermal range case.
 (3) Tee indices used although the indices were designed to give stresses in the crotch region not at the weld.

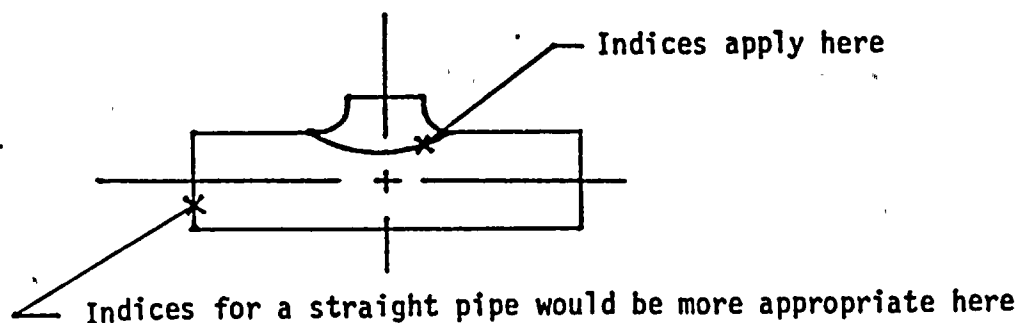
It must be noted that the recirculation loops at NMPI have less butt welds than other BWR designs. Butt welds have lower Stress Rule Index values and, therefore, would be less than 1.2. This fact would make the SRI values, as a whole, higher than for other plants with more pipe-to-pipe butt welds in their designs.

Table 2 is a comparison of the maximum stress rule index and the number of cracks in a given heat affected zone (Reference 1) at a specific location. These data do not correlate very well leading one to believe that the carbon content, previous cold working and heat treating of the pipe at a specific location contribute more cracking than the magnitude of the stress in the pipe. The actual locations may be found in Figure 2 for loop 15.

Samples of the Nine Mile Point recirculation piping have been analyzed for carbon content. The results of this analysis indicate that the carbon content range is between 0.042 and 0.075 percent. The carbon content is greater than the 0.035 percent upper bound therefore indicating the pipe is in the susceptible region for IGSCC.

It can be seen from Table 1 that, except for the tee, the SRI values are all very similar at a value of about 1.2. This value is equal to the threshold with respect to stress corrosion cracking as observed by GE for a large number of plants/systems surveyed.

It must be pointed out that the SRI values have been computed and presented here for reference and comparison by the reader with other plants, etc., keeping in mind that the relative values only are of most importance. The apparent higher values of SRI for the tee may be appropriate for the branch pipe weld but not for the run pipe welds since the stress indices (ASME Code) depict stresses at the crotch near the branch weld. Therefore, the SRI at the run pipe welds would be about 1.2 also.



The stress of importance with respect to IGSCC is the sustained tensile stress on the inside surface of the pipe in the heat affected zone of the weld.

A similar situation exists for elbows in that C_1 and C_2 do not apply to the HAZ.

C_1 and/or C_2 represent maximum shear stress at times. In an elbow C_1 is representative of the hoop stress in the crotch and C_2

represents hoop bending at the side.

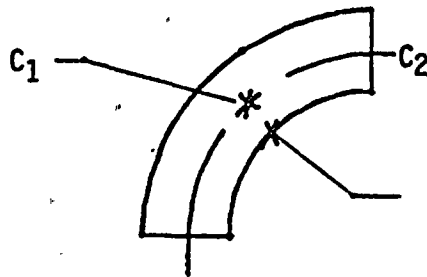


Table 2

<u>Node Number</u>	<u>Description</u>	<u>Max SRI</u>	<u>No. Cracks** Loop:</u>					<u>Total Cracks **</u>
			<u>15</u>	<u>11</u>	<u>12</u>	<u>13</u>	<u>14</u>	
101	Elbow (I)	1.391	0	0	2	1	0	3
103	Elbow (J)	1.391*	6	3	6	3	0	18
105	Tee	2.291	4	3	NA	NA	0	7
115	Tee	2.283	4	0	NA	NA	0	4
135	Valve	1.262	4	4	4	4	4	20
140	Valve	1.262*	3	4	2	4	4	17
150	Elbow (I)	1.287*	4	6	7	7	4	28
155	Elbow (J)	1.287	2	2	2	2	2	10
205	Elbow (I)	1.339	2	2	5	3	4	16

*SRI assumed equal to SRI on opposite end of component.

**Represents the number of multiply nucleated cracks at the indicated node number.

LIST OF REFERENCES

1. IGSCC Task Force Meeting Minutes, November 23, 1982.
2. TES Document No. 5838-4.
3. 1977 Edition of ASME Boiler and Pressure Vessel Code, Section III, with Addenda.
4. BWR Owners Group and EPRI Joint Presentation to NRC, October 15, 1982.

TELEDYNE ENGINEERING SERVICES

BY EAS DATE 5-23-83
CHKD. BY WJB DATE 5-23-83

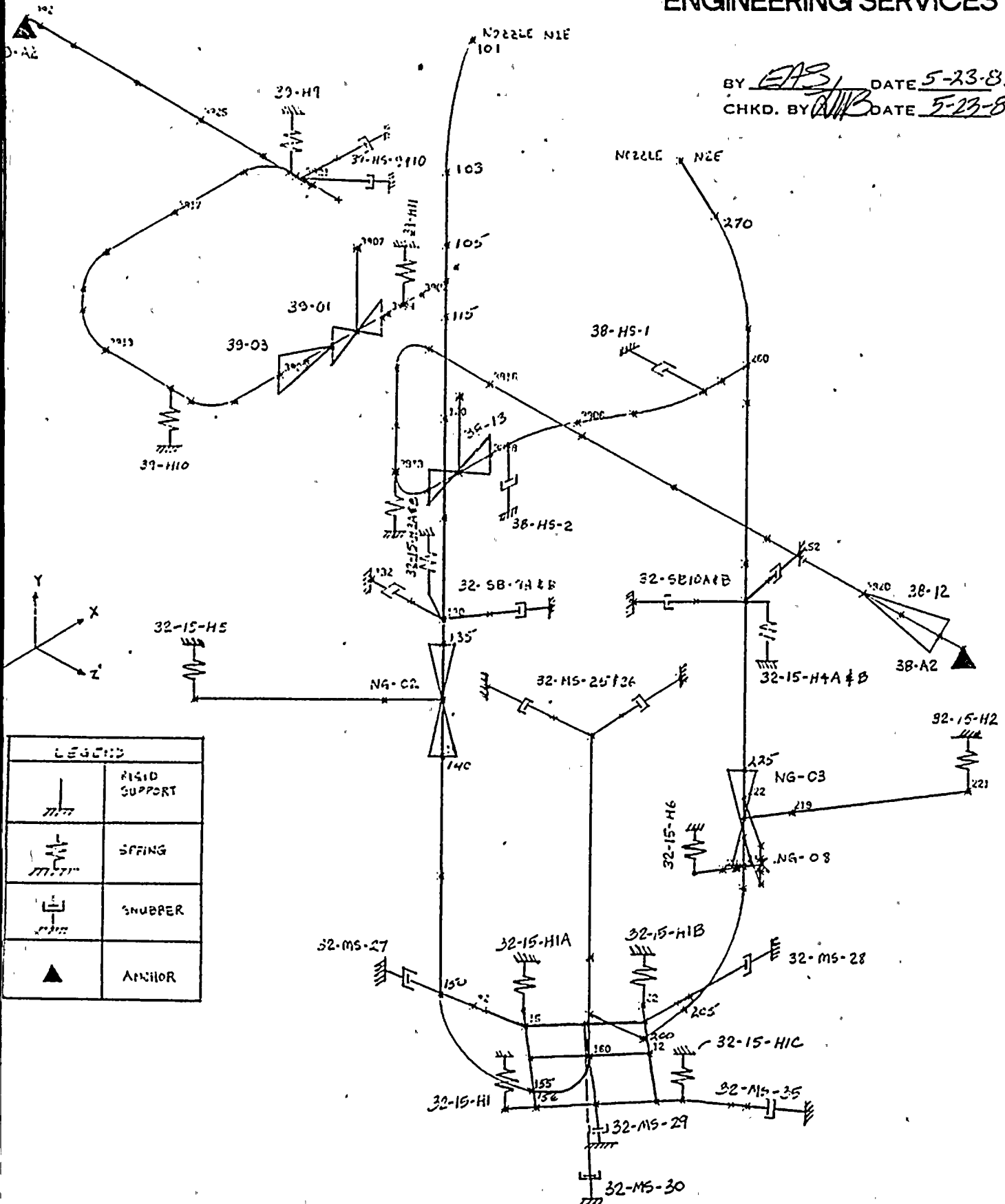


Figure 1. Node Diagram for NMP-1 Recirculation Piping System

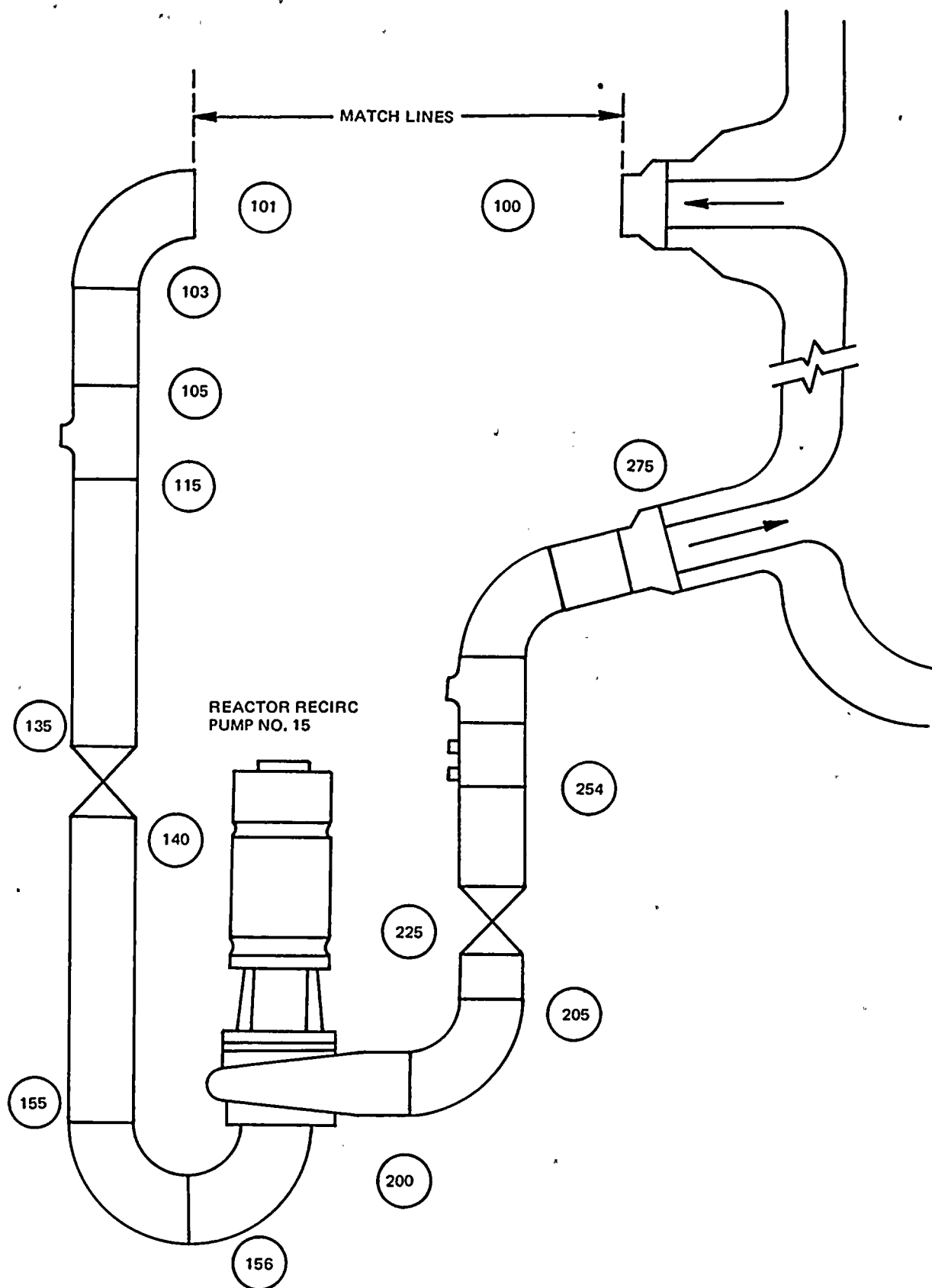


Figure 2. Node Locations for Stress Rule Indices Calculated for Loop 15.

SECTION V

MATERIALS AND FABRICATION HISTORIES

The five 28-inch recirculation loops were constructed of Type 316 stainless steel pipes, elbows and fittings. The straight sections of pipe consisted of rolled and welded plate and were fabricated by the National Annealing Box Co. The elbows and reducing tees were fabricated by the Crane Co. and were also formed from wrought plate. Following fabrication all of the wrought pipes, elbows, and reducing tees were solution annealed and water quenched. Shop welded subassemblies were prepared by the Grinnell Co. No additional heat treatment was performed.

The National Annealing Box piping was produced from four heats of material which contained 0.042% to 0.055% carbon. The elbows and reducing tees were fabricated from nineteen heats of material ranging from 0.050 to 0.075%C. In all but a few cases the heats from which specific sections of piping were fabricated is not known. The ten furnace sensitized recirculation safe ends were made from a heat of 0.054%C material.

RECIRCULATION SYSTEM CONFIGURATION

The five 28-inch diameter recirculation loops are shown in Figures 1 through 5 of Section II, "Extent and Distribution of Cracking". Each weld is identified as either a shop or field weld. The weld numbers correspond to the recirculation piping isometric diagram. Each portion of the system that includes one or more shop welds and is bounded by field welds is one subassembly. The subassembly welds (shop welds) were made by the Grinnell Co. Loops 11 and 14 are identical but differences exist among the remainder of the recirculation loops due to the number and location of reducing tees and spool pieces.

The wrought portion of the recirculation system was constructed of 31 lengths of rolled and welded piping, 15 90° elbows, 5 76° elbows, several reducing tees, and ten safe ends. The valves, pump dishes, and the elbows directly beneath the pumps were all made from cast stainless steel, and will not be discussed further since IGSCC was confined to the wrought piping. The remainder of this chapter consists of a discussion of the material and fabrication of the wrought recirculation system components.

MATERIAL AND FABRICATION

A. Pipe

The straight segments of piping were manufactured by the National Annealing Box Co. and consist of rolled and welded Type 316 stainless steel plate material. The applicable ASTM specifications are A358 for the plate and A240 for the pipe, in accordance with General Electric purchase specification 21A2103. A total of 31 straight segments of pipe were produced for Nine Mile Point 1. The part No., length, material heat No. and slab No. for each section are listed in Table 1. This data was compiled from the recirculation piping material Test Certifications, which are found in Appendix A. The parent plate material was produced by Allegheny-Ludlum. Four heats of material ranging from 0.042 to 0.055%C were used. The chemical analyses of these heats are given in Table 2. The corresponding mechanical properties are given in Table 3.

Although it is possible to determine the heat of material from which a particular pipe number was fabricated, the distribution of the pipes within the recirculation system is not known. Hence a correlation between pipe cracking and heat number cannot be developed. Table 4 lists the number of pipes from each heat and the corresponding carbon content.

The longitudinal seam welds (one per pipe) were performed by an automatic submerged-arc process per National Annealing Box procedure 7840-A. This procedure required that the as-deposited weld metal contain a minimum of 5% ferrite as determined by the Shaeffler diagram using the weld metal check analysis. The chemical composition and calculated ferrite content of the weld metal is given in Table 9.

Following welding the pipe was solution annealed per National Annealing Box procedure 7844-B, which specified heating to 1900°F-2050°F for 1 hour per inch of thickness and water quenching. This procedure required that cooling between 1700°F and 1000°F be accomplished in three minutes or less, and that rapid cooling continue to below 800°F. Electrochemical Potentiokinetic Reactivation (EPR) measurements made at the site and at the Vallecitos Nuclear Center have verified that the pipe base material is in the solution annealed condition.

B. Elbows and Tees

The 90° elbows (three per loop), 76° elbows (one per loop) and reducing tees were supplied by the Crane Co., Midwest Fitting Division. These components were manufactured in accordance with ASTM A403 Type 316 plate material. Note that each loop also contains a cast 90° elbow located directly beneath the pump.

As in the case for the straight pipes, available records do not indicate the heats of material to which particular elbows belong. The chemical analysis of the parent material is available however. Table 5 lists 10 heats used for 90° and 76° elbows, and Table 6 lists an additional 9 heats identified as having been used for reducing tees. It is likely that some of this material was used for plants other than Nine Mile, but the fittings used at Nine Mile were fabricated from among these heats. The range of C content is 0.050% to 0.075%.

On-site examination of certain sections of recirculation piping revealed heat numbers stamped on some elbows. Originally it was required that heat numbers be stamped on all of the elbows, but it is likely that many were eliminated by weld-prep machining or covered by the weld crown. The elbows on which heat numbers were found are listed in Table 7. Of these, cracking was discovered in all except one (loop 12 suction), and there was at least one cracking incident for each heat of material identified.

Available records indicate that all of the elbows and tees supplied by Crane were solution annealed per Crane Co. procedure MWP-WP316-AN1, which specified heating to 2000°F ± 25°F for one hour per inch of thickness followed by water quench. Cooling below 800°F was required in three minutes or less. EPR measurements have verified that the elbow base material is in the solution annealed condition.

C. Safe-Ends

The ten 28-inch recirculation safe-ends are Type 316 stainless steel forgings per ASTM A336. Although solution heat treated following fabrication, the safe-ends were subsequently post-weld-heat-treated with the reactor vessel, which caused them to become sensitized. All ten safe-ends were fabricated from the same heat of material, which contained 0.054%C. The chemical analysis of the safe-end material is given in Table 8:

WELDING

The GE purchase specification for the Nine Mile Point 1 recirculation system required all welded joints to be made by the inert-gas tungsten-arc process with internal inert gas purging for at least the root pass and second layer. Shielded metal arc was allowed for the remainder of the weld.

Weld filler metal was required to meet ASTM A298 or A371 or equivalent for other processes. Austenitic stainless steel weld deposits (all pressure boundary welds from safe-end to safe-end) were required to contain controlled amounts of ferrite. Both 5% ferrite minimum and %Cr \geq 1.9% Ni were allowable acceptance criteria. A summary of the austenitic filler metal used for pressure boundary welds in the recirculation system is given in Table 10. The filler identified in Table 10 as having been used by National Annealing Box and Crane was for longitudinal weld seams in pipes and elbows. The Grinnell filler metal and consumable inert rings were used for shop welds.

The heat input during welding was estimated using the equation:

$$H \text{ (joules/inch)} = \frac{\text{Current} \times \text{Voltage}}{\text{Travel Speed}}$$

and using maximum values for the current and minimum values for the travel speed. Heat input estimates for typical shop and field welds are given below:

1. Typical Grinnell Shop Weld

GTAW Root Pass:	H = 36,000 joules/inch
SMAW Second Pass:	H = 26,250 joules/inch
SMAW Cover Pass:	H = 79,800 joules/inch

2. Typical Field Welds

GTAW Root Pass:	H = 36,000 joules/inch
SMAW Second Pass:	H = 25,000 joules/inch
SMAW Cover Pass :	H = 44,550 joules/inch

TABLE 1.

SUMMARY OF NATIONAL ANNEALING BOX 28-INCH PIPE

<u>PART NO.</u>	<u>LENGTH</u>	<u>HEAT</u>	<u>SLAB</u>
7835-1	7 ft 9.25 in	340041	4
2	✓	✓	✓
3			
4			
5			
7844-1	22 ft 9.00 in	29151	2
2	22 ft 9.00 in	46550	1
3	19 ft 3.0 in	46580	1
4	15 ft 9.00 in	29151	2
5	13 ft 5.50 in	340039	6
6	✓	✓	7
7			7
8			6
9	12 ft 9.00 in	340041	3
10	12 ft 1.00 in	29151	3
11	11 ft 8.50 in	29151	1
12	✓	340041	3
13		29151	1
14		340041	3
15	9 ft 11.50 in	340041	3
16	9 ft 8.50 in	29151	3
17	3 ft 3.75 in	340039	6
18	✓	✓	7
19			7
20			6
21		29151	2
22	1 ft 4 in	✓	6
23	✓	✓	7
24			7
25			6
26		46580	1

TABLE 2.

CHEMICAL ANALYSIS OF ALLEGHENY-LUDLUM PLATE

<u>HEAT</u>	<u>C</u>	<u>Mn</u>	<u>P</u>	<u>S</u>	<u>Si</u>	<u>Cr</u>	<u>Ni</u>	<u>Mo</u>
340039	.055	1.60	.023	.010	.55	17.40	13.00	2.42
340041	.049	1.62	.024	.010	.55	17.10	13.50	2.46
29151	.049	1.63	.016	.017	.68	17.20	13.52	2.39
46580	.042	1.66	.018	.013	.45	17.62	13.40	2.77

TABLE 3.

PHYSICAL PROPERTIES OF ALLEGHENY-LUDLUM PLATE

<u>HEAT</u>	<u>SLAB</u>	<u>YS (psi)</u>	<u>UTS (psi)</u>	<u>ELONG (%)</u>	<u>RA (%)</u>	<u>BHN</u>
340039	1	44900	86700	60	67.9	156
	2	45700	86800	55	70.1	163
	3	42800	87600	50	69.6	153
	4	44200	86300	60	69.0	156
	5	43000	89500	60	69.0	156
	6	42900	88400	55	69.4	156
	7	46000	88400	52	65.7	170
29151	1	43400	83700	61	71.4	159
	2	39200	81900	64	69.3	143
340041	3	38900	82100	65	69.5	143
	4	41000	78100	70	71.0	143
	?	41300	81700	63	73.0	149
29147	4	46200	85800	55	68.0	159
46850	1	42700	32900	56	68.8	149

TABLE 4.

PIPING BREAKDOWN BY HEAT NO.

<u>HEAT</u>	<u>NO. PIPES</u>	<u>FRACTION</u>	<u>%C</u>
340039	12	39%	0.055
340041	9	29	0.049
29151	7	23	0.049
46580	3	10	0.042

TABLE 5.
CHEMICAL ANALYSIS OF CRANE CO. ELBOW MATERIAL

<u>HEAT</u>		<u>C</u>	<u>Mn</u>	<u>P</u>	<u>S</u>	<u>Si</u>	<u>Cr</u>	<u>Ni</u>	<u>Mo</u>
45015	Mill	.061	1.60	.026	.022	.49	17.13	13.37	2.50
	Check	.065	1.62	.029	.026	.50	17.11	13.34	2.58
65122	Mill	.060	1.77	.025	.011	.52	17.32	12.76	2.39
	Check	.059	1.79	.024	.014	.51	17.36	12.70	2.40
45109	Mill	.053	1.80	.025	.010	.59	17.26	13.02	2.29
	Check	.055	1.78	.028	.012	.60	17.30	13.00	2.26
44839	Mill	.057	1.53	.020	.021	.59	17.04	13.13	2.24
	Check	.060	1.50	.020	.020	.60	17.08	13.10	2.30
44842	Mill	.057	1.70	.019	.010	.45	17.13	12.86	2.24
	Check	.061	1.70	.020	.013	.47	17.10	12.80	2.19
45012	Mill	.061	1.46	.020	.020	.51	16.90	12.96	2.57
	Check	.060	1.45	.021	.020	.50	16.89	12.97	2.55
45110	Mill	.060	1.48	.022	.016	.53	17.28	13.15	2.27
	Check	.062	1.48	.020	.015	.50	17.30	13.13	2.25
65120	Mill	.061	1.55	.022	.020	.64	16.88	13.44	2.45
	Check	.063	1.59	.021	.020	.66	16.80	13.48	2.40
44840	Mill	.051	1.57	.021	.021	.63	17.18	13.22	2.25
	Check	.057	1.55	.022	.020	.59	17.17	13.18	2.20
65077	Mill	.052	1.55	.024	.013	.61	16.95	12.90	2.28
	Check	.050	1.58	.021	.012	.61	17.00	12.88	2.30

TABLE 6.
CHEMICAL ANALYSIS OF CRANE CO. REDUCING TEE MATERIAL

<u>HEAT</u>		<u>C</u>	<u>Mn</u>	<u>P</u>	<u>S</u>	<u>Si</u>	<u>Cr</u>	<u>Ni</u>	<u>Mo</u>
65121	Mill	.056	1.85	.022	.020	.61	17.17	13.09	2.20
	Check	.060	1.80	.020	.024	.59	17.11	13.10	2.22
44838	Mill	.054	1.80	.022	.017	.62	17.32	12.88	2.30
	Check	.060	1.81	.019	.021	.60	17.29	12.95	2.31
65123	Mill	.058	1.74	.024	.022	.53	17.27	13.00	2.23
	Check	.061	1.70	.020	.020	.55	17.30	13.04	2.23
45153	Mill	.059	1.64	.020	.013	.57	17.26	13.00	2.30
	Check	.060	1.65	.022	.014	.55	17.20	13.08	2.28
45030	Mill	.065	1.65	.019	.011	.62	17.13	12.92	2.47
	Check	.066	1.64	.020	.010	.62	17.20	12.89	2.42
45139	Mill	.060	1.70	.025	.028	.54	17.35	13.04	2.25
	Check	.061	1.68	.020	.026	.55	17.30	13.01	2.24
45157	Mill	.057	1.71	.025	.009	.47	17.35	13.06	2.27
	Check	.060	1.70	.021	.011	.50	17.33	13.07	2.30
45043	Mill	.066	1.69	.024	.020	.45	17.69	12.97	2.30
	Check	.062	1.70	.020	.020	.46	17.60	12.99	2.30
64788	Mill	.068	1.44	.020	.012	.63	17.25	12.91	2.01
	Check	.075	1.25	.008	.023	.52	16.47	13.43	2.04

TABLE 7.

LIST OF ELBOWS WITH KNOWN HEAT NO.

<u>ELBOW TYPE</u>	<u>LOOP</u>	<u>SURROUNDING WELDS</u>	<u>HEAT</u>	<u>%C</u>
90°	12 Suction	SW 4, FW 5	44840	0.054
76°	12 Discharge	SW 18, FW 28	45015	0.063
90°	13 Suction	SW 6, FW 9	44840	0.054
76°	13 Discharge	SW 21, FW 33	45015	0.063
76°	14 Discharge	SW 24, FW 38	45109	0.054

TABLE 8.

CHEMICAL ANALYSIS OF SAFE-END MATERIAL

<u>HEAT</u>	<u>C</u>	<u>Si</u>	<u>P</u>	<u>Mn</u>	<u>S</u>	<u>Ni</u>	<u>Cr</u>	<u>Mo</u>
E-5349	.054	.50	.020	1.69	.009	10.84	18.00	2.37

TABLE 9.

SUMMARY OF WELDING FILLER COMPOSITIONS AND
CALCULATED FERRITE CONTENT

	<u>Weld Metal Supplier</u>	<u>Heat No.</u>	<u>C</u>	<u>Mn</u>	<u>P</u>	<u>S</u>	<u>Si</u>	<u>Cr</u>	<u>Ni</u>	<u>Mo</u>	<u>N</u>	<u>% Ferrite Schaeffler</u>
National Annealing Box Company			.036	1.47	-	-	.45	18.70	12.70	2.70	-	5
			.045	1.60	-	-	.54	18.80	12.65	2.75	-	5
			.041	1.64	-	-	.64	18.80	12.35	2.78	-	6½
			.057	1.56	-	-	.58	18.40	12.20	2.64	-	4½
			.048	1.64	-	-	.60	18.80	12.15	2.78	-	6½
			.044	1.52	-	-	.64	18.80	12.25	2.62	-	6½
5-12 Crane Mid West Fitting Division	Arcos	C8036- T316 S-16-5B7F	.053	1.24	.062	.016	.51	16.84	11.18	2.17	-	5
Grinnell Company	Arcos Chro- mend 316	4N105A	.028	2.16	.014	.008	.29	18.97	12.00	2.37	-	6
	Chro- menar	7776- 316L	.011	1.88	.004	.011	.39	19.49	11.94	2.39	.045	9
	Consumable Insert Rings		.028	1.58	.021	.019	.48	19.68	13.42	2.36	--	5

SECTION VI

WATER CHEMISTRY AS A POTENTIAL CONTRIBUTING FACTOR

It is known that significant at-temperature operation with out-of-specification water quality can lead to enhancement in IGSCC susceptibility. Therefore, it is important to review the long term and transient water chemistry history at NMP-1 and to compare this history with that of other BWR plants with significantly higher and lower incidences of IGSCC.

EVALUATION OF GENERAL ELECTRIC WATER CHEMISTRY DATA BASE FOR NMP-1

This section summarizes the relevant water chemistry data from the Nine Mile Point reactor. These data are maintained in the General Electric Plant Chemical and Radiation Technology time share files. These files are submitted monthly by each utility to General Electric to demonstrate compliance to the contractual fuel warranty operating limits. The forms are sent to key punch operators who transcribe the data onto magnetic tape. While some verification effort has been made on the data from each plant, there are undoubtedly a few transcription errors which have not been corrected.

The chemistry parameters which are maintained in the data base and are plotted in this report are as follows:

1. Reactor Water

A. Weekly Average Conductivity (uS/cm at 25°C)

This is a numerical average of 5-7 daily readings in a given week.

B. Weekly Maximum Conductivity (uS/cm at 25°C)

The highest value from A in a given week.

C. Weekly Average Chloride Concentration (ppb)

This is a numerical average of 5-7 daily measurements in a given week.

D. Weekly Maximum Chloride Concentration (ppb)

The highest value from C in a given week.

E. Hydrogen Ion Concentration (pH at 25°C)

This can be a weekly average or perhaps only a single measurement in a given week.

F. Silica Concentration (ppb)

This can be a weekly average or perhaps only a single measurement in a given week.

2. Feedwater

A. Weekly Average Conductivity (uS/cm at 25°C)

Same as reactor water.

B. Weekly Maximum Conductivity (uS/cm at 25°C)

Same as reactor water.

C. Dissolved Oxygen Concentration (ppb)

This can be a weekly average or perhaps only a single measurement in a given week. Maximum data are provided when there is more than one analysis in a week.

D. Metallic Impurities (ppb)

There are many variations in presenting these data.

1. Insoluble Fe
2. Soluble Fe

3. Total Fe
4. Insoluble Cu
5. Soluble Cu
6. Total Cu
7. Total Metals (Fe, Cu, Ni, Cr)
8. Total Fe + Cu

Of these, the most important are Total Metals (dominated by Insoluble Fe) and Total Cu where fuel warranty limits have been established for these parameters.

Most of the data presented encompass the time period from plant startup in 1969 to the shutdown in early 1982. For better readability, each set of data is presented as two plots - 1969 to 1977 and 1975 to 1982. Large time gaps where data are not presented generally reflect a refueling or extended maintenance outage.

A. Reactor Water Conductivity

The weekly average and weekly maximum reactor water conductivities are shown in Figures 1-4. As a reference point for the discussion, the fuel warranty normal operational limit is 1.0 uS/cm at 25°C for steaming rates greater than 1% of rated steam flow. The warranty allows for an interval of 14 days per 12-month period where the conductivity can be in excess of 1.0 uS/cm; above 10 uS/cm the limiting condition for operation, plant shutdown is required.

An eyeball average of the data would indicate a typical conductivity of 0.4-0.5 uS/cm, with substantially better water quality observed after 1979. In an EPRI funded review of the NMP-1 water chemistry¹, it is pointed out that conductivity levels of 1-2 uS/cm were present. However, these higher conductivities were not representative of routine operation but rather correspond to the relatively frequent conductivity, mini-excursions in excess

¹R. L. Cargill (NUTECH), EPR-09-101, January 1983, "Report on the Field Investigation of Recirculation System Pipe Cracking at Nine Mile Point 1"

of 1 uS/cm that occurred in the 1971-76 period, (Figures 3 and 4). The highest conductivity observed (30.0 uS/cm) occurred in June, 1971, and was due to poor water quality in the condensate storage tank. The maximum chloride concentration during this intrusion was 232 ppb. Compared to conductivities of other BWR's, Table I, Nine Mile Point reactor water chemistry is about average. No conductivity excursions have been reported since 1979.

B. Reactor Water Chloride

The weekly average and maximum chloride readings are shown in Figures 5-8. Again as a reference, the normal operating limit for chloride ion is 200 ppb for steaming rates in excess of 1% rated steam flow. The chloride concentration may be in excess of 500 ppb for an interval of 14 days per 12-month period. The NMP 1971 Technical Specification is substantially more liberal (1000 ppb). The average chloride concentration has been in the vicinity of 40-50 ppb with a few excursions in excess of 200 ppb; no power excursions have been reported since 1977. Like conductivity, the chloride ion concentration has generally decreased since 1977.

A comparison of the geometric average of weekly maximum reactor water chloride level at NMP-1 with all other BWR's in the fuel warranty data base is presented in Table 2. Note that although NMP-1 is among the six highest plants based on the 1 standard deviation (upper 84% value) above the geometric average for this chloride concentration, its actual value of 89.5 ppb lies well below the 200 ppb specification limit and within 30 ppb of the upper 84% value of 59.2 ppb for an average plant in the data base. Thus, it does not appear that the steady state chloride levels are an IGSCC aggravating factor.

C. Hydrogen Ion Concentration (pH)

The Nine Mile Point pH data are shown in Figures 9 and 10. Routine pH measurements are not required in the General Electric fuel warranty document except when the conductivity is out of specification. The 1.0 uS/cm conductivity operational limit bounds the pH range from 5.6 to 8.6. The maximum

fuel warranty limit range is pH 4 to 10. Most pH measurements are performed in the laboratory on grab samples. Due to carbon dioxide uptake by the sample, the measurements are not extremely reliable; the high purity of the water compounds the measurement difficulty.

The pH data reported by the NMP chemistry group are consistently on the acidic side and are generally within specification. However, many data points in 1980 and 1981 fall in the range of pH 5.0 to 5.5. The average and maximum conductivity readings in the same time period cannot support the pH data, implying one or both measurements are in error.

D. Reactor Water Silica

NMP silica data are shown in Figures 11 and 12. The analysis of silica is not required in the fuel warranty document. The information is useful to provide guidance for the changeout of reactor water cleanup demineralizers. A normal operating maxima of 200 ppb has been suggested, along with a tighter administrative limit of 100 ppb.

Substantial improvement in cleanup system performance has been observed since 1978. The appearance of the trend is consistent with the cleanup demineralizers being changed once per fuel cycle. Cleanup system operation before 1978 fluctuated significantly.

E. Feedwater Conductivities

The average and maximum feedwater conductivities are shown in Figures 13-16. While there is no fuel warranty specification on feedwater conductivity, a limit of 0.1 uS/cm was established for the common effluent of the condensate treatment system. A 4-hour time interval above this limit is allowed for each incident. Routine operation is characterized by a conductivity of 0.07 uS/cm. There have been spikes in excess of 0.1 uS/cm, some of them approaching or exceeding 1.0 uS/cm. Most of these spikes appear to be the result of changing condensate demineralizers, since comparable spikes do not appear in the reactor water plots.

F. Feedwater Dissolved Oxygen

Feedwater dissolved oxygen concentrations are shown in Figures 17 and 18. Fuel warranty limits are 20-200 ppb for operation greater than 10% power. The maximum and minimum values were established to protect the carbon steel feedwater piping from generalized corrosion. Normal operation at Nine Mile Point is 30-40 ppb. No excursions in excess of 200 ppb have been reported; in a few cases the dissolved oxygen concentration has dropped below 200 ppb.

G. Metallic Impurities

The fuel warranty limitation for metallic impurities (soluble and insoluble) is 15 ppb (Fe, Cu, Ni, Cr) for operation above 50% power, with the usual interval of 14 days per 12-month period allowed for concentrations in excess of 15 ppb. Of this value, a separate limit was established for Cu (<2 ppb). For startups, less stringent limits were provided. The plots for total metals are shown in Figures 19 and 20. There have been several excursions in excess of 15 ppb, but only 4 since 1978. Copper concentrations are shown in Figure 21 and 22. No excursions in excess of the 2 ppb warranty limit have been reported.

EVALUATION OF WATER CHEMISTRY TRANSIENTS

In one study, Radiological and Chemical Technology, Inc. conducted an evaluation of conductivity and chloride transients at Nine Mile Point and 19 other BWR's (EPRI Report No. NP-1603). For each plant, attempts were made to define all the occasions where the conductivity and chloride concentrations were out of specification during operating and shutdown conditions. The Nine Mile Point data encompass the period from startup through early 1978. Table 3 shows the maximum Nine Mile Point-1 chloride and conductivity transient values for each excursion in this study. Without extrapolating or interpolating beyond the actual reported data, attempts were made by Radiological and Chemical Technology, Inc., to estimate the integral number of days that each parameter was out of specification for each event. The highest chloride concentration observed (683 ppb) occurred during a shutdown in 1977. 80% of the total integrated chloride excursions have occurred during shutdown where the probability

of stress corrosion damage to piping is extremely low, while 63% of the integrated conductivity transients have occurred during power operation. The highest at power chloride concentration and conductivity observed through early 1978 were 287 ppb and 30 uS/cm, respectively.

The maximum at power chloride and conductivity transient values for the 20 plants in the study are shown in Table 4. As can be seen, when ranked from lowest to highest, NMP-1 is 7th for chloride and 16th for conductivity. It cannot be inferred from these maximum values alone that one plant is better or worse than another in terms of potential effect of transient Water Chemistry on pipe crack propensity. In addition to these peak values, the integrated transient time history of conductivity and chloride values above the specification limit have been evaluated and are listed in Table 5. For both of these time weighted parameters, Nine Mile Point-1 lies slightly below the median for all plants indicating its performance has been typical for those plants in the evaluation.

In order to better reflect the effect of plant age on integral transient severity, Radiological and Chemical Technology attempted to normalize the previous data by dividing by plant age. The ranking of this age normalized parameter is shown in Table 6. Again, NMP-1 lies at the median value indicating typical plant performance. Further, if the absolute values of these transient chloride and conductivity parameters are examined, it is seen that the NMP-1 values are over one order of magnitude better than for the "worst" plants.

Although the EPRI study treated transient chemistry behavior in an integrated comparative sense it is also useful to examine the specific transient behavior at NMP-1.

There have been at least two significant water chemistry transients during the plant lifetime. One, which occurred in June 1971, resulted in conductivity values between 8 and 30 uS/cm over 5 hours with the reactor at temperature. The high conductivity resulted from water pumped from the waste collection tanks through exhausted waste demineralizer beds to the condensate storage tank and then into the reactor. The major impurity was

probably sulfate and the pH was not measured but could have been acid. The second known intrusion occurred in 1979¹, when chlorinated hydrocarbons were introduced into the primary coolant following valve maintenance. This transient was not included in the Radiological and Chemical Technology, Inc., EPRI study.¹

Little is known about the severity of this intrusion except that conductivity and chloride values went well above specification limits for several hours. It is possible but unlikely that these off-chemistry intrusions contributed to early IGSCC initiation in the recirculation piping which then grew slowly over several years to the final March 1982 condition. In previous cases of severe off-chemistry intrusions at other reactors, there was evidence of stress corrosion damage indicated during or shortly following the intrusions. In these cases, damage was indicated by failure of in-core low power range monitors (LPRM). At NMP-1 there was no such damage at any time.

SUMMARY

With respect to the NMP-1 coolant environment, the steady state long term conductivity values have been equivalent to that of a typical BWR, while the weekly maximum chloride levels have been somewhat higher than average although still well within specification. In addition to these steady state values, the two most significant off-chemistry transients have also been evaluated. As a result it is concluded that there is no obvious basis for believing that water chemistry played a significant role in accelerating IGSCC at NMP-1.

¹EPR-09-101 Rev. 1 - Nutech Apt.

Table 1
STEADY STATE CONDUCTIVITY - PLANT COMPARISONS
WEEKLY MAX CONDUCTIVITY, uS/cm

<u>Plant Rank</u>	<u>Geom Mean (1)</u>	<u>Geom Dispersion (2)</u>	<u>Upper 84% Value (3)</u>
1	0.145	1.69	0.25
2	0.210	1.39	0.29
3	0.174	1.82	0.32
4	0.183	2.02	0.37
5	0.287	1.44	0.41
6	0.260	1.58	0.41
7	0.265	1.73	0.46
8	0.242	2.11	0.51
9	0.285	1.79	0.51
10	0.353	1.55	0.55
11	0.347	1.61	0.56
12	0.263	2.26	0.59
13	0.341	1.74	0.59
14	0.227	2.73	0.62
15	0.401	1.90	0.76
16	0.444	1.80	0.80
17	0.524	1.55	0.81
18 (NMP-1)	0.392	2.11	0.83
19	0.393	2.17	0.85
20	0.389	2.31	0.90
21	0.451	2.04	0.92
22	0.603	1.55	0.93
23	0.463	2.15	1.00
24	0.420	2.52	1.06
25	0.499	2.29	1.14
26	0.534	2.21	1.18
27	0.751	1.61	1.21
28	0.583	2.10	1.22
29	0.866	1.46	1.26
30	0.601	2.28	1.37
31	0.547	2.68	1.47
32	0.773	2.15	1.66
33	0.824	2.08	1.71
34	0.948	2.03	1.92
35	0.851	2.32	1.97
36	1.05	1.98	2.08

Table 2
AVERAGE STEADY STATE CHLORIDE LEVELS - PLANT COMPARISONS

WEEKLY MAXIMUM CHLORIDE, ppb

<u>Plant Rank</u>	<u>Geom Mean (1)</u>	<u>Geom Dispersion (2)</u>	<u>Upper 84% Value (3)</u>
1	11.7	1.60	18.7
2	20.0	1.00	20.0
3	20.0	1.00	20.0
4	20.0	1.00	20.0
5	20.3	1.10	22.3
6	20.8	1.10	22.9
7	20.5	1.20	24.6
8	20.8	1.29	26.8
9	16.5	1.78	29.4
10	15.7	2.08	32.7
11	6.9	4.96	34.2
12	27.7	1.32	36.6
13	31.7	1.18	37.4
14	27.6	1.36	37.5
15	14.0	2.09	40.6
16	20.6	2.09	43.1
17	34.2	1.49	51.0
18	50.2	1.06	53.2
19	26.8	2.06	55.2
20	50.4	1.15	58.0
21	50.9	1.18	60.1
22	47.7	1.32	63.0
23	30.5	2.26	68.9
24	34.3	2.03	69.6
25	38.1	1.88	71.6
26	50.9	1.43	72.8
27	42.9	1.73	74.2
28	26.9	2.95	79.4
29	50.7	1.58	80.1
30	32.8	2.66	87.2
31 (NMP-1)	42.2	2.12	89.5
32	52.9	1.95	103.2
33	102.0	1.21	123.4
34	73.0	1.74	127.0
35	67.3	2.03	136.6
36	77.7	1.80	139.9

NOTES FOR TABLES 1 AND 2

- (1) Five to seven reactor water conductivity readings, and approximately three reactor water chloride readings are taken weekly, on different days. The weekly maximum is found, and its geometric mean is calculated. Geom mean is

$$\left(\prod_i^k x_i\right)^{1/k}; \text{ also, antilog of arithmetic mean of } \log x_i \text{ values.}$$

- (2) Geometric dispersion is antilog of standard deviation of $\log x_i$ values.
- (3) Upper 84% conductivity and chloride values are based on log-normality of the weekly maximums. The Upper 84% value is (Geom means \times Geom disp); also, antilog (arith mean of $\log x_i$ values + 1 std dev of $\log x_i$) values. Logs on either base 10 or e can be used throughout.

Example. For $\{x_i\} = 2, 3, 4$, geometric mean of 2.884, geometric dispersion is 1.417, and upper 84% value is 4.085.

Table 3
NINE-MILE POINT CONDUCTIVITY AND CHLORIDE TRANSIENT
VALUES (MAXIMUM AND TIME-INTEGRATED)

Year	Dates	Percent Power	Maximum Value*		Integral**	
			Cond.	Cl	Cond.	Cl
1969	12/16	34	1.30	250	0.10	10.9
1970	1/5-1/9	38	1.56		0.82	
	1/13-1/16	62	2.6		4.34	
	2/3-2/7	80	1.52		0.59	
	12/22-12/26	80	2.20		2.22	
1971	2/24	82	1.42		0.14	
	2/4-5/8	0	3.2		1.06	
	5/18-5/22	0	2.3		0.10	
	6/5-6/9	2	1.95		1.48	
	6/18-6/23	66	→30	232	4.79	3.3
	7/8	70	1.9		0.52	
	10/26-10/30	55	2.4		2.25	
	12/21-12/25	95	1.52		0.59	
	7/31-8/4	83	1.40		1.29	
	8/28	47	2.0		0.83	
1972	9/14	94	2.60	260	1.37	23.3
	9/20	74	2.0		0.86	
	9/25	64	1.5		0.43	
	10/6	81		250		14.8
	10/27-10/31	85	2.5	287	2.81	74.5
	11/30-12/4	82	1.12		0.34	
1974	4/3-4/7	0	5.10		5.32	
	6/18-6/26	0	3.4		→ 8.87	
	7/2-8/1	76	2.0	220	3.39	5.4
	11/26-11/28	93	1.2		0.32	
1976	3/21-3/22	51	1.8	238	1.23	28.1
	4/17	0		120		20.0
	4/22	63	2.2		0.96	
	4/27-4/28	85	2.2	212	0.34	0.24
1977	3/9	0	7.2	683 ←	5.36	327.7←
	6/7-6/11	0	4.0	315	1.67	299.4
	6/14-6/18	0	2.2		0.03	
	6/21-6/25	0	2.5		0.16	
	6/28-7/2	0	3.5		1.08	
	7/5-7/9	0	2.2		0.02	
	7/12-7/16	0 (hot)	1.6		0.68	
	1/17-1/21	71	3.0		7.35	
TOTALS			Reactor at power:		40.02	160.5
			Reactor shutdown:		23.67	647.1

*Units

Conductivity (uS/cm)

Chloride (ug/kg)

→ Highest value

**Conductivity (uS/cm)-da above warranty limits

Chloride (ug/kg)-da above warranty limits

Table 4
CONDUCTIVITY AND CHLORIDE MAXIMA
FOR BWR CHEMISTRY TRANSIENTS

<u>Plant Rank</u>	<u>Plant</u>	<u>Reactor at Power</u> <u>Chloride*</u>	<u>Plant</u>	<u>Reactor at Power</u> <u>Conductivity**</u>
1	7	#	19	2.0
2	8	#	18	2.7
3	12	#	17	5.0
4	15	#	11	5.8
5	16	#	16	6.0
6	19	#	15	6.2
7	1 (NMP-1)	287	20	6.8
8	14	300	10	9.2
9	13	320	7	12.
10	18	355	14	12.
11	10	370	8	13.0
12	4	374	2	13.8
13	6	400	4	14.
14	2	495	12	23.
15	17	495	3	25.6
16	11	600	1 (NMP-1)	30.
17	20	725	13	40.5
18	3	1200	9	72.
19	9	3000	5	84.
20	5	14500	6	95.

* units: $\mu\text{g/kg}$ (ppb)

** units: $\mu\text{S/cm}$

No data reported in excess of 200 $\mu\text{g/kg}$.

Table 5
CONDUCTIVITY AND CHLORIDE INTEGRALS
FOR BWR CHEMISTRY TRANSIENTS

<u>Plant Rank</u>	<u>Plant</u>	<u>Reactor at Power</u> <u>Chloride*</u>	<u>Plant</u>	<u>Reactor at Power</u> <u>Conductivity**</u>
1	7	0	18	3.2
2	8	0	8	5.7
3	12	0	19	6.7
4	15	0	10	7.6
5	16	0	11	9.5
6	19	0	7	13.7
7	13	20	16	14.4
8	18	32	5	19.
9	4	120	15	22.
10	14	120	17	22.
11	10	140	14	35.
12	17.	140	1 (NMP-1)	40.
13	1 (NMP-1)	160	4	51.
14	11	300	9	69.
15	9	1250	12	84.
16	2	1260	20	96.5
17	6	1920	13	99.
18	20	2770	2	112.
19	3	2810	3	206.
20	5	3280	6	530.

* units: ($\mu\text{g/kg}$) - days above the specified limits.

** units: ($\mu\text{S/cm}$) - days above the specified limits.

Table 6
CONDUCTIVITY AND CHLORIDE INTEGRALS
PER YEAR OF PLANT OPERATION
FOR BWR CHEMISTRY TRANSIENTS

<u>Plant Rank</u>	<u>Plant</u>	<u>Reactor at Power</u> <u>Chloride*</u>	<u>Plant</u>	<u>Reactor at Power</u> <u>Conductivity**</u>
1	7	0	8	0.9
2	8	0	10	1.2
3	12	0	18	1.2
4	15	0	11	1.7
5	16	0	7	2.6
6	19	0	19	2.8
7	13	4.0	5	3.1
8	18	12.3	9	6.2
9	10	21.5	15	6.2
10	1 (NMP-1)	28.1	1 (NMP-1)	7.0
11	14	30.0	17	7.8
12	4	40.2	14	8.8
13	17	49.9	20	12.5
14	11	52.6	4	17.1
15	9	112.9	12	17.3
16	20	359.7	13	19.8
17	6	410.8	16	30.1
18	5	537.0	2	72.4
19	2	814.5	3	83.7
20	3	816.6	6	113.4

* units: ($\mu\text{g/kg}$) - days per year of operation.
 ** units: ($\mu\text{S/cm}$) - days per year of operation.

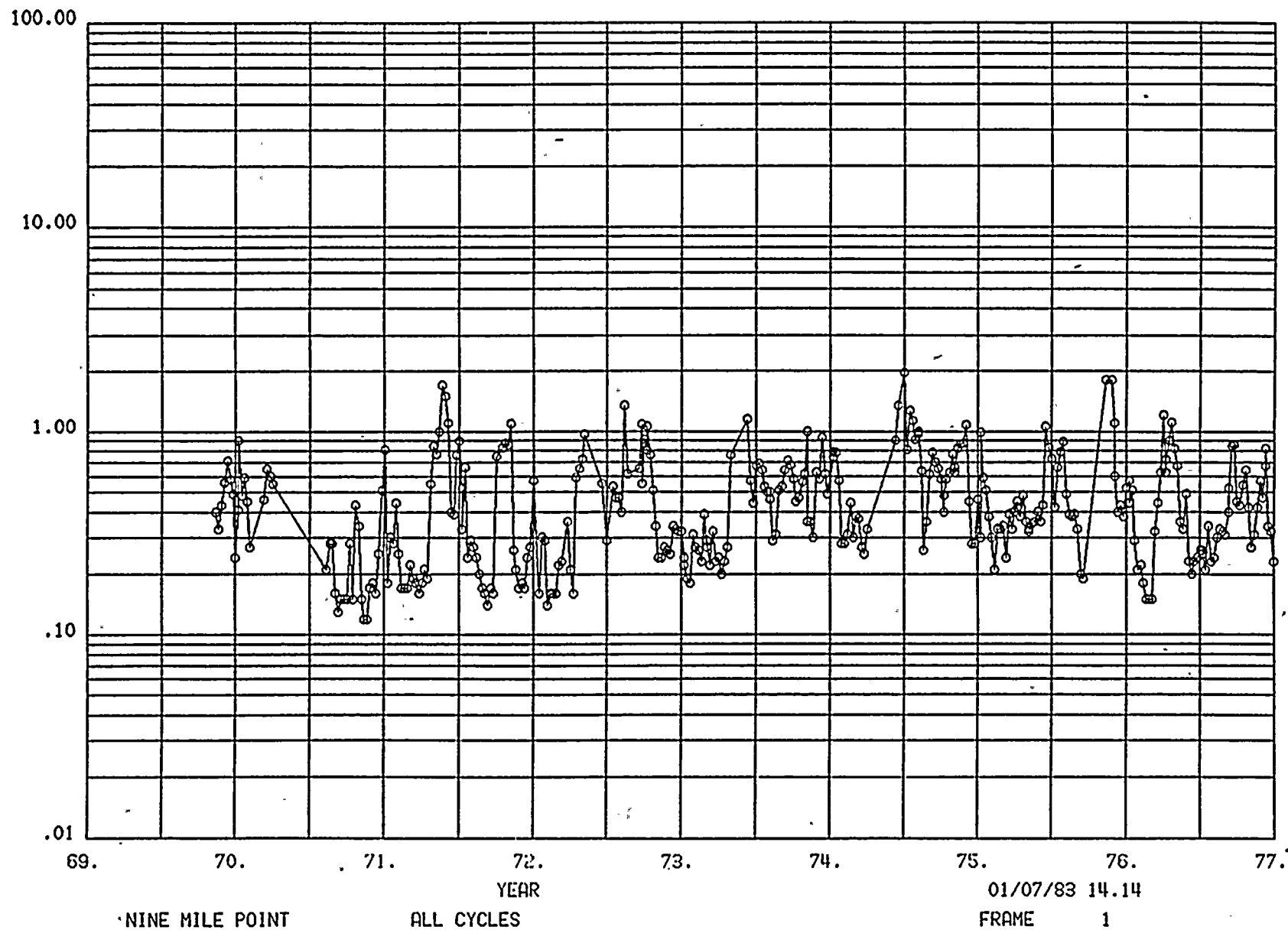
FIGURE 1
REACTOR WATER CONDUCTIVITY AVG. (UMHO/CM)

FIGURE 2

REACTOR WATER CONDUCTIVITY AVG. (UMHO/CM)

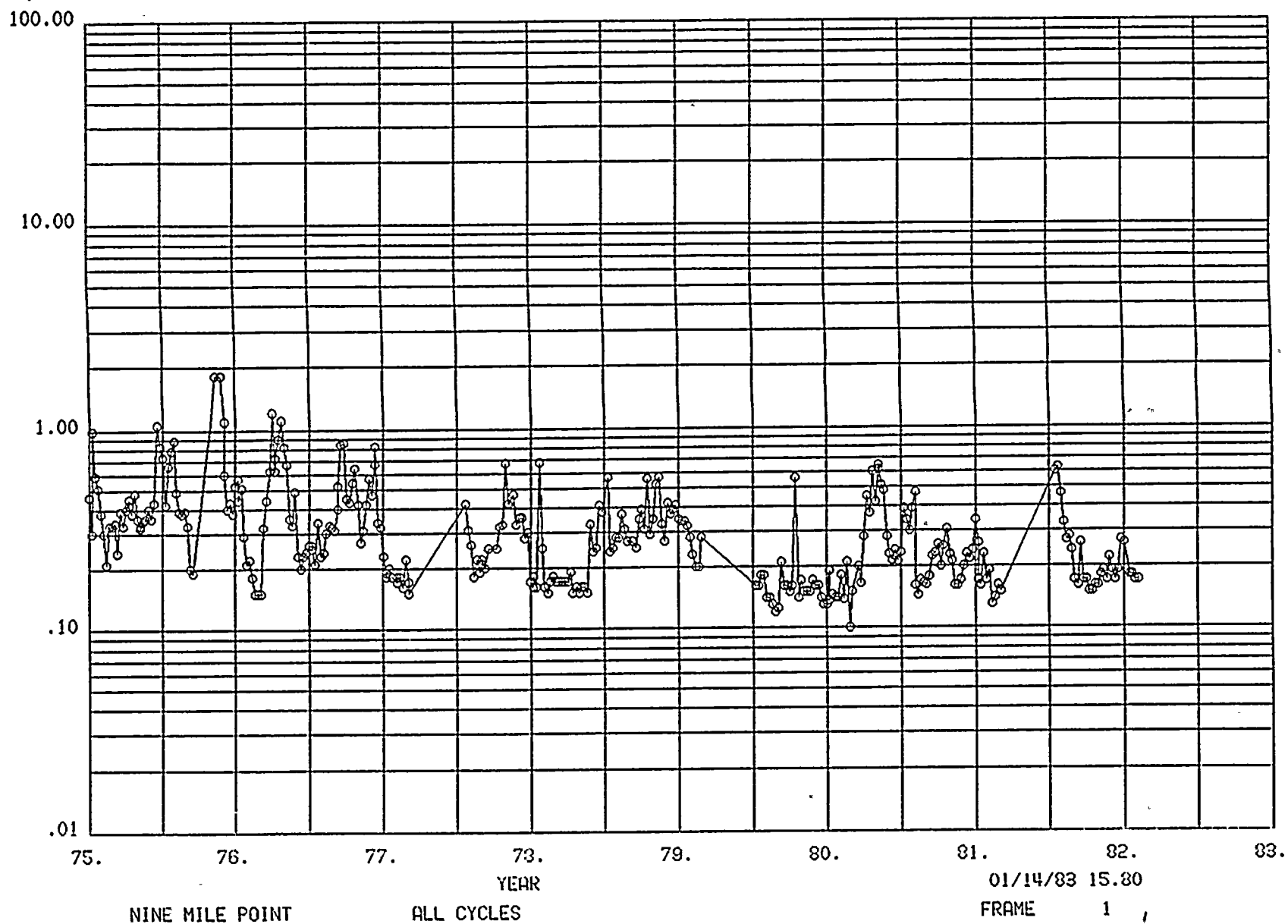


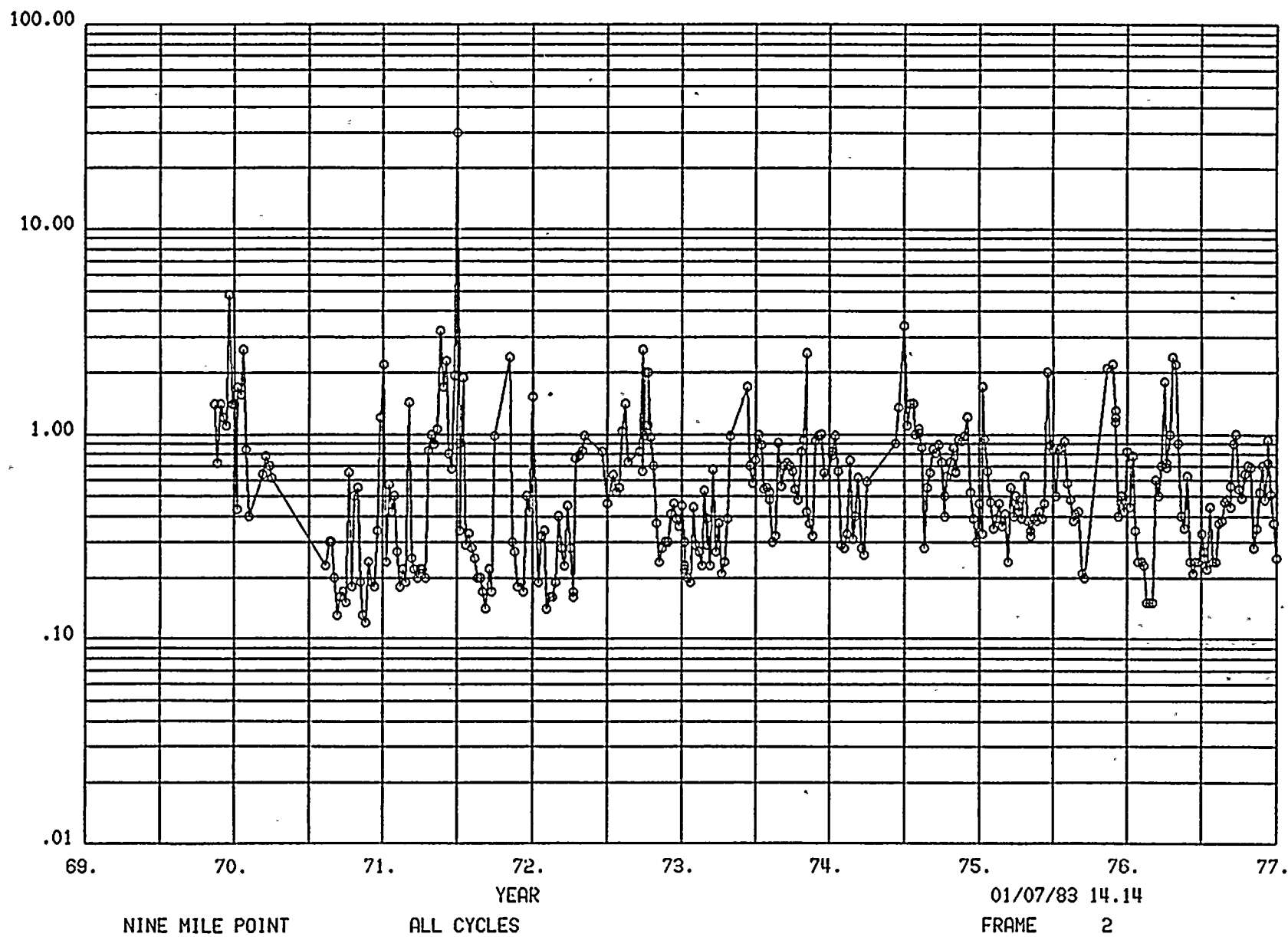
FIGURE 3
REACTOR WATER CONDUCTIVITY MAX. (UMHO/CM)

FIGURE 4
REACTOR WATER CONDUCTIVITY MAX. (UMHO/CM)

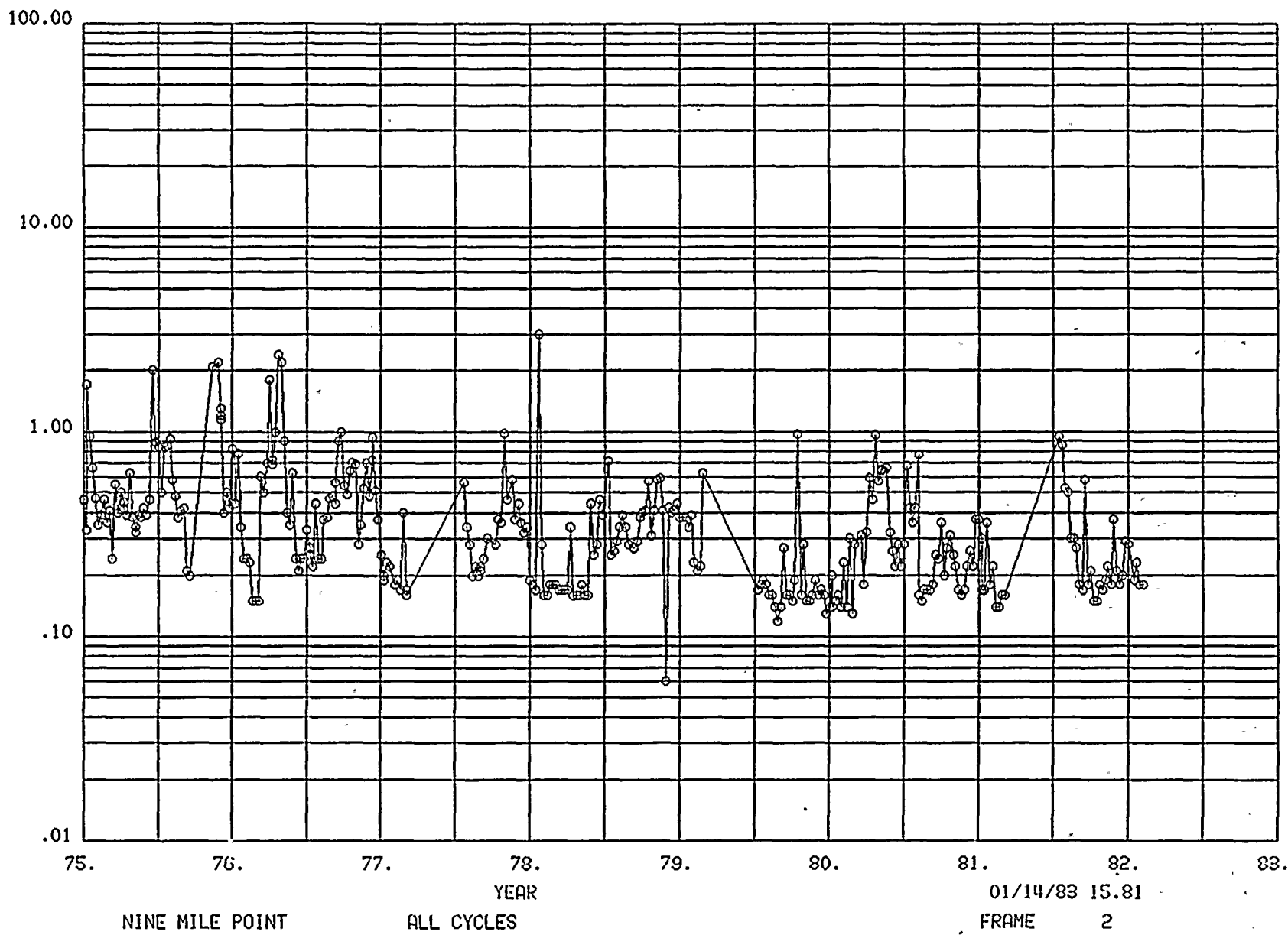
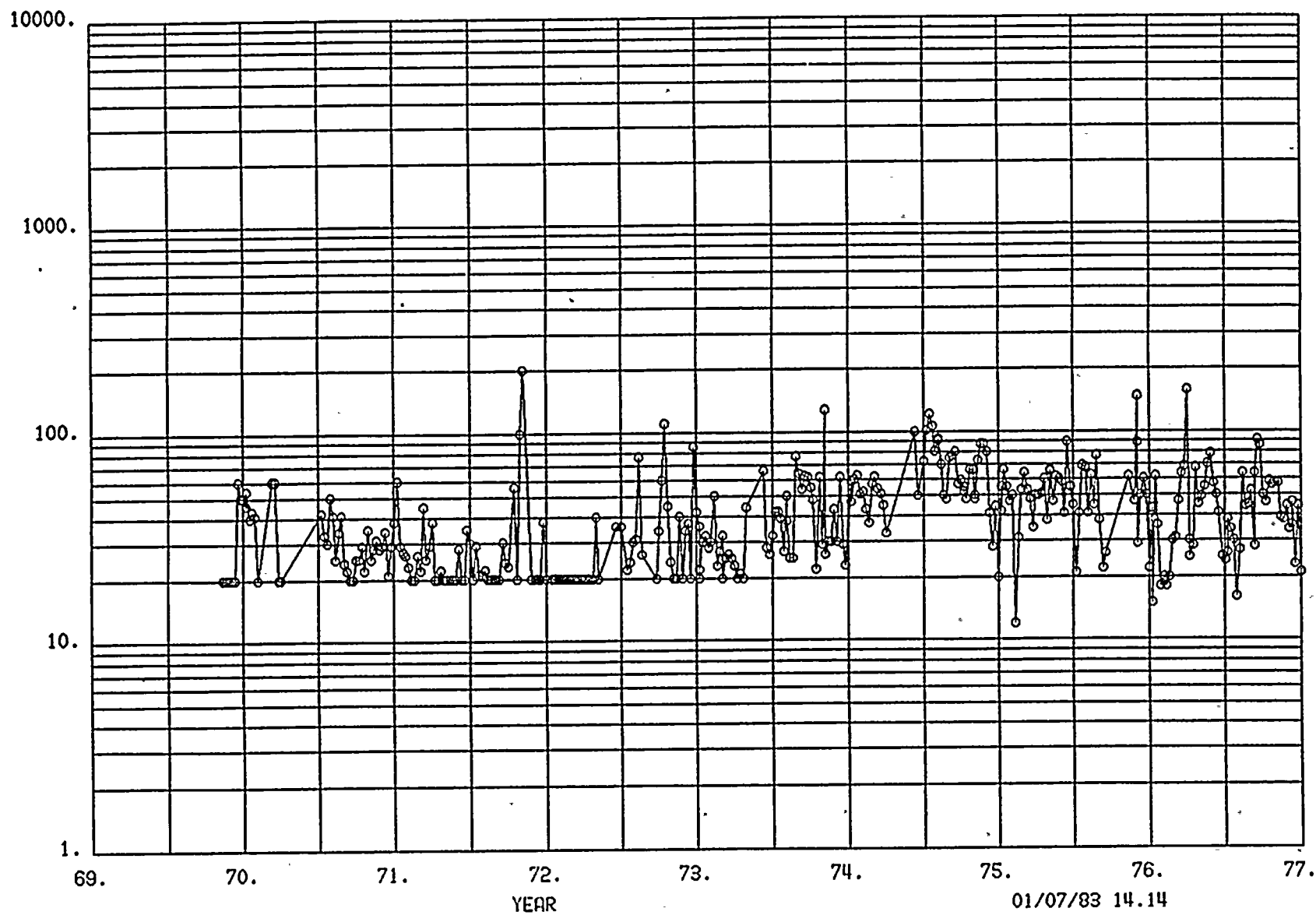


FIGURE 5
REACTOR WATER CHLORIDE AVG. (PPB)



NINE MILE POINT

ALL CYCLES

01/07/83 14.14

FRAME 3

FIGURE 9

REACTOR WATER CHLORIDE AVG. (PPB)

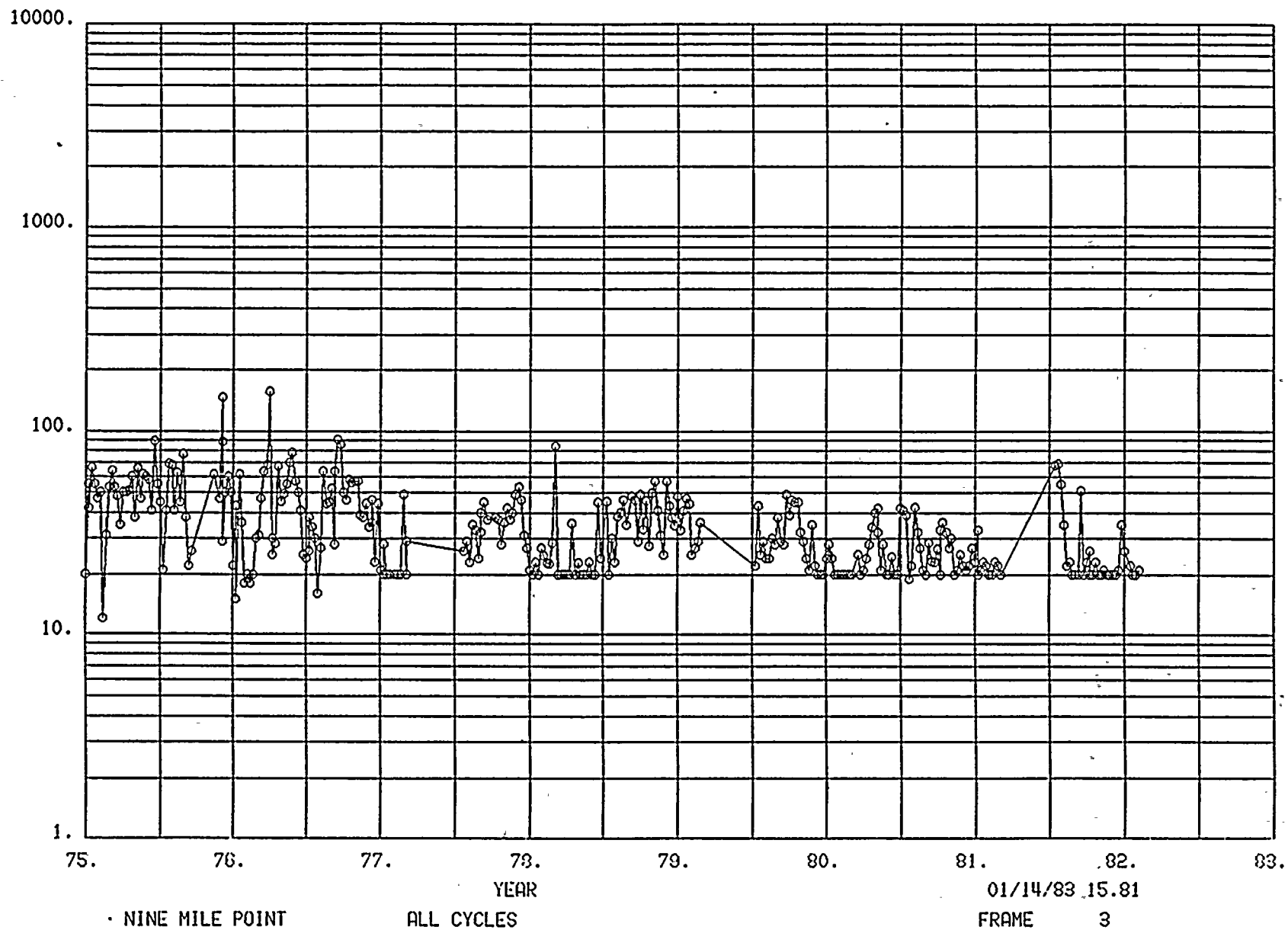


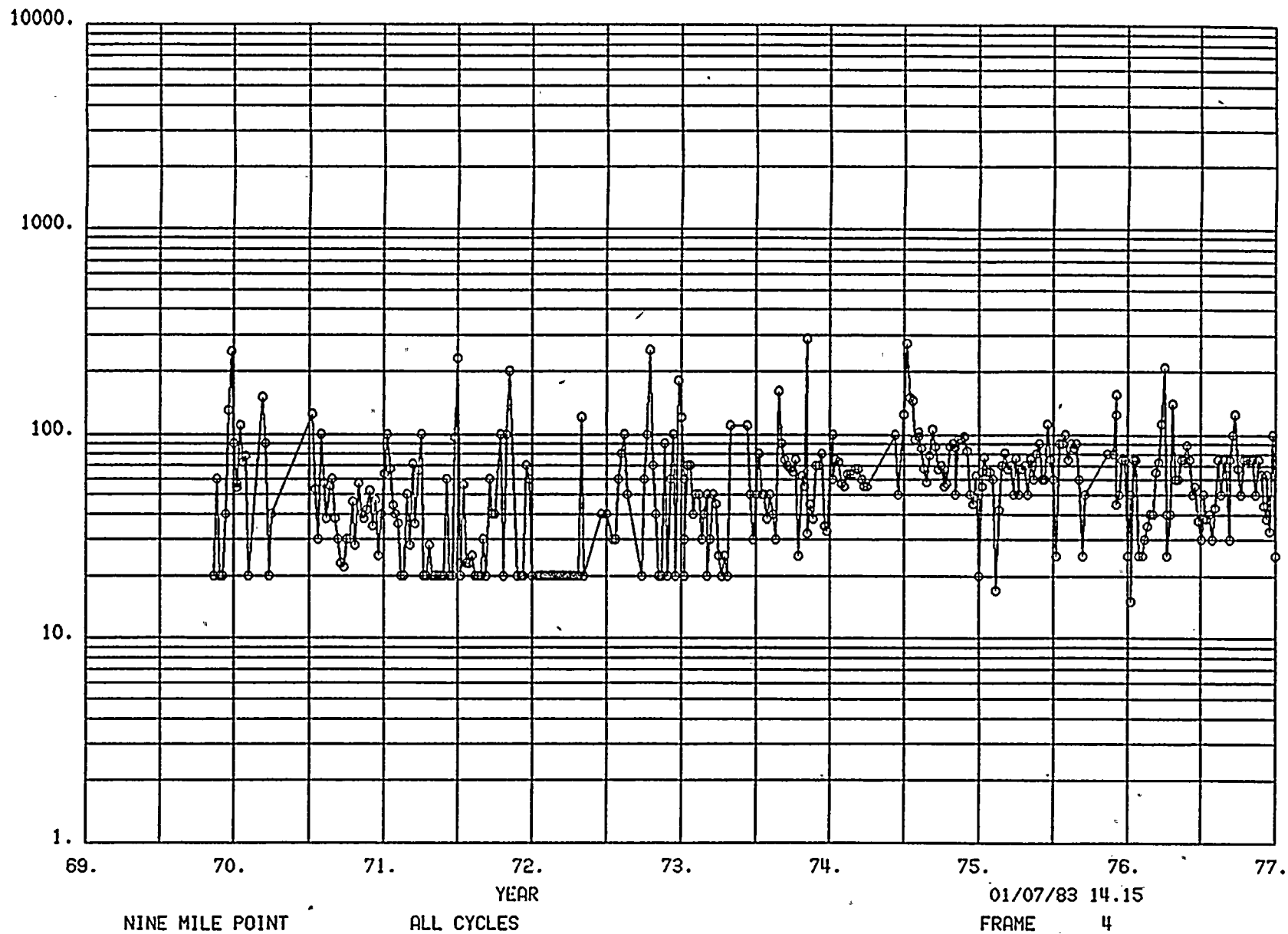
FIGURE 7
REACTOR WATER CHLORIDE MAX. (PPB)

FIGURE 8

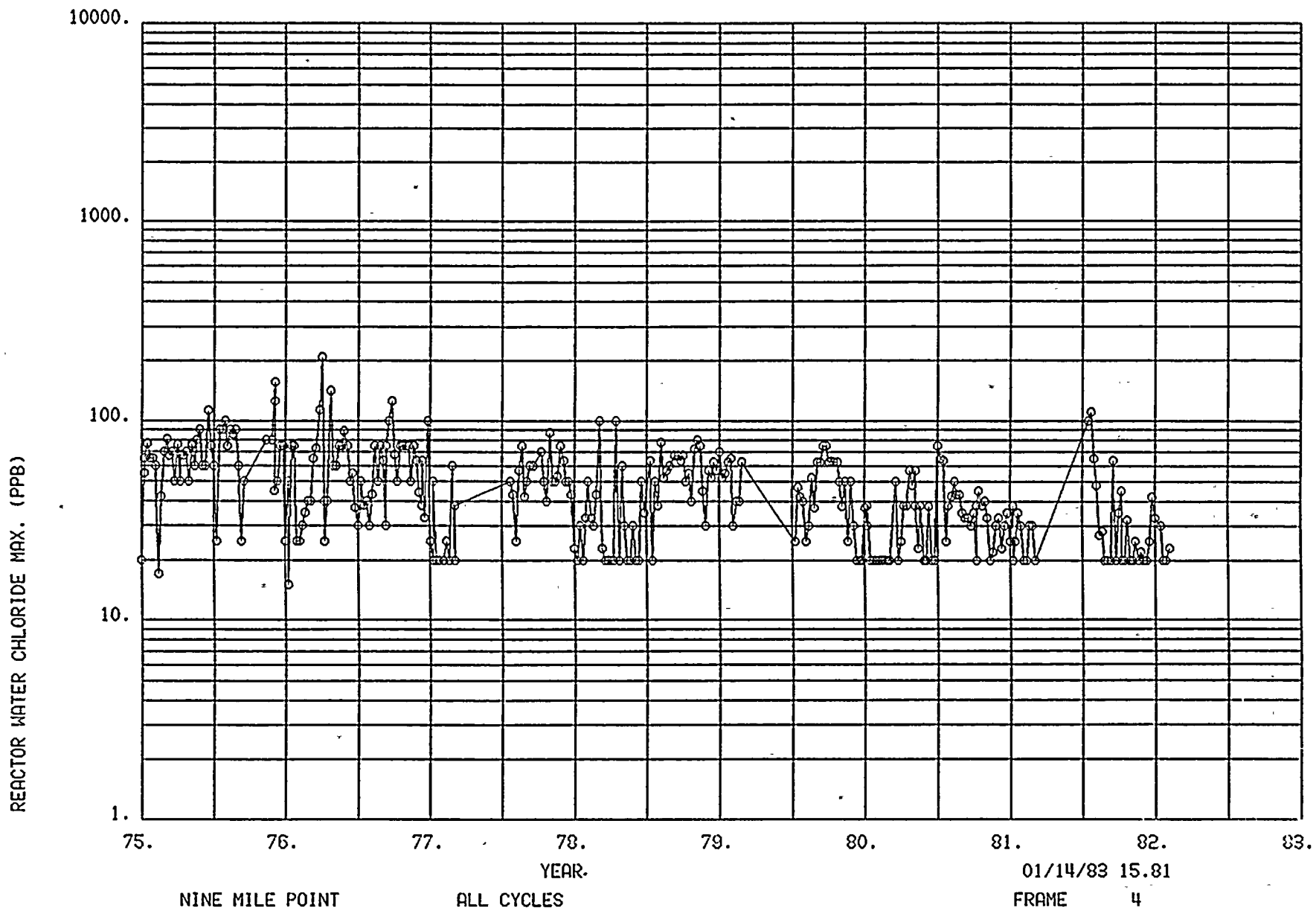


FIGURE 9

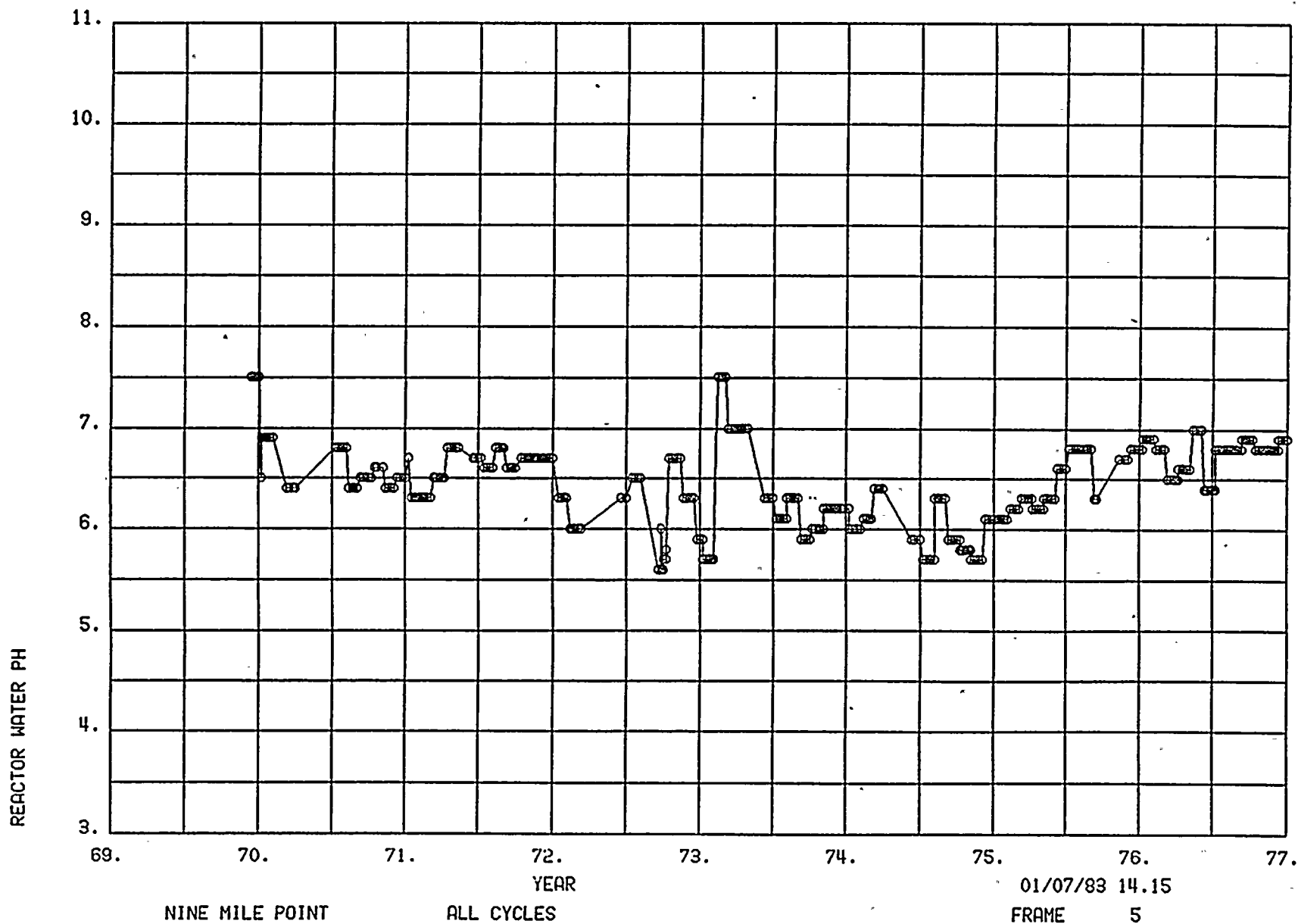


FIGURE 10

REACTOR WATER PH

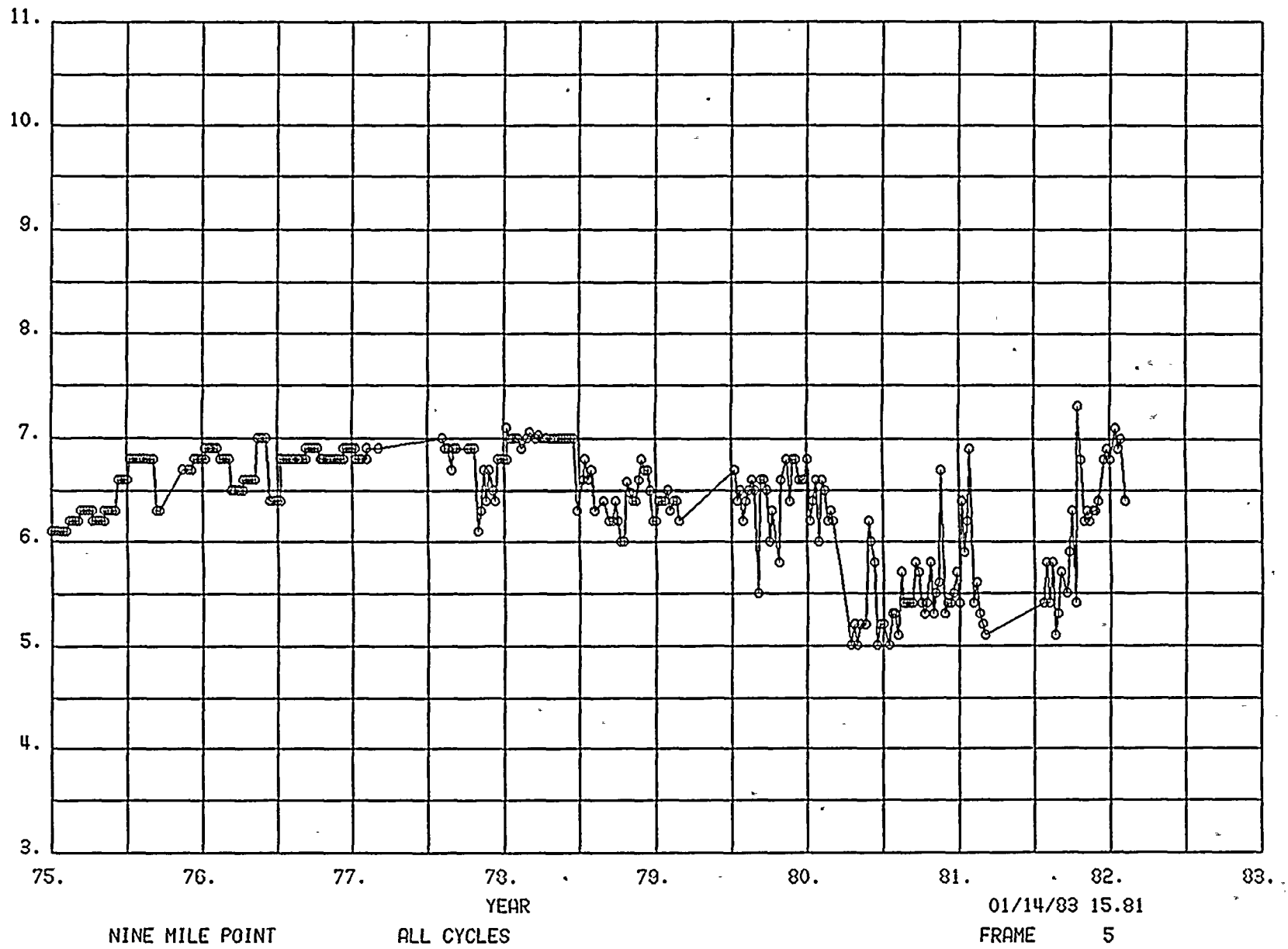


FIGURE 11

REACTOR WATER SILICA (PPB)

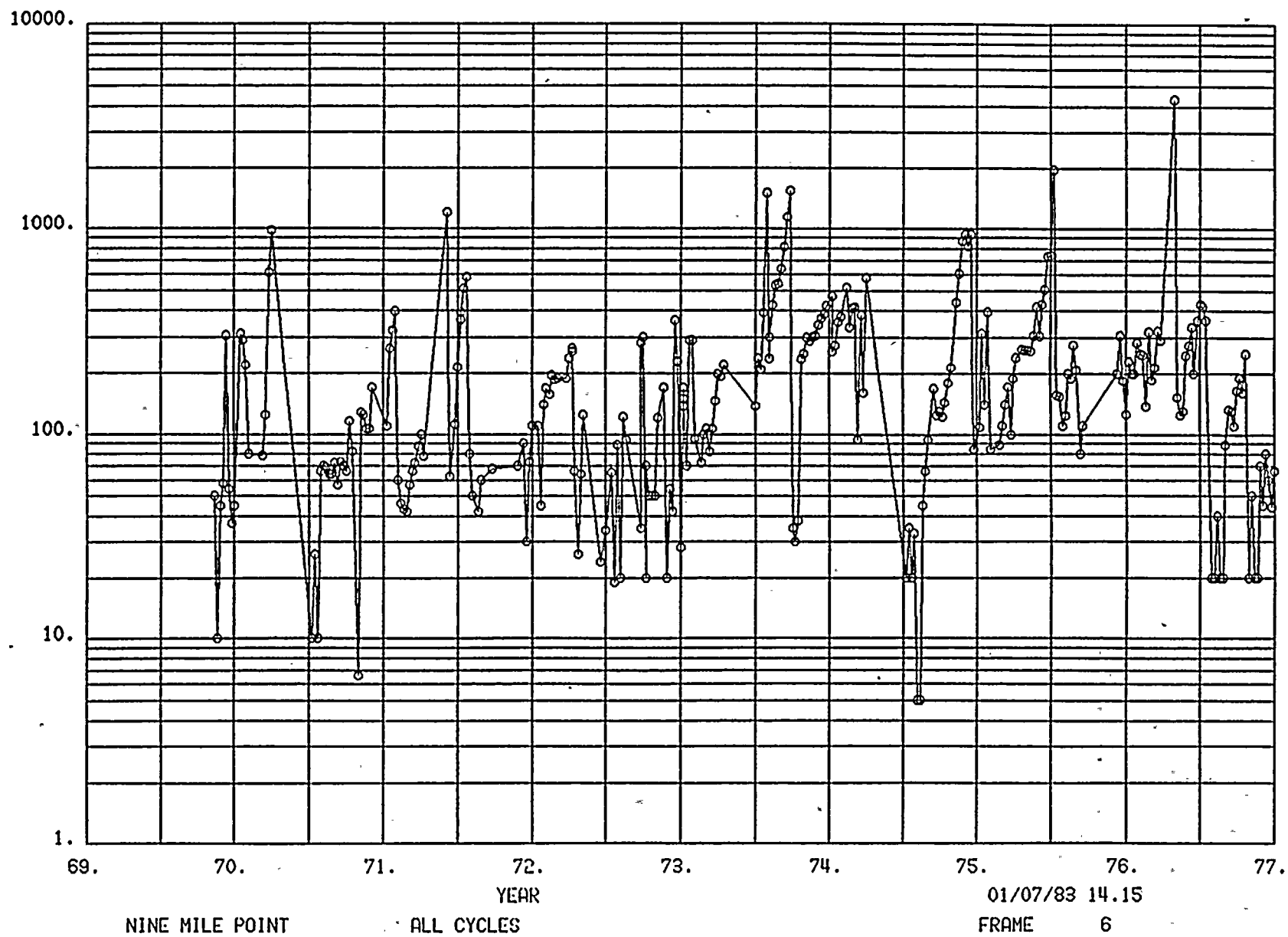
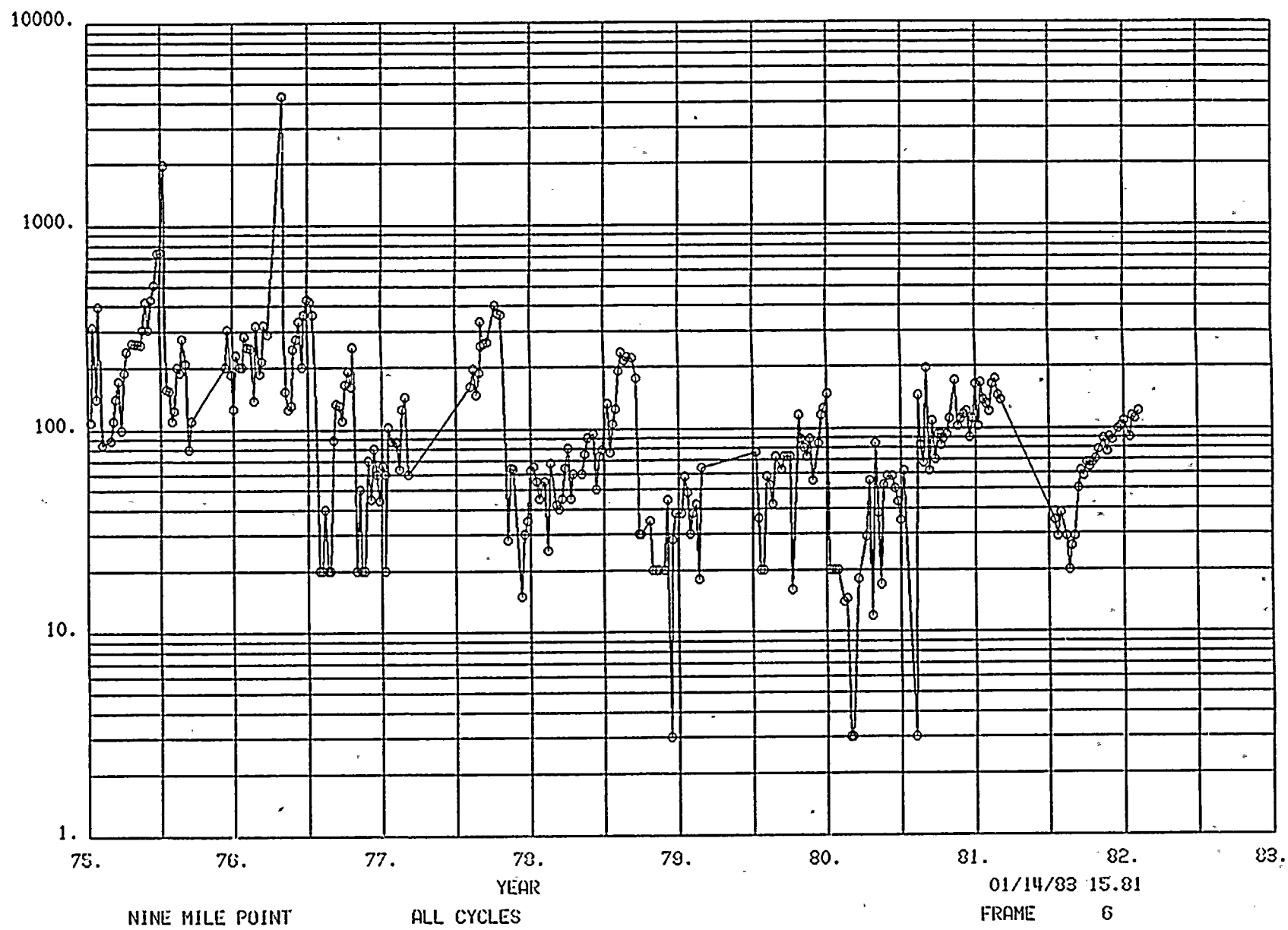


FIGURE 12

REACTOR WATER SILICA (PPB)



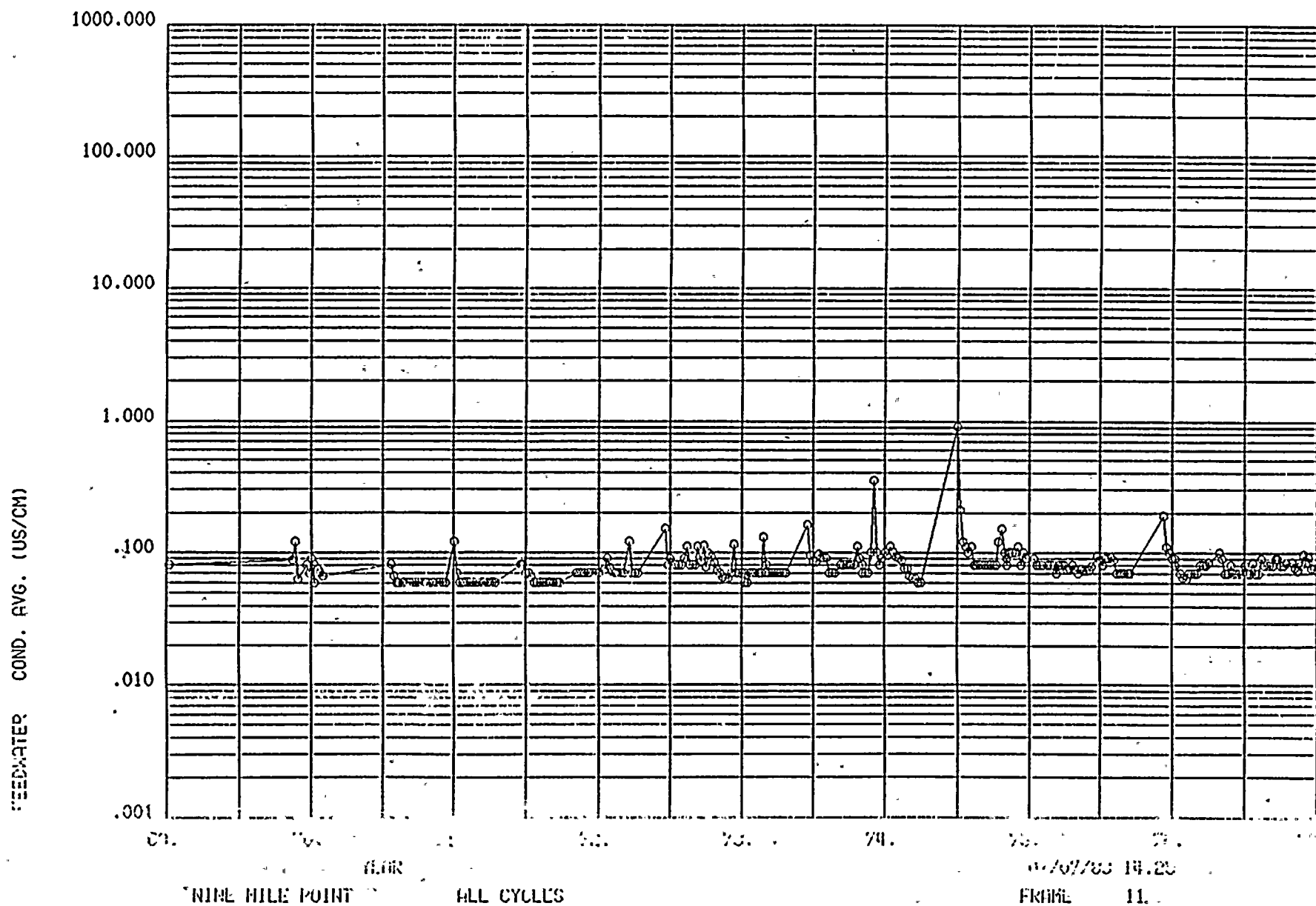
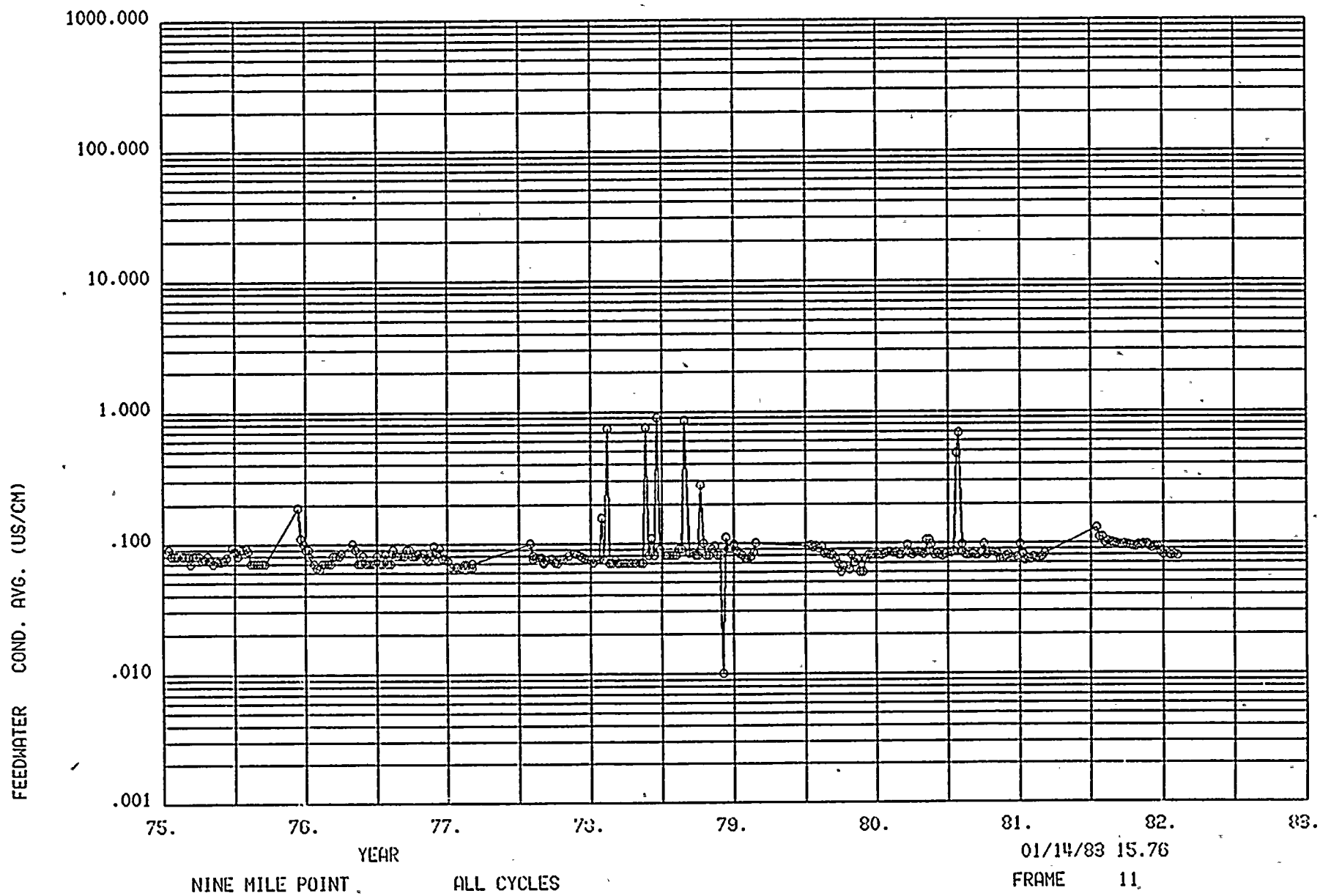


FIGURE 14



COND. XAX. (US/CM)

FIGURE 15

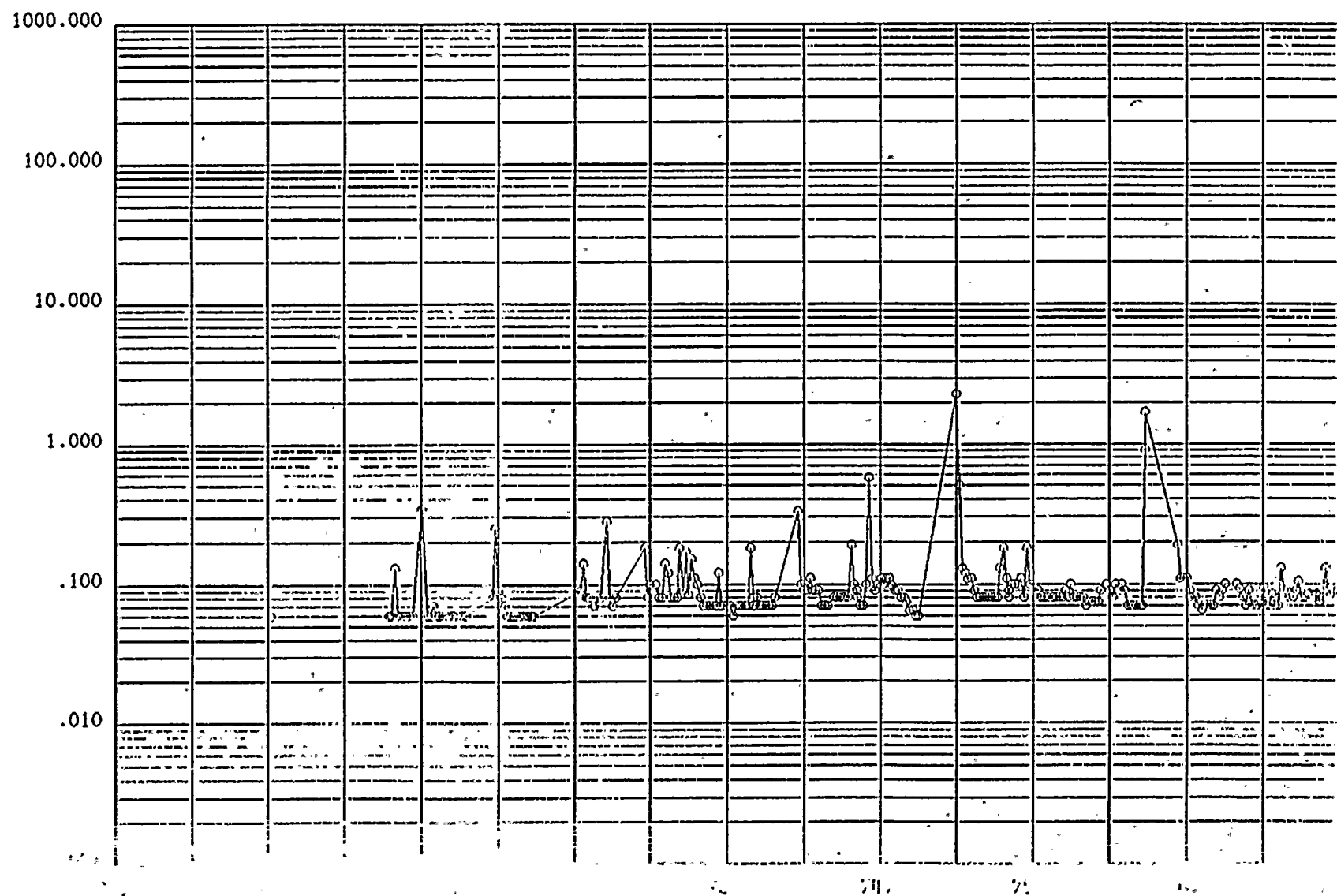


FIGURE 16

FEEDWATER COND. MAX. (US/CM)

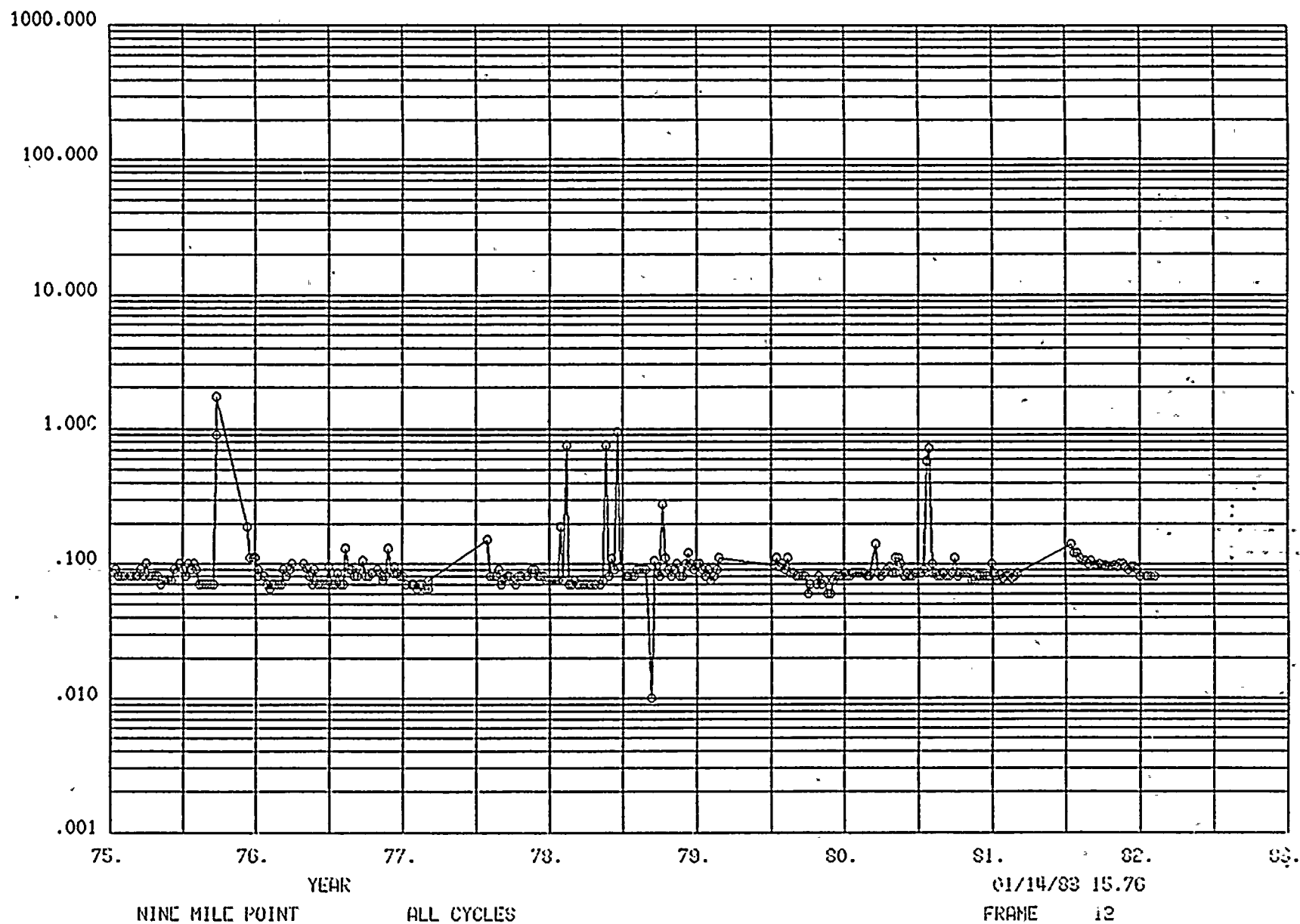


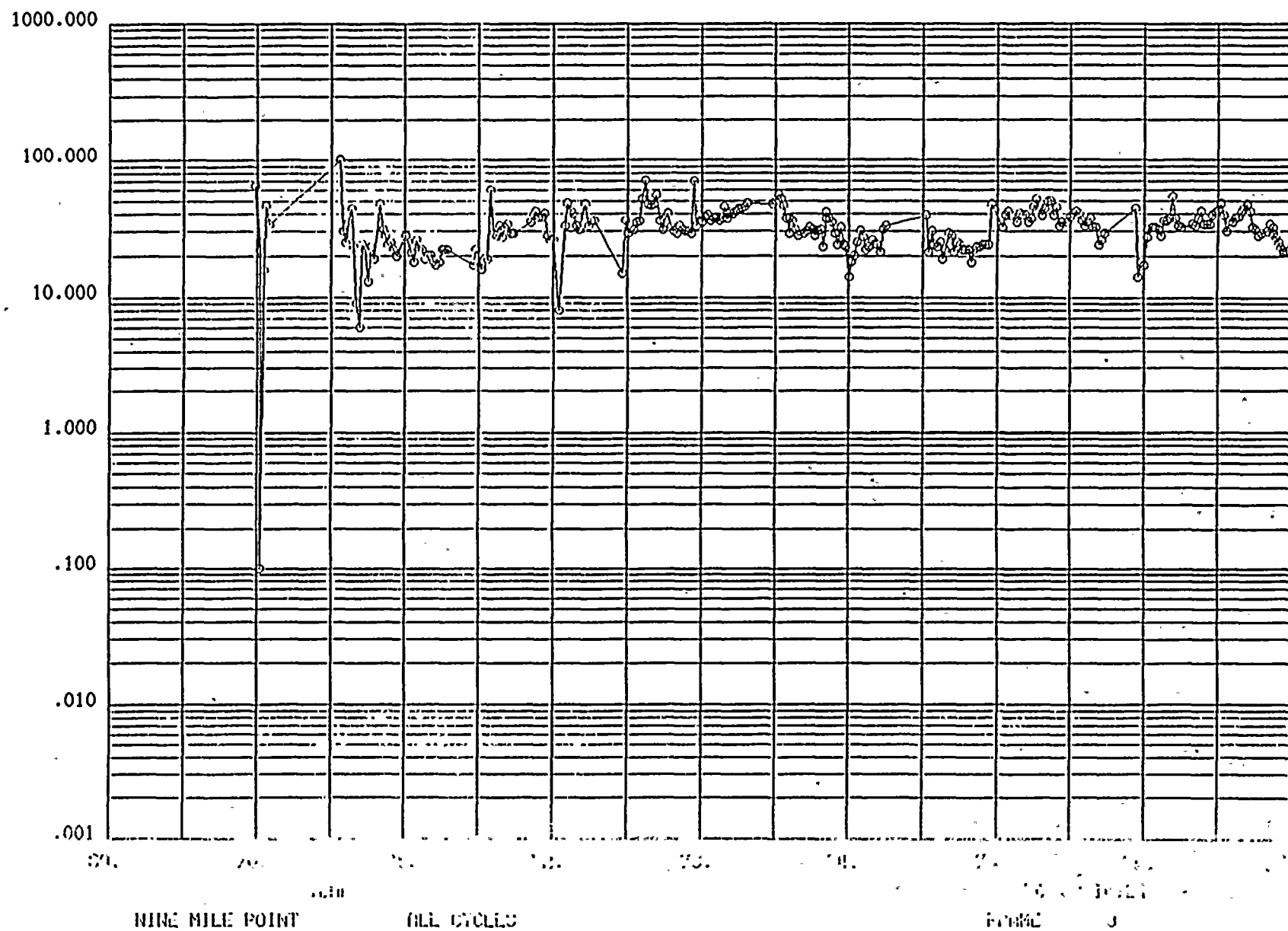
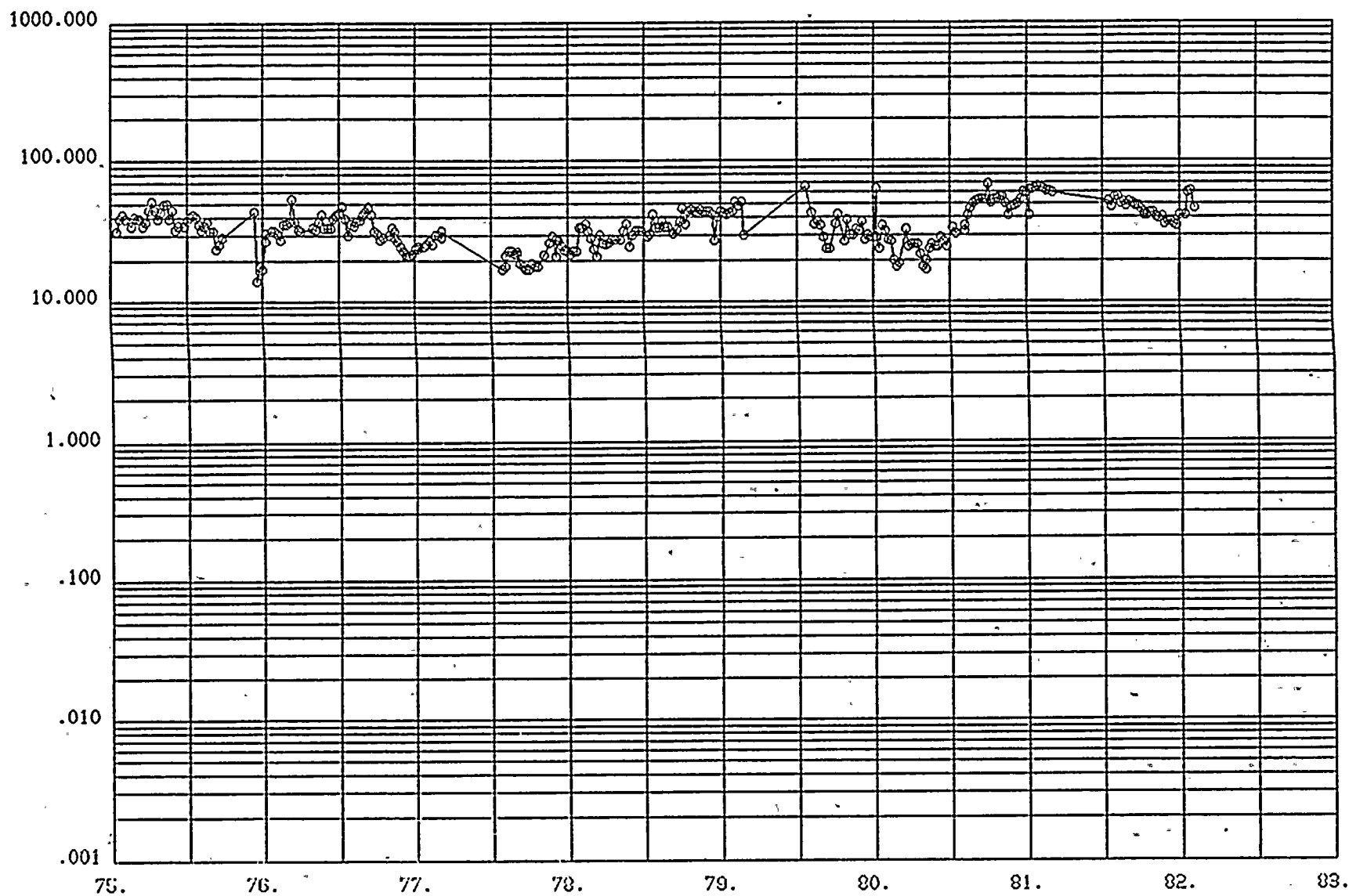
FIGURE 17
FEEDWATER OXYGEN AVG. (PPB)

FIGURE 18

FEEDWATER OXYGEN AVG. (PPB)



NINE MILE POINT

ALL CYCLES

01/14/83 15.75

FRAME 9

10-10-24 45.

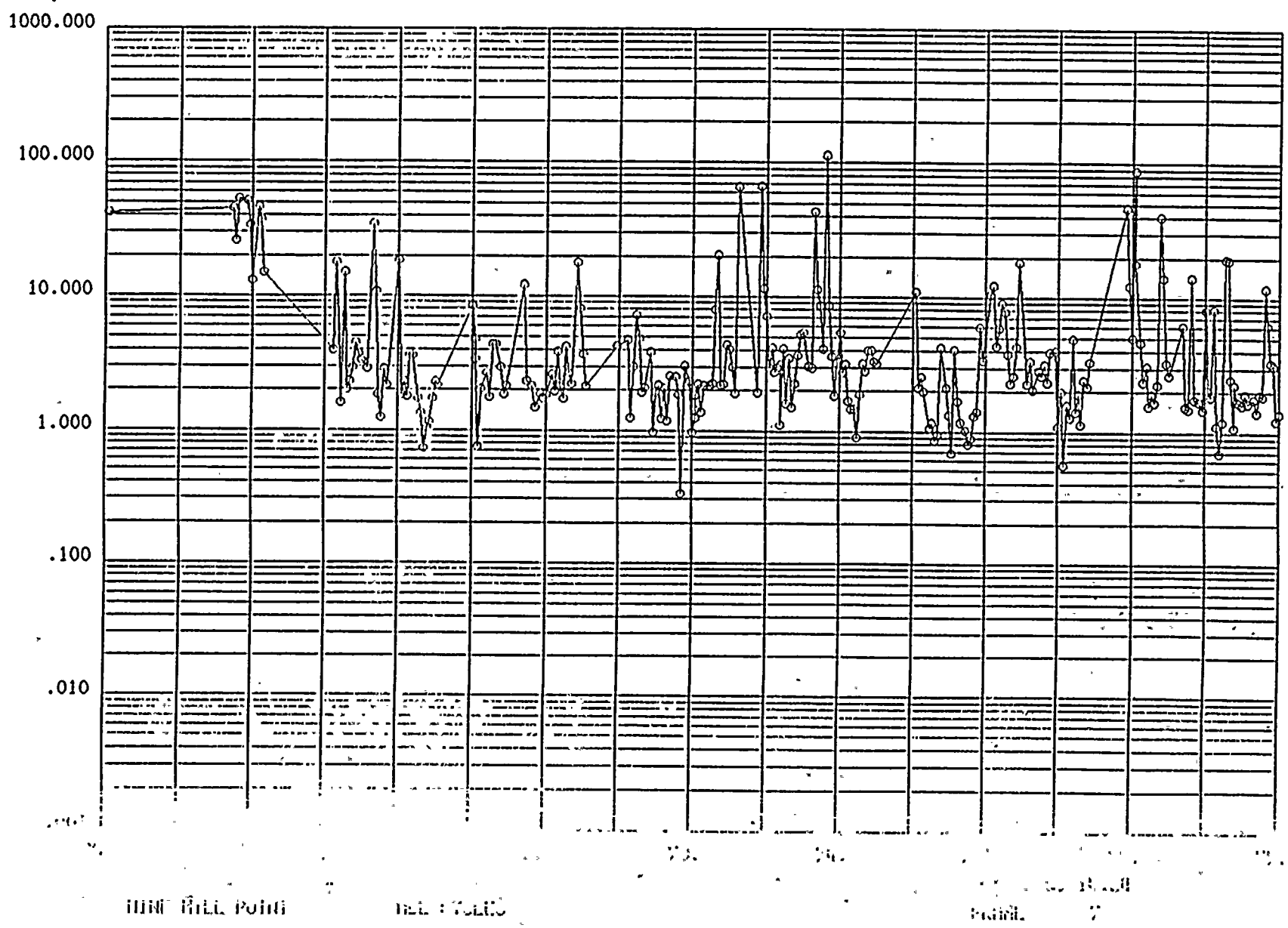


FIGURE 19 (BDD) STATION TOTAL RESERVE

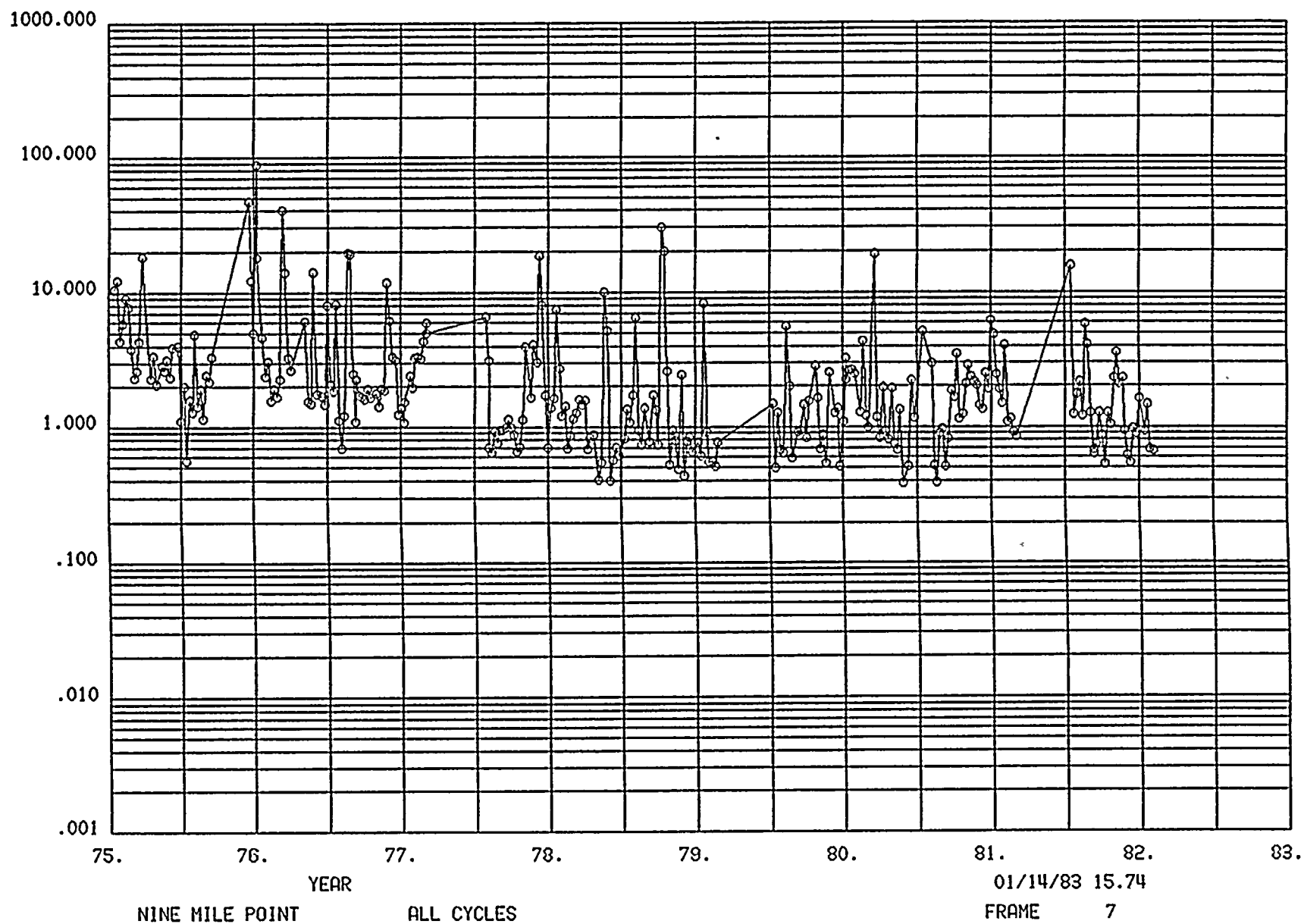
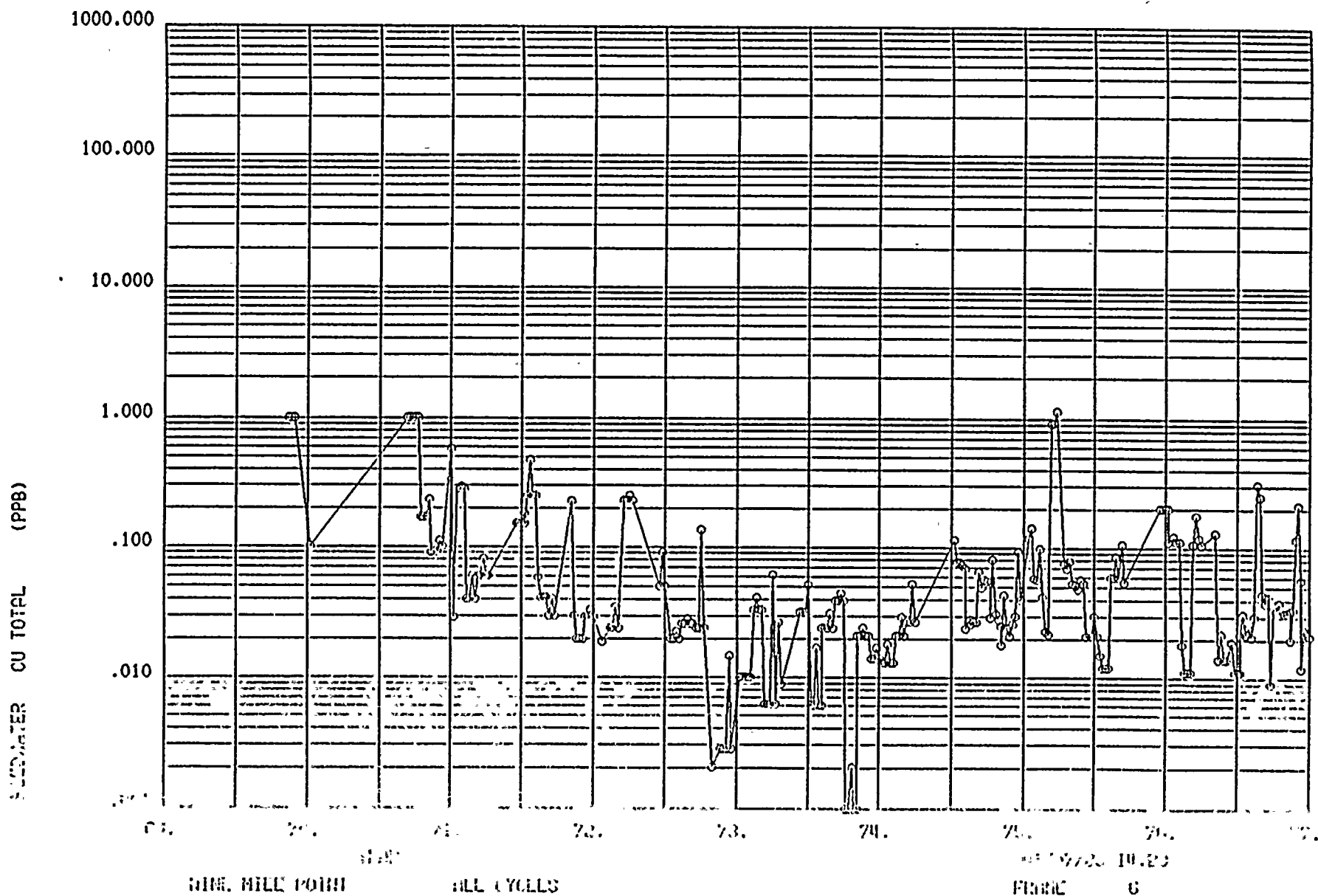
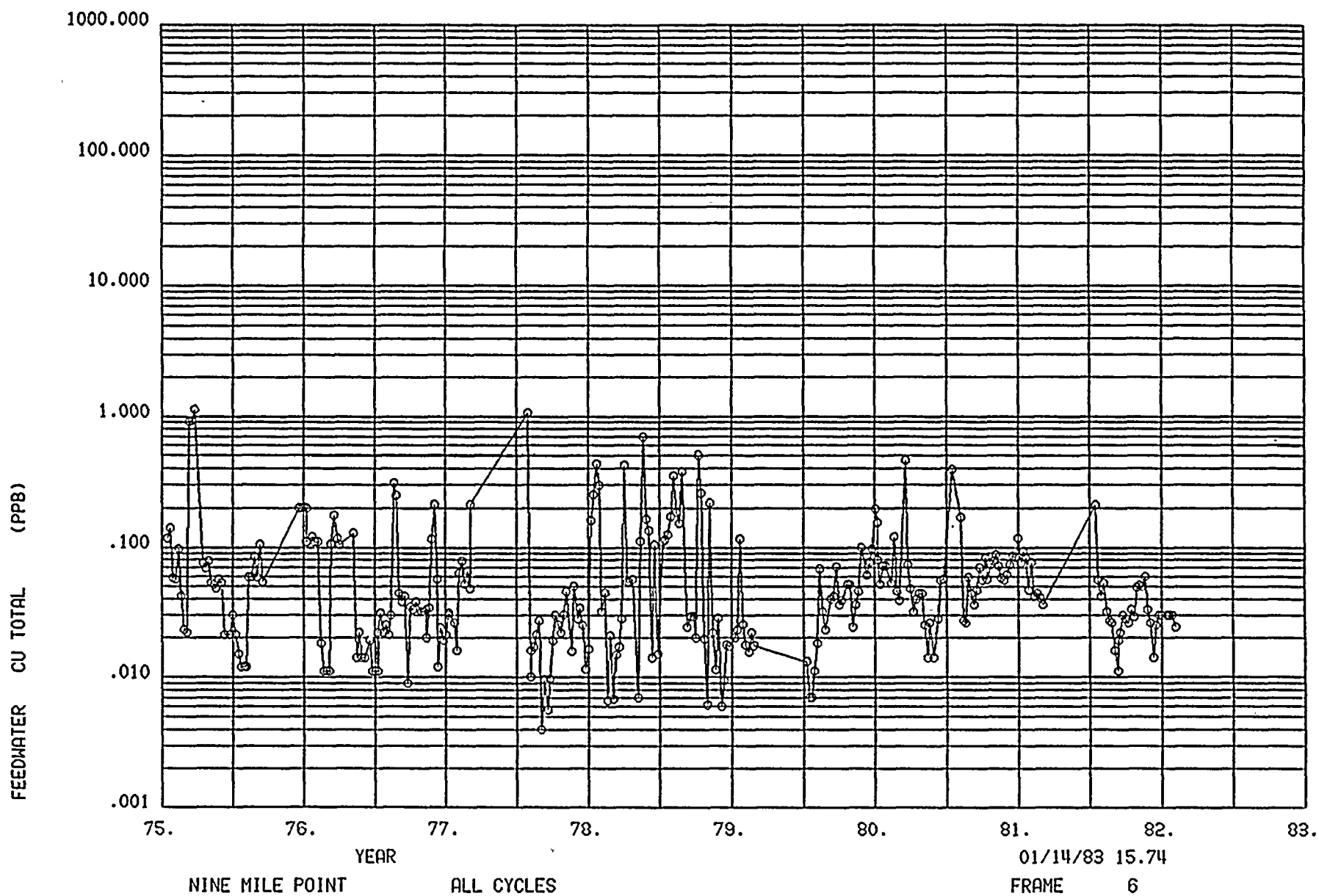
FIGURE 20
FEEDWATER TOTAL METALS (PPB)

FIGURE 21



6-37/6-38

FIGURE 22



SECTION VII

EFFECTS OF DECONTAMINATION

INTRODUCTION

The IGSCC incident on large diameter Type 316 stainless steel recirculation piping at Nine Mile Point (NMP) Unit 1 in March, 1982 provided the motivation for an in-depth analysis of several potential contributing factors to this deterioration in corrosion resistance. Since the NMP recirculation pumps were decontaminated by the London Nuclear Ltd. proprietary CAN-DECON process in April 1981, and the entire recirculation system in April-August 1982 period, it was considered prudent to determine if this process had any impact on the IGSCC propensities of the recirculation system either during the process application or subsequent operation. This section treats this concern.

Prior to discussing the potential impact of the CAN-DECON decontamination on the stress corrosion cracking tendencies of BWR piping, a brief description of this proprietary process will be presented below.

The CAN-DECON process utilizes a low temperature (85-90°C, occasionally 110°C) dilute decontamination solution (0.1 w/o) of acidic organic chelating agents (pH 3.5-4.5) plus excess hydrazine for oxygen scavenging that is circulated through the target system and through a purification system of filters and ion exchange columns. The loose crud is deposited on the filters while the ion exchange system cationic bed removes iron, cobalt, nickel, chromium, molybdenum and any other heavy metals that may be present. The process is terminated by removing the reagent on a mixed

bed column. Prior to returning to the nominal operating environment of the reactor, the target system may be re-passivated by the introduction of ethylenediaminetetracetic acid (EDTA) or oxygen free water at 150°C.

Specifically, in the case of the Nine Mile Point decontamination, two CAN-DECON decontaminations, separated by an oxidization step, were performed on recirculation pump 15, the single pump scheduled for inspection. This oxidizing step was designed to alter the morphology of the oxide films remaining after the first CAN-DECON treatment so that they would be more amenable to dissolution during the second CAN-DECON treatment. Only one decontamination was performed on the other four pumps, plus all 5 recirculation loops upto just below the vessel safe-end level. Decontamination of pump 15 lasted five days while the other four pump's treatment lasted three days each.

DECONTAMINATION AND STRESS CORROSION CRACKING

A. Laboratory Studies

Takaku et al³ investigated the effects of two undefined decontamination solutions on the IGSCC propensities of Type 304 stainless steel (0.07 w/o C) using test specimens fabricated from four inch diameter pipe weldments. The SCC tests were conducted in pure water at 288°C containing 8 ppm oxygen utilizing three testing techniques; constant extension rate test (CERT), cyclic tension test by load controlled trapezoidal stress waveform, and constant load test. Table 1 presents chemical cleaning conditions of the two reagents.

It appears that Reagent A more closely approximates the CAN-DECON decontamination solution relative to concentration and temperature. The most striking disparity in this study, aside from not knowing the exact composition of the relative proprietary solutions, is the dissolved oxygen concentration.

The results of the CERT SCC tests in 288°C pure water containing ~8 ppm oxygen are summarized in Table 2. Various mechanical parameters are utilized in the table for evaluating the materials susceptibility to SCC. The data indicate that there were no significant differences in these mechanical parameters between the as-welded specimens and the chemically cleaned specimens (either Reagent A or B). It is also important to note that the IGSCC propensity was not increased in both reagents by either severe decontamination conditions including the continuous long term cleaning of 72 hours, the extent of the decontamination cycle (three time cycles) or the presence of crevices and residual reagents (pre-cracked specimen).

Table 3 presents the results of the cyclic tension tests which were characterized by a maximum holding stress of 175% of the 288°C yield stress for 30 minutes and a strain rate of $4.2 \times 10^{-6} \text{ sec}^{-1}$. A review of this data indicates that no notable differences in IGSCC susceptibility was observed between the decontaminated and non-decontaminated specimens.

The final Takaku et al SCC study, constant load testing, was conducted at applied stresses of 150 and 175% of the 288°C yield stress. The data, as delineated in Table 4, indicates the same results as revealed in the two previous studies, that is, no significant difference was observed in IGSCC response whether the

specimens were decontaminated or not. Therefore, the Takaku et al data clearly indicate that their chemical cleaning solutions will not increase the IGSCC susceptibility of Type 304 even under exceptional cleaning cycles.

Two different types of SCC testing techniques were employed by Ishii et al⁴ in evaluating chemical decontamination cycles for BWR primary systems component materials; pipe testing and creviced bent beam (CCB) testing. The pipe tests were designed to evaluate the effects of decontamination on the propagation rate of pre-existing surface cracks in the heat affected zone of primary loop piping weld joints. The objective of the CCB testing was to determine the effects of residual decontamination reagent on the SCC behavior of Type 304 stainless steel (0.07 w/o C), Alloy 600 and X-750.

Two types of pipe tests were performed. The first pipe test procedure was characterized by a decontamination cycle with Reagent A or B (Table 1), followed with rinsing by operating the main loop with warm deionized water and followed further by pipe testing at 135% of the 288°C yield stress using a trapezoidal wave form similar to other pipe tests as described elsewhere.⁵ The second experiment was characterized by pre-cracking in pure water for ten cycles followed by the decontamination procedure used in the first experiment, and then pipe testing.

The results of Ishii et al's pipe testing is summarized in Table 5. No significant difference was observed in the time to failures (TTF) between the two types of pipe experiments (precracked and non-precracked), the type of reagent used or whether the pipe was subjected to the decontamination cycle or was exposed to only pure 8 ppm oxygen water.

The 500 hour CBB tests were performed on furnace sensitized Type 304 stainless steel, Alloy 600 and X-750 with compositions and heat treatments as presented in Tables 6 and 7, respectively. The assembly of the CBB rig with graphite wool as a crevice former is present in Figure 1. The test solutions initially contained ~8 ppm oxygen and residual reagent at 0.1% of the specified concentration for process decontamination.

Metallographic examination at test termination revealed that all three materials experience IGSCC in high temperature oxygenated water without the presence of the decontamination reagents, Table 8 and 9. In fact, the presence of a trace level of the chemical reagent appears to be beneficial. The cracking of Alloy 600 appears to be totally mitigated while the depth of cracking for Type 304 stainless steel is slightly reduced in the decontamination solution. The cracking propensities of Alloy X-750 is also dramatically reduced when the residual chemical reagents are present. Ishii et al suggest that since Reagent B acts as an oxygen scavenger, the mitigation result is not totally unexpected. Reagent A does not reduce the dissolved oxygen significantly, but still appears to have some beneficial effect.

Apparently only limited SCC testing has been performed by London Nuclear on various reactor structural materials in their CAN-DECON solutions.² Test specimen types included single and double U-bends and four-point loaded bent beams. The primary material evaluated was furnace sensitized Type 304 stainless steel and other austenitic materials.

The standard London Nuclear test sequence consists of exposing the specimens for 28 days to 288°C oxygenated (0.2-0.3 ppm) deminera-

lized water, decontaminating in a special loop, and then returning the specimens to the original autoclave for final exposure.

The results of this testing indicated that precracked sensitized Type 304 specimens were characterized by similar crack extensions regardless of whether the specimens were decontaminated or only exposed to the simulated BWR environment. No crack initiation was detected in non-precracked Type 304 specimens. However, a slight surface etching was observed on all surfaces of this material exposed to the CAN-DECON solution. Since this morphology was observed on surfaces which were in compression as well as in tension, the result is attributed to straight chemical attack on the metal oxide by the reagent, and not any stress related phenomenon.

B. Operating Experience

Prior to the April-August 1982 Nine Mile Point application, the CAN-DECON dilute chemical process had been applied to five BWR reactor water cleanup systems (Vermont Yankee - October 1979, Brunswick II - March 1980, Brunswick I - April 1981 and December 1981, Vermont Yankee - October 1981, Peach Bottom II - April 1982) and five primary recirculation pumps (Nine Mile Point 1 - April 1981). This process had also been applied to systems of the NPD 25 MWe reactor in 1972 and 1973, the full reactor system including the core with fuel in place of the Douglas Point CANDU pressurized Heavy Water Reactor in August 1975 and several subsystems and isolated heat exchanger from various other CANDU reactors. To date, there has been no evidence of corrosion of any material or malperformance of any reactor component which could be clearly associated with decontaminations. However, no data are available to verify longer term materials performance.

It appears that the only effect of the decontamination process on reactor components clearly identified to date, aside from what the solutions

are designed to accomplish, is the effect on IGSCC detectibility. For example, dye penetrant examination of safe ends at KRB following cleaning in water by soft brushing did not reveal any indications.⁷ However, dye penetrant testing following chemical decontamination by an alkaline permanganate/water rinse/oxalic acid/ammonium citrate solution at 90°C revealed crack indications.^{7,8,9} Prior to the application of this chemical decontamination procedure it was established by Kernkraftwerk Gundremmingen Betriebsgesellschaft that the chemical reagent did not affect the austenitic material and no new IGSCC was produced.^{7,10}

DISCUSSION

The study reported here was undertaken to evaluate the effects of the decontamination process per se as well as the effects on the subsequent stress corrosion cracking response on typical BWR structural materials. Although the volume of relevant available data is not extensive and principally short term in nature, the data support the contention that decontamination does not adversely affect the stress corrosion resistance of austenitic stainless steels. The investigation by Takakō et al³ and Ishii et al⁴ can be cited as evidence for this assertion since a wide variety of stress corrosion testing techniques including CERT, cyclic tension, constant load, full size pipe testing and creviced bent beam did not reveal that decontamination cycles have any accelerating deleterious effect on BWR plant materials. However, longer term tests that might reveal more subtle effects have not yet been performed.

Operating experience in BWR's after decontamination appears to be

satisfactory with no indications that the decontamination process contributed to any subsequent deterioration in corrosion performance.

The only documented effect of decontamination appears to be in the area of inspection where IGSCC in decontaminated components (see Section 8) appears to be revealed more readily after cleaning. This factor could potentially be misleading in that one might assume decontamination has created the cracks rather than provided a means for easier detection.

CONCLUSIONS

The above discussion concerning the effects of decontamination processes on the recent identification of IGSCC at Nine Mile Point indicate the following conclusions:

- 1) Laboratory testing by the reviewing investigators, utilizing a variety of stress corrosion cracking techniques, indicate that decontamination solutions do not produce IGSCC on typical BWR structural materials. In fact, in some instances, some decontamination solutions mitigated IGSCC.
- 2) Operating experience in various BWR and non-BWR plants with systems or subsystems decontaminated by the CAN-DECON process has been satisfactory to date, with no indications that chemical cleaning has resulted in malperformance of any structural material.
- 3) Although decontamination may result in more readily identifiable defects in reactor components upon inspection by ultrasonic or dye penetrant techniques, there is laboratory evidence that decontamination in itself does not contribute to or enhance the extent of cracking due to the processing per se. However, longer term tests that might reveal decontamination effects on subsequent crack initiation have not yet been performed.

- 4) It is unlikely that the decontamination of Nine Mile Point 1 recirculation pumps in April 1981 contributed to the subsequent identification of cracking of the recirculation system discovered in March of 1982. Further, the 1982 total recirculation system decontamination does not appear to have exacerbated the observed cracking. The only clear contribution decontamination appears to have had on this system is the increase in sensitivity for inspection of cracks which already existed in the system.

REFERENCES

- 1) J. C. Cutt, "Laboratory Examination of Sections from Type 316 Stainless Steel Recirculation Piping - Nine Mile Point 1, 1982" PMT Transmittal No. 82-178-41, November 17, 1982.
- 2) J. E. LeSuff letter to R. S. Tunder, "Decontamination and Stress Corrosion Cracking," January 29, 1980.
- 3) H. Takaku et al "Effects of Chemical Cleaning on the SCC Susceptibility of Type 304 Stainless Steel Pipe Weldment in 288°C High Purity," paper presented at "Decontamination of Nuclear Facilities" International Joint Meeting ANS-CNA, September 1982, Niagara Falls, Canada.
- 4) H. Ishii, M. Yajima and K. Hattori, "The Effect of Reactor Decontamination Reagent on Stress Corrosion Cracking of Austenitic Materials Under High Temperature Water" paper presented at "Decontamination of Nuclear Facilities" International Joint Meeting ANS-CNA, September 1982, Niagara Falls, Canada.
- 5) R. S. Tunder, "Alternate Alloy for BWR Applications," Final Report EPRI Project T111-1, WE 8102-03, September 1981.
- 6) P. J. Pettit et al, "Decontamination of the Douglas Point Reactor by the CAN-DECON Process" paper presented at Corrosion 78, Houston, Texas March 6-10, 1978.

- 7) H. Flache, "KRB-A Experience with Ultrasonics for Identification of Intergranular Stress Corrosion Cracking in Heavy Austenitic Steel Components," paper presented at BWR Operating Plant Technical Conference III, Lugano, Italy, October 30, 1978.
- 8) N. Eickelpasch, H. Bertholdt and M. Lasch, "In-Situ Decontamination of Components of the Primary Loop in the Gundremmigen Nuclear Power Plant," Kraftwerk Union Laboratory Report, 1978.
- 9) H. Meier and H. Peterreit, "Possibilities of Testing Forged Austenitic Steel for Intergranular Stress Corrosion Cracking with the Ultrasonic Method," Kraftwerk Union Laboratory Report R 413 No. 42/78. February 3, 1978.
- 10) R. Riess and H. Bertholdt, "Chemical Decontamination of Reactor Components" Kraftwerk Union Aktiengesellschaft, Erlanger 1978.

Table 1
TAKAKU et al³ DECONTAMINATION REAGENTS

	<u>Reagent A</u>	<u>Reagent B</u>
Concentration	0.1	5
Temperature, °C	125	90
Dissolved O ₂ , ppm	8	8
Cleaning time, hrs.	24 and 72	24 and 72

Table 2

CERT SCC TEST RESULTS, TESTED AT CONSTANT EXTENSION RATE OF $4.2 \times 10^{-6} \text{ SEC}^{-1}$ AND IN 288°C
HIGH PURITY WATER CONTAINING AIR-SATURATED DISSOLVED OXYGEN ($\sim 8 \text{ ppm}$)

Surface preparation before SCC test	Type of reagent	$\sigma_{\text{max.}}^{(1)}$, kg/mm^2	U.E. $^{(2)}$, %	T.E. $^{(3)}$, %	SCC area ratio $^{(4)}$, %	Number of specimen
As weld (no oxide film and no chemical cleaning)	—	40.7	14.9	18.2	58	4
No oxide film \longrightarrow 24 hrs. C.C. $^{(5)}$	A	40.3	15.1	18.3	60	4
	B	41.4	14.4	18.9	55	4
331 hrs. corrosion \longrightarrow 24 hrs. C.C.	A	40.6	14.5	18.5	61	4
	B	39.6	15.8	18.9	65	4
953 hrs. corrosion \longrightarrow 72 hrs. C.C.	A	36.0	10.0	14.5	65	4
	B	38.9	12.4	16.5	55	4
Decontamination cycle $^{(6)}$	A	38.4	11.3	15.5	64	2
	B	40.3	14.9	19.1	57	2
Pre-cracked specimen $^{(7)}$ \longrightarrow 24 hrs. C.C.	A	37.6	10.8	15.4	60	4
	B	40.1	13.6	17.6	50	4

(1) $\sigma_{\text{max.}}$: Maximum stress value, (2) U.E. : Uniform elongation, (3) T.E. : Total elongation,

(4) SCC area ratio: SCC area ratio on the fractured surface, (5) C.C. : Chemical cleaning,

(6) Decontamination cycle : Three times procedure of "24 hrs. chemical cleaning after approx. 330 hrs. corrosion",

(7) Pre-cracked specimen : Pre-crack introduced by CERT SCC test in 288°C pure water

Table 3

RESULTS OF CYCLIC TENSION SCC TEST, CONDUCTED UNDER LOAD-CONTROLLED CONDITION IN 288°C
HIGH PURITY WATER CONTAINING AIR-SATURATED DISSOLVED OXYGEN (~8 ppm)

Surface preparation before SCC test	Type of reagent	Number of cycle to failure	SCC area ratio ⁽¹⁾ , %	Number of specimen
As weld (no oxide film and no chemical cleaning)	—	19	64	4
No oxide film → 24 hrs. chemical cleaning	A	25	58	4
	B	31	61	4
331 hrs. corrosion → 24 hrs. chemical cleaning	A	22	60	4
	B	23	58	4
953 hrs. corrosion → 72 hrs. chemical cleaning	A	18	59	2
	B	26	64	2
Decontamination cycle ⁽²⁾	A	43	65	2
	B	27	62	2

(1) SCC area ratio : SCC area ratio on the fractured surface

(2) Decontamination cycle : Three times procedure of "24 hrs. chemical cleaning after approx. 330 hrs. corrosion in 288°C pure water"

Table 4

RESULTS OF CONSTANT LOAD SCC TEST IN 288°C PURE WATER (8 ppm dissolved oxygen)

Surface preparation before SCC test	Type of reagent	Applied stress, $\sigma_y(1)$	Time to failure, hr.	SCC area ratio(2), %	Number of specimen
As weld (no oxide film and no chemical cleaning)	—	1.50	No failure to 2100	—	2
		1.75	40	59	2
231 hrs. corrosion → 24 hrs. chemical cleaning	A	1.50	No failure to 2100	—	2
		1.75	38	62	2
	B	1.50	No failure to 2100	—	2
		1.75	43	53	2
953 hrs. corrosion → 72 hrs. chemical cleaning	A	1.50	No failure to 1900	—	2
		1.75	56	54	2
	B	1.50	No failure to 1900	—	2
		1.75	41	52	2
Decontamination cycle ⁽³⁾	A	1.50	No failure to 1900	—	2
		1.75	65	61	2
	B	1.50	No failure to 1900	—	2
		1.75	57	58	2

(1) σ_y : 0.2% offset stress in 288°C pure water

(2) SCC area ratio : SCC area ratio on the fractured surface

(3) Decontamination cycle : Three times procedure of "24 hrs. chemical cleaning after approx. 330 hrs. corrosion in 288°C pure water"

Table 5:
TIME TO FAILURE IN PIPE TESTING

Type of Decon. Reagent	Type of Experiment	1st Failure	TTF in hour 2nd Failure	3rd Failure
A	(1)	134	135	162
	(1)	133	205	206
	(2)*	158	159	172
	(2)*	182	193	222
B	(1)	203	208	237
	(1)	173	178	181
	(2)*	128	148	150
	(2)*	234	241	268

Experiment (1); DECON CYCLE + PIPE TEST

Experiment (2); PIPE TEST (10 cycles + DECON CYCLE + PIPE TEST)

TTF (hrs) in Pipe Testing				
Type of Decon. Reagent	Type Experiment	Median TTF in hour	Standard Deviation	Mean TTF in hour
A	(1)	245	1.5	268
	(2)*	240	1.4	252
B	(1)	225	1.3	264
	(2)*	320	1.8	380
NON DECON CYCLE		225	1.5	244

*includes pre-cracking time

Table 6
CHEMICAL COMPOSITION OF MATERIALS (wt. %)

<u>Material</u>	<u>C</u>	<u>Si</u>	<u>Mn</u>	<u>P</u>	<u>S</u>	<u>Ni</u>	<u>Cr</u>	<u>Fe</u>	<u>Other El.</u>
Type 304 S.S.	0.06	0.59	1.62	0.032	0.010	8.68	18.17	bal.	
Inconel 600	0.044	0.28	0.32	--	0.010	74.28	15.32	8.50	
Inconel X-750	0.04	0.09	0.05	0.004	0.005	73.60	15.57	6.62	Nb+Ta 0.85 Al 0.49

Table 7
HEAT TREATMENT OF MATERIALS FOR CBB TEST

<u>Material</u>	<u>Heat Treatment Condition</u>
Type 304 S.S.	a) 650°C x 3h AC b) 650°C x 10h AC
Inconel 600	a) 650°C x 3h AC b) 620°C x 24h AC
Inconel X-750	a) 985°C x 1h AC +705°C x 20h AC

A.C. = Air Cooling

Table 8

SCC SUSCEPTIBILITY IN 500 HR CBB TEST IN HIGH TEMPERATURE
WATER WITH RESIDUAL CHEMICAL REAGENT

<u>Material</u>	<u>Pure Water</u>	<u>Reagent A</u>	<u>Reagent B</u>
Type 304 SS (a)	10/10	6/24	7/12
Type 304 SS (b)	10/10	3/7	2/7
Inconel 600 (a)	10/10	0/7	0/7
Inconel 600 (b)	8/10	0/7	0/7
Inconel X-750	5/8	-	1/2

Table 9

MAX. CRACK PENETRATION IN CBB TEST IN HIGH TEMPERATURE
WATER WITH RESIDUAL CHEMICAL REAGENT (in μm)

<u>Material</u>	<u>Pure Water</u>	<u>Reagent A</u>	<u>Reagent B</u>
Type 304 SS (a)	991	900	760
Type 304 SS (b)	864	580	480
Inconel 600 (a)	1045	0	0
Inconel 600 (b)	324	0	0
Inconel X-750	591	-	84

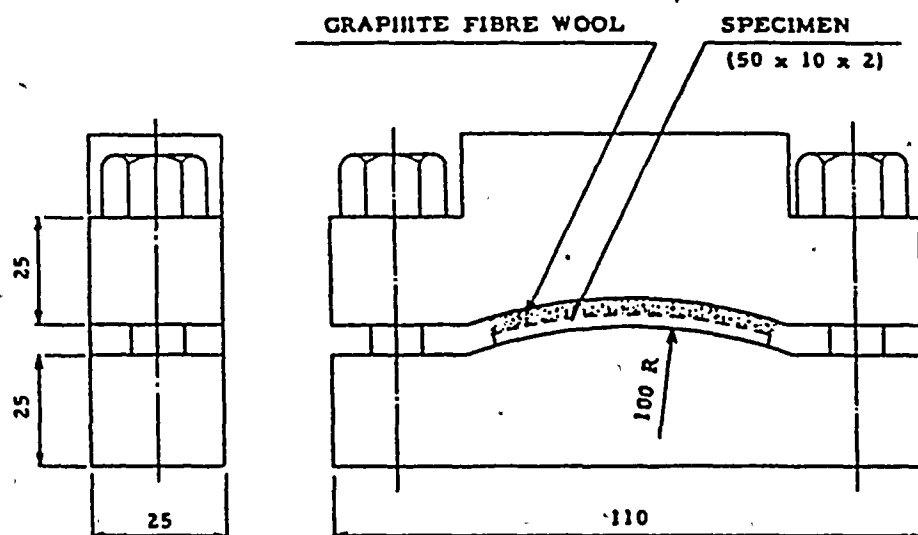


Figure 1. Assembly of Creviced Bent Beam Test Jigs

SECTION VIII ULTRASONIC EVALUATION

8.1 INTRODUCTION AND BACKGROUND

In March, 1982, during a hydrostatic test at NMP-1 evidence of leakage was observed on two 28-inch diameter recirculation system safe-ends. Subsequently ultrasonic (U.T.) examination was conducted and confirmed the presence of intergranular stress corrosion cracking in the safe-ends. In addition a recirculation pump discharge nozzle to elbow weld had U.T. indications which were confirmed, by destructive examination, to be IGSCC. These events, and those which occurred later are listed in chronological order:

8.1.1 Sequence of Events

- 3/23/82 - Visual discovery of leaking safe-ends - axial orientation.
- 3/26 to 3/31/82 - Informational examinations performed on leaking and non-leaking safe-ends. Indications reported. Safe-end activity stopped.*
- 4/1/82 - Commence informational examinations at pump end of recirculation system. Indications reported.
- 4/20/82 - Transfer measurements of cal blocks and riser elbow performed. 10 dB variance noted. (Resulted in 10 dB increase in examination sensitivity and changed recording criteria for subsequent examinations.)
- 5/6/82 - Commence ultrasonic examination of balance of recirculation piping welds following confirmation of IGSCC existing at riser elbow.*
- 6/82 to 12/82 - Ultrasonic, visual and liquid penetrant verification of cracking in removed material.

*Examinations performed and results are presented in Section 8.1.2.

(Appendix A of this section contains excerpts of the procedures used for the IGSCC oriented examinations and the examination of other austenitic S/S piping.)

The word "informational" has been applied to examinations performed during this period for several reasons. In the case of the safe-ends, the examinations, while performed in accordance with procedure, did not generate carefully plotted, detailed results. By direction and agreement, the exams were to confirm detectability of the discovered cracks and make a survey for other indications. Greater accumulation of man-rem for detailed results was considered unnecessary given known failure and necessary replacement. Further, the informational quick-look approach continued into the next examinations on the recirculation system. Strict adherence to specified procedural techniques was not maintained once additional indications had been detected. Different evaluation techniques were used as soon as the normal approach had provided evidence of cracking indications.

Transfer measurements from calibration blocks to components were made as the result of using alternative techniques for evaluation. A depth calibration approach employing small diameter side drilled holes rather than notches for calibration was desirable for aiding evaluation. It was determined that the depth calibration sensitivity was about 10 dB greater than that resulting from the notches. Subsequently, a transfer comparison was made which showed that for the recirculation pump elbow, there was a difference of 10 dB between the calibration blocks and the component, the component being the more attenuative. Primarily, this established direct application of the depth technique to examination of component and secondarily resulted in an increase of 10 dB being applied to the standard notch calibration sensitivity for the balance of the examinations performed on the recirculation system.

Part of the transfer measurement activity was devoted to making the same comparisons between the available flat and curved calibration blocks of the same material. There was approximately 2 dB difference noted. It is important to realize that the 10 dB factor did not result from a difference

between flat and curved calibration blocks, but from attenuation differences between the calibration blocks and pump discharge elbow.

A verification of the attenuation difference between the flat and curved calibration blocks was requested as a result of comments made by General Electric. The recheck confirmed the initial differential of 2 dB between calibration blocks.

8.1.2 Principle Aspects of the 1982 U.T. Examination at NMP-1

For the U.T. examination used to detect IGSCC in the NMP recirculation system, the procedure was modified from that used during previous in-service inspections (ISI). Miniature 1/2 inch and 1/4 inch search units were used and scanning was conducted at 20 dB above calibration gain. The effect of the miniature search units upon scanning was that it allowed the ultrasound to reach the weld heat affected zone (HAZ) of welds with wide weld crowns. Previously scanning was conducted at 6 dB above calibration gain and 1/2 by 1 inch search units were used. The latter restricted ability to examine the HAZ effectively.

It was also discovered in the course of U.T. examinations conducted in 1982, that the attenuation of the piping, safe-end and elbow components measured from 6 to 10 dB higher than that measured on the flat 1.5 inch thick stainless steel calibration standard. This difference in attenuation resulted in insufficient gain being used during scanning to adequately detect and record low amplitude signals.

The principal aspects of the U.T. procedure employed in 1982 at NMP-1 required the following:

- (a) Calibration for examination using 10% of thickness notches in a flat 1.5 inch thick calibration standard.
- (b) Correction for attenuation to accommodate for the higher attenuation measured on the safe-end, piping and elbow components.

- (c) Use of miniature 1/4 inch 2.25 MHz 45° angle beam and 1.5 MHz 45° dual element angle beam search units.
- (d) Recording of all indications regardless of amplitude if considered to be caused by IGSCC.
- (e) Plotting of indications using full scale drawings of the weld configuration.
- (f) Examination for axial and circumferential indications.
- (g) Training of U.T. personnel on piping samples with actual IGSCC.

Subsequent examination of recirculation piping system welds conducted at Monticello, Hatch, and TVA-2 (Browns Ferry 2) and others were performed to procedures similar to that employed at NMP-1 in 1982. Deviations if any, consisted of using strip chart recording, computers for data plotting, and calibration for examination on curved calibration standards of the same diameter and thickness as the component to be examined. The latter deviation would provide a minor increase in scanning gain, the other two would enable more exact plotting.

With respect to detection and sizing of axially oriented IGSCC in the weld HAZ, their detection is difficult. The majority of the piping welds at operating plants are in the as-welded condition or are flat topped. As a result manipulation of the search units so as to transmit ultrasound perpendicular to these axial cracks is not normally fully achieved. Instead examination is conducted from the nearest flat surface with the search unit angled toward the anticipated area of cracking. Any IGSCC detected would therefore have reduced amplitude and be difficult to size for depth. These difficulties were an impedance to the identification of axially oriented cracks at NMP-1. When observed, the indications of axially oriented cracking were generally below the recording limit. The same situation would be true for any plant with extended weld crowns or unground welds.

In order to improve the detection of axial IGSCC in weld HAZ's grinding of the piping system weld crowns is required. The degree of grinding should provide a smooth cylindrical surface without any obstructions to prohibit search unit movement. Of plants examined to date, all except plant Hatch, had unground welds.

8.2 RECIRCULATION SYSTEM ISI EXAMINATION RESULTS

For examination activities occurring prior to the 1979 refueling outage at NMP-1, no specific attention had been given to the potential for IGSCC : occurrences in the recirculation system. Neither the selection process for welds nor the examination techniques utilized reflected the requirements of NUREG 0313. Any welds that had been examined had been done in accordance with a procedure based on the requirements of Article 5 of Section V of the ASME Code.

For the 1979 outage, an augmented program had been developed in accordance with the provision of NUREG 0313, Rev. 0. Although initial drafts of this program included the entire recirculation system, it was finally decided that only the recirculation safe-ends techniques fell into the service sensitive category. The balance of the recirculation system piping welds remained in the regular ISI program.

Also in accordance with NUREG 0313, the ultrasonic examination procedure for austenitic stainless steel piping welds was modified and augmented to address detection of IGSCC; specific transducers were called out, scan speed modified, sensitivity increased, etc. However, these improvements only applied to these welds or items identified in the augmented program. In this case, the improved techniques were applied only to the safe-ends.

For the 1981 outage year a new examination procedure addressing only IGSCC detection had been developed for use on those items identified in the augmented program. While this effort further enhanced IGSCC detection, no changes were made to the selection of items to be examined, and only the safe-ends

themselves were to be examined with the improved methods. The balance of the recirculation system piping remained part of the standard ISI program. This means that prior to 1982, less than 10% of the recirculation piping circumferential welds had been examined since the NMP-1 ISI plan was implemented and none of those examinations reflected IGSCC detection considerations.

Following the safe-end leakage in 1982, indications were readily detectable in the safe-ends. It was at this point that the remainder of the recirculation piping was subjected to examination utilizing IGSCC techniques for the first time. Indications were detected in almost every weld examined once IGSCC techniques were applied.

Table 1 provides graphic and tabular information about in-situ examinations performed on the recirculation piping in 1982. (Refer to Figures 1 through 5 of Section 2 for identification of weld numbers). It will be noted that the bulk of examinations were performed on the pump suction side of the loops. This was a result of access conditions. Other pertinent information is included where appropriate, eg., welds with particularly large cracks, welds examined in 1981, etc. Except for 1982, the safe-ends themselves have been examined as part of the augmented program and are not part of this listing.

8.3 ISI INSPECTION COMPARISONS - 1979-82

During the primary system hydrotest in March 1982, leakage was visually detected at two of the ten furnace-sensitized, recirculation system safe-ends. Subsequent to the discovery of the leakage, U.T. examination of the two affected safe-ends and one other safe-end confirmed the presence of indications of intermittent cracking around the inner surface.

After the inspection of the safe-ends additional examinations were carried out in selected areas of the balance of the recirculation piping system. These first added examinations revealed indications in the heat-affected zones of recirculation pump discharge welds at the inner surface. Partial

disassembly of some of the pumps allowed access to the inner surface of the subject welds with dye penetrant examination confirming the indications as cracks. The U.T. examinations were then extended to other welds in the five loops of the recirculation system. This resulted in the identification of a large number of indications considered to be cracks.

In addressing the questions as to why certain defects in the total recirculation pipe system at Nine Mile Point were not detected in the 1981 inspection the subject must be divided into two categories. These categories are the (a) sensitized safe ends and (b) the balance of the recirculation system. Different procedures were applied to these two subdivisions of the piping system. The safe ends were part of the augmented inspection program according to NUREG 0313, while the balance of the system was not.

8.3.1 Safe Ends

Tables 2-7 derived from the ISI records of 1979-82 compare the inspection parameters of the safe ends in loops 11-15. In reviewing these and other supporting records the following factors are observed:

1. In 1982 more gain was added to the calibration sensitivity for scanning than in 1981 (typically 10dB versus 6dB).
2. Less time was devoted to a typical inspection in 1981 than in 1982.
3. The 1982 inspection took place after the presence of IGSCC had been confirmed by leakage, creating a psychology of inspection contributing to more careful examination and more willingness to call cracks.

Elaborating on the time consideration, the scanning and recording times of 1981 appear to be too short for thorough evaluation. Even without any recordable indications, they are too short for sufficient scanning to find

IGSCC. For example note the case in Table 6 of discharge safe ends #11 and 12 in 1981. About 1.5 hours were spent on the examination from one side of two circumferential joints (nozzle to safe end and safe end to pipe) and one whole safe end body. Rough estimates indicate 30 minutes for the safe end to pipe weld (safe end side only). This means one axial scan and two circumferential scans (CW and CCW) of a 28" diameter pipe took place in 30 minutes. Experience shows that rapid rates of manual scans tend to miss indications in the areas where IGSCC occurs. It is difficult to say how slow the scan should be. This must be learned by UT personnel through hands-on training on actual IGSCC specimens.

In summary, the following conclusions are reached relative to a comparison of the 1981 and 1982 NMP-1 safe-end inspection.

1. A higher sensitivity was used for the scanning in 1982.
2. The time devoted to some of the safe end examinations in 1981 appear to be too short for optimum detection of IGSCC.
3. All UT inspection in 1982 was done after the presence of IGSCC had been confirmed by leakage, probably resulting in a somewhat more careful inspection.

8.3.2 Balance of Recirculation Pipe System

Table 8 was derived from the ISI records of 1981 and 1982 for the common joints inspected in both years. In reviewing these and other supporting records the following factors are observed:

1. Prior to 1982 sampling (examination frequency) and techniques were based on Code requirements with no IGSCC consideration.
 - a. Only two joints were inspected during the 1981 ISI, namely 32-FW-10-W and 32-FW-36-W. Comparison of ISI results in 1981 and 1982 is hence limited to these two welds.

- b. The 0.5" x 1.0" 2.25 MHZ transducer used in 1981 will have a lower sensitivity to small defects (due to its large size) than the transducers used in 1982. It is expected that these indications would have been on the order of 20% DAC or less in 1981. The 1981 procedure required a 50% DAC reporting level.
 - c. In 1982 more gain was added to the calibration sensitivity for scanning than 1981 (both 10 dB and 20 dB versus 6 dB).
 - d. Indications were found in both joints in 1982 with amplitudes less than 50% DAC (10% notch) using 1/2" diameter 1.5 MHZ transducers.
 - e. More time was typically devoted to scanning and recording of data in 1982 than in 1981.
2. PT of 32-FW-36-W revealed a substantial axial crack. This crack is not detectable ultrasonically due to interference from unground weld crown.

Relative to the time devoted to inspection in 1981 versus 1982 note from Table 8 that the examination from one side of joint P32-FW-10-W plus the examination of two other circumferential joints from one side and 48 inches of axial weld from both sides took one hour and 49 minutes in 1981. It is estimated that the subject examination of joint P32-FW-10-W took about 30 minutes. Note that 3 hours and 20 minutes were devoted to the same examination in 1982.

In summary the following conclusions are considered to relate to the difference between the 1981 and 1982 inspection results on the balance of the recirculation system:

1. The procedure used in 1981 (a procedure acceptable to Section XI Appendix III) is ineffective for detection of IGSCC because of the 50% DAC reporting level.
2. Unground crowns may interfere (often do) with detection of axial cracks.
3. The time spent on scanning and recording is considerably lower for 1981 than 1982, and may be too short for optimum inspection for IGSCC.
4. IGSCC experience of inspection personnel was higher in 1982 than 1981 (availability of IGSCC samples and participation in EPRI NDE Center workshops).
5. The transducers used in 1982 resulted in effectively a more sensitive examination compared to 1981.
6. A higher sensitivity was used for scanning in 1982.
7. The same psychology of inspection after confirmation of IGSCC was present in 1982 as in the case of the safe end inspection.

8.4 EVALUATION OF ULTRASONIC EXAMINATION PERFORMANCE FOLLOWING PIPE REMOVAL

In addition to examinations performed in-situ on the recirculation system piping, a number of welds were examined subsequent to their removal. Figure 1 is a summary of examinations performed, noting procedure used and whether the in-situ examination occurred before or after initial system decontamination.

Due to a number of practical limitations, a complete in-situ and post-removal examination comparison was precluded. Six welds were examined both in-situ and after removal. A limited comparison of examination data from before and

and after in-situ chemical decontamination was also made. The following sections summarize the results of these analyses.

8.4.1 Correlation of UT and PT Data

To date, U.T. examinations on the specimens have been performed without benefit of ID PT information. This was generally followed from efforts to approximate the in-situ examination condition. Comparison of several ID PT examinations with the U.T. data suggest a relatively good correlation overall with a number of indications detected by only one of the examination methods. Where there is a lack of correlation, several possible examination conditions may be responsible.

Where a crack is identified by PT but not identified by U.T., two conditions are most likely:

1. The surface geometry precludes search unit positioning favorable to detection. This is likely to be the most frequent limitation.
2. The grain boundaries in the area of IGSCC may have deteriorated enough that local attenuation precludes U.T. response above the detection threshold.

Where an indication is identified by U.T. but not PT. the indication may result from reflection from significantly degraded grain boundaries which have not yet been opened by corrosion. Another possibility exists. The cracks may have been tight and filled with oxides, presenting the entrance of dye penetrant material into the crack.

8.4.2 Search Unit and Procedure Correlation

In order to evaluate the relative detection capability of the various U.T. techniques applied to piping, a combination of available search units were tested with three examination procedures on a flawed specimen (Figure 2).

Indications were found with all three procedures using the 45°, 1.5 MHz dual 3/8 x 3/4 inch search unit, and the 60°, 1.5 MHz 1/2 inch round search unit. Other search unit/procedure combinations were less sensitive. All but the 45°, 2.25 MHz 1/2 x 1 inch search unit detected the indications using the IGSCC oriented procedure (80A2818) which was used for 1982 Nine Mile Point recirculation system piping examinations.

As illustrated in Figure 3, indications from these tests were relatively repeatable. The high sensitivity of the 60°, 1.5 MHz .5 inch round or 45°, 1.5 MHz 3/8 x 3/4 inch dual search units are considered an acceptably reliable detector of IGSCC when used with the IGSCC-oriented procedure (80A2818) for piping similar to the Nine Mile Point recirculation system piping.

8.4.3 Effects of Chemical Decontamination on Detection

• Field Comparison

Eleven of the thirty-six welds examined in-situ were examined prior to system chemical contamination. Of these, four were identified to have 360° continuous intermittent indications, with six varying from few discrete indications to partial areas of continuous intermittent indication and one with no recordable indications.

Of twenty-six welds examinations in-situ after chemical decontamination, four had from few discrete indications to partial areas of continuous intermittent indications. These include three pipe-to-recirculation suction safe-end welds which were not directly subjected to decontamination, and will therefore be excluded from the tabulation. The fourth was limited to a one sided examination by accessibility. One weld was examined in-situ before and after chemical decontamination and had 360° intermittent indications in both examinations. All other in-situ, post-decontamination weld examinations found 360° intermittent indications.

Before Decon

Of 11 welds examined:

- 4 (36 percent of welds) had 360° intermittent indications
- 6 (54 percent of welds) had "few" discrete indications
- 1 (~10 percent of welds) had no recordable indications

After Decon

Of 22 1/2* welds examined after exposure to chemical decontamination:

- 22 (98 percent of welds) had 360° intermittent indications
- 1/2*(2 percent) had "few" discrete indications
- 0 had no recordable indications.

The effect of chemical decontamination on detection by UT is tabulated below. The results suggest that chemical decontamination may have increased the detectibility of the cracks by ultrasonic examination.

Because of this potential enhanced U.T. visibility associated with decontamination, the U.T. procedures and results were examined more closely.

Evaluation of the U.T. procedures employed revealed that they were identical for both the pre and post decontamination examinations. The only known difference was a somewhat longer examination time for the decontaminated weld. However, this difference is not considered significant.

In comparing the reported U.T. results before and after decontamination, it is important to establish that there are no significant differences, i.e., that both categories of welds are from the same population and have similar actual crack patterns. In comparing welds, it is found that except for two discharge safe-end to pipe spool welds, the weld population examined by U.T. before decontamination consisted entirely of elbow welds associated with the pumps in each loop. Since there is some uncertainty associated with whether

*Note: 1/2 weld represents a one sided examination by accessibility.

the two safe-end welds actually saw decontamination solution, the comparison was made excluding these two welds. The welds examined after decontamination were more randomly distributed. The actual welds evaluated are listed in Table 9 along with the U.T. results (i.e., whether termed continuous [360° intermittent] or discrete). Also listed is the stress rule index value for each weld as well as the post-decontamination P.T. indication length for each heat affected zone.

Post-decontamination P.T. gives the best available measure of total indication length and provides a basis for comparison between pre- and post-decontamination U.T. results. Examination and analysis of the results presented in Table 9 leads to several interesting conclusions:

The weld HAZ indication patterns and stress levels appear to represent a common population for both pre- and post-decontamination welds. This is based on; a) The average P.T. indication length (13.6% of circumference) is the same for pre- and post-decontamination. b) The cumulative distributions of HAZ P.T. indication lengths (Figure 4) is very similar for pre- and post-decontamination welds. c) The average stress rule index values for the pre- and post-decontamination welds are also very similar, 1.26 and 1.25 respectively.

Based on the above, it can be concluded that the pre- and post-decontamination welds are from a common population with similar cracking patterns and therefore the apparent reported differences in U.T. response on welds examined before versus after decontamination appear to be related to some aspect of the decontamination process. Perhaps the removal of oxide from the crack mouth by decontamination enhances U.T. visibility leading to the reporting of longer indication lengths. Additional evidence supporting enhanced U.T. visibility after decontamination is available from further analysis of the results in Table 9. It is assumed that the true indication length and circumferential distribution is best represented by the post-decontamination P.T. pattern. In Table 9, the available P.T. patterns for each weld HAZ are classified as

continuous (i.e., 360° intermittent indications), discrete, or none (no apparent indications). When only those HAZ's with continuous P.T. patterns are compared with the respective HAZ U.T. patterns, it is found that if U.T. was performed before decontamination only 33% of the continuous P.T. patterns also exhibited continuous U.T. patterns. However, if U.T. performed after decontamination, 89% of the continuous U.T. patterns also exhibited continuous P.T. patterns, indicating again that decontamination apparently significantly enhances U.T. visibility. In some other cases of continuous U.T. patterns, listed in Table 9, the corresponding P.T. patterns were non-continuous (discrete or non-existent). In these cases, it is likely that the U.T. "indications" were associated with geometric reflectors rather than cracks.

Since crack depth sizing was not attempted during the bulk of the U.T. exams, the available data are not adequate to determine whether decontamination also enhances crack depth determinations.

8.4.4 In-Situ vs. Laboratory U.T. Examination

A total of six welds were subjected to similar U.T. examinations both in-situ and after removal from the system. Due to repair and sample decontamination schedules, the balance of U.T. examinations were performed uniquely either before or after removal. All samples had been exposed to chemical decontamination.

Of the six data comparisons:

- four have numerous discrete indications in the laboratory compared to continuous intermittent indications in-situ. Of these four one weld has 100% correlation between discrete indications in-situ and laboratory.
- one has fewer discrete indications in laboratory than in-situ examination (about half of the indications in the examination correlate approximately).

- one has no laboratory indications compared to continuous intermittent indications in-situ (possible weld identification problem).

A controlled test would be required to more accurately determine the effects of cutting out the piping on detectability of existing IGSCC cracks. It does not appear, based on the limited sample, that there is any substantial difference in IGSCC crack detectability between in-situ post chemical decontamination examinations and post removal examinations using the same U.T. examination procedure. In the reduced radiation exposure environment of the laboratory, sizing and discrimination of small cracks is improved as expected.

8.4.5 Crack Depth Information

Due to the small through-wall dimension of typical IGSCC cracking relative to search unit beam width, it is probable that typical sizing parameters ("W" measurements and metal path change) are characterizations of the search unit beam spread, not necessarily the crack depth. (Figure 5.)

This is substantiated by review of the basic trigonometric parameters. These demonstrate that neither the plotted ID reflection of the crack tip (Figure 6) nor 6 dB down beam angle from the crack corner (Figure 5) satisfy the empirical metal path data for the 6 dB down "W₂" position.

It is most likely that the "W₂" (6 dB down) position represents the point at which the crack corner reflects the spread beam from the forward search unit edge. Thus, the metal path may result from the angle of beam divergence rather than from an extended "vee" path (Figure 8).

It is concluded that the distance from maximum signal, "W_m" to the 6 dB down point "W₂" suggests an upper limit on IGSCC crack depth but that the actual crack depth is considerably smaller than this limit. Additional studies have been initiated to improve sizing techniques; however, these techniques have not been applied to the Nine Mile Point welds.

TABLE 1
ISI EXAMINATIONS PERFORMED ON NMP-1 RECIRCULATION
PIPING WELDS IN 1982

RECIRCULATION LOOP 11

<u>WELDS EXAMINED</u>	<u>DESCRIPTION</u>	<u>'82 EXAM DATE</u>	<u>RESULTS</u>	<u>COMMENTS</u>
FW-2	Pipe/Valve	5/29	Circ. indications	IGSCC Techniques
FW-3	Valve/Pipe	5/29	Circ. indications	IGSCC Techniques
SW-3	Pipe/Elbow	6/1	Circ. indications	IGSCC Techniques
FW-4	Elbow/Elbow	5/4	Circ. indications	IGSCC Techniques
FW-26	Pump/Elbow	5/6	Circ. indications	IGSCC Techniques
SW-16	Pipe/Pipe	8/6	Circ. indications	IGSCC Techniques

NOTE:

Visual detection of leakage on this loop - safe end on pump discharge leg.

RECIRCULATION LOOP 12

<u>WELDS EXAMINED</u>	<u>DESCRIPTION</u>	<u>'82 EXAM DATE</u>	<u>RESULTS</u>	<u>COMMENTS</u>
FW-6	Pipe/Valve	6/2	Circ. indications	IGSCC Techniques
FW-7	Valve/Pipe	5/31	Circ. indications	IGSCC Techniques
SW-5	Pipe/Elbow	5/31	Circ. indications	IGSCC Techniques
FW-8	Elbow/Elbow	5/8	Circ. indications	IGSCC Techniques
FW-31	Pump/Elbow	5/6 & 6/12	Circ. indications	IGSCC Techniques
SW-20	Pipe/Elbow	8/6	Circ. indications	IGSCC Techniques

RECIRCULATION LOOP 13

<u>WELDS EXAMINED</u>	<u>DESCRIPTION</u>	<u>'82 EXAM DATE</u>	<u>RESULTS</u>	<u>COMMENTS</u>
FW-32	Pipe/Safe End	3/31	Circ. indications	IGSCC Techniques
FW-10 (Note 1)	Pipe/Valve	6/4	Circ. indications	IGSCC Techniques
FW-11	Valve/Pipe	6/4	Circ. indications	IGSCC Techniques
SW-8	Pipe/Elbow	6/4	Circ. indications	IGSCC Techniques
FW-12	Elbow/Elbow	5/8	Circ. indications	IGSCC Techniques
FW-36 (Note 1)	Pump/Elbow	4/30	Circ. indications	First evidence of cracking detected here using non-IGSCC procedure 4/2/82, at 20% DAC.

Note 1: Weld nos. FW-10 and FW-36 were examined in 1981 - no indications reported.

Note 2: Weld no. SW-6 contained .5" deep crack. Data obtained after removal.

Table 1 (Continued)

<u>WELDS EXAMINED</u>	<u>DESCRIPTION</u>	<u>'82 EXAM DATE</u>	<u>RESULTS</u>	<u>COMMENTS</u>
FW-14	Pipe/Valve	6/3	Circ. indications	IGSCC Techniques
FW-15	Valve/Pipe	6/3	Circ. indications	IGSCC Techniques
FW-11	Pipe/Elbow	6/3	Circ. indications	IGSCC Techniques
FW-16	Elbow/Elbow	5/8	Circ. indications	IGSCC Techniques
FW-41	Pump/Elbow	5/6	Circ. indications	IGSCC Techniques

RECIRCULATION LOOP 15

<u>WELDS EXAMINED</u>	<u>DESCRIPTION</u>	<u>'82 EXAM DATE</u>	<u>RESULTS</u>	<u>COMMENTS</u>
SW-13	Pipe/Tee	5/26	Circ. indications	IGSCC Techniques
FW-18	Tee/Pipe	6/2	Circ. indications	IGSCC Techniques
FW-19	Pipe/Valve	6/2	Circ. indications	IGSCC Techniques
FW-20	Valve/Pipe	6/2	Circ. indications	IGSCC Techniques
FW-14	Pipe/Elbow	6/4	Circ. indications	IGSCC Techniques
FW-21	Elbow/Elbow	6/3	Circ. indications	IGSCC Techniques
FW-46	Pump/Elbow	4/2	Circ. indications (75% DAC)	First UT evidence of cracking detected here using IGSCC procedure. (75% DAC). PT and film metallurgical verification.

NOTE 1: Visual detection of leakage this loop -
Safe end on pump suction leg.

NOTE 2: Weld No. SW-12 contained .55" deep
crack. Data obtained after removal.

TABLE 2
INDICATIONS

	SUCTION					DISCHARGE				
	11	12	13	14	15	11	12	13	14	15
1979	NO	NO	GEO	GEO	?	NO	NO	NO	NO	NO
1980	--	--	GEO	--	--	--	--	--	--	--
1981	GEO	GEO	GEO	GEO	NO	NO	NO	NO	NO	NO
1982	--	--	--	--	IGSCC ¹	IGSCC	--	IGSCC	--	--
DP/LEAK	*2	*3	*3	*3	LEAK	LEAK	*3	*3	*3	*3

NOTES:

1. Leaking crack investigated by UT, no examination performed.
2. No cracking found in DP examinations by NDE Center at Battelle Columbus Laboratories (BCL)
3. DP investigation at plant or BCL not completed and documented

NO - Inspection performed, no reportable indications

-- - No inspection

GEO - Inspection performed, geometry indications reported

DP/LEAK - Determination of flaw by leakage or dye penetrant indication

TABLE 3
SEARCH UNIT (NAME/MHz)

	SUCTION					DISCHARGE				
	11	12	13	14	15	11	12	13	14	15
1979	AERO/1.6	AERO/1.6	AERO/1.6	AERO/1.6	AERO/1.6	SUSI-10/ 1.5	AERO/1.6	AERO/1.6	SUSI-10/ 1.5	DUEL/1.5
1980	--	--	AERO/1.6	--	--	--	--	--	--	--
1981	AERO/1.5	SUSI-10/ 1.5	SUSI-10/ 1.5	SUSI-10/ 1.5	SUSI-11/ 1.5	SUSI-39/ 1.5	SUSI-39/ 1.5	SUSI-10/ 1.5	SUSI-10/ 1.5	SUSI-10/ 1.5
1982	--	--	--	--	--	SUSI-10/ 1.5	--	SUSI-10/ 1.5	--	--

AERO/N Aerotech transducer of frequency N, MHz

SUSI-X/N Search Units Systems, Inc. transducer, Model X,
frequency of N, MHz

TABLE 4
SENSITIVITY* (CAL. SENSITIVITY WITH P8F-1.5-1), CAL/SCAN

	SUCTION					DISCHARGE				
	11	12	13	14	15	11	12	13	14	15
1979	43/?	49/?	41/?	38/?	43/?	77/?	45/?	47/?	39/?	62/?
1980	--	--	40/46	--	--	--	--	--	--	--
1981	47/53	55/61	55/61	55/61	68/74	40/46	40/46	98/104	102/108	102/108
1982	--	--	--	--	--	44/54	--	55/65	--	--

*All except Suction #13, 1980 were with Sonic Mk-I. (USL-31 for Suction #13).

TABLE 5
TEMPERATURE (CAL. BLOCK/COMPONENT °F)

	SUCTION					DISCHARGE				
	11	12	13	14	15	11	12	13	14	15
1979	63/84	64/86	64/81	67/80	63/84	72/96	80/90	65/85	65/86	73/90
1980	--	--	110/132	--	--	--	--	--	--	--
1981	65/86	65/86	65/86	65/86	74/99	75/95	75/95	76/96	65/86	65/85
1982	--	--	--	--	--	88/100	--	72/88	--	--

TABLE 6
SCANNING AND RECORDING TIME (HR. MIN.)

	SUCTION					DISCHARGE				
	11	12	13	14	15	11	12	13	14	1 15
1979	2.50	2.05	0.55	3.00	2.50	3.00	3.00	1.30	2.00	2.48
1980	--	--	1.50	--	--	--	--	--	--	--
1981	1.25	2.13	2.12	2.13	2.20	1.30	1.30	1.40	1.40	1.40
1982	--	--	--	--	--	6.20 ¹ 1.45	--	2.15	--	--

NOTE: The listed times are the time between calibration time and final check. This typically includes inspection for scanning of nozzle/safe end weld (safe end side), safe end body and safe end/pipe weld (safe end side).

¹Elapse time includes activities other than examination. Scanning and recording time consists of two 1-2 hour periods.

TABLE 7
UT PERSONNEL (LEVEL)

	SUCTION					DISCHARGE				
	11	12	13	14	15	11	12	13	14	15
1979	II,I	III,II	II,II	III,II	II,I	II,I	II,I	II,I	II,I	II,I
1980	--	--	III,II	--	--	--	--	--	--	--
1981	II,I	III,III	II,I	III,III	II,I	III,III	III,III	II,I	II,II	II,I
1982	--	--	--	--	--	III,II III,III	--	III,III	--	--

TABLE 8
OVERALL COMPARISON COMMON JOINTS 1981, 1982

	1981		1982		
	P32-FW-10W	P32-FW-36W	P32-FW-10W	P32-FW-36W	
Indication	NO	NO	5-10% DAC (100% DAC at +10dB)	20% DAC	50% DAC at +10dB
UT Instrument	MK-1	MK-1	USL-38	MK-1	
Search Unit	AEROTECH 1/2"x1" RECT. 2.25 MHz	AEROTECH 1/2"x1" RECT. 2.25 MHz	AEROTECH 1/2" ♦ 1.5 MHz	AEROTECH 1/2" ♦ 2.25 MHz	AEROTECH 1/2" ♦ 1.5 MHz
Cal. Block	PBR-1.050-1	PBR-1.050-1	PBR-1.050-1	PBR-1.050-1	
Sensitivity Cal.(dB)/Scan	72/78	72/78	42/62	31/41	38/58
Temperature (°F) Cal. Blk/Component	67/72	67/72	68/76	62/80	62/70
Scan & Record Time (Hr. Min.)	9.15/11.04 1.49 ^a	9.15/11.04 1.49 ^a	8.40/11.60 3.20 ^a	9.45/15.15 5.30 ^a	9.00/10.30 1.30 ^a
UT Personnel	II,I	II,I	III,II	III,II	II,I

APRIL

MAY

- ^a This total time includes scanning both joint P32-FW-10W and P32-FW-36W from one side only plus 1 other circumferential welds from one side only and 4 - 12" sections of longitudinal weld from both sides.
- ^b Time for scanning P32-FW-10W from one side only.
- ^c Time for scanning P32-FW-36W from one side only plus three other circumferential welds from one side only.
- ^d Time for scanning P32-FW-36W from one side only.

TABLE 9
SUMMARY OF COMPARATIVE U.T. AND P.T. RESULTS
Welds U.T.'d Before Decon, P.T.'d After Decon

Weld	HAZ	Stress Rule Index	Classification		P.T. Indication	% Circumference With P.T. Indications
			UT	PT		
FW-4	Elbow	1.3	D	D	Circ. Ind.	8
FW-26	Elbow	1.2	C	D	Circ. Ind.	5
FW-22	Pipe	1.2	N	D	Circ. + Axial	5
	Safe-End	1.2	D	C	Circ. + Axial + Leak	10
FW-8	Elbow	1.3	D	C	Branched Circ.	40
FW-31	Elbow	1.2	C	C	Branched Circ.	26
FW-12	Elbow	1.3	C	C	Branched Circ.	44
FW-36	Elbow	1.2	D	D	Circ. + Axial	1
FW-32	Pipe	1.4	D	C	Circ. + Axial	6
	Safe-End	1.4	D	C	Circ. + Axial	3
FW-41	Elbow	1.2	C	D	Circ. + Axial	3
FW-21	Elbow	1.3	D	D	Circ.	5
FW-46	Elbow	1.2	D	C	Circ.	21
1.26 Avg.						13.6 Avg.

Welds U.T.'d After Decon, P.T.'d After Decon

SW-2	Tee	2.1(1.7)*	N	N	No Ind.	0
	Pipe	2.1(1.7)*	D	N	No Ind.	0
FW-2	Pipe	1.2	C	-	-	-
FW-3	Pipe	1.2	C	-	-	-
SW-16	Pipe	-	C	N	No Ind.	0
	Pipe	-	C	N	No Ind.	0
SW-3	Pipe	1.2	C	N	No Ind.	0
	Elbow	1.2	C	D	Circ.	2
FW-5	Safe-End	1.2	D	N	No Ind.	0
	Elbow	1.2	D	N	No Ind.	0
FW-6	Pipe	1.2	C	-	-	-
FW-7	Pipe	1.2	C	-	-	-
SW-17	Elbow	1.2	D	N	No Ind.	0
	Pipe	1.2	N	N	No Ind.	0
SW-5	Pipe	1.2	C	D	Axials	1
	Elbow	1.2	N	D	Circ.	2
FW-31	Elbow	-	C	C	Branched Circ.	26
SW-20	Elbow	1.2	C	D	Circ.	2
	Pipe	1.2	C	C	Circ.	13
SW-19**	Pipe	1.2	C	C	Branched Circ.	55-60
	Pipe	1.2	C	C	Branched Circ.	25-30

*SRI = 1.7 if treated as branch connection; 2.1 if treated as Tee.

**U.T. performed after pipe removal.

C = 360° Intermittant Indications

N = No Indications

D = Discrete Indications

TABLE 9 (Continued)
SUMMARY OF COMPARATIVE U.T. AND P.T. RESULTS
Welds Y.T.'d, P.T.'d After Decon (Cont'd)

Weld	HAZ	Stress Rule Index	Classification		Post Decon P.T. Indication	% Circumference With P.T. Indication
			UT	PT		
FW-9	Safe-End	1.2	D	C	Circ. + Axial	>50%
	Elbow	1.2	D	N	No Ind.	0
SW-7	Pipe	1.2	D	-	-	-
FW-10	Pipe	1.2	C	-	-	-
FW-11	Pipe	1.2	C	-	-	-
SW-8	Pipe	1.2	C	C	Circ. + Axial	42
	Elbow	1.2	C	C	Circ. + Axial	16
FW-14	Pipe	1.2	C	-	-	-
FW-15	Pipe	1.2	C	-	-	-
SW-11	Pipe	1.2	C	C	Circ. + Axial	14
	Elbow	1.2	C	C	Circ. + Axial	15
FW-16	Elbow	1.3	C	C	Branched Circ.	18
FW-17	Safe-End	1.2	D	D	Circ. + Leak	22
	Elbow	1.2	N	N	No Ind.	0
SW-12	Elbow	1.2	C	D	Circ.	11
	Pipe	1.2	C	C	Circ.	17
SW-13	Pipe	2.1(1.7)*	C	-	-	-
	Tee	2.1(1.7)*	N	-	-	-
FW-18	Tee	2.1(1.7)*	N	-	-	-
	Pipe	2.1(1.7)*	C	-	-	-
FW-19	Pipe	1.2	C	-	-	-
FW-20	Pipe	1.2	C	-	-	-
SW-14	Pipe	1.2	C	C	Circ. Ind.	8
	Elbow	1.2	C	N	No Ind.	0
SW-6**	Pipe	1.2	C	C	Branched Circ.	45-50
	Elbow	1.2	C	C	Branched Circ.	35-40
SW-23**	Pipe	1.2	N	C	Branched Circ.	30-35
	Elbow	1.2	C	C	Branched Circ.	20-25
SW-10**	Tee	2.1(1.7)*	N	-	-	-
	Pipe	2.1(1.7)*	N	-	-	-
SW-26**	Elbow	1.2	C	C	Branched Circ.	20-25
	Pipe	1.2	C	C	Circ.	5-10
SW-25**	Pipe	1.2	C	D	Circ. Ind.	0-5
	Pipe	1.2	C	D	Branched Ind.	0-5
		1.25 Avg. +				13.6 Avg.

+ Average based only on welds with PT results.

*SRI = 1.7 if treated as branch connection; 2.1 if treated as Tee.

**U.T. Performed after pipe removal.

C = 360° Intermittent Indications

N = No Indications

D = Discrete Indications

Loop No.	Weld No.	IN SITU UT (Procedure* - Data Sheet*)	Before/After Initial Decon	Other NDE (Data Sheet*)		
				80A2818 (UT)	80A2819 (PT)	80A4022 (UT)
11	FW-1-W				SP-03	
11	SW-1-W				SP-02	
11	SW-2-W	2818-19	After	EP-UT-10		
11	FW-2-W	2818-17	After			
11	FW-3-W	2818-17	After			
11	FW-4-W	2818-6,7	Before			
11	FW-26-W	2818-8	Before			
11	SW-16-W	2818-49	After	EP-UT-1		
11	FW-22-W	2818-1	Before			
11	SW-3-W	2818-24	After	EP-UT-7	EP-PT-6	EP-DC-3
11	SW-17-W			EP-UT-8	EP-PT-7	EP-DC-2
12	FW-5-W	2818-SP-01	After		SP-05	
12	FW-6-W	2818-30	After			
12	FW-7-W	2818-22	After			
12	SW-5-W	2818-23	After	EP-UT-4	EP-PT-3	EP-DC-4
12	FW-8-W	2818-10	Before			
12	FW-31-W	2818-9/47	Before/After			
12	SW-20-W	2818-51	After	EP-UT-5	EP-PT-4	EP-DC-5
12	SW-19-W			EP-UT-12		
12	SW-4-W				SP-04	
13	SW-6-W			SP-04,05,06	SP-06	
13	FW-9-W	2818-SP-01	After	SP-02,03	SP-07	
13	SW-7-W				SP-08	
13	FW-10-W	2818-36	After			
13	FW-11-W	2818-35	After			
13	SW-8-W	2818-37	After	EP-UT-09		
13	FW-12-W	2818-11	Before			
13	FW-36-W	2818-4, SP-07	Before			
13	SW-23-W			EP-UT-06	EP-PT-05	EP-DC-01
13	SW-22-W			SP-09		

Figure 1. Summary of Examinations Performed

Loop No.	Weld No.	IN SITU UT (Procedure* - Data Sheet*)	Before/After Initial Decon	Other NDE (Data Sheet*)		
				80A2818 (UT)	80A2819 (PT)	80A4022 (UT)
13	FW-32-W	2818-3	Before			
14	FW-14-W	2818-31	After			
14	FW-15-W	2818-32	After			
14	SW-11-W	2818-33, SP-08	After	EP-UT-11		
14	FW-16-W	2818-12	After			
14	FW-14-W	2818-9	Before			
14	SW-26-W			EP-UT-02	EP-PT-01	EP-DC-07
14	SW-25-W			EP-UT-03	EP-PT-02	EP-DC-06
15	FW-17-W	2818-SP01	After			
15	SW-12-W	2818-46	After			
15	SW-13-W	2818-14	After			
15	FW-18-W	2818-28	After			
15	FW-19-W	2818-27	After			
15	FW-20-W	2818-26	After			
15	SW-14-W	2818-38,39	After			
15	FW-21-W	2818-5,7	Before			
15	FW-46-W	2309-4	Before			

Figure 1. Summary of Examinations Performed (Continued)

PROCEDURE	TRANSDUCER	CAL BLOCK	SCAN SENS (dB)	REMARKS
80A2309	A	CURVED	36	
REV 1	B	P8R-1.050-1	70	
	C	↓	50	
	D		42	
	E		44	
	F		42	
80A2818	A	CURVED	36	
REV 1	B	P8R-1.050-1	70	
	C	↓	50	
	D		42	
	E		44	
	F		42	
80A0835	A	FLAT	60	
REV 0/FC-3	B	P8F-1.5-1	73	
	C	↓	63	
	D		50	
	E		51	
	F		60	
80A2818	E	CURVED	62	FC 1, 2, 3, AND 5
REV 1	E	P8R-1.050-1	62	DATA AT BATTELLE
				SCAN 20 dB > REF
				RECORD 10 dB > REF
				DATA AT NMP 1

NOTES: 1) TRANSDUCER INFORMATION

LTR	MFG	ANGLE (°)	SIZE	FREQ	TYPE
A	AERO	45	3/8 x 3/4 in.	1.5 M	DUAL
B	AERO	60	0.5 in.	1.5 M	γ
C	SUSI	45	3/8 x 3/8 in.	1.5 M	DUAL
D	AERO	45	0.5 in.	2.25 M	γ
E	AERO	45	0.5 in.	1.5 M	γ
F	AERO	45	1/2 x 1 in.	2.25 M	γ

2) ALL SCANNING WAS
PERFORMED AT
BATTELLE ON WELD
RING P-32-SW-8-W
EXCEPT EXAM
INDICATED IN
REMARKS ("DATA
AT NMP 1")

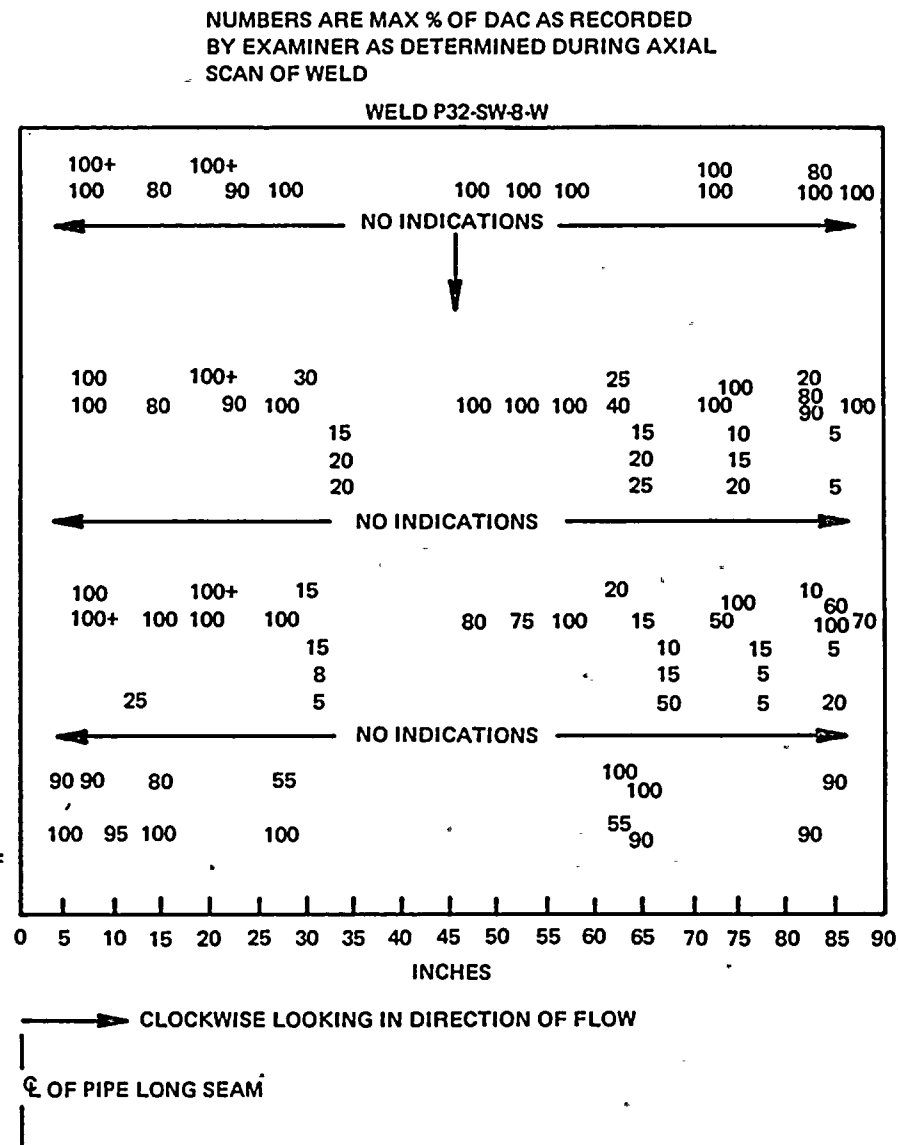


Figure 2. Summary of Recordings - Using Various Transducers
and Nine Mile Point Unit 1 Procedures.

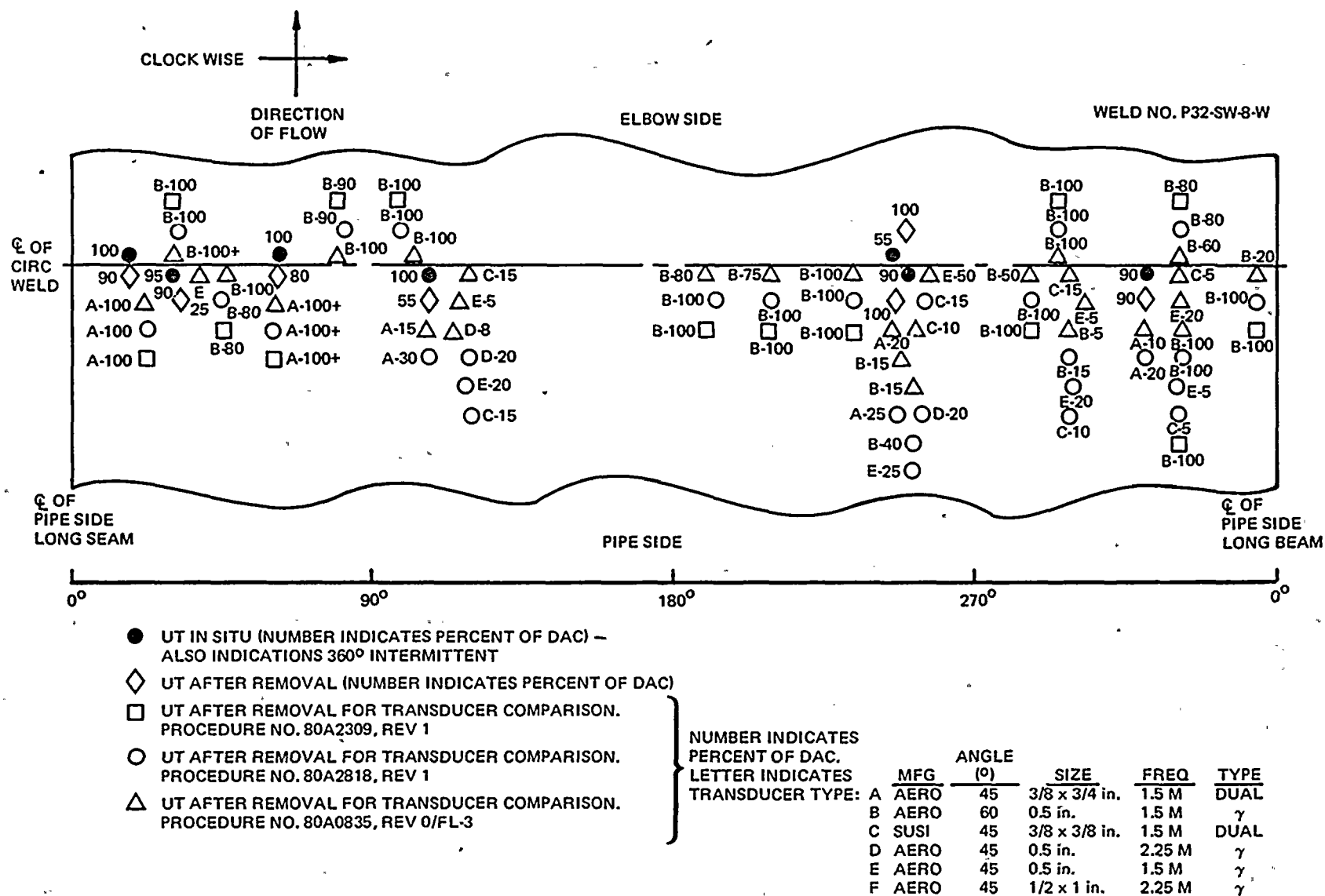


Figure 3. Graphical Display of Recorded Indications

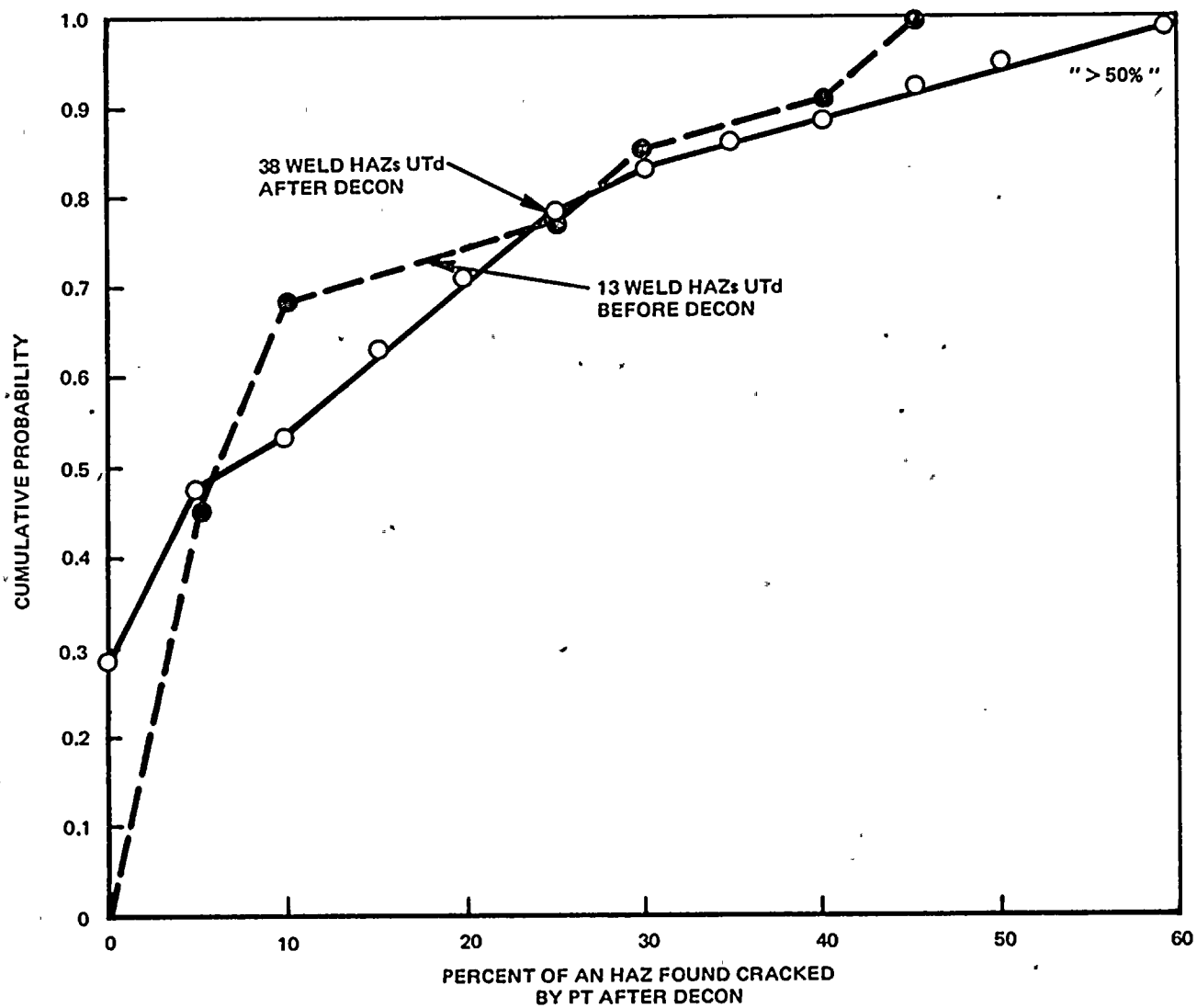


Figure 4. Cumulative Probability of Percent of an HAZ Found Cracked by P.T. After Decon

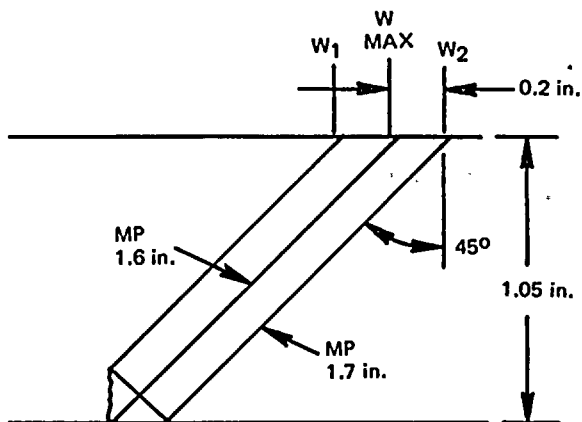


Figure 5. Typical Measured Data

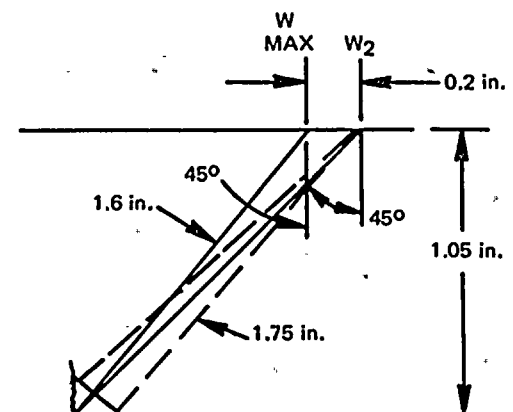


Figure 6. Minimum Theoretical Metal Path

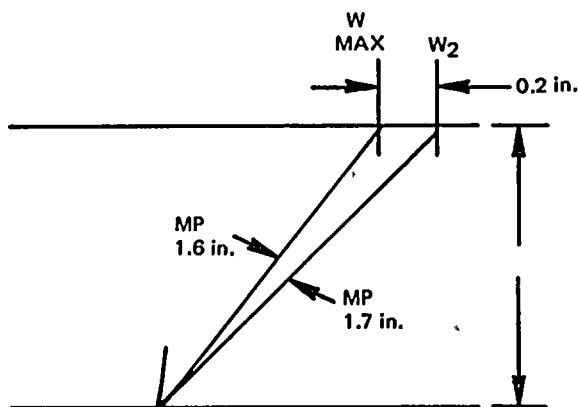


Figure 7. Typical Dimensions

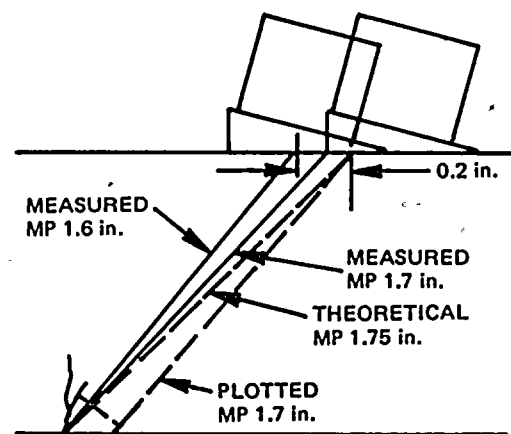


Figure 8. Possible Condition

APPENDIX A

Procedure Excerpts

The following paragraphs are taken from the procedures used for (1) IGSCC oriented examinations and (2) other austenitic piping, respectively. This material illustrates the salient differences in examination methods.

1. 80A2818, Rev. 1 - Applied to Safe Ends, '81 and '82; applied to Recirculation Piping '82 (following IGSCC confirmation), "Ultrasonic Examination of Stainless Steel Piping for Intergranular Stress Corrosion Cracking (IGSCC)."

5.2.1 The rate of search unit movement shall not exceed two (2) inches per second. The search unit shall be swiveled a full 90° during axial scanning (45° left and 45° right).

6.1 Examination Contractor's Equipment

The following test equipment or its equivalent shall be provided by the Examination Contractor (as a minimum) for examination of welds when specified in this procedure:

1. Pulse echo ultrasonic instrument
2. Search Unit: dual 1.6 MHz or 1.5 MHz for $T \geq 0.375"$
3. Search Units: 0° ; $1/4"$ - $1/2"$ dia.; 5.0 MHz
4. Search Unit: 1.6 MHz, $1/2"$ dia.; single element for $T < 0.375"$
5. Wedges: 45° shear and longitudinal, $1/2"$, 60° shear for wall thickness 0.200" and less

8.2.2 Angle Beam Calibration: 1-1/2 Vee Technique

One and one-half vee path calibration shall be the preferred method of calibration for the examinations described in this procedure and shall be accomplished as follows:

1. Obtain maximized signal response from the notches and mark the signal response positions on the instrument's CRT screen.
2. Maximize the signal from the notch producing the highest response and set its amplitude to 80% FSH.

9.2 Additional Straight Beam Examination (When indications are detected)

9.2.1 In order to accurately plot indications, the ID and OD weld contour must be established. The OD contour shall be recorded with the use of a contour gauge. The ID contour is established by performing a thickness check of the weld and adjacent base material to establish the location, depth and slope of any existing counterbore.

9.2.2 The thickness and contour data is then plotted on a full scale weld profile. Angle beam recordings are transferred to this plot to determine the true nature of all indications.

9.3 Angle Beam Examination

9.3.1 The scan sensitivity shall be a minimum of 2X (6 dB) greater but no more than 10 dB greater, than the calibration reference sensitivity level.

9.3.2 The search unit shall be swiveled (45° each way) as it is moved along a rectilinear scan pattern to ensure a minimum of 25% overlap of the transducer width. This is required to detect cracks which may be oriented at odd angles.

9.3.3 The examiner shall pay particular attention to indications which originate adjacent to the weld root and up to 0.5" out from the root. These typical locations of IGSCC are of ID origin.

9.3.4 Any such indications which may be considered as counterbore must be verified by 0° thickness check.

10. Evaluation Criteria

10.1.1 Indications from the weld crown and from other OD geometric origins may be ignored. The liquid penetrant examination will cover this area.

10.1.2 All other indications regardless of amplitude shall be recorded ...

2. 80A2309, Rev. 1 - Applied to Recirculation Piping, '81, "Ultrasonic Examination Procedures for Austenitic Piping."

6.1 Examination Contractor's Equipment

The following test equipment or its equivalent shall be provided by the Examination Contractor (as a minimum) for examination of welds specified in this procedure.

1. Pulse echo ultrasonic instruments

2. Search Units: 1/4" through 1-1/8" dia., 2.25 MHz, 0°

3. Search Units: 1/2" through 1-1/8" dia., 5.0 MHz, 0°
4. Search Units: 2.25 MHz (all sizes) for angle beam wedges.

8.3.2 Sensitivity Calibration; 1-1/2 Full Vee Technique

One and one-half vee path calibration shall be the preferred method of calibration for the examinations described in this procedure and shall be accomplished as follows:

1. Obtain maximized signal responses from the notches and mark the signal response positions on the instrument's CRT screen.
2. Maximize the signal from the notch producing the highest response and set its amplitude to 80% FSH.
3. Without changing sensitivity settings, maximize successive notch indications and mark their peak amplitudes on the CRT screen, and on the Calibration Data Sheet.

9.2 Straight and Angle Beam Examination of WRV

- 9.2.1 All straight and angle beam examinations of the WRV shall be performed at a scanning sensitivity level, a minimum of 2X (6 dB), but no more than 10 dB greater than the calibrated reference sensitivity level.
- 9.2.2 The search unit shall be swiveled as it is moved along at a recilinear scan pattern to ensure a minimum of 25% overlap of the transducer width.
- 9.2.3 For the locations and the numbers of the welds, refer to the Program Plan. Examinations shall not be considered complete until all recordable indications have been evaluated.

10. Evaluation Criteria

- 10.1 All indications showing a signal amplitude \geq 50% of DAC, at the strongest location, shall be plotted full scale. If the indication is nongeometric, the examiner shall continue recording until all necessary data is obtained.

APPENDIX B

Transducer Usage for Safe End Examination

The following tabulation illustrates the various types of transducers used for safe end examinations in 1981. The inconsistency in transducer size could cause some variation in examination results.

<u>Safe End</u>	<u>1981</u>	<u>1982</u>
#11 Discharge (leak)	SUSI 39	SUSI 10
#12 Discharge	SUSI 39	N/A
#13 Discharge	SUSI 10	SUSI 10
#14 Discharge	SUSI 10	N/A
#15 Discharge	SUSI 10	N/A
#11 Suction	Aerotech 3/8 x 7/8 Dual, 1.5 MHz	N/A
#12 Suction	SUSI 10	N/A
#13 Suction	SUSI 10	N/A
#14 Suction	SUSI 10	N/A
#15 Suction (leak)	SUSI 11	SUSI 10 (incomplete)
SUSI 10 = 3/8" x 3/8" Dual, 1.5 MHz		
SUSI 11 = 1/4" x 1/4" Dual, 1.5 MHz		
SUSI 39 = 1/2" x 1/2" Dual, 1.5 MHz		

SUSI = Search Unit Systems, Inc.

SECTION IX

APPARENT CRACK GROWTH RATES - GENERIC IMPLICATIONS

The leaking axial through-wall cracks in two furnace sensitized safe ends discovered in March 1982, were not detected during ISI nine months earlier (1981). Through-wall crack growth in a 28-inch safe end in nine months or less is completely unexpected based on previous crack growth assessments of furnace sensitized safe ends. Therefore, it was important to establish the rate at which IGSCC would propagate from the true U.T. detectability threshold to through-wall leakage. To accomplish this, it was necessary to:

1. Measure actual crack growth rate of a NMP-1 Type 316 furnace sensitized safe end.
2. Evaluate the through-wall residual stresses for the NMP-1 safe end geometry in the region of cracking.
3. Assess for that geometry the U.T. detectability threshold to establish the size of crack that might have gone undetected during the 1981 ISI.

A. MATERIALS DATA BASE

Previous tests have been conducted to measure crack growth rates of furnace sensitized 304 stainless steel under constant loads.¹ The objective was to support a methodology used to predict crack growth behavior in large diameter pipes exposed to service environments. Tests were conducted in 0.2 ppm O₂ and 8 ppm O₂ high purity, high temperature (550°F) water. The 0.2 ppm low oxygen environment and sensitized material condition is representative of service conditions. Figure 1 presents the data obtained from these tests along with two evaluation curves.¹ The upper bound curve represents a high degree of

sensitization due to post weld heat treatment. The lower bound curve represents data for moderate degrees of sensitization. The shape of the lower curve was selected to display characteristic stress corrosion cracking behavior. These data results are the basis for predictions used to explain field experience.

B. CRACK GROWTH RATES OF NINE MILE POINT MATERIAL

A test program was initiated to characterize furnace sensitized safe end material from the Nine Mile Point plant that had exhibited field cracking. Constant load crack growth tests were performed using a .9T-WOL (Wedge-Open Loaded) specimen, shown in Figure 2. This specimen was fabricated from NMP 316 stainless steel safe end material, Heat #E-5349.

Testing was conducted in the General Electric Small Environmental Fatigue Test (SEFT) machine which is a 100 kip capacity hydraulic test machine. A computerized data acquisition system (Figure 3) was utilized to measure in-situ compliance data. This data is obtained from a Linear Variable Differential Transformer (LVDT) mounted on the specimen face, as shown in Figure 4.

The SEFT test vessel was supplied with high pressure/temperature water environment provided by a high flow test loop (Environmental Fatigue Loop II) in General Electric's Experimental Mechanics Laboratory. The loop included a canned rotor pump which provided sufficient flow to insure that the specimen was subjected to a refreshed environment. Dissolved oxygen level was controlled by a gas control system that continually

purged a gas mixture through the makeup tank supplying water to the loop. A schematic of the test loop is shown in Figure 5. The level of dissolved oxygen and conductivity of the loop water was continuously monitored during testing. Table 1 lists the environment specifications.

The .9T-WOL specimen was fatigue precracked in room temperature air prior to test to produce a $\sim .100$ " long precrack. A test load of 5000 pounds was chosen to produce a stress intensity level (K) of $\sim 37 \text{ ksi}\sqrt{\text{in}}$. The loading was divided into two phases, shown in Figure 6. Phase I (cyclic loading) was to insure that an active crack existed. Phase II (constant loading) was the primary test phase wherein all crack growth data is obtained.

The total time on test for the 316 stainless steel specimen was 1351 hours, with the initial 248 hours under cyclic loading (Phase I). At the test completion, the specimen was broken apart and the total crack growth measured using an x-y traversing bed optical microscope. The fracture surface morphology indicated an average of ~ 0.020 " of intergranular stress corrosion crack growth (IGSCC) under the constant load phase. The average crack growth rate at a K level of $37 \text{ ksi}\sqrt{\text{in}}$ was determined to be 1.6×10^{-5} in/hr, with an upper bound of 7.5×10^{-5} in/hr for the heavily attacked regions.

The results from the constant load tests performed on 316 SS Nine Mile Point safe end material are plotted with the data base from previous tests in Figure 7. The data lie among other data that is from heavily sensitized material, typical of post weld heat treated material. The crack growth behavior, therefore, is consistent with previous test results on highly sensitized material and supports the GE crack growth prediction methodology.

C. MODEL QUALIFICATIONS AND PREDICTIONS

Predictive methods developed as part of the Large Pipe Program¹ were used to evaluate crack growth behavior in the safe end heat affected zone of the Nine Mile Point large diameter recirculation system. The predictive methodology developed assumes the existence of a fully circumferential/or axial flaw. These geometries are consistent with those observed for Intergranular Stress Corrosion Cracking (IGSCC) in butt-welded pipes. In addition to determining the rate of growth of these flaws, it is necessary to determine the critical flaw size for net section collapse to demonstrate that adequate margin still existed at NMP so that the plant could have operated for at least one additional 12-18 month cycle without exceeding Code type structural margins. The methodology for calculating this size and for adding a factor of safety to calculate a smaller "acceptance flaw size" are discussed in Reference 1.

The time required for a crack of some initial known size to grow to this acceptance flaw size is the subject of this section. The calculated crack growth under operating conditions, Δa , can be used to establish the appropriate time increment between inspections. The methodology for determining the growth of the flaw size uses LEFM to determine the stress intensity factor at the crack tip and includes residual stress as well as other applied loads. The assumption is made that the stress intensity factor, K , is the principal factor controlling the rate of crack growth. It is a function of the flaw geometry, component geometry, and the stresses. Crack growth rates as a function of stress intensity were determined from laboratory data and are used for the crack growth predictions.

The crack growth rates depend on material condition, loading history, and environment. To predict the behavior of heavily sensitized material, upper bound crack growth rates are generally used to assure the most conservative prediction crack deepening. These upper bound rates have been derived from tests performed in severely sensitized material, in a condition expected to be worse than that in as-welded pipe. For as-welded pipes, the behavior would be expected to be similar to or slower than that predicted by expected (or average) IGSCC crack growth data and much slower than the upper bound data that can be used to bound field experience accurately.

Circumferential Flaw

The methodology required input operating stresses and input throughwall residual stresses. These stresses were used to define the stress intensity as a function of crack depth for the pipe configuration. It is assumed that the crack is fully circumferential. This output was used with the crack growth data to develop crack depth as a function of time using a time-step integration to arrive at the crack length. This methodology is described in Reference 1.

The input stresses for the Nine Mile Point large pipe are given in Table 2. For the crack growth calculations, the total operating stress was used to derive the stress intensity, K , as a function of depth listed in Table 3. The throughwall residual distribution was picked to be representative. It is shown on a plot of measured residual stresses in

Figure 8. Through-wall residual stresses were obtained from a comparable pipe-to-safe-end weld from a large diameter recirculation segment from the KRB plant after operating for approximately the same number of years as NMP-1. The heavy line superimposed on the other data of Figure 8 is the experimentally measured through-wall residual stress distribution from the furnace sensitized safe end. These residual stresses were obtained by direct strain gage measurements and were determined with a high confidence of accuracy. (Ref. 2.) The measured results for the KRB safe end, which is similar in design to the NMP-1 safe end, are typical of the band of the experimentally determined data for large diameter pipes. Figure 8 illustrates the comparison, and lends confidence to the use of the existing through-wall residual stress data base.

Residual axial stresses were also calculated analytically using finite element methods (Figure 9). The magnitude of the predicted stresses agreed very well with the experimentally determined residual stresses and those used for the crack growth analysis. The listing of stress intensity as a function of crack depth is listed in Table 4. Because the method uses linear elastic fracture mechanics, these two K-solutions for operating stresses and residual stresses are superimposed to arrive at the driving force for crack growth.

The crack growth data used is displayed in Figure 7. For the evaluations performed, two crack growth evaluation curves were used: the upper bound, shown as the solid line and expected IGSCC crack growth shown as a dashed line. The expected curve is comprised of a crack growth rate as a function of K that is one-third ($1/3$) that of the upper bound. This rate curve fits the data well and therefore represents a good estimate of growth for highly sensitized stainless steel.

The crack size as a function of time assuming upper bound rates is given in Table 5 and displayed in Figure 10. The table lists the stress intensity and crack growth rate used as well as the crack size and time. Table 6 lists the crack size as a function of time using expected IGSCC crack growth rates. Figure 11 displays these results.

Using the results of the predictions for the Nine Mile Point safe end, it is possible to summarize the time for a starting crack, a_0 , to grow to a maximum allowable size, a_c . Table 7 shows the time to grow to 50% of the thickness as a function of initial size. The table displays times for both crack growth evaluation curves. Growth is more rapid initially (up to 20%) than at greater depth due to the compressive nature of the residual stresses. Beyond 50%, the time for additional growth is still significant due to the nature of the residual stresses.

For a degree of sensitization expected in the safe end, an initial circumferential crack of depth 5% of wall is predicted to grow to 20% of wall in about one year and from 20% to 50% of wall in an additional six years. By way of contrast, a prediction using the upper bound growth rates shows the initial 5% flaw would grow to 20% of wall in a few thousand hours and from 20% to 50% in an additional two years. The decrease in growth rates as the crack depth increases is again due to the compressive nature of the residual stress field in the mid-thickness of the safe end.

The allowable circumferential flaw size curve for a 28-inch safe end is shown in Figure 12. The acceptance line represents a safety factor of 2.773, while the

cross-hatched failure region indicates net section collapse. Average and maximum crack depths representative of those found at Nine Mile Point are plotted, as well as their calculated crack growth in a period of 18 months (using the upper bound crack growth rates). It can be seen that even the worst case cracks still remain below the acceptance line after the 18 month period.

Even in the event that a growing crack were to cross the acceptance case on the failure diagram, it is likely that a portion of the crack would penetrate the wall well before entering the net section collapse region. Typical cracks have considerable variability in depth. The crack depth profile of Loop 15, SW-12 is shown on Figure 13. Because the deepest parts of the crack are typically the fastest growing (Figures 10, 11), it is expected that a small fast growing crack front would penetrate the wall in advance of the remainder of the cracks, producing a leak-before-break condition.

Axial Crack

The fracture mechanics methodology for an axial crack analysis requires hoop pressure and residual stress levels to define the stress intensity as a function of crack depth. A pressure stress of 15.5 ksi and residual hoop stress of 38.5 ksi were used as representative stresses. The residual hoop stress was calculated analytically using finite element methods similar to those used for the axial through-wall residual stress (Figure 14). The magnitude of the residual stress was assumed to be constant through wall for the crack growth calculations. The initial flaw size was estimated to be 10% of

the thickness. The stress intensity (K) for this crack length was 27.8 ksi $\sqrt{\text{in.}}$. It can be determined from the crack growth data curves (Figure 10) that a K level of ~ 28 ksi $\sqrt{\text{in.}}$ places the crack growth rates at a plateau of 6×10^{-5} in/hr for 0.2 ppm oxygen environment. Assuming this rate, it would be predicted that the crack would grow to a length of ~ 0.50 in. in 9 months of operation. It would require an additional 12 months to propagate the crack through-wall at these plateau rates.

Even for a limiting case, using the highest 0.2 ppm O_2 , 288°C data for furnace sensitized Type 304 SS, one can calculate that the maximum growth that could have occurred in the last 10 months of operation; 5220 hours of actual operation, would still not be through wall. From Figure 10 this rate is 1.2×10^{-4} in/hr. The total crack extension determined from this upper bound rate is 0.626 inches. If one presumes that the crack was 15% through wall prior to this last period of operation, 0.158 in. in the 1.05 in. thick safe end, the flaw would have been predicted to be 0.784 in. deep at the end of the ten month period. This is approximately 75% of the total thickness.

The allowable axial flaw size was determined for a 28-inch safe end (stress ratio = 0.92) and is shown in Figure 15. The acceptance curve contains a safety factor of 3 and is indicated as a solid line. The dashed line is the present extension of the code acceptance limits; however it does not accurately model the crack as it approaches through wall. The cross-hatched area represents the failure region. A crack growth curve is shown for an initial flaw size of 0.105 in. It can be seen that the crack growth falls within the acceptance limits and well below the failure region (supporting leak before break).

D. U. T. DETECTABILITY vs GEOMETRY vs CRACK GROWTH RATE

The results of Section 8 indicate that the 1982 examination was more sensitive than the 1981 examination, such that axially oriented cracks with a depth less than a 20% wall thickness might not have been detected in 1981. However, assuming a 20% wall crack was present in 1981, a higher than expected residual stress and an abnormally high crack growth rate would be required to drive the crack through-wall in the time between the 1981 and 1982 exam dates. A crack growth rate for a sensitized material subjected to a more normal residual stress field would require an axial crack pre-existing in 1981 to be 40 to 50 percent wall thickness. To help resolve this disparity, a study was performed to develop a U.T. detectability vs. weld joint geometry vs. growth rate correlation:

- a) An analytical residual stress analysis was developed and results were compared with experimentally determined thru-wall stress profiles to establish a residual stress estimate for axial cracks in the furnace sensitized NMP safe-end welds (this subject is discussed earlier in this section).
- b) A section of a cracked NMP safe-end was characterized by U.T. examination, and select cracks were removed for a three dimensional profiling.

A 20 inch circumferential segment of loop 11 pipe-to-safe-end weld FW-22 was selected to develop this U.T. detectability vs. weld joint geometry vs. growth rate correlation.

In 1981 U.T. examinations were performed at a gain of approximately 6 dB over the reference gain used on the calibration block. As a result, the safe-end scan was effectively performed at reference gain.

Prior to removal from the recirculation system of the plant in April 1982, NES had examined this weld, and, using improved techniques with a scan gain of 10 to 14 dB over reference gain, they had reported the finding of axial and circumferential indications adjacent to a through-wall leaking axial crack. For the 1982 U.T. examinations, transfer measurements of cal blocks and safe-end components were performed. A 6 dB variance was noted. As a result, the 1982 examinations were performed at a scan gain of 20 dB over reference, and the recording criteria was changed accordingly. The effective scan gain of approximately 14 dB over reference produced an 1982 examination significantly more sensitive than the 1981 examination.

Figure 16 is a composite photograph of the PT indications on the inner surface of the pipe segment. The 7 cracks are identified by number. After the section was removed from the plant, personnel of the J. A. Jones Center, and General Electric performed a U.T. examination. At the J. A. Jones Center, the indications were examined with a 45° shear wave crystal at 2.25 MHZ. General Electric used a 45° crystal at a frequency of 1.5 MHZ. In addition to duplicating the improved techniques applicable to detection of IGSCC as used by NES in 1982, GE personnel also performed a U.T. examination with the less sensitive techniques used in the 1981 ISI program. (See Section 8 for a full discussion.) On the basis of these examinations, four cracks (cracks #1, 4, 6, and 7) were selected for sectioning and determination of the

crack profile. Crack 1 could be detected only with the improved techniques (35% FSH at a gain of 16 dB above reference). Using the 1981 techniques this crack would not be a reportable indication. Crack 4 was a stronger reflector. (42% FSH at a gain of 16 dB above reference.) This crack would be only marginally detectable with the 1981 technique of using a scan gain of 6 dB above reference. Crack 6 would have been called a reportable indication using the 1981 NES techniques. Crack 7, on the pipe side of the weld, was nearly invisible, even at the 20 dB gain, unless the examination was made from the surface of the weld crown. And even then, the detectability was poor (5% FSH at reference gain). During a normal ISI, using the improved IGSCC detection methods, crack 7 would likely have gone undetected. The Table below summarizes the detectability of the cracks selected for sectioning.

<u>Crack</u>	<u>Detectable* by 1981 ISI Methods</u>	<u>1982 Improved Techniques*</u>
1	No	Yes
4	Marginally	Yes
6	Yes	Yes
7	No	Marginally

Sectioning of the cracks for determining profile involved first mounting the sample for metallographic examination to view the crack on the ID pipe surface. This surface was polished, etched, and photographed for each sample.

Subsequent to the original polish and etch, the metallographic sample was ground to expose a plane 0.050 in. below the original surface. This plane

*With unground weld crown.

was polished, etched and photographed. Then, the samples were again ground to a depth of approximately 0.100 in. below the original surface and again polished, etched, and photographed. This sequential grinding, polishing and etching was repeated at 0.050 inch intervals for each specimen until the crack disappeared. Figures 17 and 18 are sketches of crack profiles resulting from the sequential sectioning and photographing. Similar results are obtained for each crack.

<u>Crack</u>	<u>Detectable* by 1981 ISI Methods</u>	<u>Detectable* by 1982 Improved Techniques</u>	<u>Actual Crack Depth</u>
6	Yes	Yes	0.052 in. (50% wall) and 0.20 in. deep secondary crack)
4	Marginally	Yes	0.610 in. (58% wall)
1	No	Yes	0.620 in. (59% wall)
7	No	Marginally	0.400 in. (38% wall)

The summary table suggests the limit of detectability for axial cracks during the 1981 examination without grinding the weld crowns first was approximately 45% to 60% thru-wall. With the improved technique cracks with depths less than 38% were detectable. (Further study would be required to establish the actual lower limit of detectability of an axial crack in the configurations observed at NMP-1.) Axial crack 7 on the pipe side of the wall has poor detectability primarily due to the interference of the extended weld crown with the placement of the U.T. crystal.

*With unground weld crown.

It can be concluded from this study that because of the U.T. methods employed and the presence of unground extended weld crowns at the safe end to pipe/elbow welds, axial cracks up to 45 percent thru-wall were probably present at the time of the 1981 ISI examination, but not detected. With the improved methods used in the 1981 ISI examination, the axial cracking of this depth would have been detected.

Based on the previously discussed crack growth analysis, cracks in 1981 of 45 percent of wall could be expected to grow through wall and leak in the 9 month period from 1981 to March 1982.

E. REFERENCES

1. "The Growth and Stability of Stress Corrosion Cracks in Large Diameter BWR Piping," Final Report, EPRI NP-2471, July 1982.
2. "Metallurgical Examination and Destructive Assay of Piping Samples from KRB Nuclear Reactor," Prepared by Southwest Research Institute, San Antonio, Texas, EPRI NP-2382-SY-LD, Project T114-2, May 1982.

Table 1
ENVIRONMENTAL CONDITIONS FOR TESTING IN
SIMULATED BWR SERVICE CONDITIONS

Temperature	$550^{\circ}\text{F} \pm 10^{\circ}\text{F}$
Pressure	$1230 \text{ psi} \pm 20 \text{ psi}$
Oxygen	$0.2 \text{ ppm} \pm 0.1 \text{ ppm}$
Conductivity	$0.5 \text{ } \mu\text{mho} \pm 0.2 \text{ } \mu\text{mho}$
pH	$6.5 \pm 0.5 \text{ at } 25^{\circ}\text{C}$

Table 2
ASSUMED OPERATING STRESSES USED IN CRACK
GROWTH EVALUATION*

28" Pipe - Nine Mile Point

1. Pressure stress - 7.75 ksi
2. Dead weight - 1.0 ksi
3. Thermal stress - 2.0 ksi
4. Pressure on crack- 1.0 ksi

*Based on discussions with H. S. Mehta

Table.3

STRESS INTENSITY VS. DEPTH, FOR NINE MILE POINT PIPE,
DUE TO OPERATING STRESSES

CRACK DEPTH	KI STRESS INTENSITY
0.0100	2.30583
0.0310	4.08272
0.0520	5.31730
0.0730	6.33535
0.0940	7.22892
0.1150	8.07485
0.1360	8.90918
0.1570	9.70982
0.1780	10.46521
0.1990	11.24126
0.2200	12.02106
0.2410	12.83732
0.2620	13.65144
0.2830	14.46498
0.3040	15.27913
0.3250	16.17742
0.3460	17.17701
0.3670	18.19022
0.3880	19.21713
0.4090	20.25776
0.4300	21.33305
0.4510	22.46566
0.4720	23.60859
0.4930	24.76767
0.5140	25.94277
0.5350	27.17912
0.5560	28.46388
0.5770	29.80780
0.5980	31.15064
0.6190	32.51215
0.6400	33.94177
0.6610	35.44672
0.6820	36.97302
0.7030	38.52035
0.7240	40.08842
0.7450	41.74820
0.7660	42.50064
0.7870	45.89518

GCRAK01 Assumptions:

MAX. CRACK DEPTH OF 0.800 INCH

PLATE THICKNESS OF 1.050 INCH

CIRCUMFERENTIAL CRACK IN CYLINDER $YR/TI=10$

Input and calculated throughwall operating stresses

POINT	X-VALUE	Y-VALUE	Y-CALC	Y-DIFF
1	0.	0.11750E 02	0.11750E 02	0.11921E-06
2	0.20000E 00	0.11750E 02	0.11750E 02	0.
3	0.40000E 00	0.11750E 02	0.11750E 02	-0.11921E-06
4	0.60000E 00	0.11750E 02	0.11750E 02	-0.11921E-06
5	0.80000E 00	0.11750E 02	0.11750E 02	0.11921E-06

Table 4

STRESS INTENSITY VS. DEPTH DUE TO THROUGHWALL RESIDUAL
STRESS FOR NINE MILE POINT PIPECRACK
DEPTH KI STRESS
INTENSITY

0.0100	5.93721
0.0310	9.62835
0.0520	11.42018
0.0730	12.31079
0.0940	12.61334
0.1150	12.54303
0.1360	12.19546
0.1570	11.56701
0.1780	10.69747
0.1990	9.62164
0.2200	8.46867
0.2410	7.07731
0.2620	5.59904
0.2830	3.99231
0.3040	2.27471
0.3250	0.60638
0.3460	-0.97495
0.3670	-2.60699
0.3880	-4.27190
0.4090	-5.95080
0.4300	-7.61939
0.4510	-9.26703
0.4720	-10.88335
0.4930	-12.44728
0.5140	-13.93933
0.5350	-15.41424
0.5560	-16.87622
0.5770	-18.21725
0.5980	-19.41113
0.6190	-20.43018
0.6400	-20.92663
0.6610	-20.79440
0.6820	-20.33514
0.7030	-19.51371
0.7240	-18.29372
0.7450	-17.29147
0.7660	-16.57651
0.7870	-15.39785

GCRAK01 Assumptions:

MAX. CRACK DEPTH OF 0.800 INCH:

PLATE THICKNESS OF 1.050 INCH

CIRCUMFERENTIAL CRACK IN CYLINDER (R/T)=10

Input and calculated throughwall residual stresses:

POINT	X-VALUE	Y-VALUE	Y-CALC	Y-DIFF
1	0.	0.30000E 02	0.21490E 02	-0.14904E 01
2	0.10500E 00	0.14000E 02	0.11091E 02	0.23086E 01
3	0.17000E 00	0.	-0.53014E 00	0.53014E 00
4	0.21000E 00	-0.50000E 01	-0.49637E 01	-0.36275E -01
5	0.31500E 00	-0.19000E 02	-0.15853E 02	-0.21473E 01
6	0.42000E 00	-0.21000E 02	-0.20753E 02	-0.24681E 00
7	0.52500E 00	-0.18000E 02	-0.16843E 02	0.84880E 00
8	0.63000E 00	-0.70000E 01	-0.88800E 01	0.99998E 01
9	0.70000E 00	0.	0.17088E 01	-0.17088E 01

Table 5
CRACK DEPTH VS. TIME FOR NINE MILE POINT PIPE
MADE USING UPPER BOUND da/dt

NINEMILE-11.75KSI,AVG.RS,FS da/dt

Wall Thickness= 1.05 (in) ,

Initial Crack Depth= .0525 (in)

a (in)	a/t (in)	K(load) ksi/in	K(resid) ksi/in	K(total) ksi/in	da/dt (in/hr)	Time (hours)
.053	.050	5.34	11.43	16.77	2.98E-05	0
.076	.072	6.40	12.09	18.49	3.84E-05	700
.097	.092	7.33	12.59	19.92	4.67E-05	1200
.116	.110	8.10	12.40	20.50	5.03E-05	1600
.137	.130	8.93	12.18	21.11	5.43E-05	2000
.153	.146	9.54	11.59	21.14	5.46E-05	2300
.175	.166	10.36	10.81	21.18	5.48E-05	2700
.196	.187	11.16	9.70	20.85	5.26E-05	3100
.217	.207	11.91	8.57	20.48	5.02E-05	3500
.237	.225	12.67	7.29	19.96	4.69E-05	3900
.255	.243	13.38	6.07	19.45	4.38E-05	4300
.276	.263	14.21	4.49	18.70	3.96E-05	4800
.295	.281	14.97	2.98	17.96	3.56E-05	5300
.315	.300	15.79	1.37	17.16	3.16E-05	5900
.333	.318	16.59	-.05	16.54	2.87E-05	6500
.353	.336	17.52	-1.54	15.97	2.62E-05	7200
.373	.355	18.48	-3.10	15.39	2.37E-05	8000
.393	.374	19.49	-4.68	14.81	2.14E-05	8900
.414	.394	20.56	-6.31	14.25	1.94E-05	9900
.434	.413	21.62	-7.92	13.70	1.75E-05	11000
.454	.432	22.67	-9.49	13.18	1.58E-05	12200
.474	.451	23.72	-10.94	12.78	1.46E-05	13500
.494	.470	24.87	-12.39	12.47	1.37E-05	14900
.514	.489	26.03	-13.86	12.17	1.29E-05	16400
.533	.507	27.12	-15.23	11.89	1.21E-05	17900
.553	.526	28.29	-16.54	11.75	1.18E-05	19600
.573	.546	29.57	-17.81	11.76	1.18E-05	21300
.593	.565	30.88	-19.09	11.79	1.19E-05	23000
.613	.584	32.18	-19.74	12.44	1.36E-05	24600
.634	.603	33.53	-20.19	13.33	1.63E-05	26000
.653	.622	34.89	-20.61	14.28	1.95E-05	27100
.675	.643	36.51	-20.22	16.28	2.75E-05	28100
.694	.661	37.89	-19.47	18.42	3.81E-05	28700
.716	.682	39.48	-18.60	20.88	5.28E-05	29200
.733	.698	40.82	-17.91	22.91	6.80E-05	29500
.756	.720	42.70	-16.99	25.71	9.63E-05	29800
.773	.737	44.17	-16.58	27.59	1.22E-04	29970
.793	.756	45.30	-16.58	28.72	1.41E-04	30120

Table 6
CRACK DEPTH VS. TIME FOR NINE MILE POINT PIPE
(EXPECTED IGSCC da/dt ASSUMED)

NINE MILE-11.75KSI, AVG. RS, FS/3 da/dt

Wall Thickness= 1.05 (in)

Initial Crack Depth= .0525 (in)

a (in)	a/t (in)	K(load) ksi/in	K(resid) ksi/in	K(total) ksi/in	da/dt (in/hr)	Time (hours)
.053	.050	5.34	11.43	16.77	9.93E-06	0
.073	.069	6.27	12.01	18.28	1.24E-05	1900
.093	.089	7.21	12.60	19.80	1.53E-05	3400
.113	.107	7.97	12.43	20.40	1.66E-05	4600
.133	.127	8.80	12.22	21.02	1.79E-05	5800
.153	.146	9.55	11.59	21.14	1.82E-05	6900
.173	.165	10.30	10.87	21.17	1.83E-05	8000
.193	.184	11.03	9.88	20.91	1.77E-05	9100
.214	.204	11.79	8.75	20.54	1.69E-05	10300
.234	.222	12.54	7.50	20.05	1.58E-05	11500
.253	.241	13.32	6.18	19.49	1.47E-05	12800
.273	.260	14.10	4.71	18.81	1.34E-05	14200
.293	.280	14.91	3.10	18.02	1.20E-05	15800
.313	.298	15.69	1.57	17.26	1.07E-05	17500
.334	.318	16.62	-.11	16.52	9.53E-06	19600
.353	.336	17.52	-1.55	15.97	8.73E-06	21600
.378	.360	18.73	-3.49	15.24	7.71E-06	24600
.393	.374	19.48	-4.67	14.81	7.15E-06	26600
.414	.394	20.57	-6.32	14.25	6.46E-06	29600
.433	.412	21.55	-7.81	13.74	5.88E-06	32600
.455	.433	22.72	-9.57	13.16	5.25E-06	36600
.475	.453	23.81	-11.05	12.75	4.84E-06	40600
.494	.471	24.91	-12.44	12.46	4.57E-06	44600
.517	.492	26.19	-14.07	12.13	4.26E-06	49600
.533	.508	27.16	-15.29	11.87	4.03E-06	53600
.553	.527	28.32	-16.57	11.75	3.93E-06	58600
.573	.546	29.57	-17.81	11.76	3.94E-06	63600
.593	.564	30.86	-19.07	11.79	3.96E-06	68600
.613	.584	32.20	-19.74	12.45	4.56E-06	73600
.633	.602	33.46	-20.17	13.29	5.39E-06	77600
.656	.625	35.10	-20.68	14.42	6.67E-06	81600
.678	.646	36.72	-20.11	16.61	9.67E-06	84600
.694	.661	37.86	-19.48	18.38	1.26E-05	86100
.714	.680	39.35	-18.66	20.69	1.72E-05	87500
.733	.698	40.86	-17.88	22.98	2.29E-05	88500
.754	.718	42.60	-17.04	25.55	3.15E-05	89300
.776	.739	44.37	-16.58	27.79	4.18E-05	89900
.794	.756	45.30	-16.58	28.72	4.70E-05	90300

Table 7⁴
 TIME REQUIRED FOR STARTING FLAW TO GROW TO 50% AND 75% FLAW -
 NINE MILE POINT PIPE*

(Circumferential Crack Geometry Assumed)

A. Upper Bound da/dt

<u>a (initial)</u>	<u>a (final)</u>	<u>Time</u>
5%	50%	2.45 yr
10%	50%	2.25 yr
20%	50%	1.95 yr
30%	50%	1.60 yr
40%	50%	1.0 yr
50%	75%	1.85 yr

B. Expected IGSCC da/dt

<u>a (initial)</u>	<u>a (final)</u>	<u>Time</u>
5%	50%	7.35 yr
10%	50%	6.75 yr
20%	50%	5.85 yr
30%	50%	4.80 yr
40%	50%	3.0 yr
50%	75%	5.45 yr

*80% usage assumed

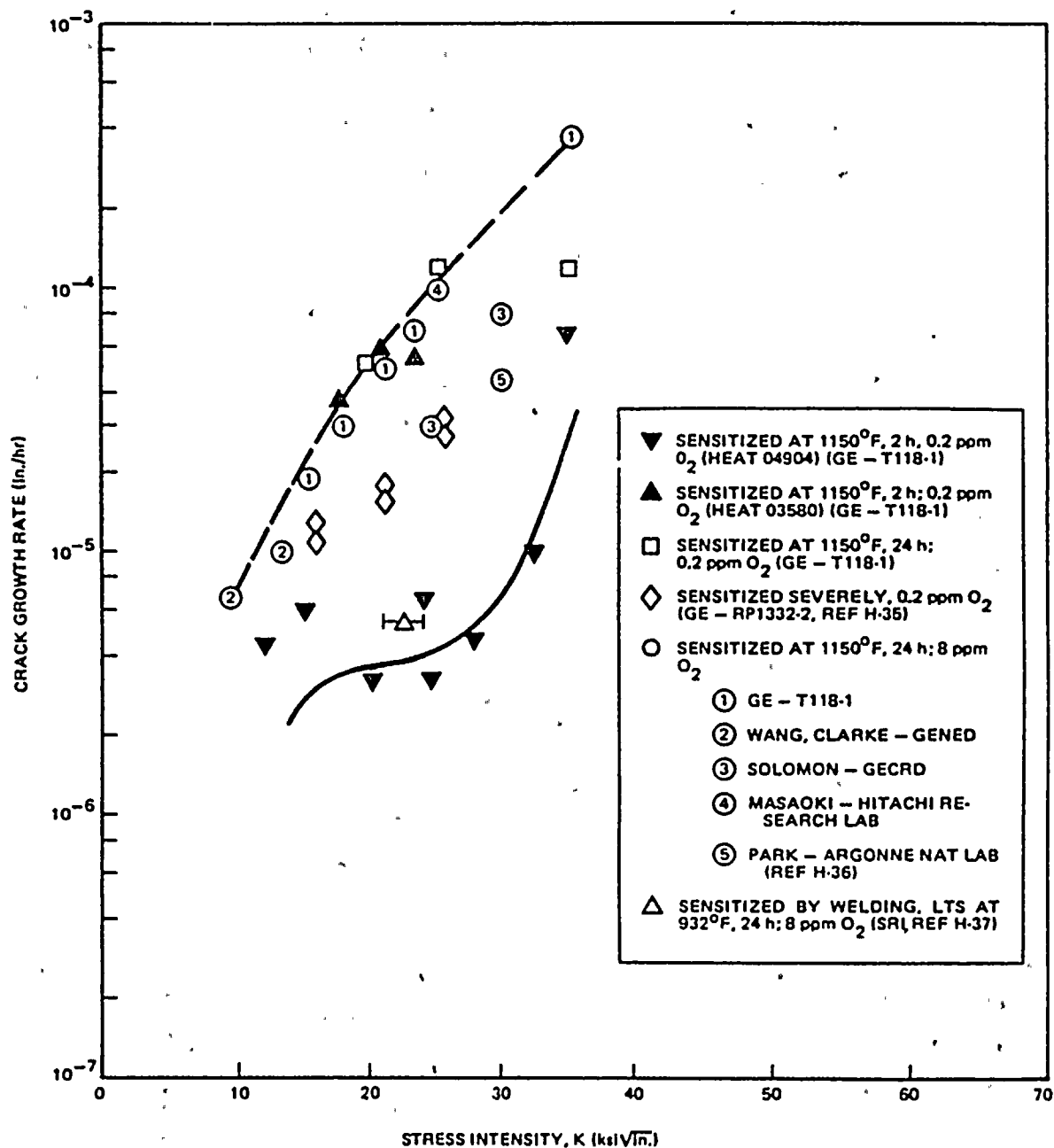
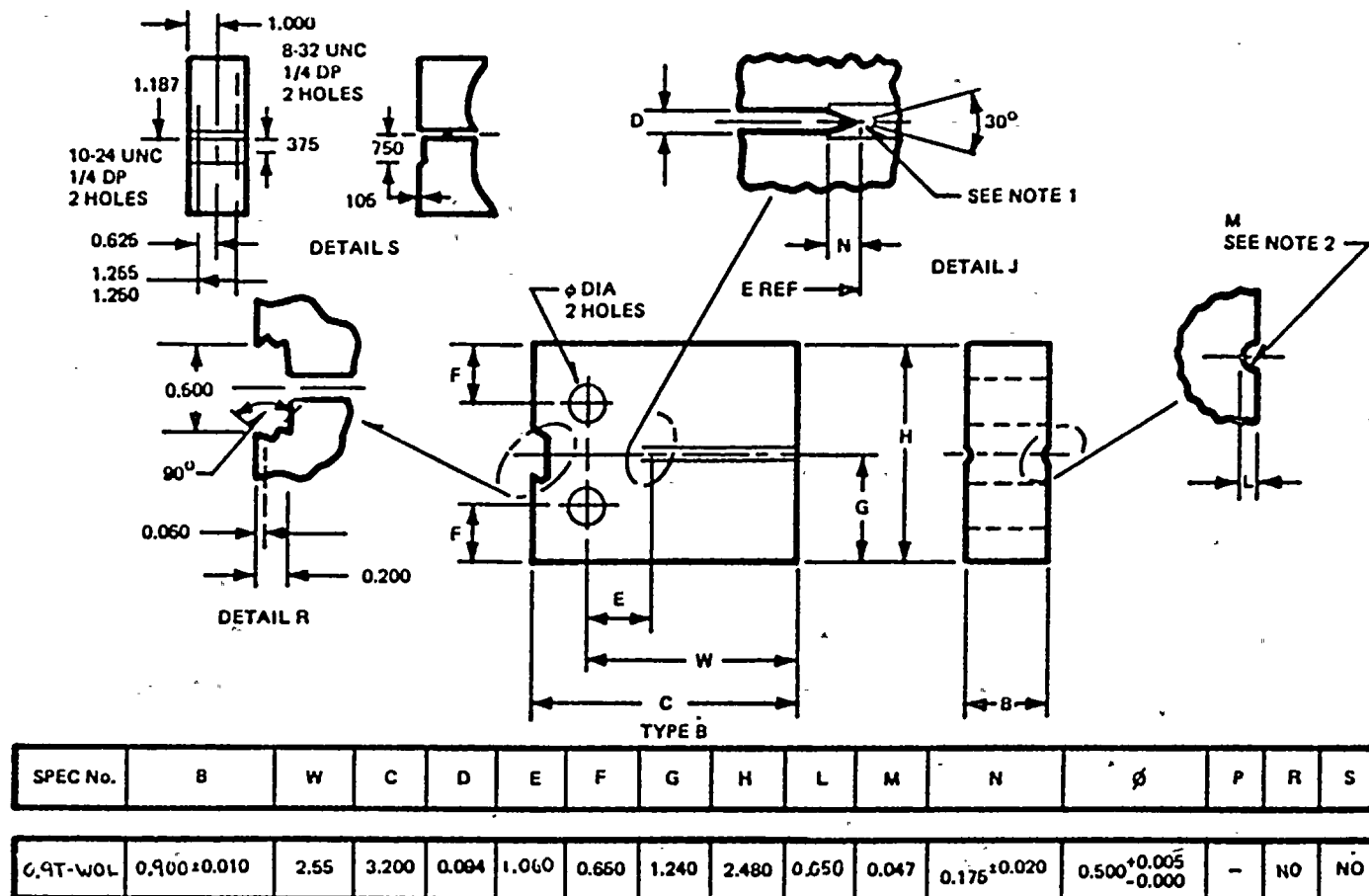


Figure 1. Summary of Constant Load Crack Growth Data (Curves are evaluation curves.) Data collected in 0.2 ppm O₂ and 8 ppm O₂ water. Different levels of sensitization examined. (Reference 1)



NOTES:

1. 0.007 in. MAXIMUM RADIUS (EDM)
2. LAY MARKS TO FALL PARALLEL TO AXIS OF RADIUS SURFACE
FINISH TO BE 32

Figure 2. WOL Specimen for Crack Growth Rate Study

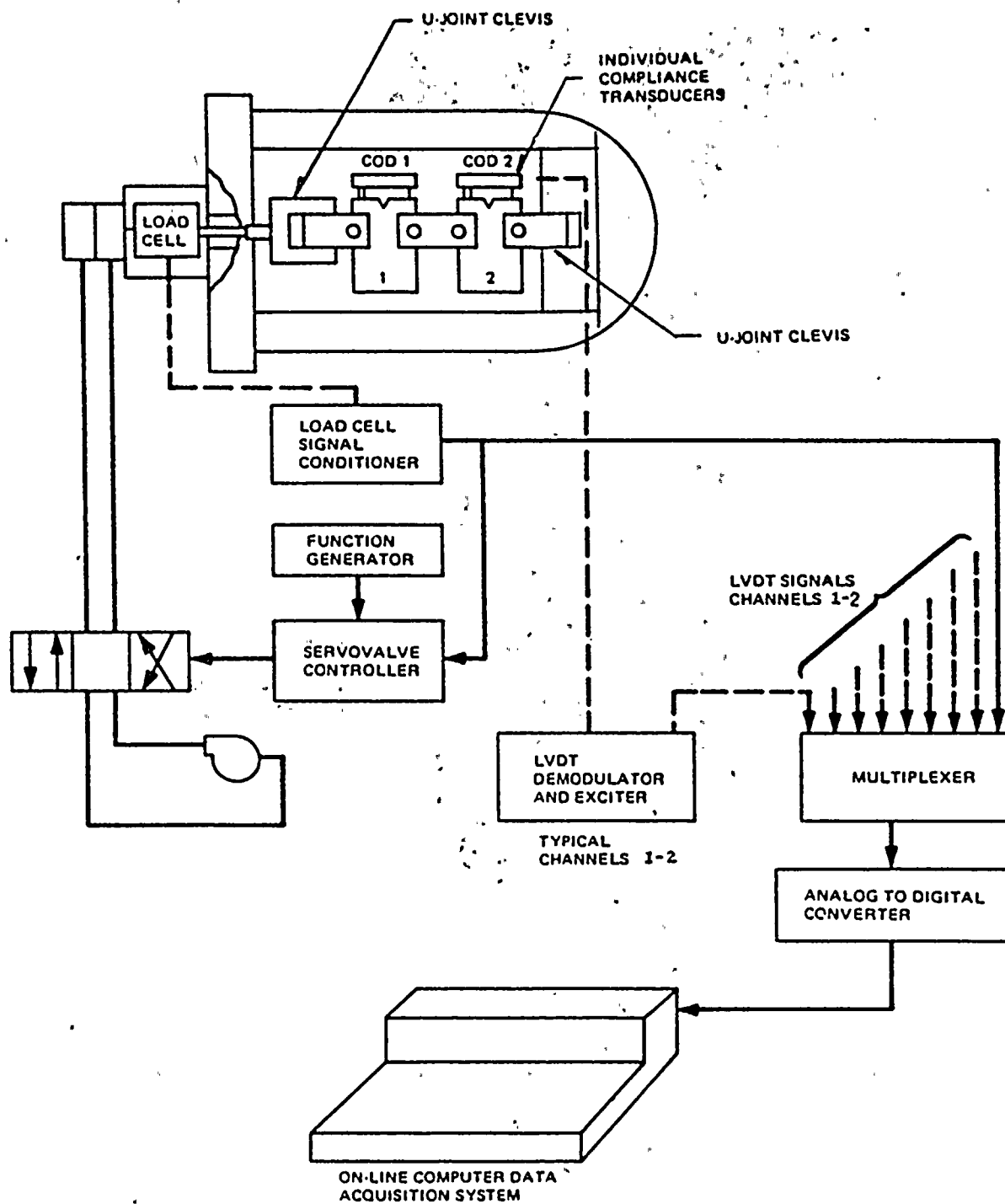


Figure 3. Schematic of SEFT, Multispecimen Environmental Test Facility

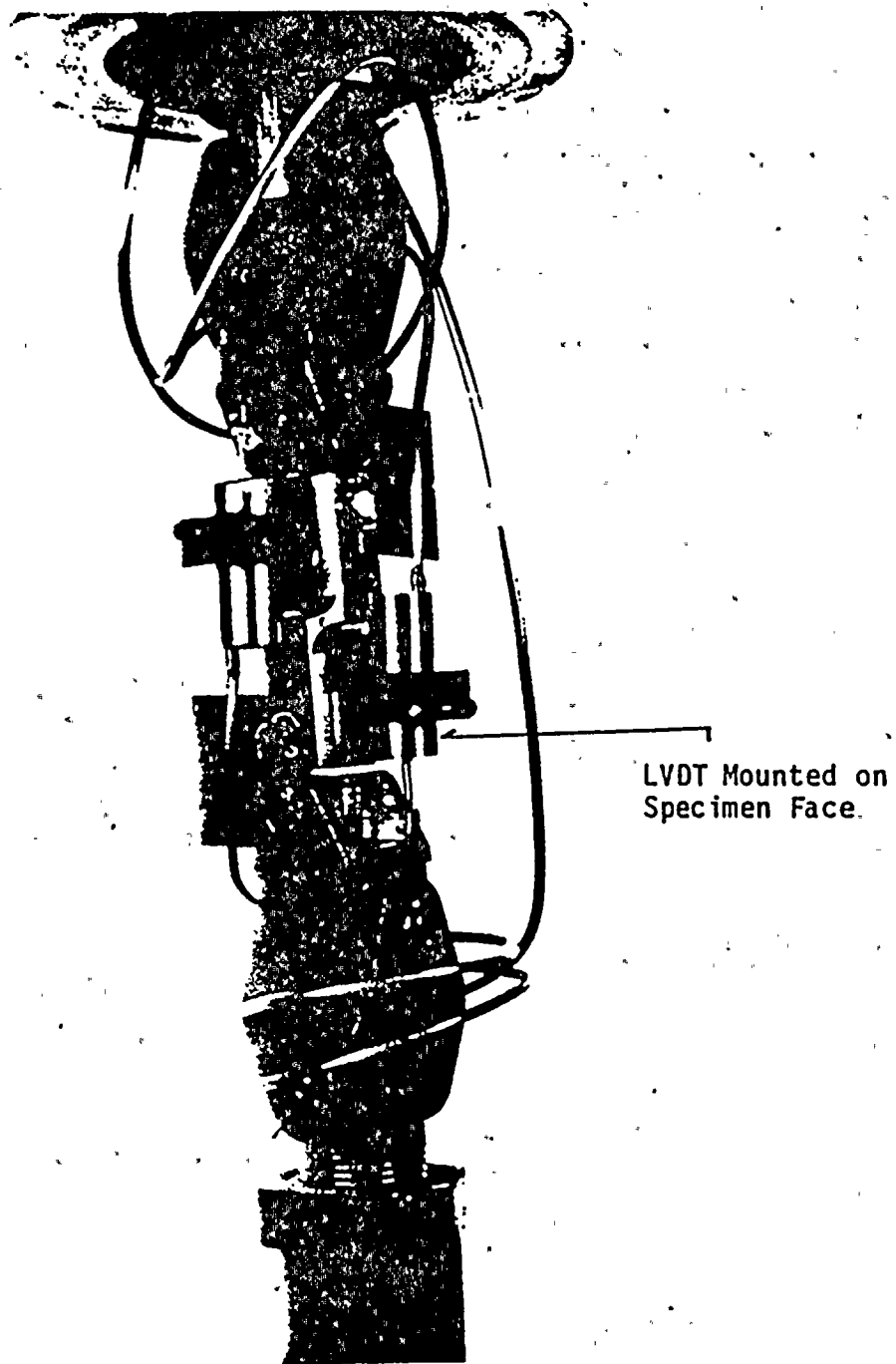


Figure 4. SEFT Vessel Specimen Chain

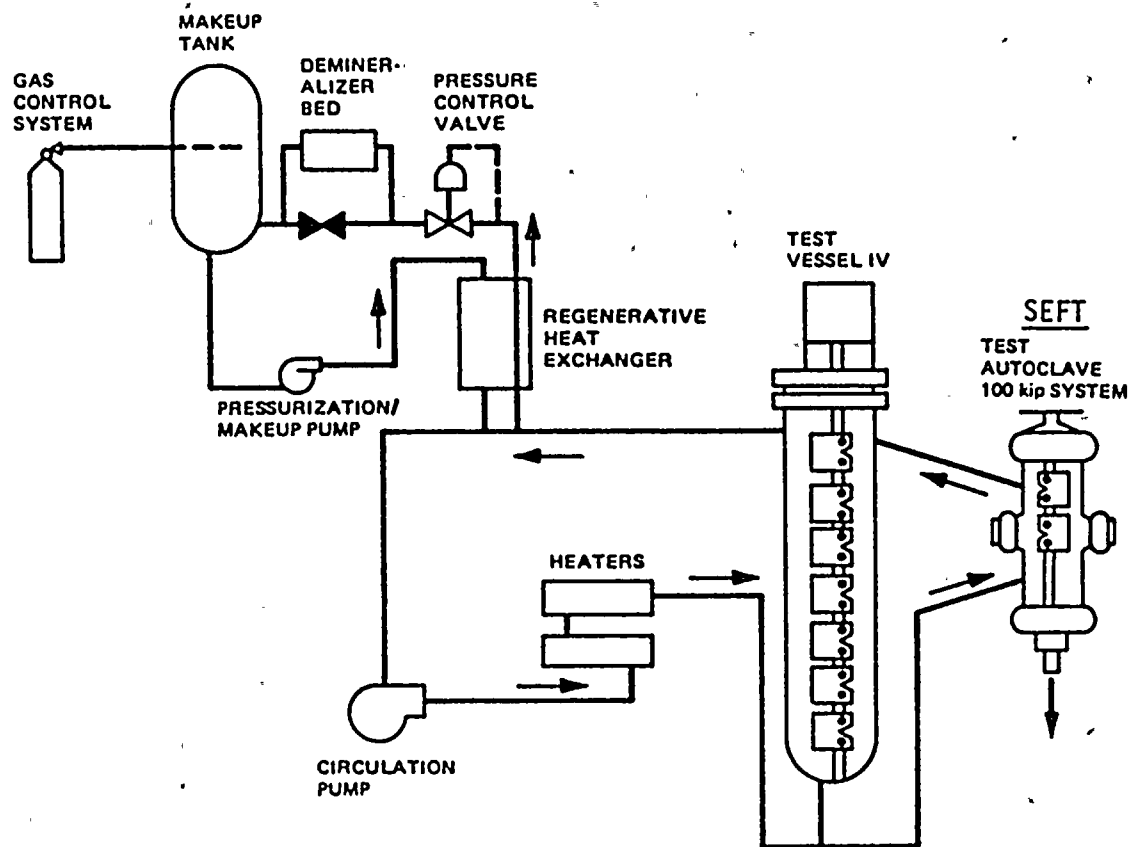
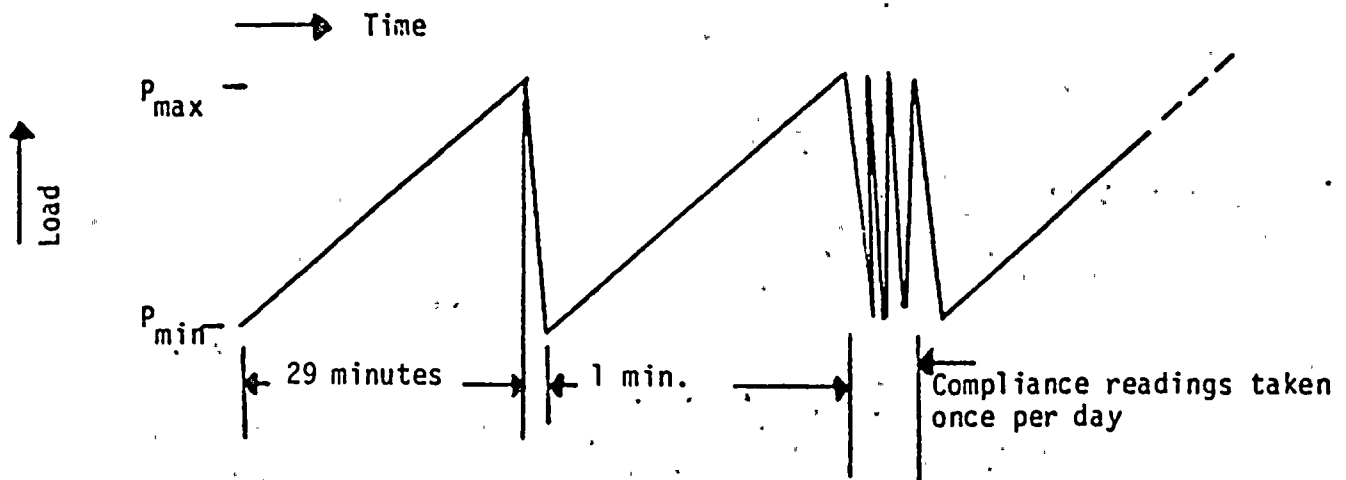


Figure 5. Simulated BWR Water Test Loop

Phase 1: SLOW CYCLIC LOADING



Phase 2: CONSTANT LOAD

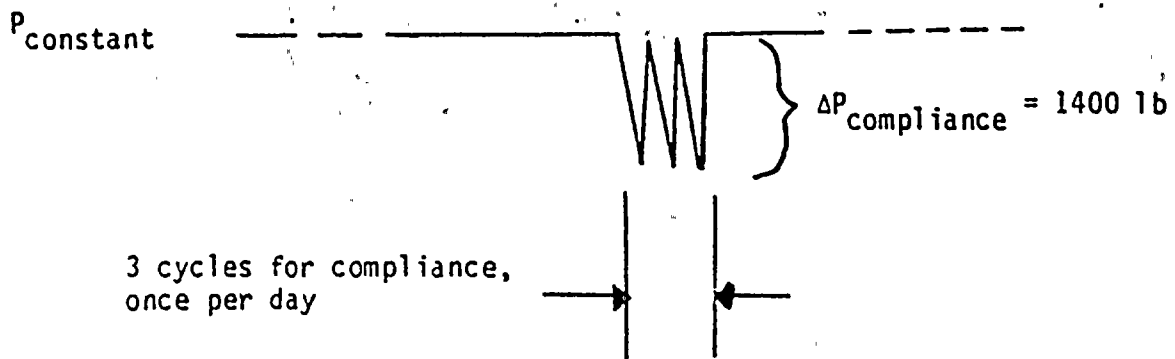


Figure 6. Loading

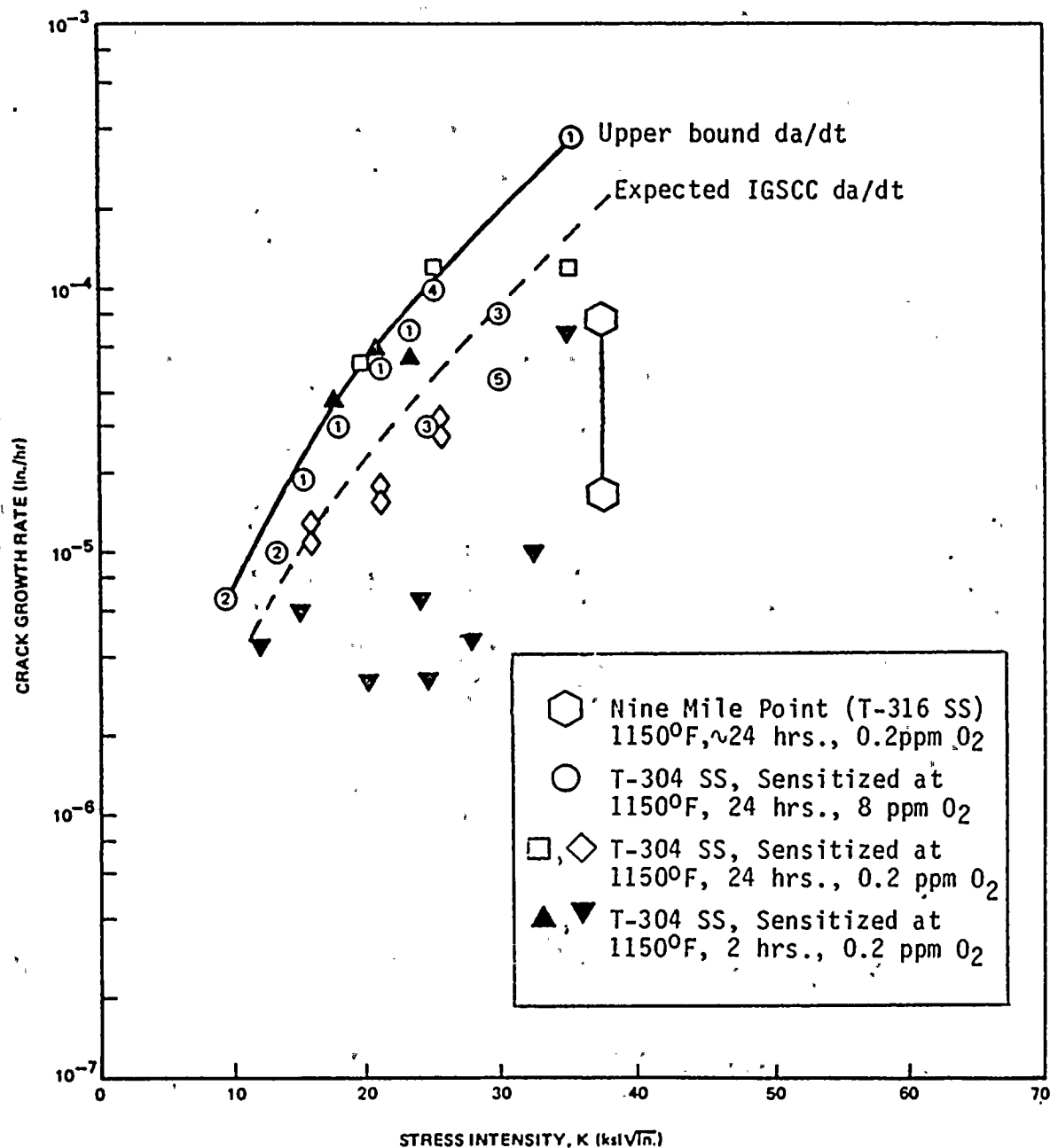


Figure 7. Summary of Constant Load Crack Growth Data (Curves are evaluation curves.) Data collected in 0.2 ppm O₂ and 8 ppm O₂ water. Different levels of sensitization examined.

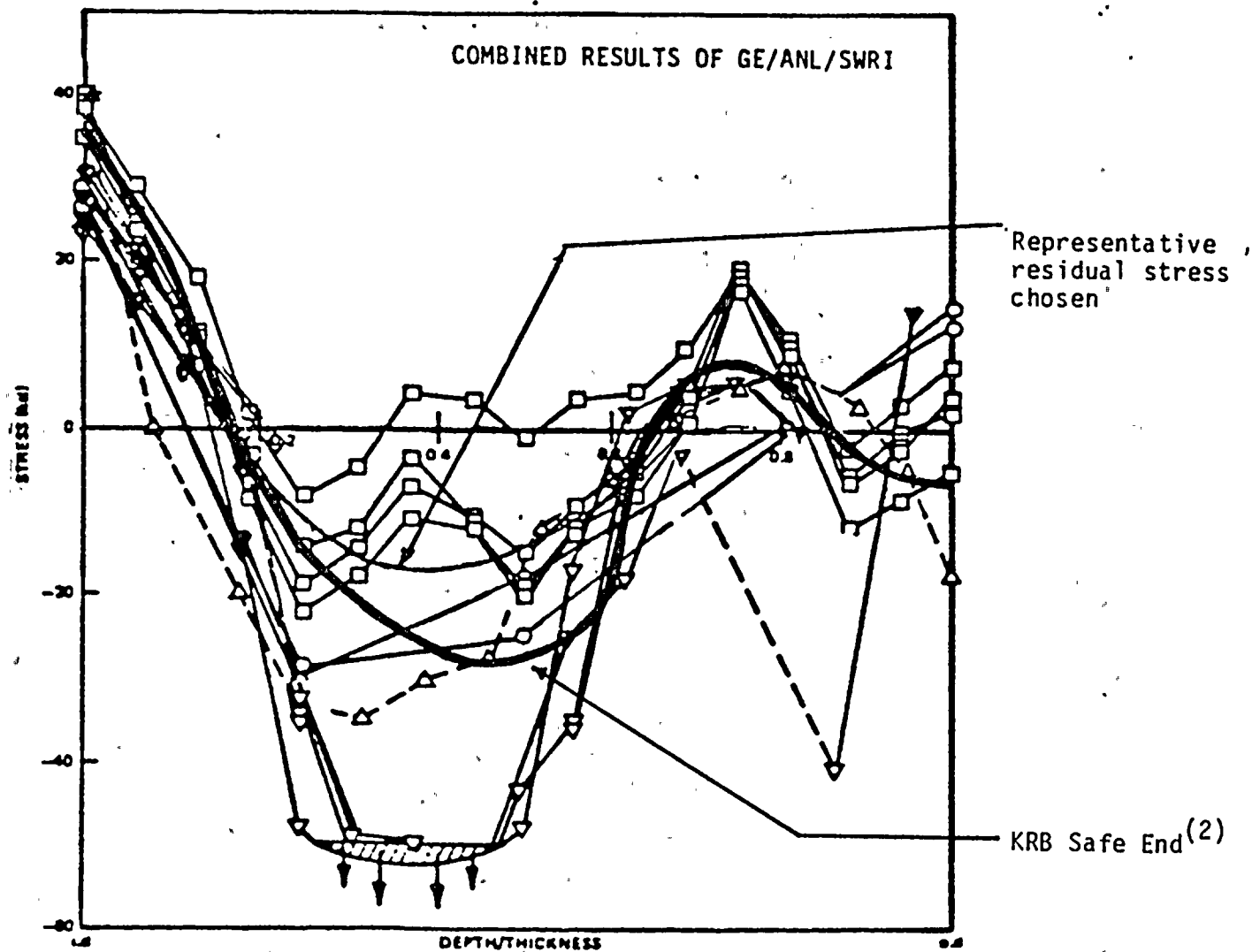


Figure 8. Residual Stress Measurements for Large Diameter Piping

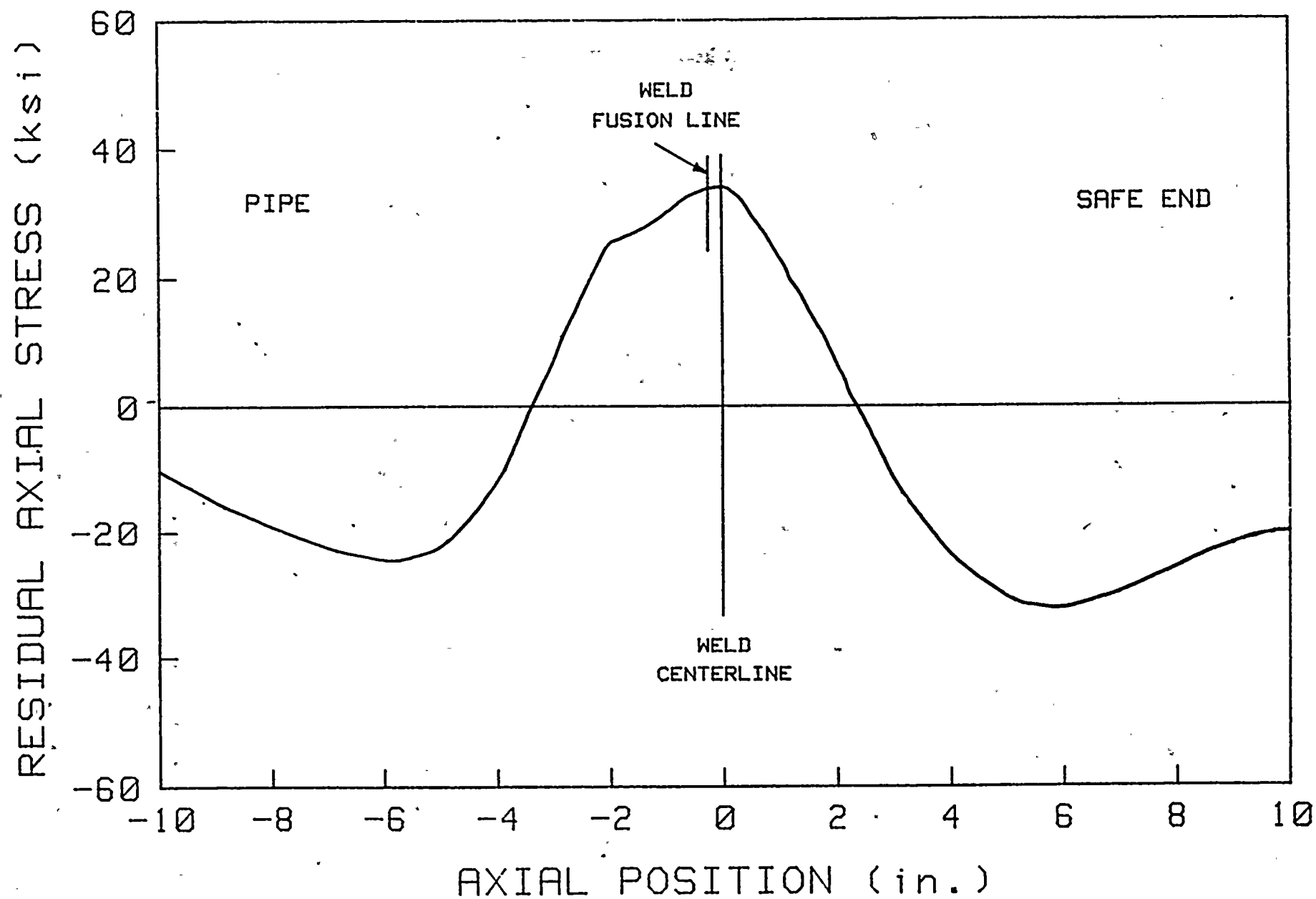


Figure 9. Nine Mile Point Residual Axial Stress on I.D.

9-30

DEPTH/THICKNESS

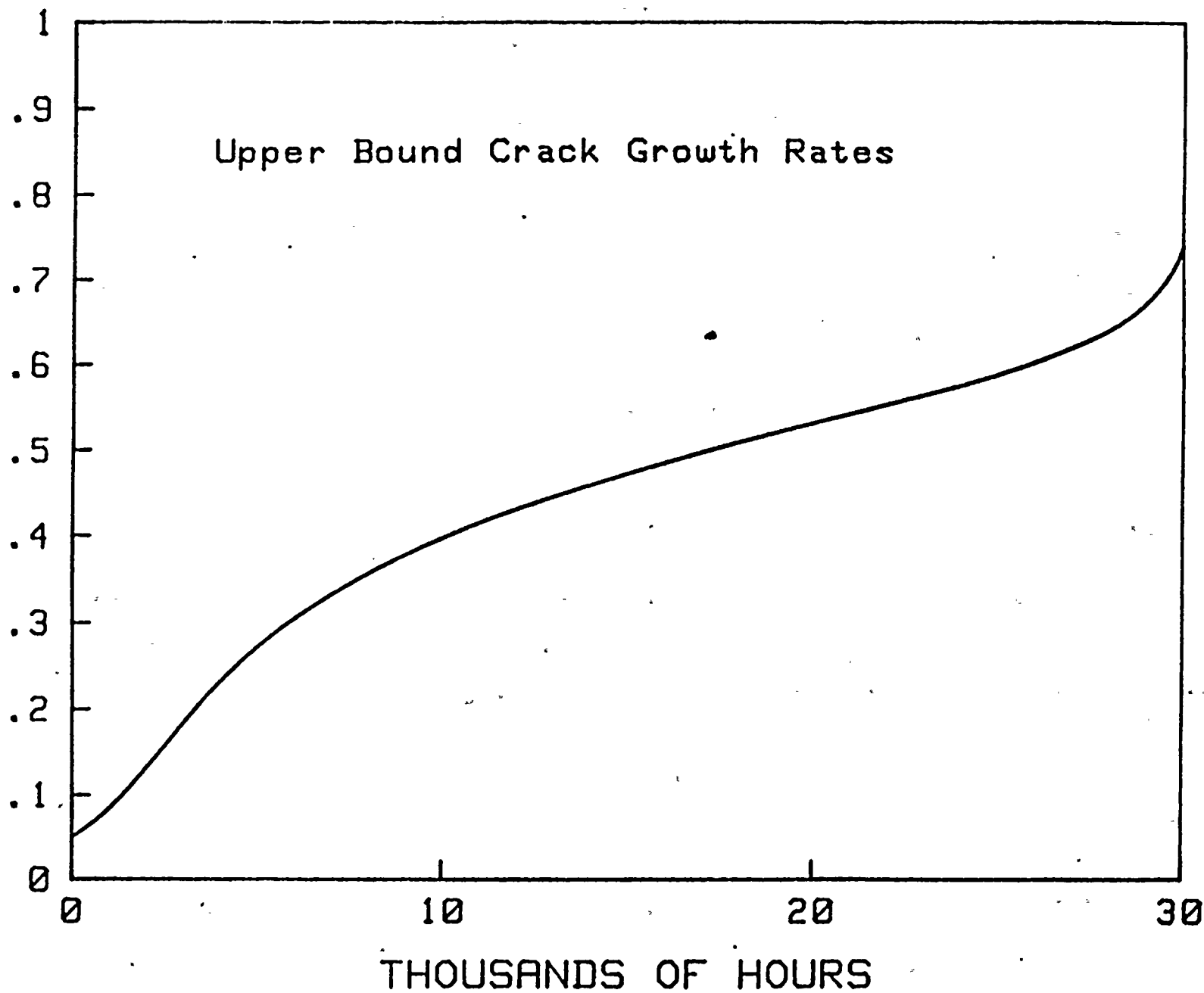


Figure 10. Crack Depth vs. Time - Nine Mile Point Pipe

DEPTH/THICKNESS

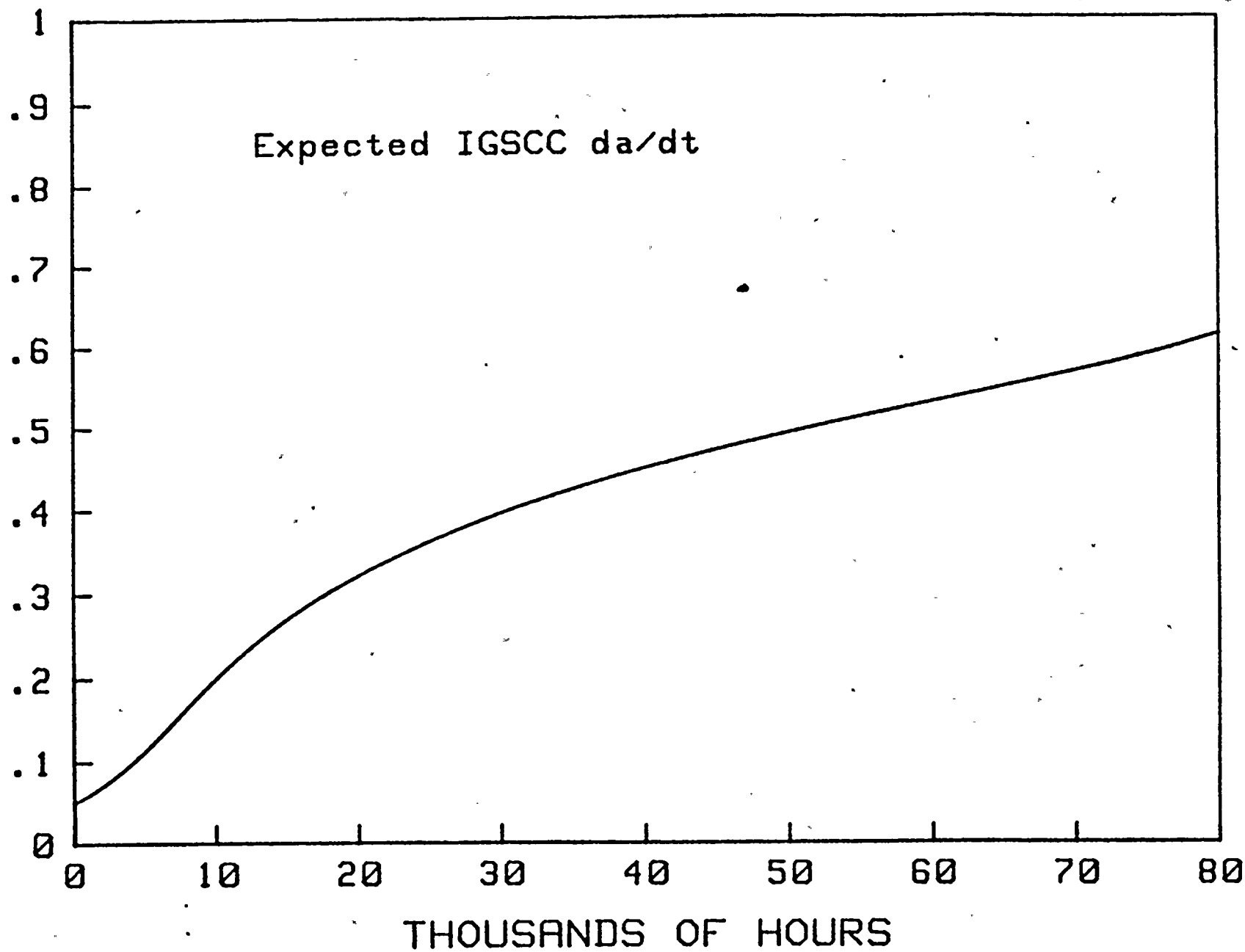
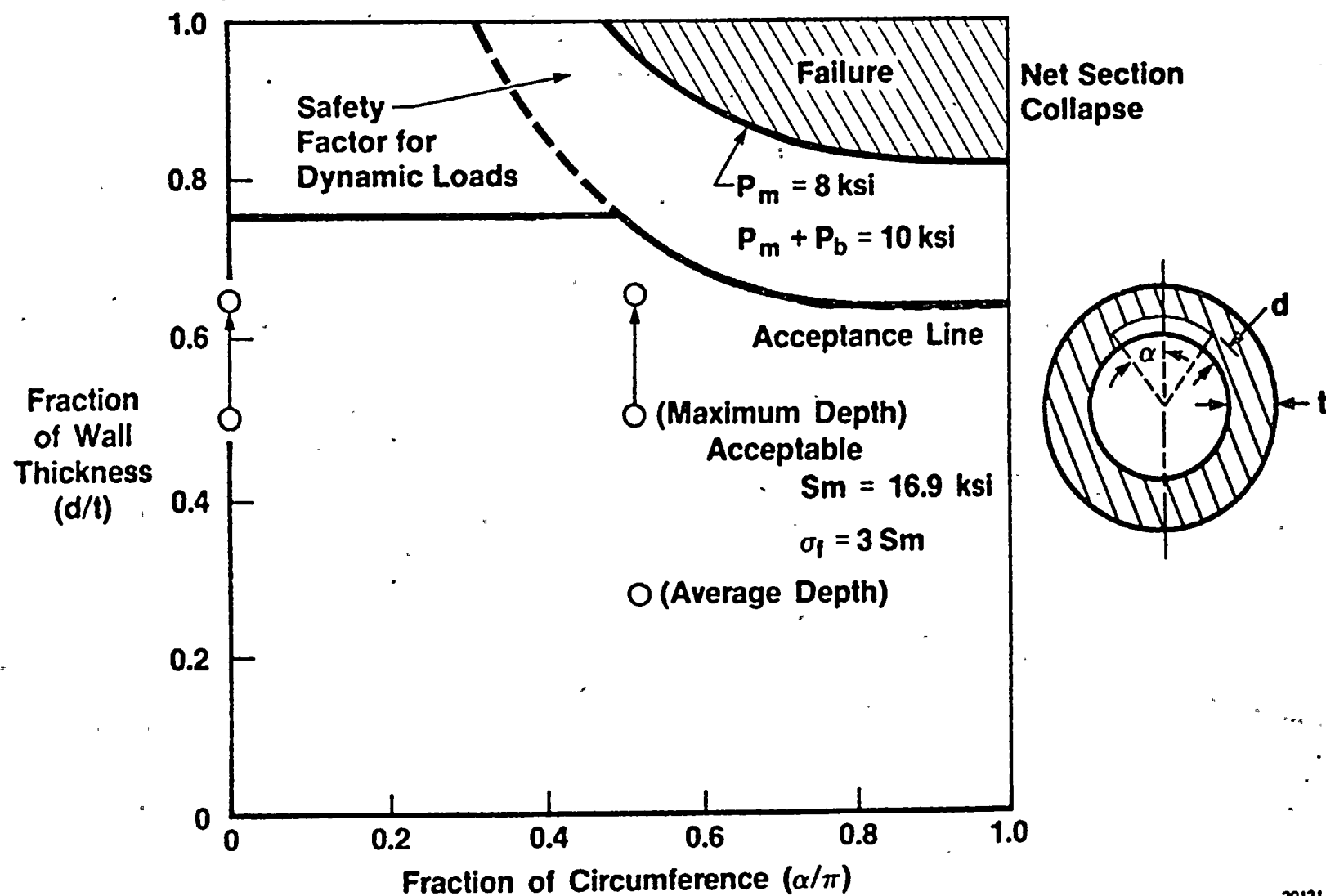


Figure 11. Crack Depth vs. Time - Nine Mile Point Pipe

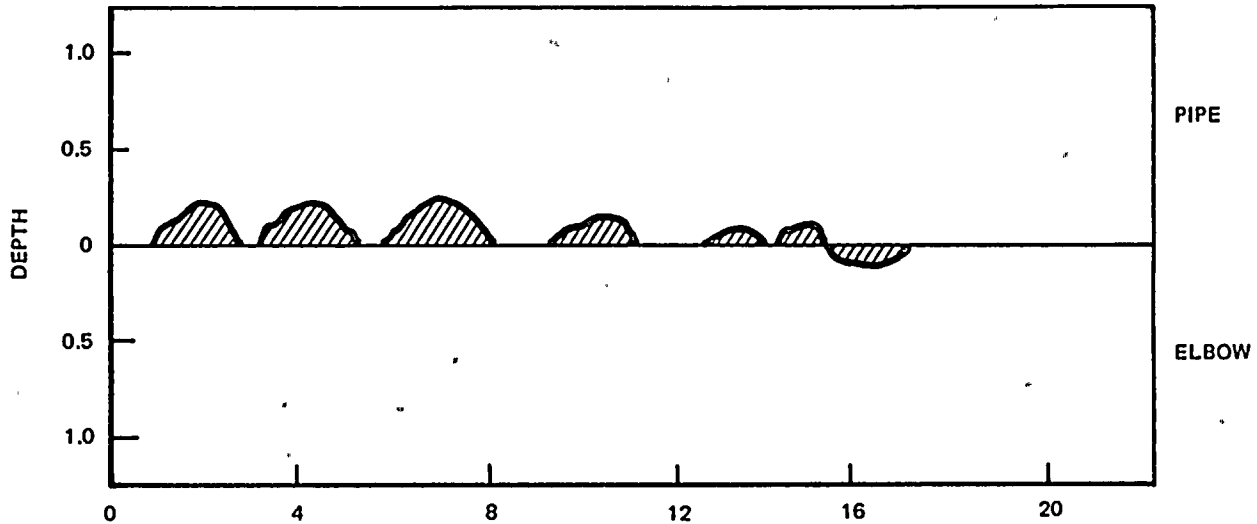


30131-46

Figure 12. Crack Growth in 18 Months (Upper Bound)

NINE MILE POINT-1
28-IN. RECIRCULATION SYSTEM
LOOP 15, SW-12

90° SECTION EXAMINED AT VNC



CRACK* LENGTH (in.)	CRACK** DEPTH (in.)	POSITION
0.88	0.275	PIPE - 2 in.
1.00	0.240	PIPE - 4 in.
1.13	0.276	PIPE - 6 in.
0.88	0.205	PIPE - 10 in.
0.31	—	PIPE - 12 in.
0.44	0.107	PIPE - 13 in.
0.50	0.100	PIPE - 14 in.
0.88	0.137	ELBOW - 16 in.

*DETERMINED BY PT

**DETERMINED BY METALLOGRAPHY

Figure 13. Crack Depth Profile

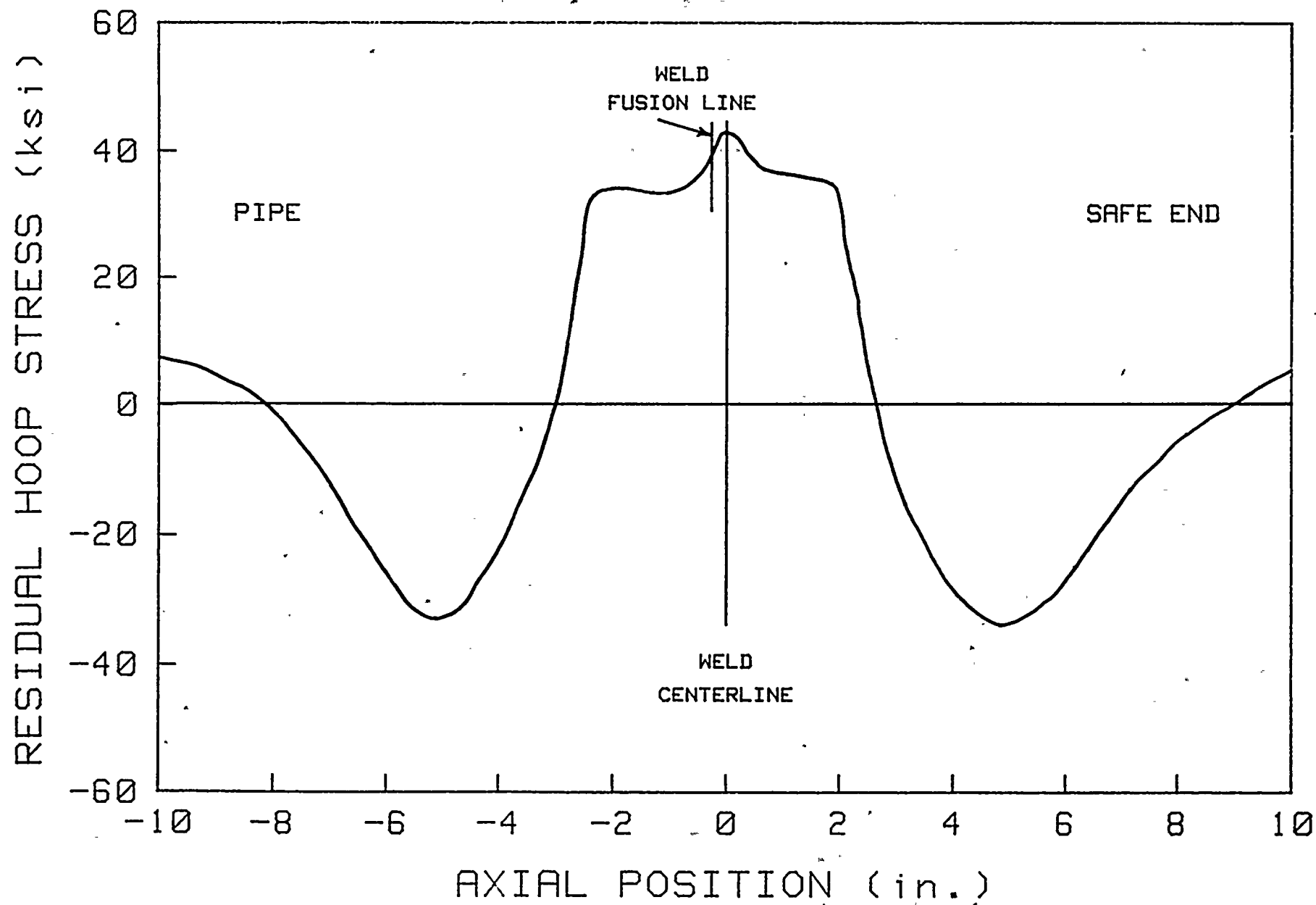


Figure 14. Nine Mile Point Residual Hoop Stress on I.D.

9-35/9-36

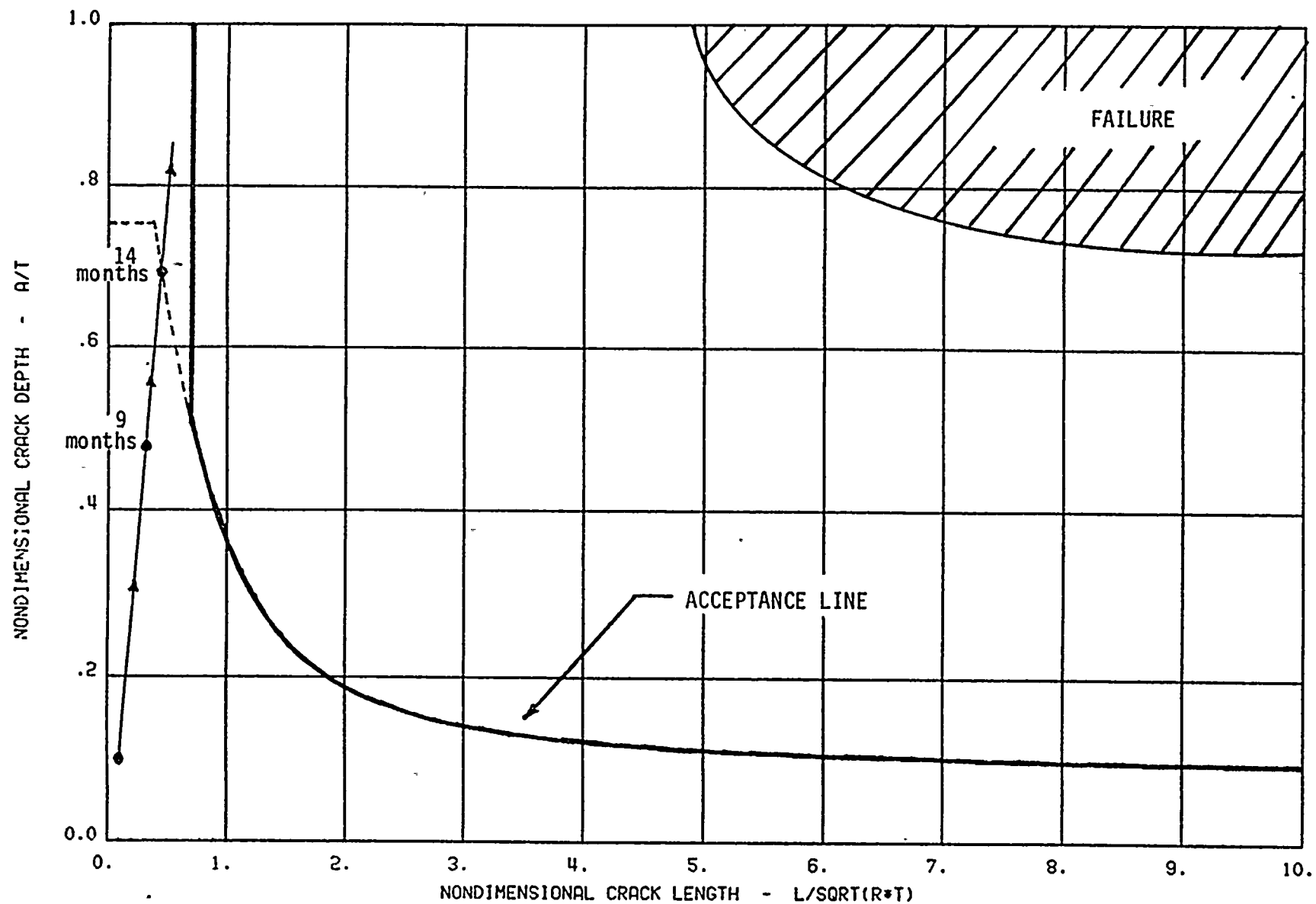


Figure 15. Allowable Axial Flaw Size; Stress Ratio = 0.92; Safety Factor = 3.0

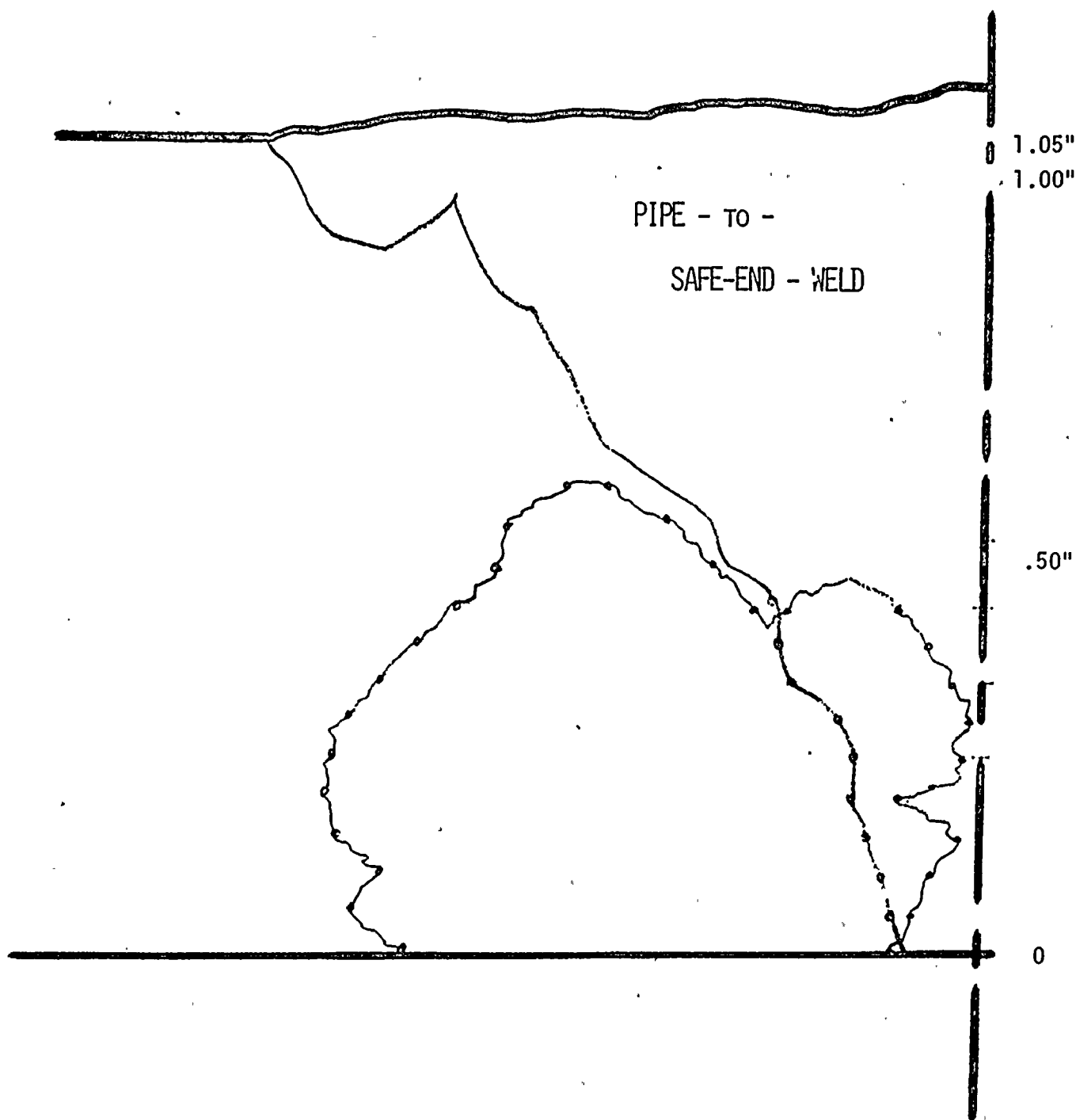


Figure 17. Profile of axial IGSCC crack #1 (of Figure 16) removed from the safe end side of safe-end-to-pipe weld FW-22 of NMP-1 recirculation loop 11. The crack, with a maximum depth of approximately 59% wall, is situated entirely below the weld crown. This crack would not have been a reportable indication as a result of the 1981 ISI examination.

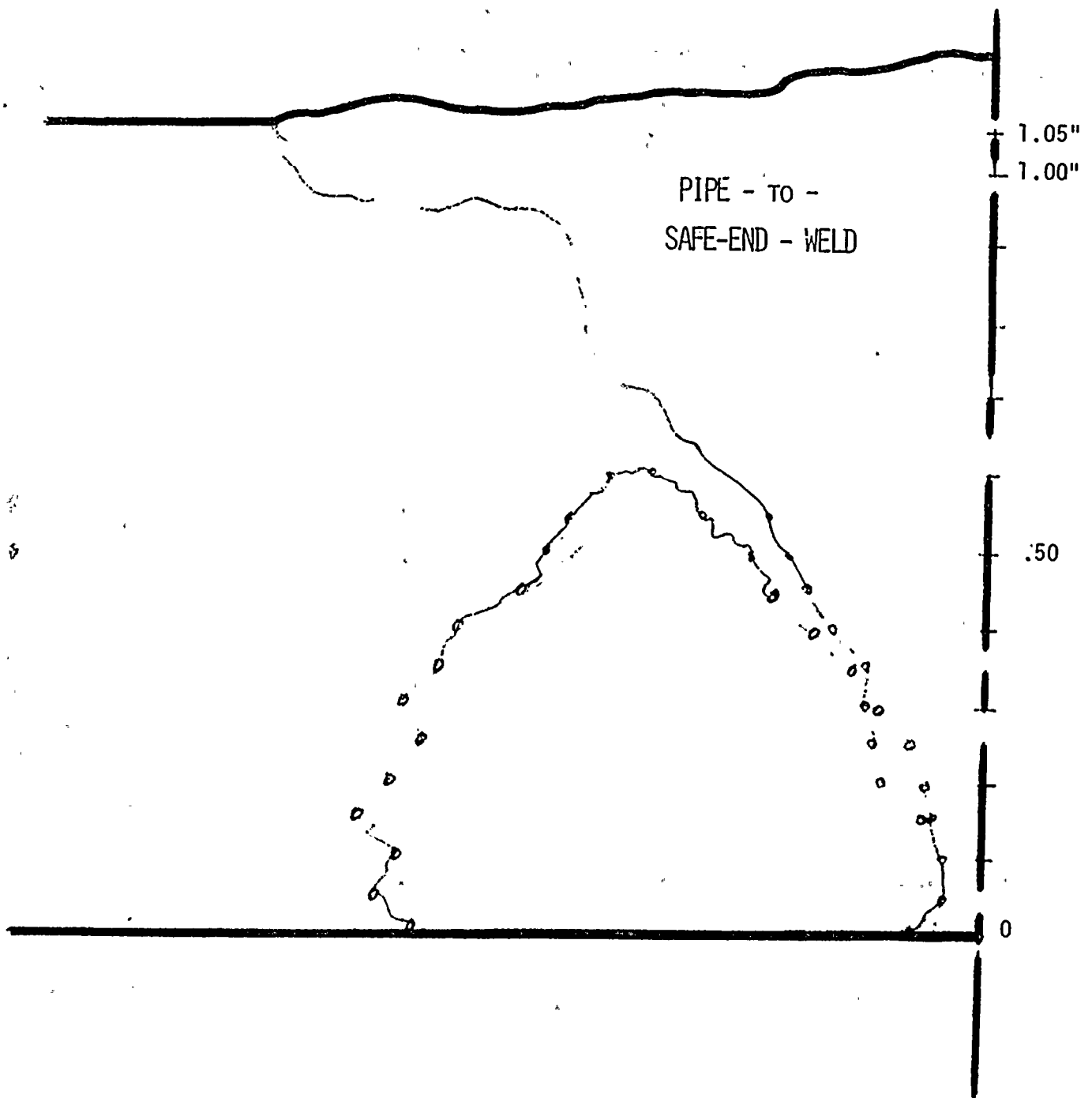


Figure 18. Profile of axial IGSCC crack #4 (of Figure 16) removed from the safe end side of safe-end-to-pipe weld FW-22 of NMP-1 recirculation loop 11. This crack, with a depth of approximately 58% wall would have been marginally detectable with the ISI procedures used in the 1981 examination.

SECTION X
STRESS CORROSION PERFORMANCE OF
TYPE 316 NUCLEAR GRADE SS

INTRODUCTION

The recent incident of intergranular stress corrosion cracking (IGSCC) of large diameter Type 316 stainless steel recirculation piping at Nine Mile Point Unit 1 (NMP-1) in March 1982¹ provided the motivation for a generic review of the relative stress corrosion propensities of Type 316 Nuclear Grade, Type 316 and Type 304 stainless steel. Type 316 Nuclear Grade stainless steel is one of two (also Type 304 Nuclear Grade) qualified replacement materials for BWR primary coolant piping applications as was developed by the General Electric Company and sponsored by the Electric Power Research Institute under Project T111-1 and reported in EPRI NP-2671-LD, Final Report.² Type 316 stainless steel was the material of fabrication at NMP-1 and Type 304 stainless steel was the primary piping structural material for the BWR (reference material). Some discussion of Type 304L stainless steel will be made where appropriate.

Table 1 reveals the chemical similarities among these alloys. The manganese, silicon, phosphorus and sulfur specifications are identical. The main alloying differences between the 304 and 316 grades are the substitution of nickel for chromium plus the addition of molybdenum for increased pitting (and sensitization) resistance in the 316 grades. The Type 316 Nuclear Grade material has a carbon content not exceeding 0.020

weight percent in the ladle analysis. The nitrogen content of this alloy is also controlled to counter-balance the loss in strength due to the decrease in carbon content.

The selection of a Nuclear Grade material was based on the need to provide a material of high reliability and no unexpected results.

The selected Type 316 Nuclear Grade stainless steel also provides the most resistance to improper treatment and handling. It is now generally accepted that Type 316NG has more overall margin than alternate austenitic stainless steel in BWR environments relative to intergranular stress corrosion cracking (IGSCC) resistance due to its lower carbon content and Mo additions.

The general format of this analysis will be developed from the overall outline below:

- 1) A detailed theoretical analysis of the influence of molybdenum and carbon on the properties of austenitic stainless steels relative to resistance to IGSCC.
- 2) A review of sensitization and oxygenated high temperature water tests of the IGSCC resistance of these austenitic alloys.

THEORETICAL ANALYSIS

Armijo^{3,4,5} analyzed the theoretical aspects of the influence of molybdenum and carbon on the properties of austenitic stainless steels with particular emphasis on sensitivity to IGSCC. The analysis was based on the documented influences of molybdenum and carbon on the thermodynamics, structure, precipitation kinetics and corrosion behavior of austenitic stainless steels.

A. Thermodynamics

Thermodynamic evaluations of the influence of alloy composition on the sensitization (grain boundary precipitation and concurrent chromium depletion) of austenitic stainless steels have been made by Tedmon et al.^{6,7} Strawstrom and Hillert⁸ and Cihal⁹. These studies have ranged from basic to semi-empirical and have resulted in findings that are strictly limited to isothermal "equilibrium" conditions, e.g., furnace sensitization.

Tedmon et al approach calculates the chromium concentration in the grain boundaries of stainless steels as a function of temperature and alloy composition. If the chromium content in equilibrium with the carbide phase is calculated to be less than 13% at a given temperature the alloy is assumed to be susceptible to intergranular corrosion and by interference, intergranular stress corrosion cracking.

In general, these studies agree that the most important element promoting sensitization is carbon. Nickel also promotes sensitization but to a lesser degree than carbon, while alloying elements such as Cr, Mo, Ti and Nb suppress sensitization. Elements such as Mn, Si, P and S appear to have no effect. For the alloys under consideration (Table 1) it is evident that maximum resistance to sensitization is associated with low carbon and nickel contents and high Cr and Mo contents. The relative effectiveness of these elements has been addressed by Tedmon, et. al.⁷ and by Romero and Romeo.⁹

It has been shown that the change in the Cr concentration in the grain boundary is reduced by about 0.25 -0.5% for each 1% increase in Ni and increased by about 0.8% for each 1% increase in Cr.^{7*} Thus a one percent increase in Cr content can offset the sensitizing effects of a 2 - 4% increase in Ni.

Similarly, a 1% increase in Mo content is as effective as a 1 - 2% increase in Cr content in suppressing sensitization.¹⁰ These latter calculations are supported by Cihal⁹ who concludes that the effective chromium concentration (Cr^1) is given by:

$$Cr^1 = \% Cr + 1.7 (\% Mo), \quad (1)$$

and the effective carbon concentration (C) is given by:

$$C^1 = \% C + 0.002 (\% Ni - 10). \quad (2)$$

He further relates equations (1) and (2) by:

$$Cr^1 = 100 C^1 + 16 \quad (3)$$

as the condition required for immunity from sensitization. These equations reduce to:

$$\% Cr + 1.7 \% Mo = 100 \% C + 0.2 \% Ni + 16 \quad (4)$$

It is evident from equation (4) that a one percent increase in Cr content can offset the sensitizing effects of a 5% increase in Ni, and that a 1% increase in Mo is as effective as 1.7% Cr in reducing sensitization.

The calculations based on the Tedmon model^{6,7,10} are in qualitative agreement with those of Cihal.⁹ The two major points of agreement are that the detrimental effect of Ni is smaller than the beneficial effect of Cr, and the beneficial effect of Mo is similar to that of Cr. Calculations were made of the relative sensitization behavior of average compositions of 316 and 304 stainless steels. As shown in Figure 1, the Tedmon model shows that 316 stainless steels of varying carbon contents would have a slightly greater propensity for sensitization than Type 304 stainless steels. However, the Cihal model for the same alloy compositions, as shown in Figure 1, would yield the opposite conclusion. For example, the values of $(Cr^1 - 100C^1)$ for 316 and 304 stainless steels containing 0.06% carbon would be ~15 and ~13 respectively. According to the Cihal

*Calculated for alloys of base composition 18% Cr, 10% Ni, 0.06% C and sensitized at 600°C.

model a value of approximately 16 or higher is required for immunity from sensitization. Thus the 316 stainless steel should have greater resistance.

It is concluded that the alloy compositions for 316 and 304 stainless steels have essentially the same net thermodynamic resistance to sensitization. The uncertainties in the thermodynamic data on the influence of Mo, Ni, and Cr on the activity coefficients of carbon in austenite are sufficient to make the calculated differences in furnace sensitization resistance inconsequential.

B. Kinetics

The sensitization of stainless steels during welding is controlled by the rates of diffusion of carbon and chromium. At elevated temperatures, carbon diffusion limits the carbide precipitation rate whereas chromium diffusion is limiting at lower temperatures. Low temperature sensitization rates can be significantly increased by prior cold working of the steel or by prior quenching from very high solution heat treating temperatures. Both processes create a supersaturation of atomic vacancies which in turn increase the Cr diffusion rates.

Conversely, sensitization rates can decrease by decreasing the concentration of mobile vacancies. Molybdenum appears to have such an effect.

The atomic diameters of the main alloying elements in austenitic stainless steels are very similar: Fe - 2.52\AA , Ni - 2.49\AA , Cr - 2.57\AA . The smallest and largest atoms differ from the average by only $\sim 1.5\%$. Molybdenum, however, has an atomic diameter of 2.8\AA and is thus $\sim 11\%$ larger than the average. This larger atom creates severe compressive strains in the crystal lattice that can be accommodated by the creation and trapping of atomic vacancies, or by the segregation of Mo atoms to vacancy rich grain boundaries or free surfaces. Because of effects such as vacancy trapping, Mo should have a strong effect in reducing the rate

of chromium diffusion (particularly at low temperatures). There is ample evidence in the literature to support this contention.

Narita¹¹ observed (by transmission electron microscopy) slower rates of carbide precipitation in Type 316 than in Type 304 stainless steel. As shown in Table 2, chrome carbides were observed in grain boundaries of Type 304 stainless steel specimens after 650°C heat treatments of 0.5 to 1 hour, but were detected in Type 316 stainless steel only after a 6 hour heat treatment. Narita concluded that the slower carbide precipitation in Type 316 stainless steel was consistent with its higher creep resistance, i.e., lattice strains produced by the Mo suppress vacancy migration as well as dislocation motion. He further postulated that intergranular corrosion resistance would increase with Mo-containing steels.

Elen and Glas¹² also observed the effect of the Mo strain field in a study of boron distribution in Types 304L and 316L stainless steels. In this study an alpha particle tracking technique capable of detecting ppm boron concentrations in austenitic stainless steels¹³ was used. Direct evidence was obtained showing boron segregation in the grain boundaries of cold worked 304L and heavy boron precipitation in grain boundaries of sensitized material. In contrast, no boron segregation was observed in cold worked 316L and only slight boron precipitation in grain boundaries of sensitized material. These findings are shown in Table 3.

In a concurrent study Elen and Glas¹² also evaluated the effects of B concentration on the recrystallization of 304L and 316L stainless steels. They found that increasing the boron content of 304L from 3 ppm to 50 ppm suppressed recrystallization. Increasing the boron content of 316L from 1 ppm to 35 ppm did not change the recrystallization behavior. They concluded that this effect was consistent with a mechanism in which boron is held in the strain fields of the Mo in the 316L steel.

Another example of the effect of the Mo strain field in the stainless steel crystal lattice is given by Barnes, Aldag and Jerner.¹⁴ In this study a very sensitive Auger electron spectroscopy technique was used to study the surface and near surface (0-30 Å) concentrations of elements in mill-annealed Type 304 and 316 stainless steels. The authors interpreted these results in terms of surface segregation. An alternated explanation (since higher Cr concentrations were also observed on the metal surface) is that Mo enrichment occurs in the oxide film. In either case it is evident that high concentrations of Mo are available at the surface of the metal to form protective oxide films.

SENSITIZATION AND CORROSION TEST RESULTS

A. Crack Initiation

As stated in Section 2 above, the major kinetic effect of Mo addition to stainless steel appears to be the reduction in Cr diffusion rates. Because Cr diffusion controls low temperature carbide precipitation, the benefits of Mo to intergranular corrosion and intergranular stress corrosion resistance should be evident in materials that have been sensitized at low temperatures. The data of Hamada et al¹⁵ provides good support for this effect. The comparative intergranular corrosion resistance of Type 316 and 304 stainless steel with the identical carbon contents (0.05 w/o) is presented in Table 4. These Strauss test results indicate no weld sensitization or corrosion resistance degradation due to subsequent Low Temperature Sensitization (LTS) at 500°C for 24 hours is observed on the Type 316 stainless steel. This acid test result was verified by constant extension rate testing (CERT), Figure 2.

Further investigation by Hamada et al was designed to determine the reason for Type 316 stainless steel's excellent SCC performance. The

prior CERT specimen was machined from an actual weldment using the interior of the piping material. An additional CERT test (interrupted CERT) using a nearly full thickness specimen with the original surfaces preserved revealed test results as displayed in Figure 3. In this instance, the post-test inside surface is characterized by several cracks in the heat affected zone (HAZ). It appears, however, that the extent of cracking would be limited to the surface layer based on the microstructural and fracture morphological examinations. A further examination of the hardness and sensitization profiles through the thickness, Figure 4 reveals that both the ID and OD surface regions are significantly harder and more sensitized.

Similar results were obtained by Edstrom and Ljungberg¹⁶ relative the degree of sensitization on Type 304 (0.054 w/o C), Type 316 (0.054 w/o C), 304L (0.020 w/o C) and Type 316 L (0.025 w/o C) stainless steels using the test after various sensitizing heat treatments (550-750°C). The material compositions and results are summarized in Tables 5 and 5 respectively.

It is evident from Table 5 that both normal carbon and high carbon 316 stainless steels start to sensitize at higher temperatures (550 - 600°C), however, the 316 grades sensitize at significantly slower rates than the 304 grades. The very strong effect of Mo is evident at 550°C where the sensitization time for 316 was as slow as that for 304L and 316L. It should also be noted that the low temperature rates of sensitization for 316L were slower than the rates for 304L even though the former contained a 25% higher carbon content. Similar results were also obtained by Ebling and Scheil.¹⁷

Akashi and Kawamota¹⁸ demonstrated the effects of molybdenum additions on the SCC susceptibility of sensitized stainless steels in oxygenated (20ppm) high temperature water (250°C) using the creviced bent beam (CBB)

technique and the Strauss test. The chemical compositions of the alloys studied are presented in Table 7.

Figures 5 - 8 present the time-temperature - SCC diagrams of Type 304, 316 and 316L stainless steels as derived from the CBB test, respectively, where the maximum crack depth is plotted as a function of various sensitization heat treatments. Figure 5 clearly indicates that Type 304 stainless steel is highly susceptible to SCC over a wide range of sensitization time and temperature. The areas of significant susceptibility ranges from low temperature/long duration to high temperature/short duration.

Type 316 stainless steel is characterized by considerable susceptibility to SCC although not nearly as severe as the Type 304; Figure 6. The area of SCC in this particular investigation shifted towards higher temperatures by approximately 50°C. This result demonstrates the effect of molybdenum suppressing the growth of chromium carbide on the basis of the classic chromium depletion theory.¹⁹

The T-T-SCC diagram of Type 304L stainless steel, Figure 7, appears to be quite similar to that of Type 304 stainless steel except that the maximum crack depth is considerably smaller, thus suggesting and verifying the increased resistance to SCC of Type 304L stainless steel due to lower carbon contents.

The T-T-SCC diagram of Type 316L stainless steel, Figure 8 indicates that the SCC susceptibility of this alloy is slightly lower than that of Type 304L stainless steel concurrent with the previous results of Types 316 and 304 stainless steels. The temperature shift in this diagram is also approximately 50°C duplicating the Type 316/Type 304 shift.

Figure 9 presents the CBB data for Type 316 and 304 stainless steel in a single plot where the regions selected are based on crack depths exceeding 200 μm in depth. Similar results are obtained in the Strauss test based on intergranular penetration exceeding 500 μm in depth, Figure 10.

The presence of molybdenum delays sensitization at lower temperatures.

A sensitization study on Types 304 (0.053 w/o C) 316 (0.07 w/o C) and 316 L (0.027 w/o C) stainless steel by Mori et al²⁰ also using the Strauss test revealed similar results, Figure 11. It should be noted that Type 316 stainless steel shifted to longer times and higher temperatures as compared to Type 304 stainless steel despite the higher carbon content on the Type 316 (0.07 vs. 0.053) stainless steel.

Hattori et al²¹ investigated the effect of carbon content on sensitization for seventeen heats of Type 304 and sixteen heats of Type 316 stainless steel pipe material. Figures 12 and 13 present the relationship between sensitization resistance and carbon content for pipe welds prepared with grinding plus welding and grinding plus welding plus LTS for Types 304 and 316 stainless steel, respectively. These figures indicated that in each alloy family, the materials with the carbon content less than 0.02 w/o (Nuclear Grade) are fully resistant to weld sensitization and LTS. It was also revealed that Type 316 stainless steel has a significantly greater margin in terms of resistance to weld sensitization.

This conclusion is further substantiated when an examination of typical ID weld sensitization profiles is performed on heats of Type 304 and 316 stainless steel of approximately the identical carbon contents, Figures 14 and 15. It is clear from this data that the weld HAZ of Type 304 stainless steel can occur over a significantly wider area. This is readily explainable based on the previous discussions on the effects of molybdenum on suppressing sensitization.

Another direct sensitization comparison between Types 304 and 316 stainless steel with identical carbon contents was made by Hataya et al.²² Table 8 presents the Strauss test results of Type 304 and 316 stainless steel welded joints. The penetration depth increases by the additional

LTS heat treatment but the penetration depth of Type 316 stainless steel is less than that observed for Type 304 stainless steel. When the identical materials are heat treated at 750°C for 100 minutes the depth of attack is greater in the Type 316 stainless steel, Table 9. This is explained by the previous T-T-SCC diagrams where the "nose" temperature for Type 316 stainless steel is approximately 750°C. When the specimens are subsequently LTS'd at 500°C for 24 hours, the depth of penetration dramatically increases for Type 304 stainless steel reflecting the lack of molybdenum in the matrix. A comparison of the results of Tables 8 and 9, indicates that the penetration depth of the simulative heat treated steels are slightly larger than those obtained in welded joints, in general, and the simulative heat treatment for 100 minutes at 750°C seems to be equivalent to the welding heat cycle for Type 304 stainless steel but significantly more severe for Type 316 stainless steel.

A correlation among carbon content degree of sensitization as measured by the Electrochemical Potentiokinetic Reactivation (EPR)²³ technique and SCC for Type 304 and 304L stainless steel was derived by Kass et al²⁴ as exhibited in Figure 16. This figure is characterized by a plot of the number of cycles to failure vs. carbon content for pipe specimens² tested at 136% of the 0.2% offset yield strength in 8 ppm oxygenated 288°C water. It is readily apparent from this figure that the lower the carbon content, the greater the number of cycles to failure. The maximum EPR data (sensitization value) for each heat are plotted as superscripts for each data point. It appears that the test data fall into four categories:

- 1) carbon contents of less than ~0.03 w/o with no failures after 2000 or 3000 cycles
- 2) carbon contents of ~0.042 w/o with failures after several

hundred cycles

3) carbon contents of ~ 0.045 w/o with failures at roughly 2000 cycles

4) carbon contents of 0.05 w/o or more with failures within 100 cycles

It is important to note that of the four groups, group 2 had lower carbon content but shorter life than group 3 and that the extremely small difference in carbon contents between 0.045 and 0.05 w/o results in extremely large differences in cyclic life. The disparity in cyclic life between groups 2 and 3 is explainable in terms of the ERR data. Although group 3 is characterized by a higher carbon content, the degree of sensitization (DOS) was significantly less than that for group 2. It was also noted that the yield stress and thus the test stress for group 4 was higher than those for groups 2 or 3. A similar type of relationship for carbon content vs. time to failure (no EPR measurements) for Type 316 stainless steel is illustrated in Figures 17 and 18.

A comparison of CERT test results of Type 316 and 316L stainless steels, Table 10 by Clarke and Hughes²⁵ is presented in Table 11. The data indicates that all three as-welded Type 316 stainless steel heats (M6985, 0.065 w/o C; 037050, 0.070 w/o C; 037049, 0.069 w/o C) suffered IGSCC in the CERT test. Both heats 037049 and 037050 welded specimens also failed intergranularly after the LTS treatment and the extent of attack was significantly greater than the as-welded condition alone. The third specimen (M6985) tested in the welded plus LTS condition failed in CERT primarily by ductile fracture with minor IGSCC and cleavage fracture present. This result is considered to be a reflection of normal scatter in SCC behavior. None of the Type 316 L stainless steel specimens were susceptible to IGSCC in the CERT in either heat treatment.

The results of the EPR tests conducted on weld profile specimens are delineated in Table 12. The EPR values correlate with the results of the CERT testing, that is, all the Type 316 L stainless steel specimens were resistant to sensitization ($P_a < 2.0 \text{ C/cm}^2$). The maximum degree of sensitization for the Type 316 stainless steel specimens generally occurred at 2.5 mm (100 mils.) from the fusion line. The EPR values for these Type 316 stainless steel specimens were low compared to typical Type 304 stainless steel samples where P_a values generally range between 4 and 40 C/cm^2 in the welded condition. As discussed previously, molybdenum additions to the Type 316 steels influences chromium diffusion such that the width of the chromium depleted zone is reduced. Table 13 combines the above CERT test data (Table 11) with some pipe test results. The correlation between these two testing techniques is also excellent.

Hishida²⁶ performed a metallurgical study to correlate the sensitization response of Type 316 and 316L as measured by the oxalic acid test, Strauss test and CERT tests. The results are summarized in Figures 19 and 20. Similar to the results of Clarke and Hughes, the correlation among these three sensitization techniques is excellent. All three testing techniques reveal approximately the same regions of sensitization for each alloy. Figure 21 indicates a comparison based on only CERT testing in 290°C 8 ppm oxygenated water. As seen previously, the ranking of sensitization propensities for these austenitic materials is Type 304, 316, 304L and 316L stainless steel.

B. Crack Propagation

All of the data reported above involved crack initiation. It is considered prudent to also briefly examine the data relevant to crack propagation in these stainless steels. Motivated by the relative paucity of data concerning this component of the SCC phenomenon, Akashi et al²⁷

performed a series of CBB tests to determine the SCL velocity of Types 304 (0.064 w/o C) and 316 (0.058 w/o C) stainless steel.

Figure 22 illustrates the results for sensitized Type 304 and 316 stainless steels exposed to 20 ppm oxygen 250°C water. The 50% probability values of the maximum crack depths are plotted versus the test duration in this figure. It is apparent that the time prior to crack initiation in these tests can be considered incubation period. The propagation rate for sensitized Type 304 and 316 stainless steel is approximately 2×10^{-9} m/sec. The data suggests that the SCC velocity is not affected by the degree of sensitization and/or alloying elements although the incubation period is significantly influenced by these two factors. Thus it appears that crack initiation dominates the difference in IGSCC response for these two alloys and that the majority of test results obtained to date has been focused in the proper area.

DISCUSSION

A review of the theoretical aspects of molybdenum bearing stainless steels compared to the non-molybdenum bearing grades indicates that the former should be more resistant to sensitization at lower sensitization temperatures and thus more IGSCC resistant in the welded condition than the latter. The results of recent high temperature constant extension rate tests, low temperature sensitization studies, crevice bent beam studies, various acid sensitization tests, electropotentiodynamic reactivation studies and full size pipe tests can be cited as extremely strong verification of this theoretical analysis. In a convincing number of instances Type 316L stainless steel (or Nuclear Grade) clearly demonstrated its superior IGSCC resistance over Type 304 and 316 stainless steel.

Normal carbon level Type 316 stainless steel, theoretically and as demonstrated by

laboratory testing, has only slightly more resistance to IGSCC than Type 304 stainless steel due to the presence of molybdenum. The results of statistical full size pipe testing can be cited as evidence to support this statement since no factor of improvement was identified with these severe testing techniques.²

Therefore, the events at Nine Mile Point Unit 1 cannot be considered as being totally unexpected. The carbon contents of the IGSCC cracked piping for an elbow and pipe material are within the normal range for nominal grade Type 316 stainless steel, 0.065 and 0.049 w/o C, respectively.¹ Type 316 stainless steel is more resistant to sensitization than Type 304 stainless steel, but is not immune. However, the replacement piping, Type 316 Nuclear Grade, does appear to be "immune" to weld sensitization and thus IGSCC due to the synergistic beneficial effects of molybdenum and lower carbon content.

E. CONCLUSIONS

In conclusions, the above literature survey and analysis of recent laboratory test programs concerning the IGSCC resistance of Type 316 and Type 316 Nuclear Grade to reference Type 304 stainless steel for BWR piping have revealed the following:

- 1) A review of the theoretical aspects of the influence of Mo and C on the properties of austenitic stainless steels has led to the following findings:
 - a) Mo additions have thermodynamic benefits similar to Cr; i.e., both offset the sensitizing effects of Ni and C. Within the limits of available thermodynamic data the normal-carbon and low-carbon grades of Type 304 and 316 stainless steels have

equivalent resistance to furnace sensitization.

- b) Mo additions significantly decrease the rate of sensitization at temperatures below 650°C, and increase the rates at higher temperatures. This effect produces a net benefit because the most severe sensitization (chromium depletion) occurs at low temperatures. This effect is probably the major benefit of 316 over 304 grades with respect to weld sensitization.
 - c) Mo additions promote the stability of passive surface films and improve pitting and crevice corrosion.
 - d) The combinations of these benefits theoretically indicate that Type 316 and 316L (Nuclear Grade) stainless steels should have greater resistance to sensitization and intergranular stress corrosion cracking than 304 and 304L, respectively.
- 2) A review of the laboratory test data (CERT testing, acid tests, full size pipe testing, creviced bent beam tests, electrochemical techniques) on the IGSCC propensities of Types 316 Nuclear Grade, 316 and 304 stainless steel in BWR type environments have revealed the following:
- a) Type 316 stainless steel is more resistant to low temperature sensitization (500 - 600°C) than Type 304 stainless steel but starts to sensitize at higher temperatures (700 - 750°C).
 - b) The surface layer of Type 316 stainless steel as influenced by local cold work/local sensitization has a detrimental impact on subsequent IGSCC performance.
 - c) Nuclear Grade piping materials (<0.02 w/o C) are fully resistant to weld sensitization and LTS.
 - d) Weld sensitization profiles on Type 316 and 304 stainless steels with identical carbon content reveal that the weld HAZ of Type 304

stainless steel can occur over a significantly wider area.

- e) Extremely small differences in carbon content $\sim(0.005 \text{ w/o})$ can have significant influences on the IGSCC response of Type 304 stainless steels.
 - f) The degree of sensitization as measured by the electrochemical potentiokinetic reactivation (EPR) technique, indicates that Type 316 stainless steel is low compared to typical Type 304 stainless steel due to Type 316 stainless steels' reduced chromium depleted zone.
 - g) Since the crack propagation of sensitized Type 316 and 304 stainless steel as measured by the CBB technique are approximately the same, the SCC velocity is not affected by the relative degree of sensitization and/or alloying elements present although the incubation period (initiation) is significantly influenced by these two factors.
 - h) The overall ranking for stress corrosion cracking resistance in the BWR environment for the discussed stainless steels is Type 316 Nuclear Grade \gg Type 316 $>$ Type 304. Although Type 316 stainless steel is more resistant to SCC than Type 304 stainless steel it is not significantly superior to be considered a sensitization resistant as-welded BWR piping material.
- 3) The cracking at Nine Mile Point Unit 1 cannot be considered as being totally unexpected. The additional IGSCC margin Type 316 stainless steel provides over Type 304 stainless steel is not significant enough to impact overall BWR plant performance.

REFERENCES

- 1) J.C. Cutt, "Laboratory Examination of Sections from Type 316 Stainless Steel Recirculation Piping - Nine Mile Point 1, 1982" PMT Transmittal No. 82-178-41, November 17, 1982.
- 2) R.S. Tunder et al, "Alternative Alloys for BWR Pipe Applications," EPRI NP-2671-LD, Project T111-1, Final Report, October 1982.
- 3) B.M. Gordon and J.S. Armijo, "A Comparison of Type 316L with Types 316, 304 and 304L Stainless Steel for Small Diameter BWR Piping," PCBA Memo No. 19, April 30, 1976.
- 4) B.M. Gordon, "The Use of Type 316L Stainless Steel As An Alternative BWR Piping Material," PME Transmittal No. 77-688-57, September 20, 1977.
- 5) J.S. Armijo, "Influence of Molybdenum and Carbon Content of the Microstructural and Corrosion Properties of Austenitic Stainless Steels," FM&MD Transmittal No. 76-58, March 23, 1976.
- 6) C.S. Tedmon, D.A. Vermilyea, and J.H. Rosolowski, Journal of the Electrochemical Society, 118, 192 (1971).
- 7) C.S. Tedmon, and D.A. Vermilyea, and J.H. Rosolowski, Journal of the Electrochemical Society, 118, 192 (1971).
- 8) C. Strawstrom and M. Hillert, Journal of Iron and Steel Inst., 207, 77 (1969).
- 9) V. Cihal, Corrosion-Treatments-Protection-Finition, 18 441 (1970).
- 10) V. Romero and G. Romeo, Fuel Development Memorandum - 126, July 1975.
- 11) K. Narita, Trans, Japan Institute of Metals, 4, 15 (1963).
- 12) J.D. Elen and A. Glas, J. Nucl. Mat., 34 182 (1970).
- 13) J.S. Armijo and H.S. Rosenbaum, J. Appl. Phys., 38 2064 (1967).
- 14) G.J. Barnes, A.W. Aldag, and R.C. Jerner, J. Electrochem. Soc., 119, 684 (1972).
- 15) I. Hamada et al private communication November 6, 1978.
- 16) J.O. Edstrom and L. Ljungberg, Chemical Engr., 114, Dec. 1964.
- 17) H.F. Ebling and M.A. Scheil, ASTM Special Tech. Pub. No. 369, Advances in the Technology of Stainless Steels and Related Alloys, April (1965).
- 18) M. Akashi and T. Kawamoto private communication, October 15, 1977.

- 19) V.G. Herbsleb and K.J. Westenfeld, Werkstoffe und Korrosion, 27, 404 (1976).
- 20) Y. Mori et al private communication, November 6, 1978.
- 21) S. Hattori et al private communication, December, 1979.
- 22) F. Hataya et al private communication, May 1979.
- 23) W. L. Clarke, "The EPR Method for the Detection of Sensitization in Stainless Steels," GEAP-24888, February 1981.
- 24) J. N. Kass, W. L. Walker, A. J. Giannuzzi, Stress Corrosion Cracking of Welded Type 304 and 304L Stainless Steel Under Cyclic Loading," Corrosion Vol. 36, No. 6, June, 1980.
- 25) W. L. Clarke and N. R. Hughes, "Comparison of EPR and CERT Results for Types 316 and 316L Stainless Steel," May 1979.
- 26) Hishida private communication, December 1979.
- 27) Akashi et al private communication, May 1979.

Table 1

CHEMICAL COMPOSITION LIMITS AND RANGES FOR TYPE 304, 316 AND
316 NUCLEAR GRADE STAINLESS STEELS

<u>Number</u>	<u>C</u> <u>max</u>	<u>Mn</u> <u>max</u>	<u>Si</u> <u>max</u>	<u>P</u> <u>max</u>	<u>S</u> <u>max</u>	<u>Cr</u>	<u>Ni</u>	<u>Mo</u>	<u>N</u>
304	0.08	2.00	1.00	0.045	0.030	18.00 - 20.00	8.00 - 12.00	-	-
316	0.08	2.00	1.00	0.045	0.030	16.00 - 18.00	10.00 - 14.00	2.00 - 3.00	-
316NG	0.020	2.00	1.00	0.045	0.030	16.00 - 18.00	10.00 - 14.00	2.00 - 3.00	0.060 - 0.100

TABLE 2

OBSERVATIONS OF CARBIDE PRECIPITATION
IN STAINLESS STEELS (Narita¹¹)

<u>HEAT TREATMENT</u>		<u>TYPE 304</u>	<u>TYPE 316</u>
Temp (°C)	Time (hours)		
650	0.5	Carbides barely detectable	None observed
650	1.0	Carbides clearly observed	None observed
650	3.0	Carbides clearly observed	None observed
650	6.0	Carbides clearly observed	Carbides detectable
650	24.0	Large carbides clearly observed	Small carbides clearly observed

TABLE 3

PERCENT ¹⁰B IN GRAIN BOUNDARIES OF 304L AND
316L STAINLESS STEELS (Elen and Glas¹²)

TEMP (°C)	PERCENT ¹⁰ B			
	0.5 hour	1 hour	4 hours	5 hours
	<u>304L/316L</u>	<u>304L/316L</u>	<u>304L/316L</u>	<u>304L/316L</u>
600	5/Not Tested	5/0	5/Not Tested	5/0
700	5/ "	15/0	15/ "	18/0
800	26/ "	33/0	37/ "	30/0
900	33/ "	43/0	47/ "	55/Detectable

304L - 9 ppm ¹⁰B
316L - 35 ppm ¹⁰B

Table 4

STRAUSS TEST RESULTS OF VARIOUS
STAINLESS STEEL WELDMENTS

<u>Material</u>	<u>%C</u>		<u>A W</u>	<u>LTS'ed</u>
316	0.05	HAZ	0	0
		depo.	0	0
316L	0.01	HAZ	0	0
		depo.	0	0
304	0.05	HAZ	x	x
		depo.	0	x
304L	0.021	HAZ	0	0
		depo.	0	x

0: Attack Free

X: IG Attack

Data of Hamada et al¹⁵

TABLE 5
ALLOY COMPOSITIONS TESTED BY
EDSTROM AND LJUNDBERG¹⁶

<u>Steel</u>	<u>C</u>	<u>Ni</u>	<u>Wt. Percent</u>		<u>N</u>
			<u>Cr</u>	<u>Mo</u>	
304	.054	8.5	18.2	-	.023
316	.054	12.2	17.7	2.52	.026
304L	.020	10.7	18.4	-	.030
316L	.025	13.4	16.0	2.50	.027

TABLE 6
THERMAL EXPOSURES LEADING TO
DETECTABLE SENSITIZATION¹⁶

<u>TEMPERATURE °C</u>	<u>304</u>	<u>316</u>	<u>304L</u>	<u>316L</u>
750°C	none	0.3	none	none
700°C	0.4	0.3	none	10
650°C	0.4	0.5	5	6
600°C	0.9	4	5	20
550°C	5.0	200	100	200

Table 7

CHEMICAL COMPOSITION OF ALLOYS STUDIED (%)⁽¹⁸⁾

<u>Type</u>	<u>C</u>	<u>Si</u>	<u>Mn</u>	<u>P</u>	<u>S</u>	<u>Ni</u>	<u>Cr</u>	(%) <u>Mo</u>
304	0.06	0.49	1.19	0.025	0.010	8.78	18.56	
304L	0.018	0.59	0.96	0.025	0.015	9.91	18.19	
316	0.05	0.96	0.60	0.029	0.006	13.02	17.40	2.48
316L	0.014	0.72	1.00	0.029	0.004	12.48	17.58	2.40

Table 8

STRAUSS TEST RESULTS OF WELDED JOINTS WITH
TYPE 304 AND TYPE 316 4B PIPES(22)

<u>Type</u>	<u>C (%)</u>	<u>Penetration Depth (μm)</u>	
		<u>As Welded</u>	<u>As Welded +500°C x 24h</u>
304	0.050	117	2230
316	0.051	≤ 20	33

Table 9

STRAUSS TEST RESULTS OF SIMULATIVE HEAT
TREATED TYPE 304 AND TYPE 316(22)

<u>Type</u>	<u>C (%)</u>	<u>Penetration Depth (μm)</u>	
		<u>750°C x 100 min</u>	<u>750°C x 100 min +500°C x 24h</u>
304	0.050	200	2260
316	0.051	283	920

Table 10

CHEMICAL COMPOSITION OF TYPES-316 AND -316L STAINLESS STEEL
USED IN CHARACTERIZATION STUDY (Wt %)(25)

<u>Alloy</u>	<u>Heat</u>	<u>C</u>	<u>Mn</u>	<u>S</u>	<u>P</u>	<u>Si</u>	<u>Mo</u>	<u>Cr</u>	<u>Ni</u>
316	037049	0.069	1.69	0.012	0.004	0.53	2.22	17.36	10.25
316	037050	0.070	1.65	0.015	0.003	0.56	2.24	18.24	11.38
316	M6985	0.065	1.70	0.014	0.021	0.50	2.36	17.18	13.30
316L	00630	0.018	1.68	0.003	0.025	0.38	2.15	16.22	11.62
316L	037040	0.024	1.68	0.013	0.004	0.53	2.19	17.46	10.28
316L	037041	0.020	1.70	0.012	0.005	0.54	2.19	18.02	11.32
316L	D63104	0.009	1.63	0.004	0.025	0.45	2.46	17.00	13.10

Table 11

CERT RESULTS FOR TYPES-316 AND -316L STAINLESS STEEL TESTED IN
289°C WATER WITH 8 ppm O₂ AT $\dot{\epsilon} = 4 \times 10^{-5}/\text{min}(25)$

Condition ^a	Alloy	Weldment	Heat	Maximum Breaking Stress (ksi)	Failure Time (h)	RA (%)	E (%)	IGSCC ^b
AW	316L	A-A	037041	73.3	62.5	40.4	12.3	No
AW		B-B		74.0	71.5	49.0	15.5	No
AW+LTS		A-A		73.4	73.5	53.1	16.4	No
AW+LTS		B-B		76.5	58.0	41.4	12.8	No
AW	316L	A-A	037040	75.8	90.5	50.4	19.7	No
AW		B-B		74.2	64.5	42.7	12.7	No
AW+LTS		A-A		76.7	77.5	47.6	17.7	No
AW+LTS		B-B		74.1	61.5	55.9	14.3	No
AW	316L	A-A	D63104	73.5	78.0	51.6	16.6	No
AW		B-B		78.2	103.0	48.4	22.6	No
AW+LTS		A-A		77.4	79.0	56.7	18.1	No
AW+LTS		B-B		77.1	98.0	53.6	20.9	No
AW	316	A-A	M6985	71.6	68.0	34.9	17.4	Yes
AW		B-B		76.3	94.5	40.8	20.4	No
AW+LTS		A-A		78.5	80.0	45.9	16.8	No
AW+LTS		B-B		76.9	101.0	44.7	20.9	No
AW	316	A-A	037050	64.4	46.5	17.7	10.3	Yes
AW+LTS		A-A		45.6	17.5	6.9	4.0	Yes
AW	316	A-A	037049	67.7	32.5	19.1	7.1	Yes
AW+LTS		A-A		52.4	17.0	10.3	3.6	Yes
AW	316L	A-A	00630	73.8	85.0	61.7	19.6	No
AW+LTS		A-A		75.2	89.0	53.5	19.6	No

^aAW = As-Welded; LTS = Low-Temperature Sensitized (500°C/24 h)

^bScanning electron microscopic examination

Table 12

EPR RESULTS FOR TYPES-316 AND -316L WELDMENTS TESTED AT 30°C
IN 0.5 M H_2SO_4 + 0.01 M KSCN AT 6 V/h(C/CM²)(26)

Alloy	Heat	Weldment	Distance from Weld Fusion Line (mils)				
			F1	50	100	150	Base Metal
316L ↓	037041 ↓	A-A	$\leq 10^{-3}$	—	—	—	—
		A-A	↓	$\leq 10^{-3}$	$\leq 10^{-3}$	—	$\leq 10^{-3}$
		B-B	↓	↓	—	—	—
		B-B	↓	↓	—	—	$\leq 10^{-3}$
316L ↓	037040 ↓	A-A	$\leq 10^{-3}$	—	—	—	—
		A-A	0.096	$\leq 10^{-3}$	$\leq 10^{-3}$	—	$\leq 10^{-3}$
		B-B	$\leq 10^{-3}$	—	—	—	—
		B-B	$\leq 10^{-3}$	$\leq 10^{-3}$	$\leq 10^{-3}$	—	$\leq 10^{-3}$
316L ↓	D63104 ↓	A-A	$\leq 10^{-3}$	—	—	—	—
		A-A	↓	$\leq 10^{-3}$	$\leq 10^{-3}$	—	$\leq 10^{-3}$
		B-B	↓	—	—	—	—
		B-B	↓	$\leq 10^{-3}$	$\leq 10^{-3}$	—	$\leq 10^{-3}$
316L	00630	A-A	$\leq 10^{-3}$	$\leq 10^{-3}$	$\leq 10^{-3}$	$\leq 10^{-3}$	$\leq 10^{-3}$
316L	00630	A-A	0.23	$\leq 10^{-3}$	$\leq 10^{-3}$	$\leq 10^{-3}$	$\leq 10^{-3}$
316	037050	A-A	1.87	—	—	—	—
316	037050	A-A	0.52	1.40	2.00	0.56	$\leq 10^{-3}$
316	037049	A-A	0.55	—	—	—	—
316	037049	A-A	0.51	1.17	1.17	0.26	$\leq 10^{-3}$
316 ↓	M6985 ↓	A-A	0.20	—	—	—	—
		A-A	0.14	0.13	0.31	0.34	$\leq 10^{-3}$
		B-B	0.18	—	—	—	—
		B-B	0.33	0.50	0.70	0.43	$\leq 10^{-3}$

Table 13

CERT AND PIPE TEST RESULTS FOR TYPES 316 AND 316L STAINLESS STEEL
TESTED IN 8 ppm OXYGEN AT 289°C

Alloy	Heat	w/o C	CERT IGSCC	Pipe Test TTF, hrs
316L	037041	0.020	No	> 2500, NF
	037040	0.024	No	> 1780, NF
	D63104	0.009	No	> 1844, NF
	00630	0.018	No	not tested
316	M6985	0.065	Yes	not tested
	037050	0.070	Yes	164
	037049	0.069	Yes	28
	03019	0.059	No	> 1850, NF

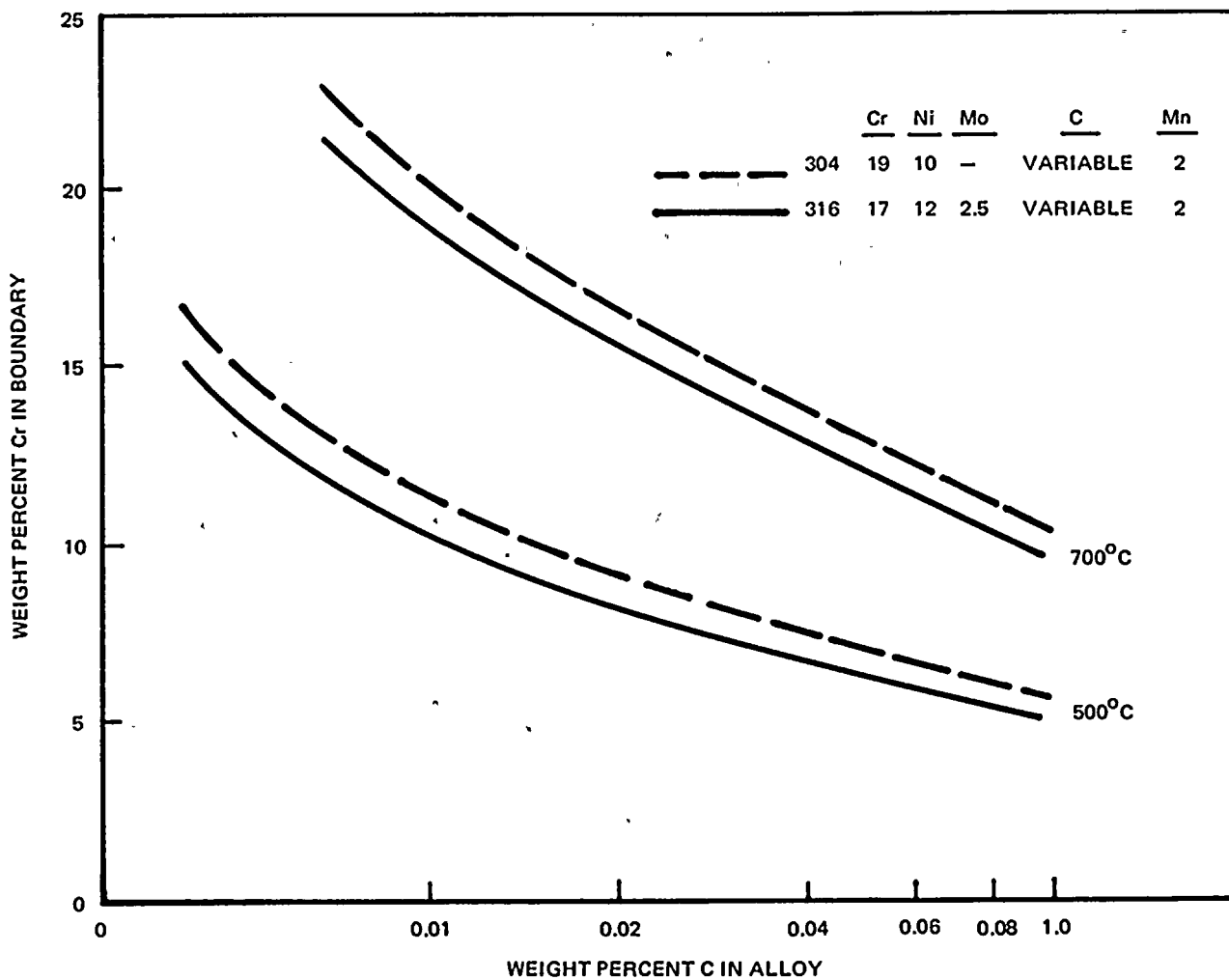
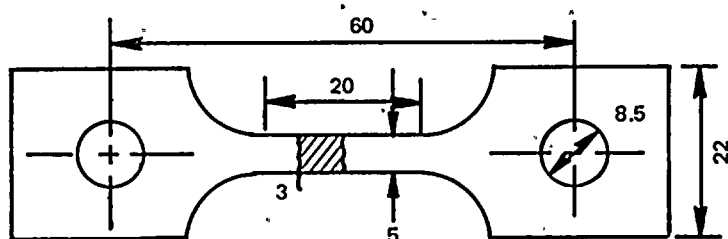
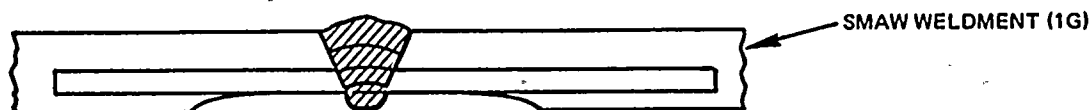


Figure 1. Comparison of Calculated Grain Boundary Cr Concentrations for Sensitized 304 and 316 Stainless Steels of Varying Carbon Contents⁽⁹⁾

CHEMICAL COMPOSITION

0.05C, 0.47Si, 1.62Mn, 0.028P, 0.008S, 12.25Ni, 16.60Cr,
2.12Mo (4-in. DIA SCH 80 SEAMLESS TUBE)



TEST CONDITION

288 C, 85 afg
DO = ~ 8 ppm
 $\dot{\epsilon} = 8.3 \times 10^{-7} / S$

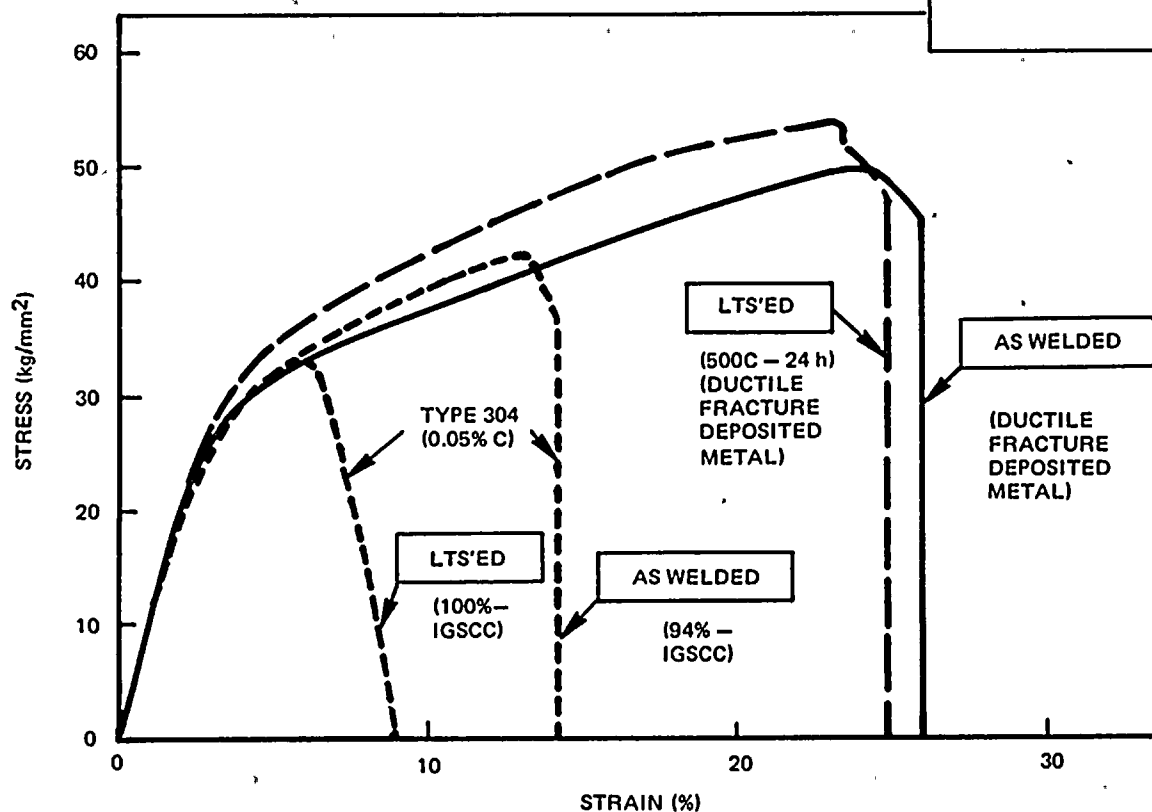
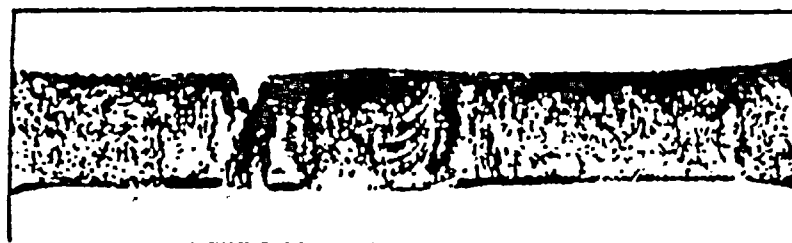
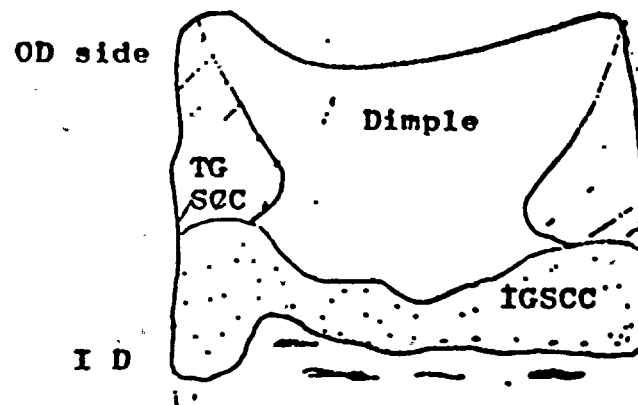


Figure 2. CERT Test Results of the Type 316 SS Weldment in As-Welded and LTS'ed(15)

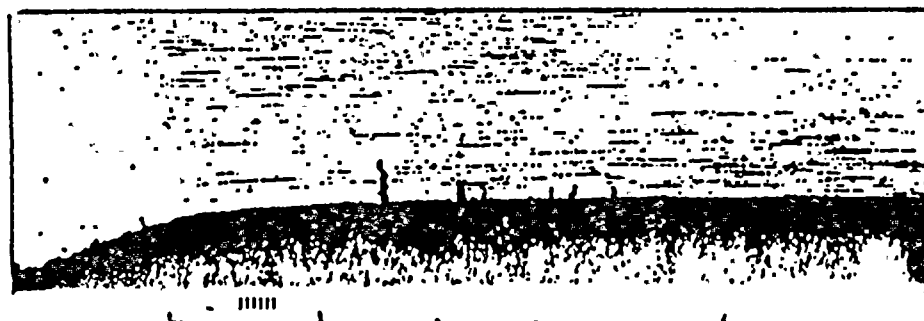


appearance view

10mm



I D



cross section

10mm



0.1 mm



fracture surface

2 mm

Figure 3. Interrupted CERT Test Result and Microexamination of a Nearly Fully Thickness Specimen of the Present Type 316 SS Weldment⁽¹⁵⁾

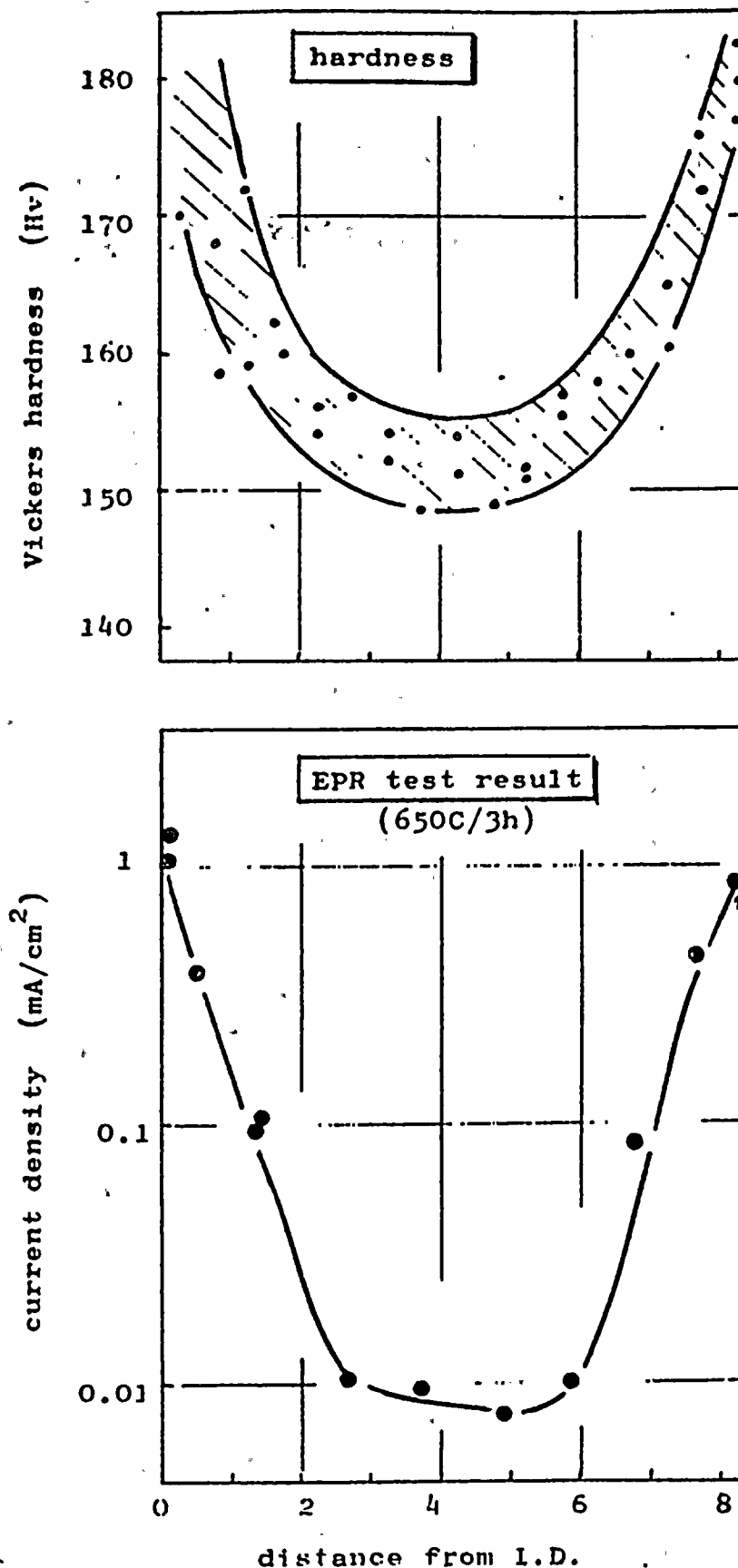


Figure 4. Hardness and Sensitization Profiles Through the Thickness⁽¹⁵⁾

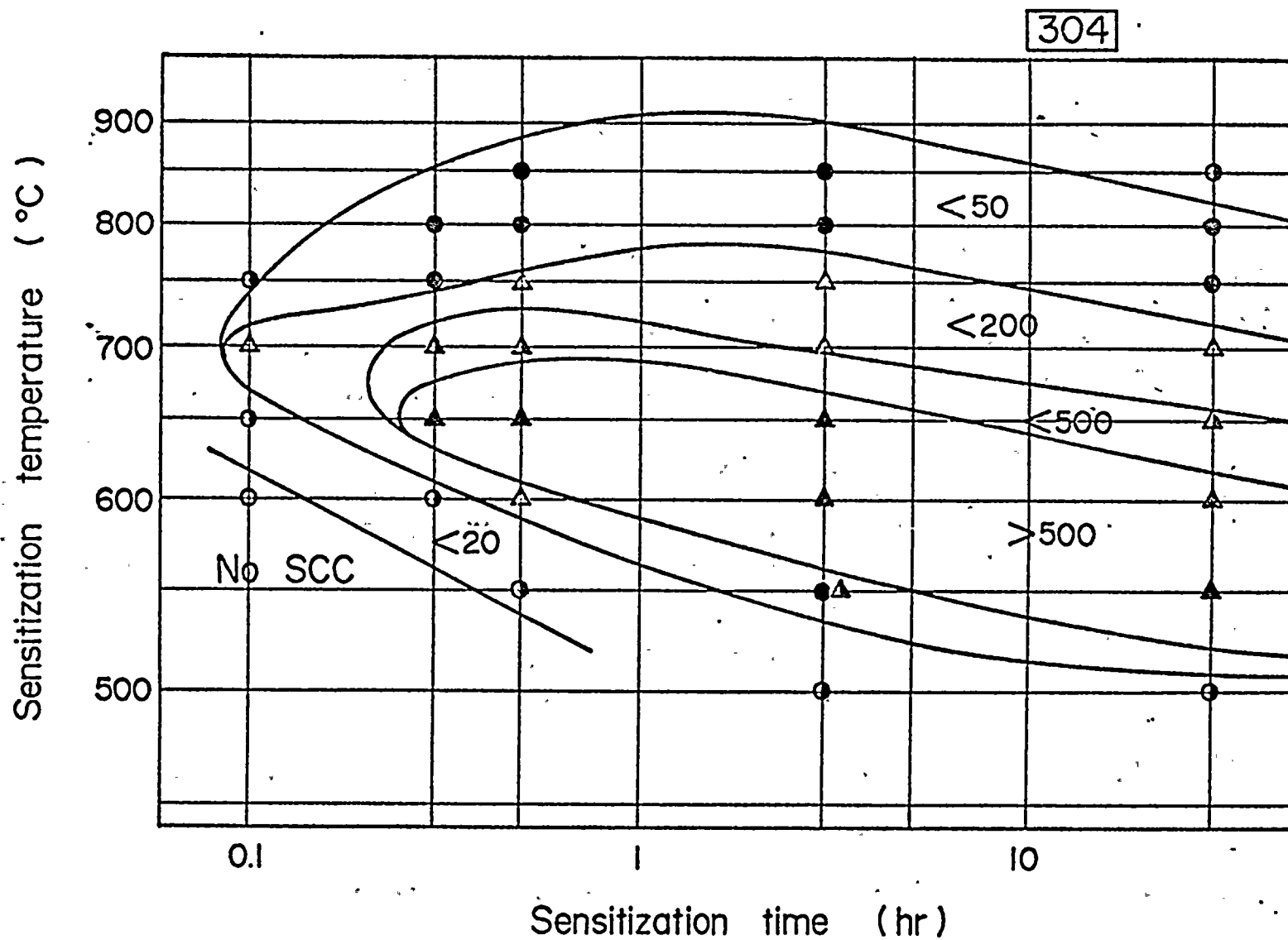


Figure 5. T-T-SCC Diagram for 304 Stainless Steel in Oxygenated Water at 250°C
(CBB Test, 20 ppm DO, 310 hr)(18)

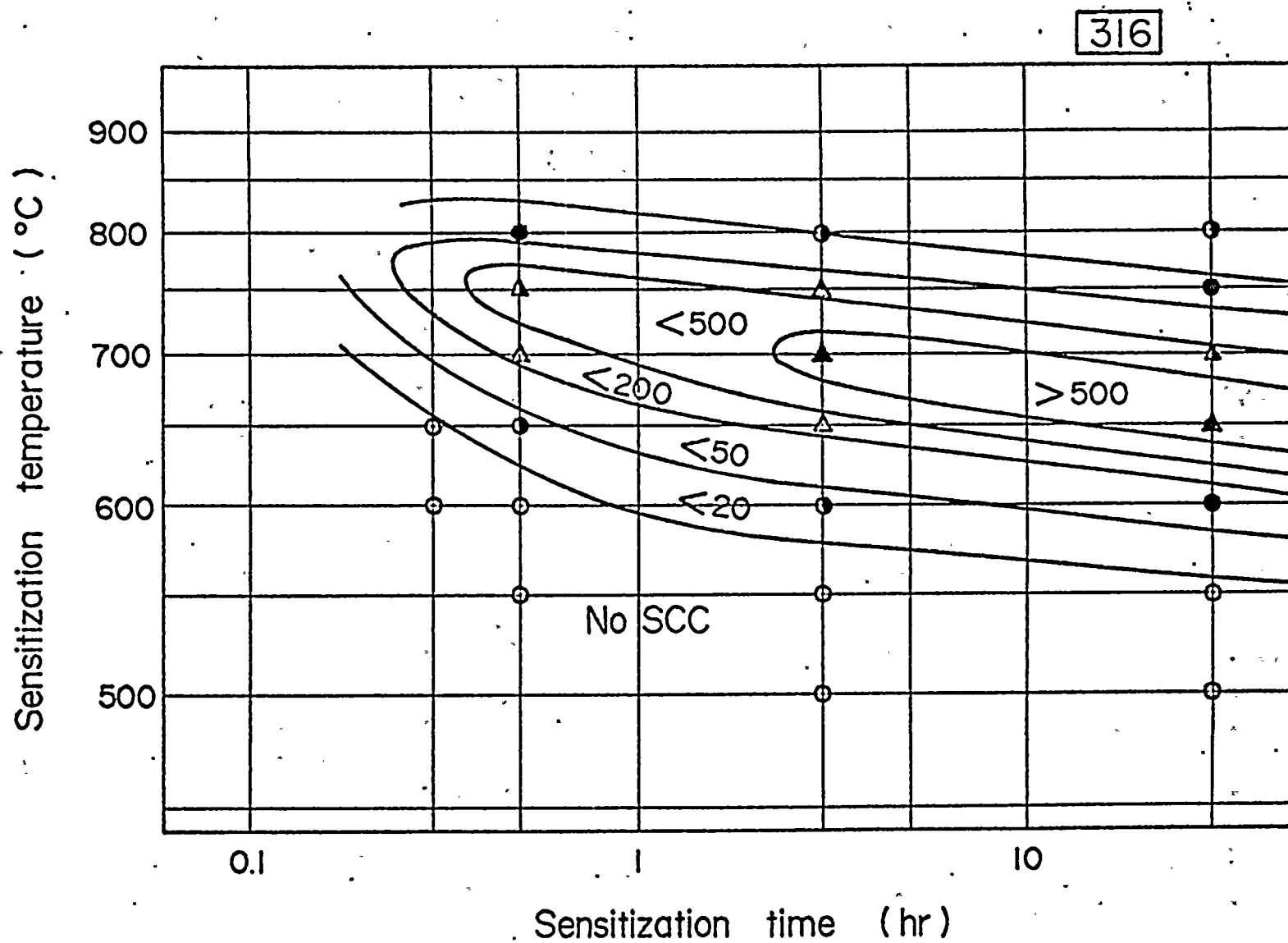


Figure 6. T-T-SCC Diagram for 316 Stainless Steel in Oxygenated Water at 250°C
(CBB Test, 20 ppm DO, 310 hr)⁽¹⁸⁾

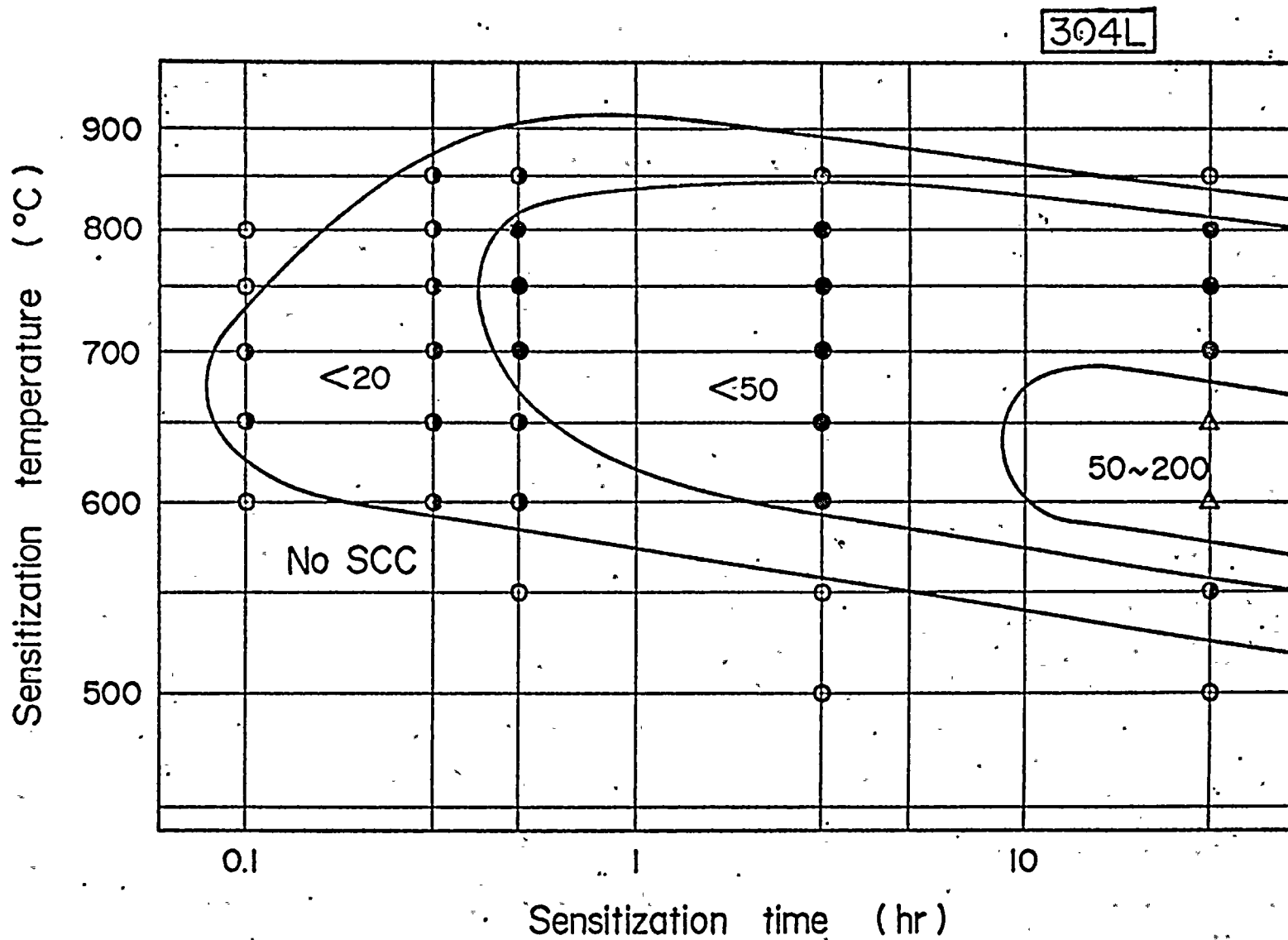


Figure 7. T-T-SCC Diagram for 304L Stainless Steel in Oxygenated Water, at 250°C
(CBB Test, 20 ppm DO, 310 hr)(18)

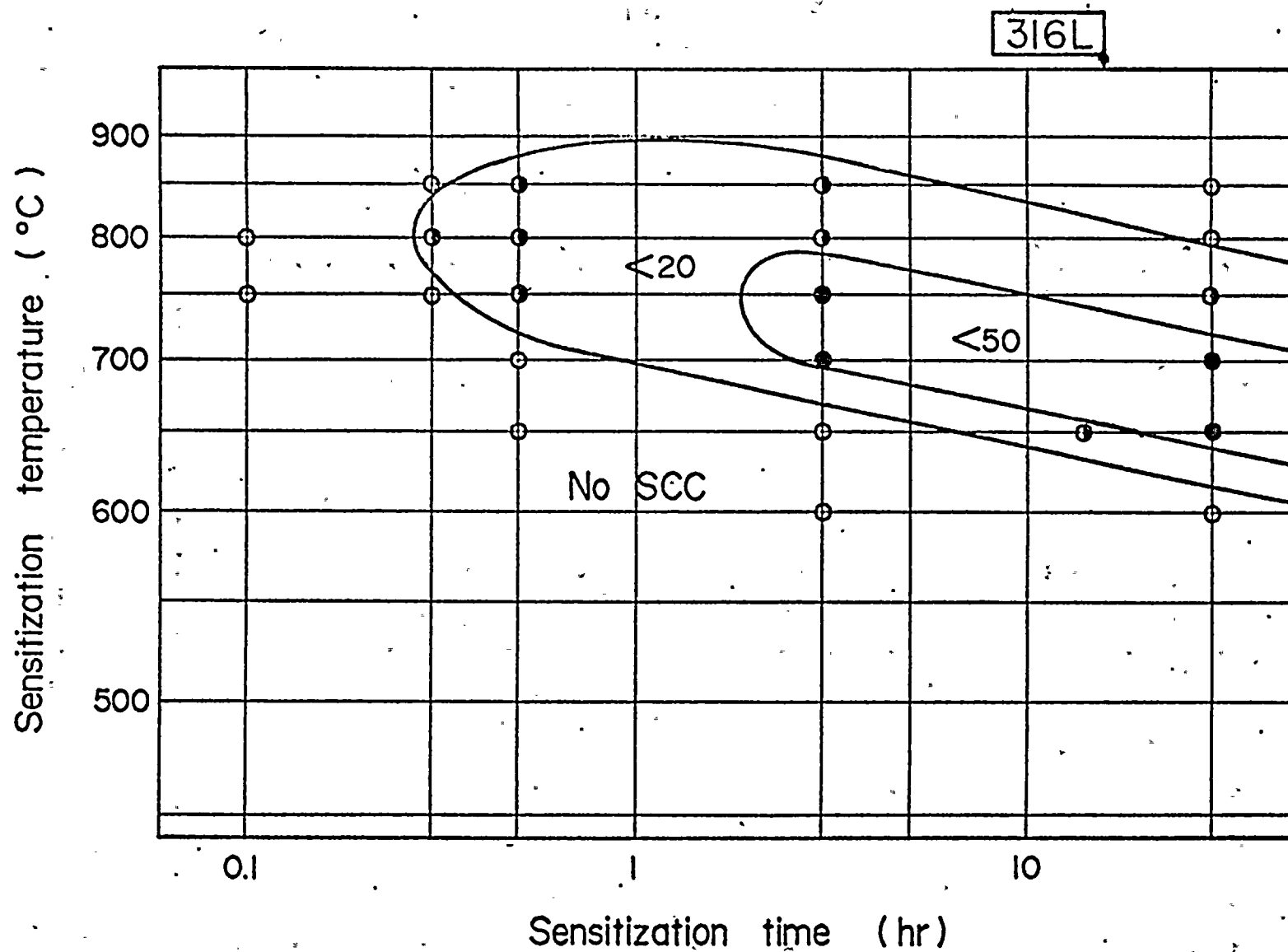


Figure 8. T-T-SCC Diagram for 316L Stainless Steel in Oxygenated Water at 250°C
(CBB Test, 20 ppm DO, 310 hr)(18)

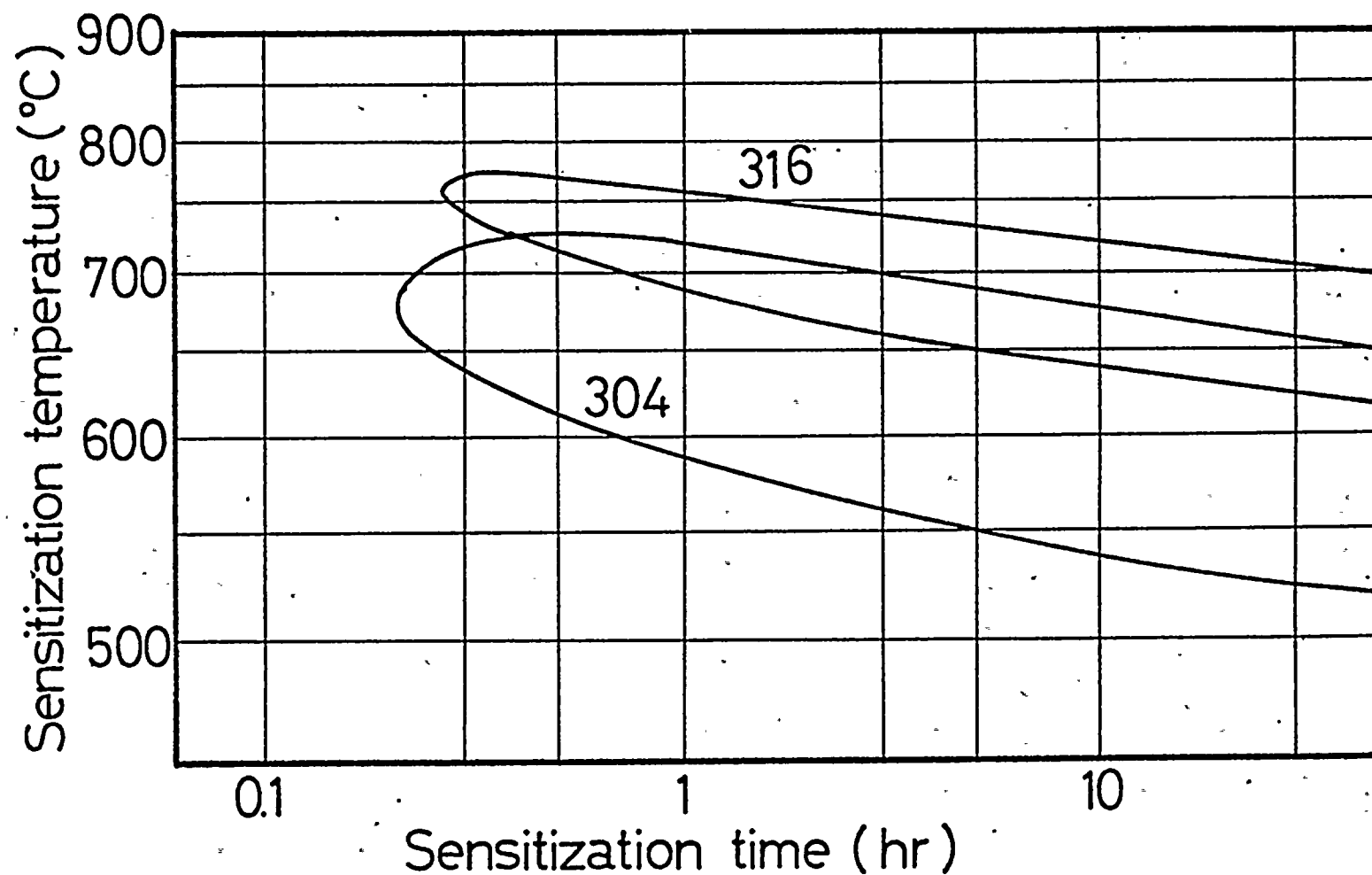


Figure 9. TTS Curves for 304 and 316 Stainless Steels Evaluated by 310 hr CCB Test in 250°C Water with 20 ppm DO (Crack Depth >200 μm) (18)

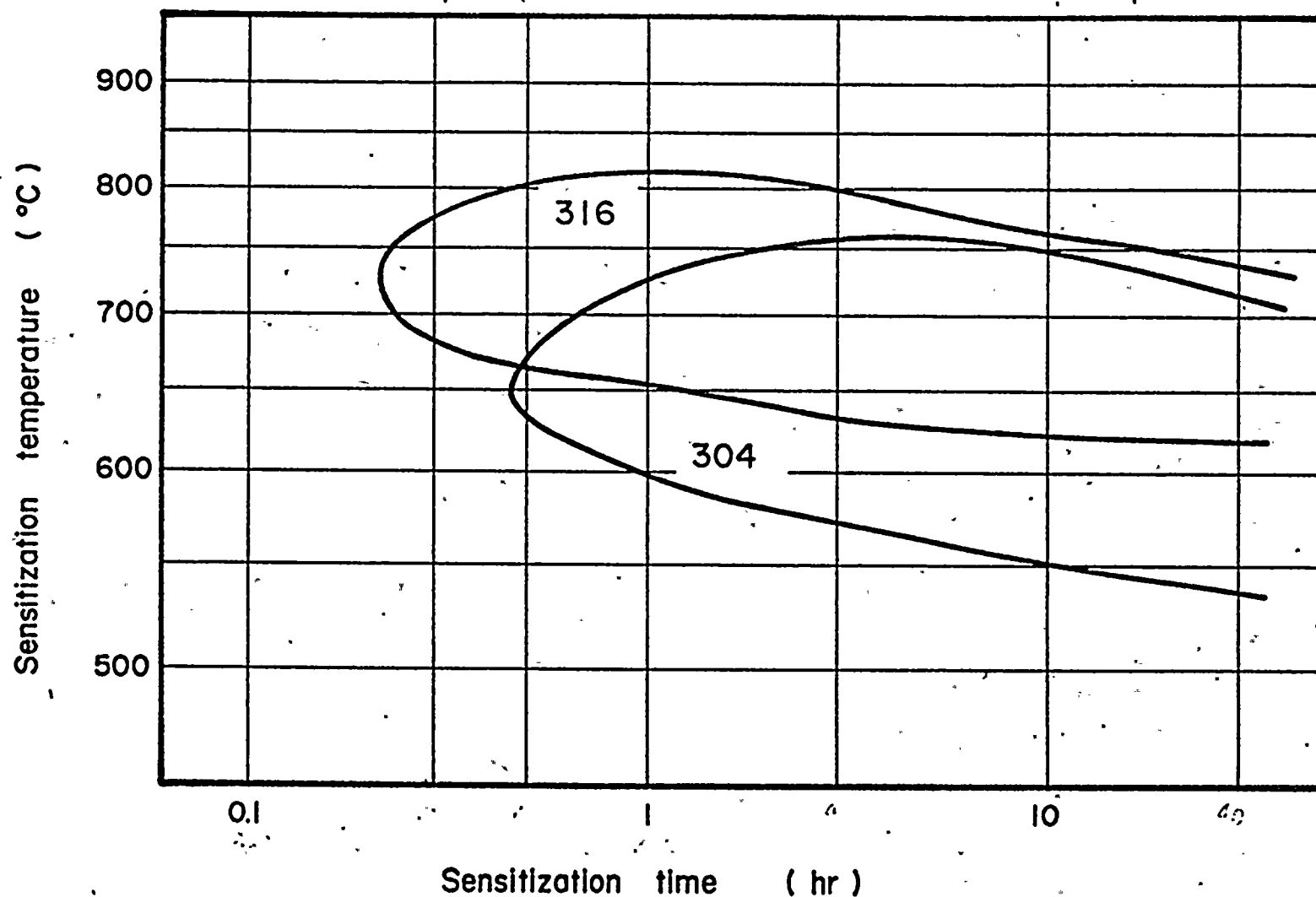


Figure 10. TTS Curves for 304 and 316 Stainless Steels Evaluated by 100 hr A262E Test (Penetration $\geq 500 \mu\text{m}$)⁽¹⁸⁾

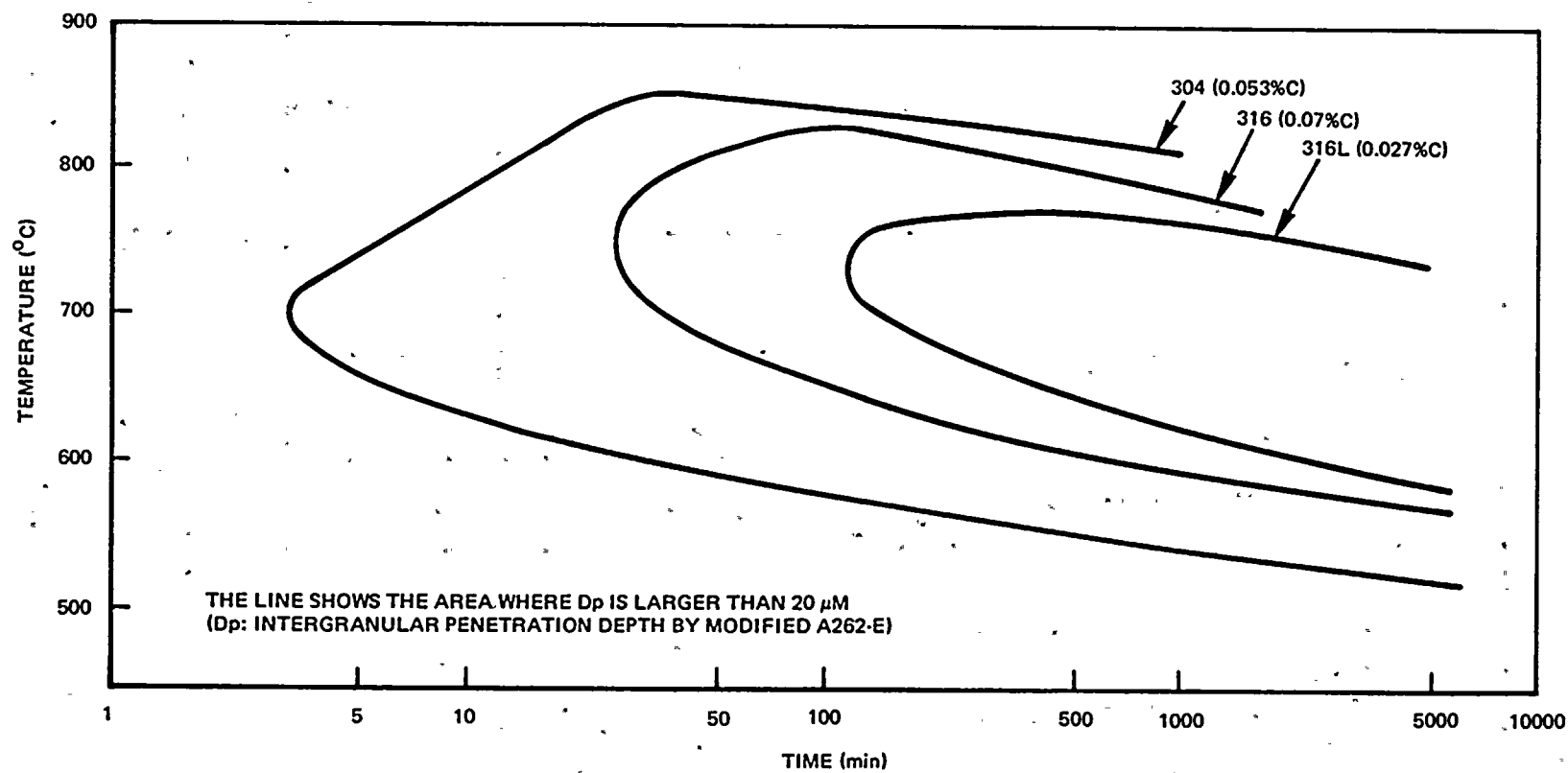


Figure 11. Time - Temperature - Sensitization Diagrams of Type 316 and 316L.
Compared with Type 304(18)

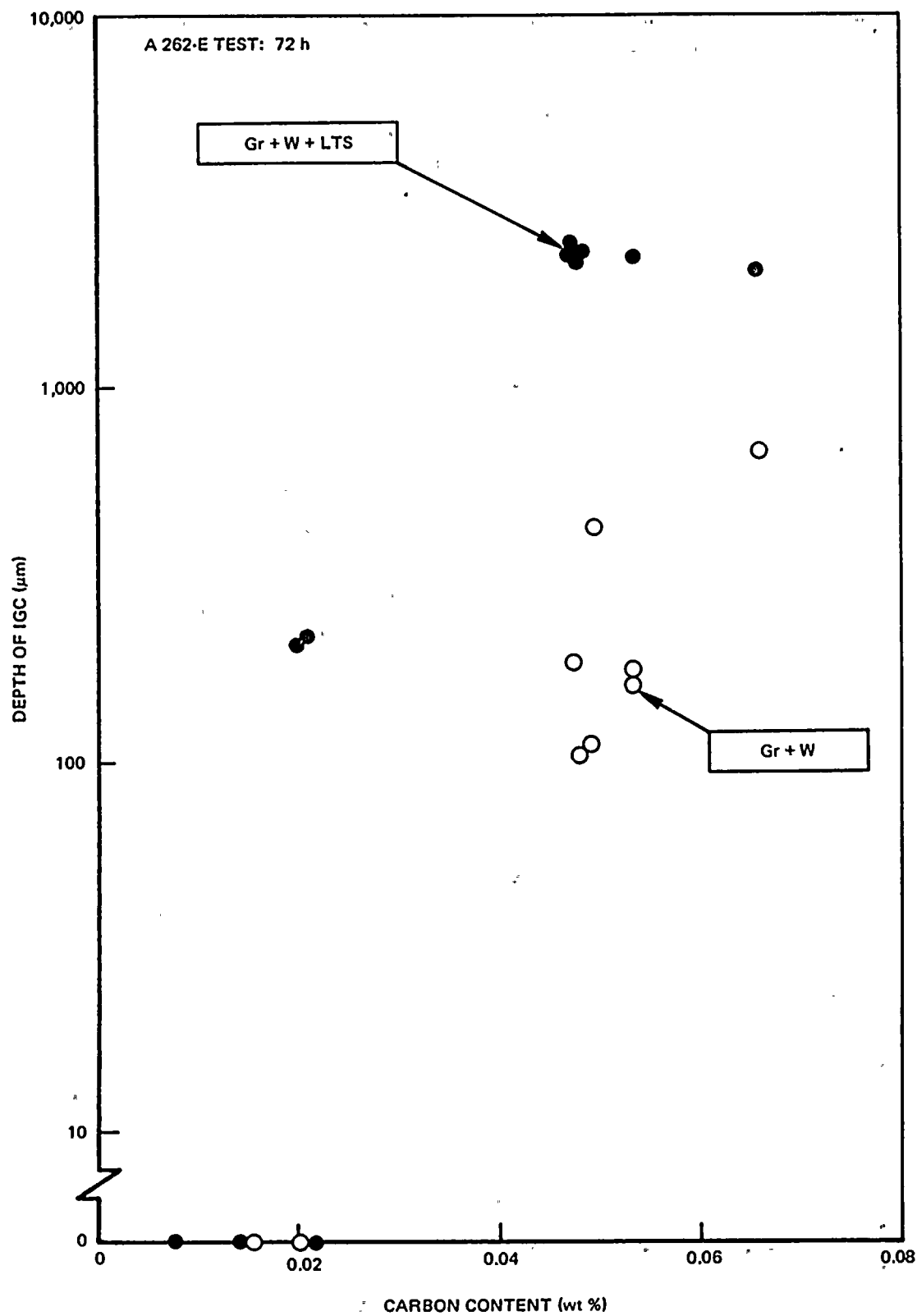


Figure 12. Effect of Carbon Content on Weld Sensitization of Type 304 Family⁽²¹⁾

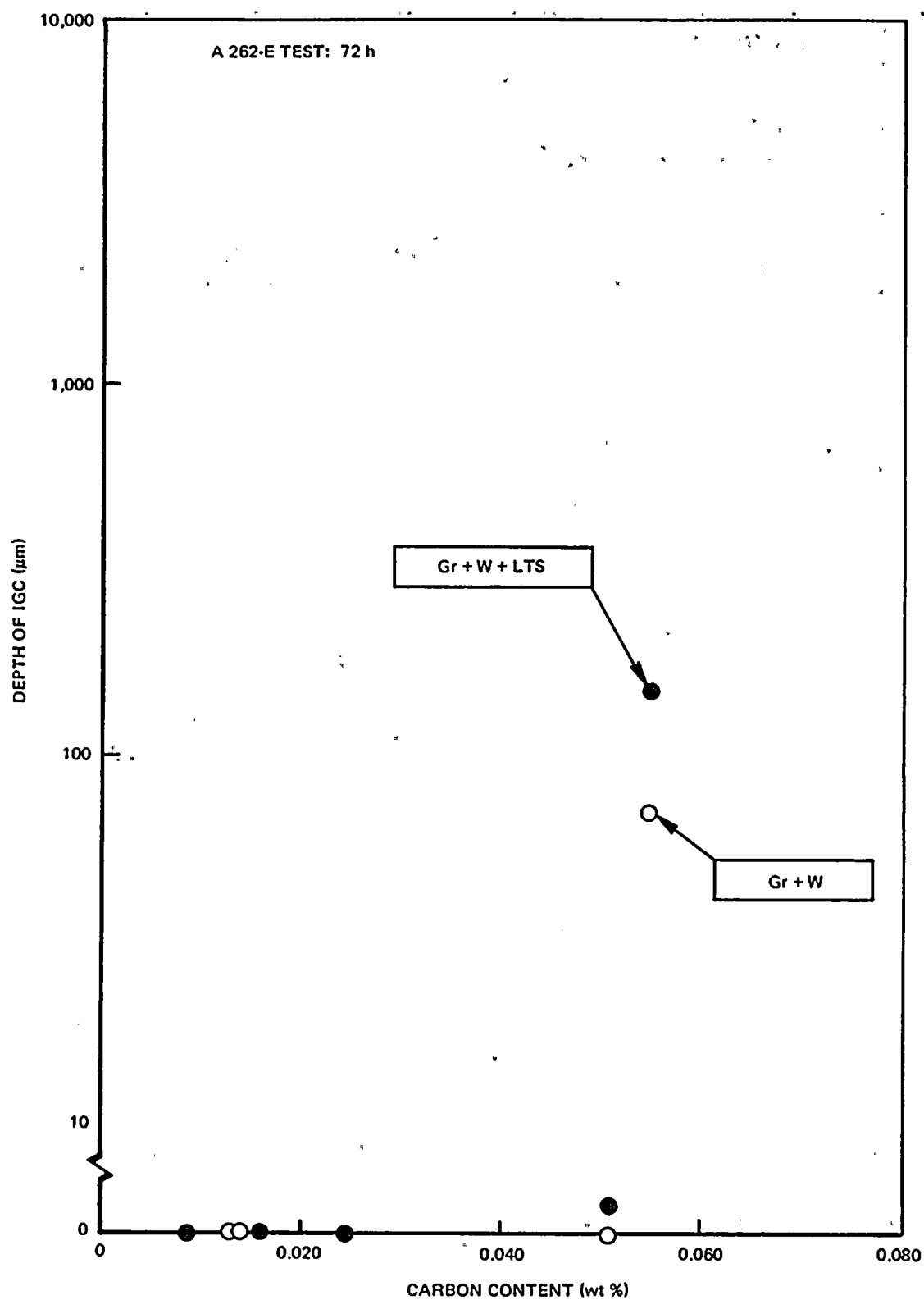


Figure 13. Effect of Carbon Content on Weld Sensitization of Type 316 Family⁽²¹⁾.

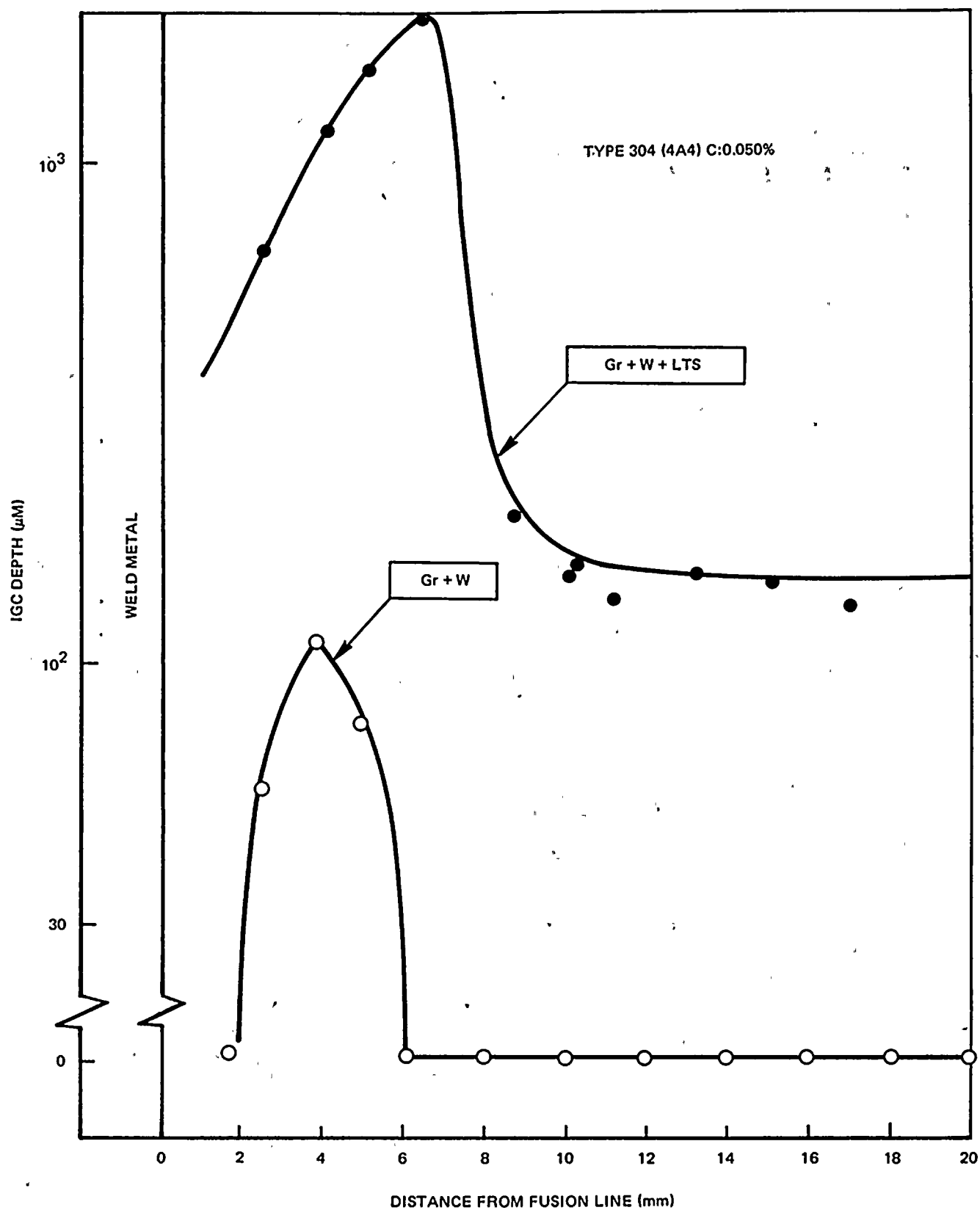


Figure 14. Sensitization Profile in Weld HAZ of Type 304
Given by A-262-E Test(21)

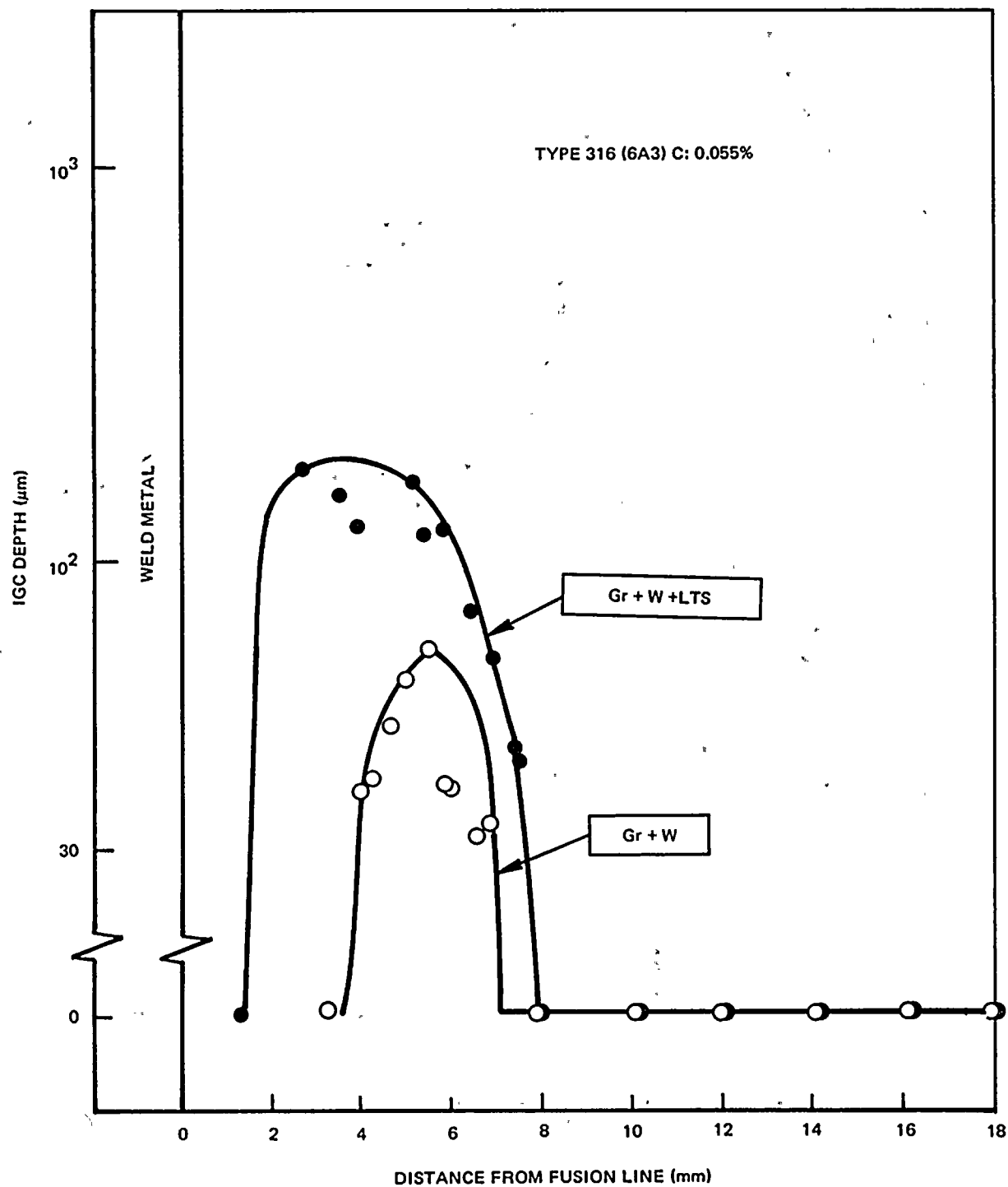


Figure 15. Sensitization Profile in Weld HAZ of Type 316
Given by A-262-E Test(21)

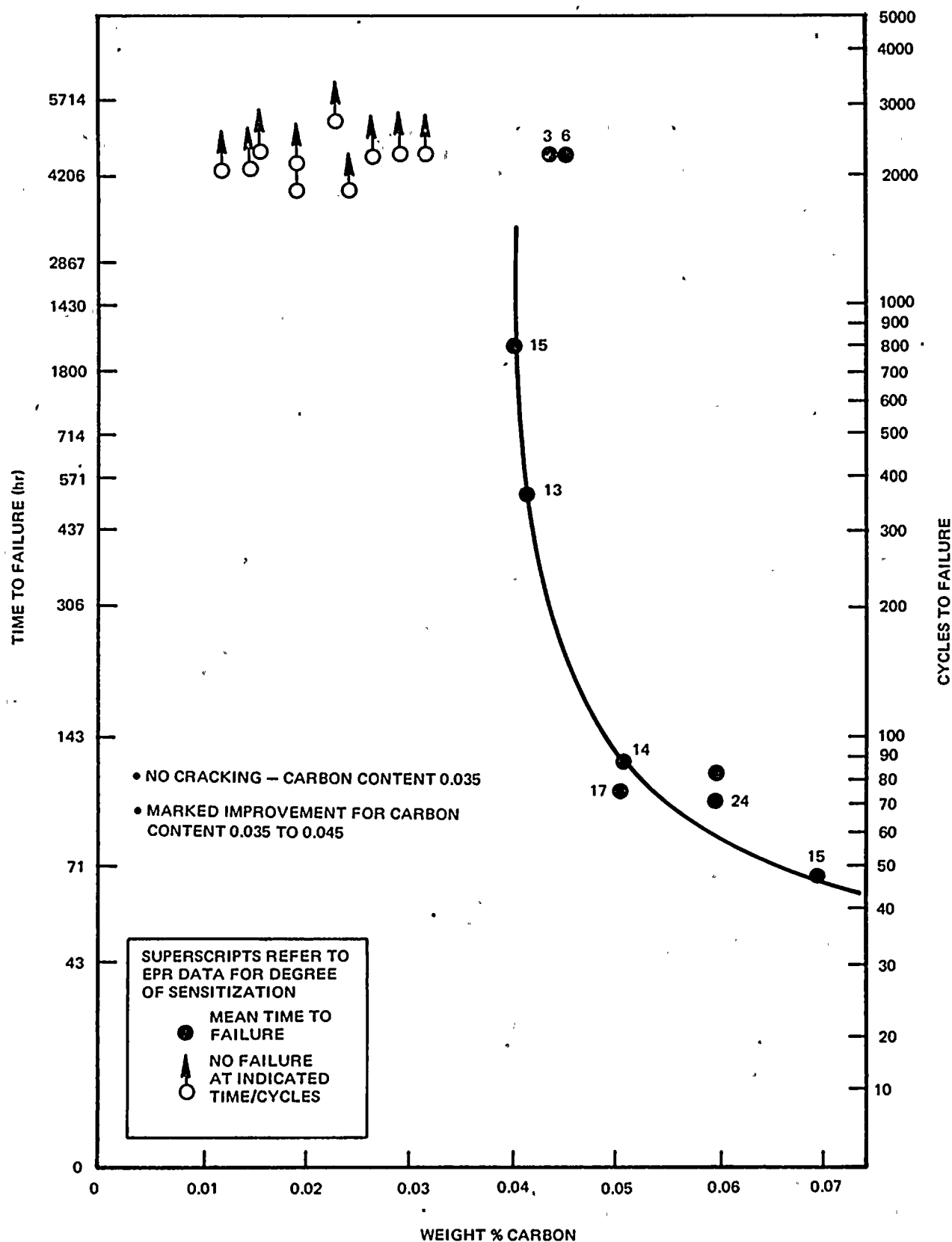


Figure 16. Failure Time vs. Pipe Material Carbon Level(24)

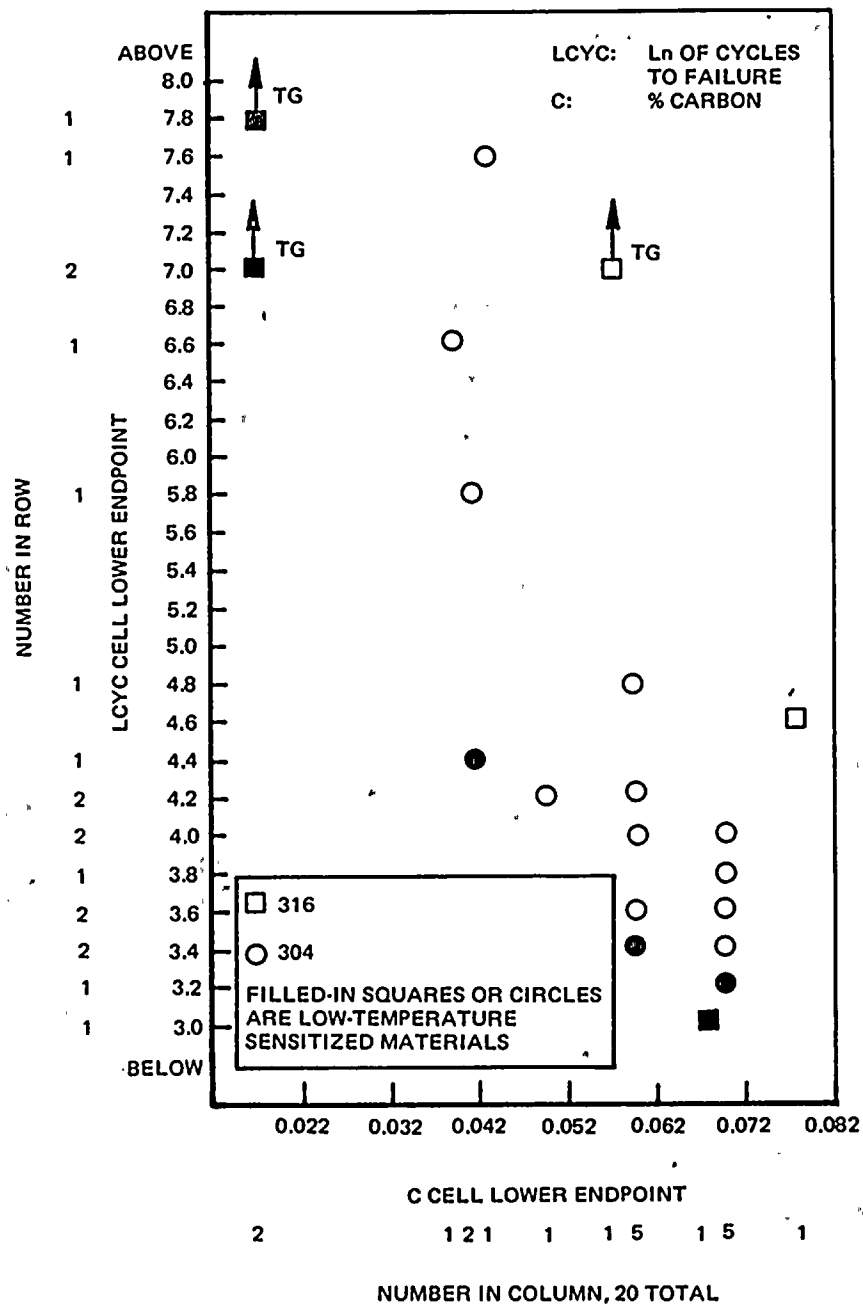


Figure 17. Log of Cycles to Failure as a Function of Carbon Content for Type 304 and 316 Stainless Steel(24)

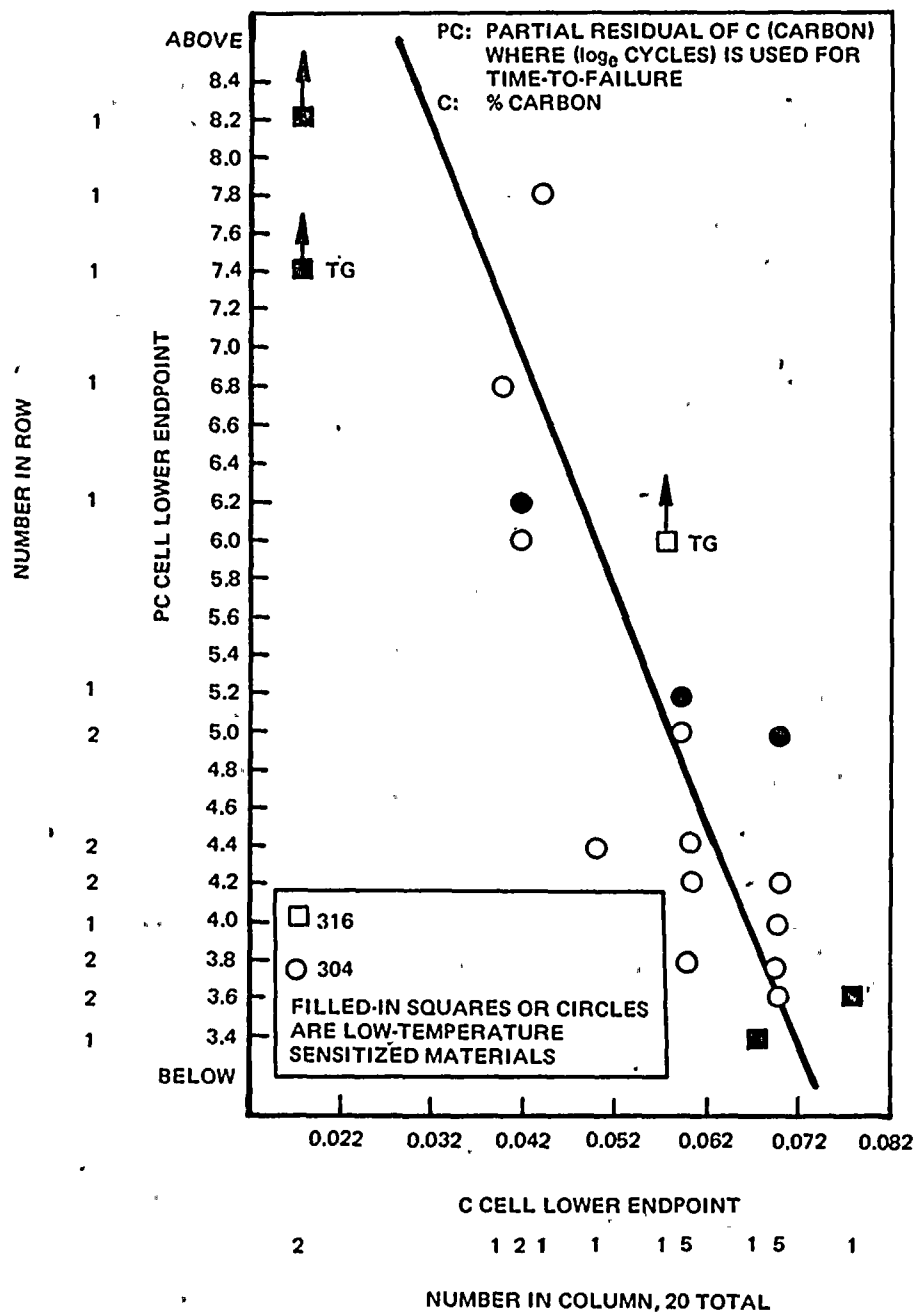
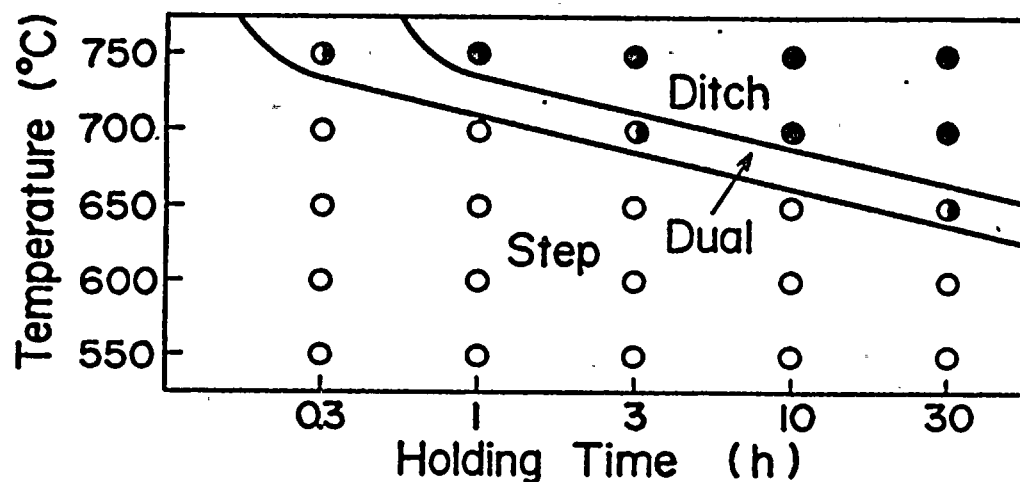
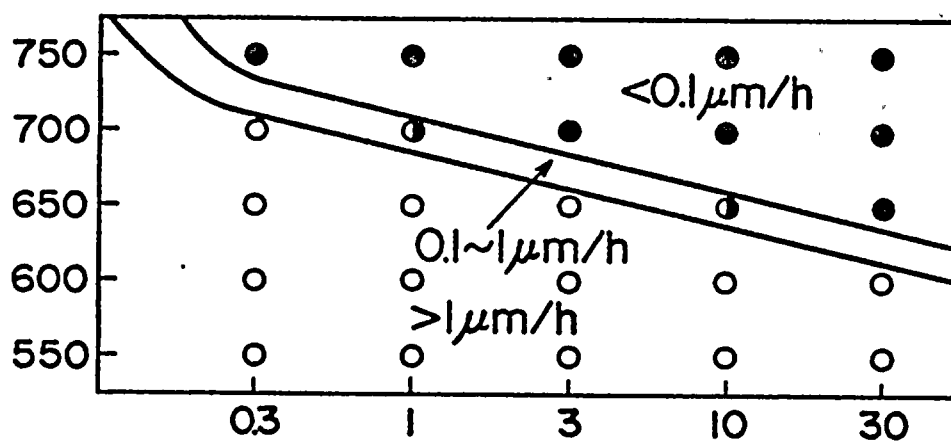


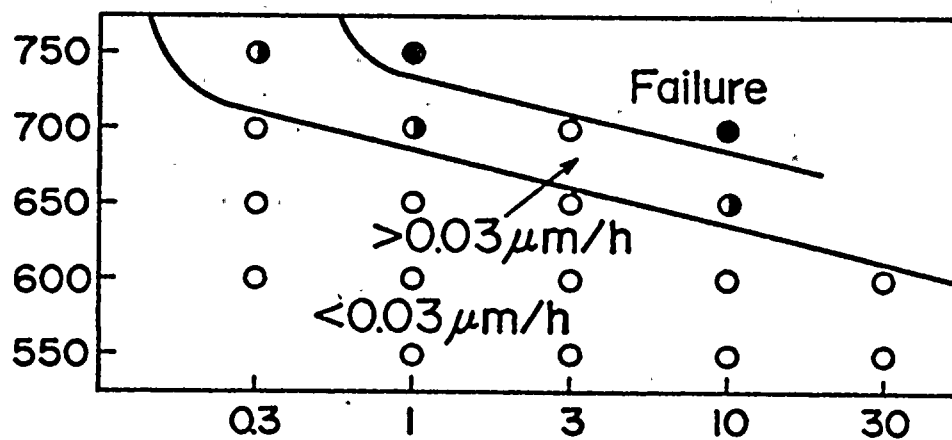
Figure 18. Partial Residual of Carbon Time to Failures
Type 304 and 316 Stainless Steel(24)



a. by ASTM A-262 A

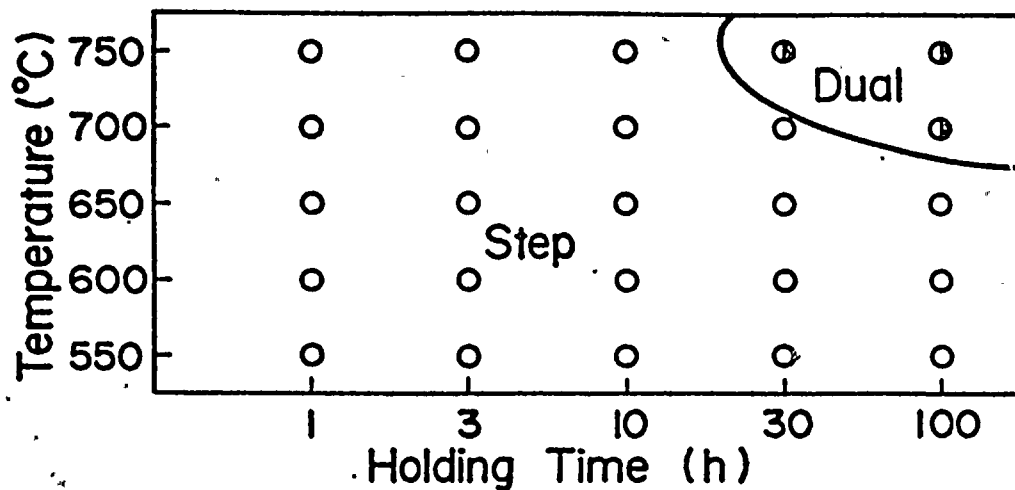


b. by modified ASTM A-262 E

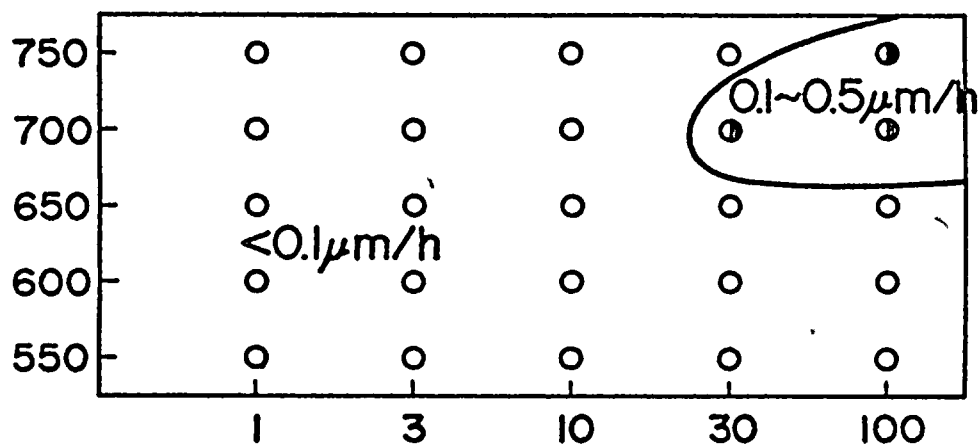


c. by CERT

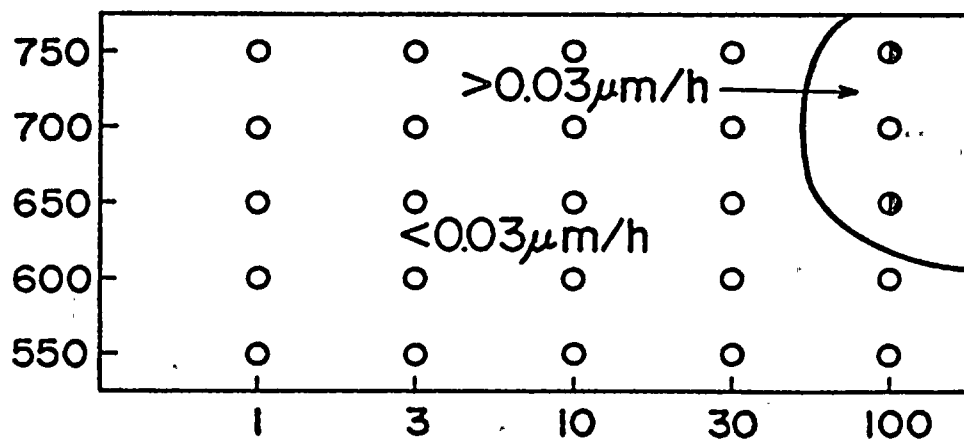
Figure 19. T-T-S and T-T-SCC Curves of Type 316 Stainless Steel⁽²⁶⁾



a. by ASTM A-262 A



b. by modified ASTM A-262 E



c. by CERT

Figure 20. T-T-S and T-T-SCC Curves of Type 316(LC) Stainless Steel⁽²⁶⁾

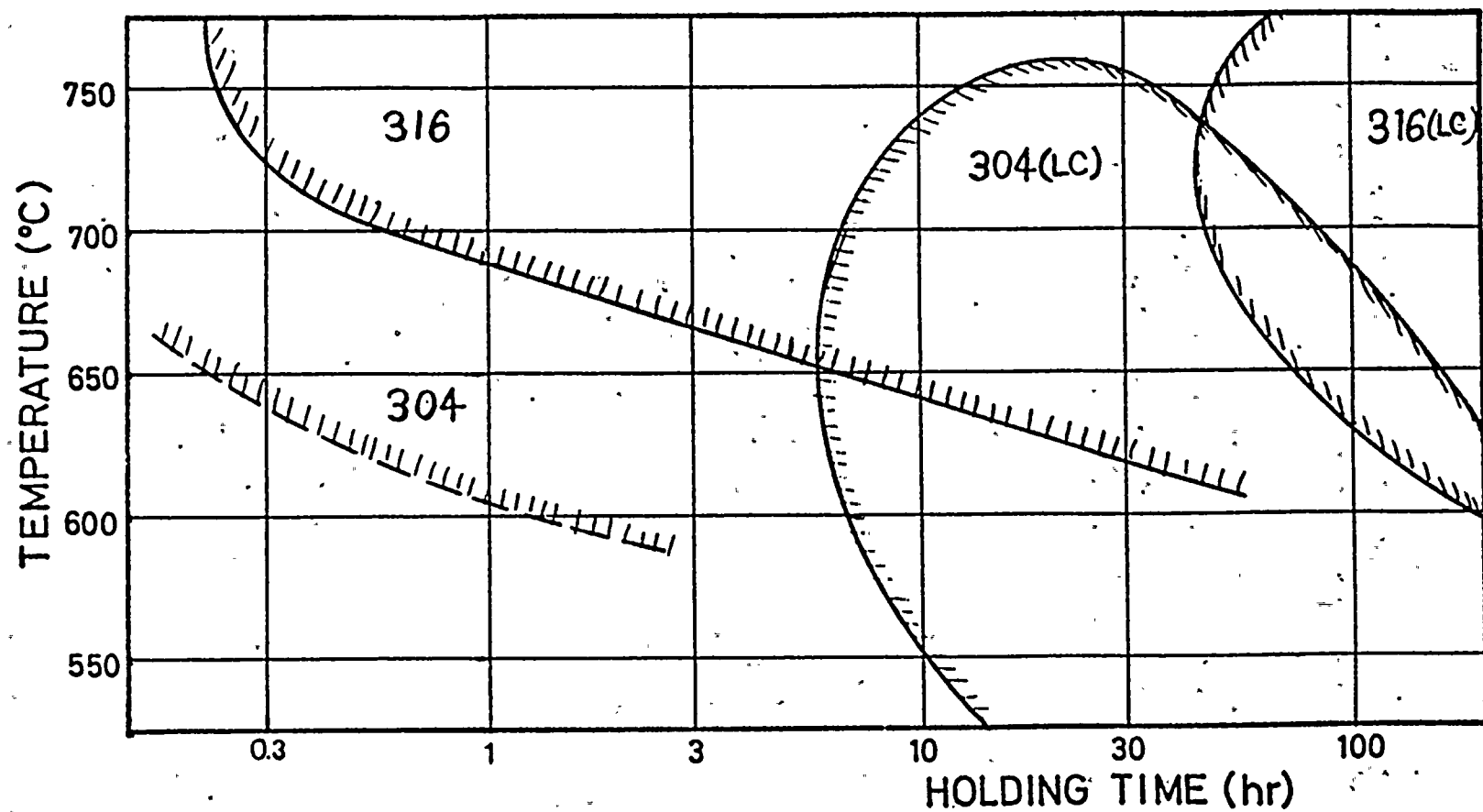


Figure 21. Comparison of SCC Susceptible Regions for Austenitic Stainless Steels Detected by CERT in 290°C Pure Water with 8 ppm Oxygen(26)

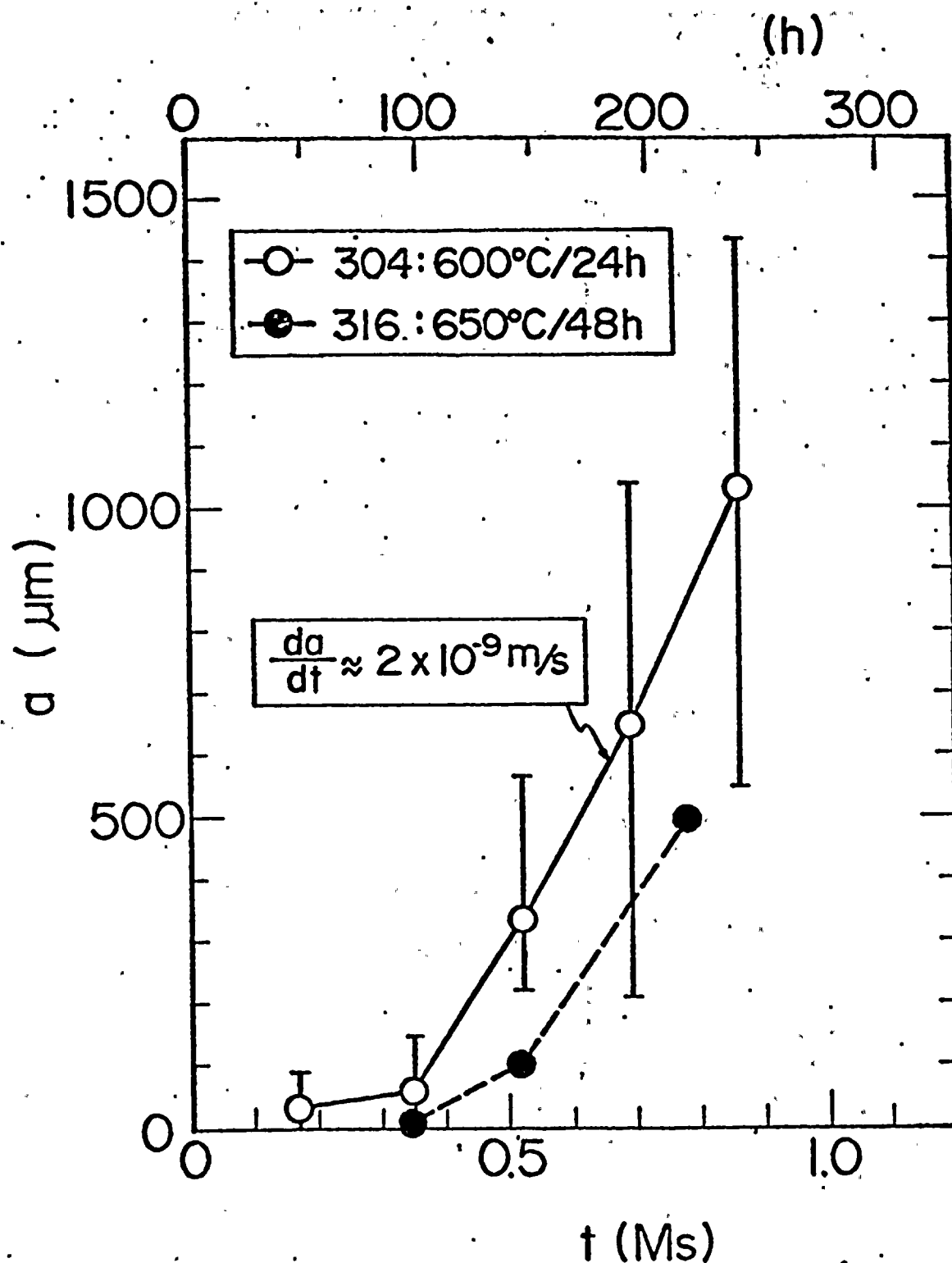


Figure 22. CBB Results for Crack Propagation of Type 316 and 304 Stainless Steel in 20 ppm O_2 at 250°C (27)

SECTION XI
EVALUATION OF RECIRCULATION SYSTEM
REPAIRS/REPLACEMENT

SAFE END REPLACEMENT

The existing furnaces sensitized intake and discharge safe ends on all recirculation system loops have been replaced with new safe ends of the same dimensions but of Type 316 nuclear grade (low carbon) stainless steel. This material has been solution heat treated following all shop fabrication. Removal of the existing safe ends and installation of the new safe ends at the reactor nozzles was accomplished through Newport News Industrial (NNI) Procedure Plan Numbers CWI 1399-K, 1-11 through 1-15 and CWI 1399-K, 2-11 through 2-15.

In the process of removing the existing safe end on loop number 15 at the intake (suction) nozzle, a partial cut was inadvertently made into the reactor nozzle parent material. This cut was approximately 7/16 inches deep and was deemed to be weld repairable using NNI Procedure Plan No. 1399-K W 3 and welding Procedure CWI 1399K-9.

Shop and field weld material is Type 308 stainless steel with .02 percent maximum carbon content and a ferrite number of eight minimum.

All field welds have been 100 percent radiographically examined. Shop welds were 100 percent ultrasonically examined.

PIPE REPLACEMENT

The existing recirculation system piping, between safe ends and pump nozzles, both suction and discharge sides of all five loops have been replaced with new pipe of the same dimensions but of Type 316 nuclear grade stainless steel. All of this new material has been solution heat treated following shop fabrication. Shop and field weld material is Type 308 stainless steel with .02 percent maximum carbon content and a ferrite number of 8 minimum.

Shop welds and field weld edge prepared areas have been 100 percent ultrasonically examined. Field welds have been 100 percent radiographically examined. All RT and UT has been performed and evaluated in accordance with Section XI of the ASME Boiler and Pressure Vessel Code in effect at time of contract.

EXPECTED PERFORMANCE OF REPAIRS/REPLACEMENTS

Type 316 nuclear grade stainless steel is highly resistant to Intergranular Stress Corrosion Cracking (IGSCC) in the welded condition. Laboratory tests have confirmed that the higher carbon grade Type 316 is less susceptible than Type 304 and that low carbon (less than .02 percent), Nuclear grade 316 is the least susceptible overall. The Type 308, low carbon weld material used is also highly resistant to IGSCC. These materials coupled with excellent quality control and examination of the base material as well as shop and field welds, coupled with a relatively low operating stress environment will ensure a long, acceptable performance level for the new recirculation piping and safe ends.

APPENDIX A

MILL TEST CERTIFICATES AND TEST REPORTS
FOR NIAGARA MOHAWK CO.

NINE MILE POINT-1
PRIMARY RECIRCULATION PIPING

	<u>Page</u>
A. Mill and Check Test Certifications for Straight Spool Pieces (Allegheny Ludlum, Jessop Steel, and National Annealing Box Co.)	A-1
B. Test Certifications for Elbows and Tee Sections. . . .	A-18
C. Chemical Analyses of Weld Filler and Consumable Insert Rings	A-21



ALLEGHENY LUDLUM STEEL CORPORATION

Special Steels for Industry

PLEASE REMIT TO: P.O. BOX 2159, PITTSBURGH 30, PENNSYLVANIA

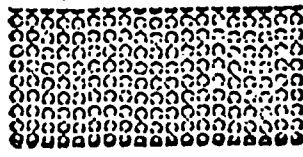
7846-44
7844

ADDRESS NO. MESSAGE NO. INQUIRY NO. SHIPMENT NO. DATE BEFORE

GOVT CONTRACT NO. VENDOR CODE NO. CUSTOMER ORDER NUMBER AND DATE DATE MILL ORDER NUMBER 52-503-033

000000 10030613615 0747123100156 COATESVILLE, PA.

NATIONAL ANNEALING BOX CO.
WASHINGTON, PA.



CERTIFICATE OF TEST

ALLEGHENY STAINLESS STEEL TYPE 316 CARBON .04 TO .08 HOT ROLLED
ANNEALED AND PICKLED TO ASME SA-280

W-52126

3/17/65

KALP AND GORDON

ITEM	WEIGHT SHIPPED	QUANTITY SHIPPED	SIZE	WIDTH - DIA - OD	GA - THICK - WALL	LOGAN ATT	SLAB
5	6740	1	78-3/4	X1-1/8	1.016	240039	2
	6740	1					3
6	5244	1	78-3/4	X1-1/8	1.016		5
8	5109	1	78-3/4	X1-1/8	1.016		1
15	7781	1	84-3/4	X1-3/8	1.094	29151	1
	7781	1				340041	3

6 PLATES

NATIONAL ANNEALING BOX CO.

RECEIVED
MAR 24 1965

WASHINGTON, PA.

W-52126

40001#-1

APPROVED
MAR 29 1965
BY [Signature]

ALLEGHENY LUDLUM STEEL CORPORATION

CERTIFICATE OF TEST

CHEMICAL ANALYSIS

HEAT NO	C	MN	P	S	SI	CR	NI	
340039	0.55	1.60	0.03	0.10	55	17.40	12.00	242
29151	0.49	1.63	0.16	0.17	60	17.20	13.52	239
340041	0.49	1.62	0.24	0.10	55	17.10	13.50	246

PHYSICAL PROPERTIES

HEAT	TEST	YIELD STRENGTH	TENSILE STRENGTH	ELONG	ROCKWELL	COLD BEND	R.P.
340039	2	45700	86800	55	162	OK	70.1
"	3	42800	87600	50	153	OK	69.6
"	5	43000	89500	60	156	OK	69.0
"	1	44900	86700	60	156	OK	67.9
29151-14-11-13		43400	83700	61	157	OK	71.4
340041-34-12-14		38900	82100	65	143	OK	69.5

CORE LOSS TEST

10000 B - 15000 B

60 CYCLES

ITEM	LOT NUMBER	WATTS PER POUND	ITEM	LOT NUMBER	WATTS PER POUND

CORE LOSS IN ACCORDANCE WITH THE AMERICAN SOCIETY FOR TESTING MATERIALS SPECIFICATION A.34

RESULT IS ABOVE CERTIFIED
ALLEGHENY LUDLUM STEEL CORPORATION

R. J. Fulton



ALLEGHENY LUDLUM STEEL CORPORATION

Special Steels for Industry

PLEASE REMIT TO: P.O. BOX 2159, PITTSBURGH 30, PENNSYLVANIA

7-17-60-14
7844

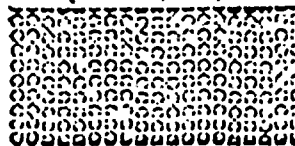
ADDRESS	MESSAGE	INDUSTRY	SHIPMENT	DATE
NO.	NO.	NO.	NO.	NO.

CONTRACT NO.	VENDOR CODE NO.	CUSTOMER ORDER NUMBER	DATE	MILL ORDER NUMBER
000000	10030693615	30009	07-17-60	52-503-053

PRIORITY	BEST	IND	CUST CODE	PRODUCT	DATE	BLANK	DATE	ACCEPTING MILL
000000	000000	000000	000000	000000	000000	000000	000000	000000

COATESVILLE, PA.

NATIONAL ANNEALING BOX CO.
WASHINGTON, PA.



CERTIFICATE OF TEST

ALLEGHENY STAINLESS STEEL TYPE 316 CARBON .04 TO .08 HOT ROLLED
ANNEALED AND PICKLED TO ASME SA-400.

W-52222 NUMBER & DATE							3/26/65	
KULP AND GORDON							33957	
ITEM	WEIGHT SHIPPED	QUANTITY SHIPPED	W	H	WIDTH - BA - OD (INCHES)	GA - THICK - WALL (INCHES)	LENGTH OF PART (FEET)	REMARKS
5	6743 6743 13486	1 1 1	78	3/4	X 1-1/8	X 285	340039	IC
8	5109	1	78	3/4	X 1-1/8	X 216	"	P
12	6277 6277 12554	1 1 1	84	3/4	X 1-3/32	X 229	"	P
16	2814 33957	1 1	78	3/4	X 1-1/8	X 119	23147	IC
6 PLATES								
APPROVED NATIONAL ANNEALING BOX CO.								
APR 19 1965								
BY <i>[Signature]</i>								
APR 12 1965								
WASHINGTON, PA.								
W-52222 33957-1								

CERTIFIED CHEMICAL ANALYSIS AND PHYSICAL PROPERTIES
ON REVERSE SIDE

ALLEGHENY LUDLUM STEEL CORPORATION

CERTIFICATE OF TEST

14.

CHEMICAL ANALYSIS

ITEM	HEAT NO	C	MN	P	S	SI	CP	NI						
									316					
									710					
340039	055	1.60	0.23	0.10	.55	1210	1300	242						
29147	040	1.59	0.14	0.15	.56	1236	1375	296						

PHYSICAL PROPERTIES

ITEM	HEAT	TEST	YIELD STRENGTH	TENSILE STRENGTH	ELONG %	ROCKWELL BHN	COLD BEND	REMARKS
340039	1		44900	86700	60	156	OK	67.9
"	4		44200	86300	60	156	OK	68.0
"	6-15-17		42900	88400	55	156	OK	69.4
"	7-15-23		46000	88400	52	170	OK	69.7
29147	4		46200	85800	55	159	OK	69.0

CORE LOSS TEST

10000 B - 15000 B

60 CYCLES

ITEM	LOT NUMBER	WATTS PER POUND	ITEM	LOT NUMBER	WATTS PER POUND

CORE LOSS IN ACCORDANCE WITH THE AMERICAN SOCIETY FOR TESTING MATERIALS SPECIFICATION A-34

RESULT AS ABOVE CERTIFIED
ALLEGHENY LUDLUM STEEL CORPORATION

E. J. Fulton



ALLEGHENY LUDLUM STEEL CORPORATION

Special Steels for Industry

PLEASE REMIT TO: P.O. BOX 2159, PITTSBURGH 30, PENNSYLVANIA

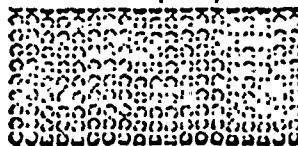
2 copy 15
7844

ADDRESS TO: MESSAGE DATE	INDUSTRY NUMBER DATE	SHIPPING METHOD	NOT BEFORE
GOVT CONTRACT NO	VENDOR CODE NO	CUSTOMER ORDER NUMBER	DATE
38000	38000	38000	38000
000000	1003064365	0747123101	55
COATESVILLE, PA.			

MILL ORDER

32-503-073

NATIONAL ANNEALING BOX CO
WASHINGTON, PENN.



CERTIFICATE OF TEST

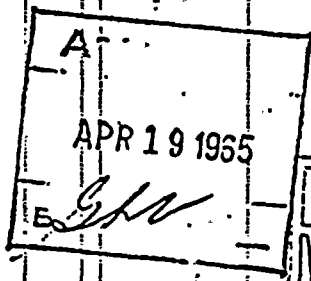
STEEL TYPE 316 CARBON .04 TO .03 HOT ROLLED
ANNEALED AND PICKLED TO ASME SA-240

INVOICE NUMBER & DATE	DATE SHIPPED
W-52431	4-15-65

VIA	CAR INITIAL & NO	GROSS	TARE	NET
HIGHWAY EXPRESS				

ITEM	WEIGHT SHIPPED	QUANTITY SHIPPED	WIDTH - DIA - OD	GA - THICK - WALL	INVT#SLAB
1	6528	1	85X1-5/16X20	340041	4
2	6570	1	85X1-5/16X19S	"	4
7	5039	1	72-3/4X1-1/4X213	340039	2
8	7536	1	84-3/4X1-3/32X275	29151	2
10	6572	1	84-3/4X1-3/32X250	46580	1

5 FLTS



NATIONAL ANNEALING BOX CO.

APR 15 1965

WASHINGTON, PA.

CERTIFIED CHEMICAL ANALYSIS AND PHYSICAL PROPERTIES
ON REVERSE SIDE

ALLEGHENY LUDLUM STEEL CORPORATION

CERTIFICATE OF TEST

16

CHEMICAL ANALYSIS

ITEM	HEAT NO	C	MN	P	S	SI	CU	NI	AS
340041	049	1.62	0.04	0.10	.55	1710	1350	246	
340039	055	1.60	0.023	0.10	.55	1740	1300	242	
29151	049	1.63	0.16	0.17	.68	1720	1352	239	
46580	042	1.66	0.19	0.13	.45	1762	1340	277	

PHYSICAL PROPERTIES

ITEM	HEAT	TEST	YIELD STRENGTH	TENSILE STRENGTH	ELONG %	ROCKWELL	COOL	TEMP
340041	4		41000	78100	70	143	OK	710
340039	2		45700	86800	55	163	OK	70.1
29151	2		39200	81900	64	143	OK	69.3
46580	1		42700	82900	56	149	OK	68.8

CORROSION TEST

10000 B - 15000 B

60 CYCLES

ITEM	LOT NUMBER	WATTS PER POUND	ITEM	LOT NUMBER	WATTS PER POUND

CORROSION IN ACCORDANCE WITH THE AMERICAN SOCIETY FOR TESTING MATERIALS SPECIFICATION A-34

RESULT AS ABOVE CERTIFIED
ALLEGHENY LUDLUM STEEL CORPORATION

R. J. Fulton

ALLEGHENY LUDLUM STEEL CORPORATION

Special Steels for Industry

PLEASE REMIT TO: P.O. BOX 2159, PITTSBURGH, PENNSYLVANIA 15230

7844

17

										MILL ORDER	
ADDRESS TO NO.	MESSAGE NO. DATE	INQUIRY NUMBER DATE	SHEET COUNT BLOD.	NOT BEFORE						DATE	NUMBER
GOVT CONTRACT NO.			VENDOR CODE NO.		CUSTOMER ORDER NUMBER	AND	DATE	IS NO. FILED		DATE	NUMBER
			38600								82-070-050
PRIORITY	DIST.	IND.	CUST. CODE	PRODUCT	MATL.	RSM.	DST.	ACCEPTING MLL			
FOR			00016	UTS	181	TO		UNCLASSIFIED - F1			

1. NATIONAL ASSOCIATION OF SEC. CO.
2. MEMBERSHIP, PA.

CERTIFICATE OF TEST

[illegible]

INVOICE NUMBER & DATE		DATE SHIPPED	
11-20-57		11-20-57	
CAR INITIAL & NO.	GROSS	TARE	NET

ITEM	WEIGHT SHIPPED	QUANTITY SHIPPED	S H	WIDTH - DIA. - O.D. INCHES	G.A. - THICK - WALL INCHES	LENGTH OR PART NO.
3	2910	1		340041	1 3/32	- 1.044 276
4	1928	1		29151	1 3/32	- 1.044 250
5	2828	1		29151-2	1 3/32	- 1.044 252
6	340039	1		340039	1 1/64	- 1.016 223
8 PAGES						
<div style="float: right; border: 1px solid black; padding: 5px; transform: rotate(-15deg);"> APPROVED JUL 28 1955 </div>						
ORIGINAL ANNEALING BOX CO.						
JUL 28 1955			NET WEIGHT OF INVOICE			

NATIONAL ANNEALING BOX CO.

JUL 28 1955

WASHINGTON, PA.

**CERTIFIED CHEMICAL ANALYSIS AND PHYSICAL PROPERTIES
ON REVERSE SIDE**

ANAL

ALLEGHENY LUDLUM STEEL CORPORATION

CERTIFICATE OF TEST

CHEMICAL ANALYSIS

ITEM	HEAT NO.	C	MN	P	S	SI	CR	NI	Mo					
5	10041	0.41	1.0	0.01	0.10	0.55	17.0	13.5	2.4					
	29151	0.49	1.63	0.16	0.17	0.68	17.0	13.5	2.39					
34	0039	0.55	1.60	0.23	0.0	0.55	17.4	13.0	2.4					

PHYSICAL PROPERTIES

ITEM	HEAT	TEST	YIELD STRENGTH	TENSILE STRENGTH	ELONG %	ROCKWELL	COLD BEND		
5	10041		41500	81500	62	177	OK	15.0	
	29151	-3-10-16	43400	83700	61	159	OK	21.4	
	29151	-2-	39200	81900	64	143	OK	69.3	
34	0039	-7	460.00	88400	52	170	OK	65.7	

CORE LOSS TEST

10000 B - 15000 B

60 CYCLES

ITEM	LOT NUMBER	WATTS PER POUND	ITEM	LOT NUMBER	WATTS PER POUND

CORE LOSS IN ACCORDANCE WITH THE AMERICAN SOCIETY FOR TESTING MATERIALS SPECIFICATION A-34

RESULT AS ABOVE CERTIFIED
ALLEGHENY LUDLUM STEEL CORPORATION

CHIEF INSPECTOR

JESSOP STEEL COMPANY

WASHINGTON, PENNSYLVANIA

CERTIFICATE OF TEST

DATE Apr. 30, 1965

National Annealing Box Co.

SHIPPED TO

7844

Washington, Penna.

GENTLEMEN: WE SHIPPED TO YOU VIA SHIPPING MEMO # MATERIAL LISTED BELOW:

Grade 316

HEAT NO. YOUR ORDER NO. OUR ORDER NO. SIZE QUANTITY

38936 MT-682410

HEAT NO.	YIELD STRENGTH LBS PER SQ IN	TENSILE STRENGTH LBS. PER SQ. IN.	ELONG. % IN 2"	RED. OF AREA	HARDNESS	BEND	CORROSION	GRAIN SIZE
T/R 12965		340041	SL Y					
1 - 7844		29151	SL 1					
1 - 7835		340041	SL 3					
3 - 7840		46580	SL 1					
		29151	SL 2					
		340041	SL 6					

PARENT METAL BLOCK				CHEMICAL COMPOSITION (WHEN CALLED FOR BY SPECIFICATION)								SO Number			
PC. #	C.	MN.	P.	S.	SI.	NI.	CR.	V.	MO.	W.	CU.	CO.	FE.		
4 - 5	.049	1.64	.023	.011	.48	13.60	17.20		2.42		7835				
11 - 13	.047	1.60	.013	.018	.62	13.65	17.40		2.26		7844				
12 - 14	.049	1.62	.023	.014	.48	13.60	17.10		2.42		"				
3 - 26	.048	1.54	.021	.014	.43	13.75	17.80		2.46		"				
1	.048	1.60	.014	.016	.62	13.70	17.30		2.30		"				
5-17-22	.047	1.52	.020	.011	.57	13.10	17.40		2.20		"				
25 thru 29	.041	1.54	.012	.021	.52	13.70	17.40		2.75		7810				
5 - 11	.051	1.56	.018	.011	.58	13.10	17.40		2.30		"				
10 - 16	.037	1.56	.018	.012	.56	13.10	17.40		2.32		"				

DECLARED TO UNDER OATH BEFORE ME

JESSOP STEEL COMPANY

THIS 30th DAY OF Apr. 1965

BY [Signature] METALLURGIST

APPROVED

MAY 7 1965

BY [Signature]

JESSOP STEEL COMPANY

WASHINGTON, PENNSYLVANIA

CERTIFICATE OF TEST

DATE Nov 19, 1965

National Annealing Box Co
Washington
Pennsylvania

SHIPPED
TO

GENTLEMEN: WE SHIPPED TO YOU VIA

SHIPPING MEMO #

MATERIAL LISTED BELOW:

Type ASME SA-240 (316)

HEAT NO.	YOUR ORDER NO.	OUR ORDER NO.	SIZE	QUANTITY
	33936	MT-682410		

HEAT NO.	YIELD STRENGTH LBS PER SQ IN	TENSILE STRENGTH LBS. PER SQ. IN.	ELONG. % IN 2"	RED. OF AREA	HARDNESS	BEND	CORROSION	GRAIN SIZE
T/R 111965								
41015-1		- Ferrite -	5%					
29151-2		"	6-1/2%					
340041-4		"	5%					
340041-4		"	5%					

Weld Metal Drillings

CHEMICAL COMPOSITION (WHEN CALLED FOR BY SPECIFICATION)

HEAT NO.	C.	MN.	P.	S.	SI.	NI.	CR.	V.	MO.	Heat No.	So Number
1-2-3	.056	1.60			.53	12.40	18.60		2.78	41015-1	7839-4
#1	.041	1.64			.64	12.35	18.80		2.78	29151-2	7844-4
1-2-3	.036	1.47			.45	12.70	18.70		2.70	340041-4	7835-4
4-5	.045	1.60			.54	12.65	18.80		2.75	340041-4	7835-4

DECLARED TO UNDER OATH BEFORE ME

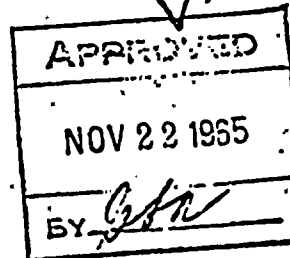
THIS 19th DAY OF Nov 1965

FORM 50 Rev. 8-60

BY

JESSOP STEEL COMPANY

METALLOGIST



JESSOP STEEL COMPANY

WASHINGTON, PENNSYLVANIA

CERTIFICATE OF TEST

DATE Dec 17, 1965

National Annealing Box Co
Washington
Pennsylvania 15301

SHIPPED
TO

ENTLEMEN: WE SHIPPED TO YOU VIA SHIPPING MEMO # MATERIAL LISTED BELOW:

Type 316

HEAT NO. YOUR ORDER NO. OUR ORDER NO. SIZE QUANTITY

40595

MT-745540

HEAT NO. YIELD STRENGTH TENSILE STRENGTH ELONG. RED. OF HARDNESS BEND CORROSION GRAIN

121765

CHEMICAL COMPOSITION (WHEN CALLED FOR BY SPECIFICATION)

So Number Ferrite

HEAT NO.	C.	MN.	P.	S.	SI.	NI.	CR.	V.	MO.	W.	Grain Size	Ferrite
Q #3-26												
6580-1	.057	1.56			.53	12.20	18.40		2.64		7844-4	4-1/2
C #7-19-24	.048	1.64			.60	12.15	18.80		2.78		"	6-1/2
40039	.044	1.52			.64	12.25	18.80		2.62		"	6-1/2

DECLARED TO UNDER OATH BEFORE ME

HIS 17th DAY OF Dec 1965

OPM 50 Rev. 8-60

JESSOP STEEL COMPANY

BY:

DEC 27 1965

E. *[Signature]*

NATIONAL ANNEALING BOX CO.

WASHINGTON, PENNA.

MATERIAL RECORD

INSPECTION

PURCHASER GRINNELL CORPORATION

TYPE EQUIPMENT ASTM-A358-CL-1 FGE SPR RIAR103

ASME-SA-240 T-316 SS (25.661 ID X 1.232 MIN WALL)

YEAR BUILT 1965 (SO 7835)

DWG. NO. 116-2137-4 REV O

SERIAL NO. 7835-1 ETC.

PUR. ORDER NO. W-7359 NIAGARA-MOHAWK

INSPECTED BY G. WARE, ROBINSON (G) TITTINGTON (GE)

LABORATORY TEST REPORT

KDJ #322
10/10/69

PART NO.	MANUFACTURER OF MATERIAL	HEAT NO. / SERIAL NO.	SLAB OR TEST NO.	CHEMICAL										PHYSICAL FOR R.R.A.				
				C.	MN.	P.	S.	SIL.	CR	NI	MO.			ULT. STRENGTH.	EL. LIMIT	ELONG%	BEND	FRACTURE
7835	ALUM 38809	340041	4	.049	1.62	.024	.010	.55	17.10	13.50	2.46			78100	41000	70	OK	71.0
1	PM-CHECK	Tessop 38936	TR-42965	.049	1.64	.023	.011	.48	17.20	13.60	2.42			79250	(52 TESTS)	-	OK	(11-16-65)
7-9/4	WM-CHECK	Tessop 38936	TR-111965	.036	1.47	-	-	.45	18.70	12.70	2.70	*						
7835	ALUM 38809	340041	4	.049	1.62	.024	.010	.55	17.10	13.50	2.46			78100	41000	70	OK	71.0
2	PM-CHECK	Tessop 38936	TR-42965	.049	1.64	.023	.011	.48	17.20	13.60	2.42			79250	(52 TESTS)	-	OK	(11-16-65)
7-9/4	WM-CHECK	Tessop 38936	TR-111965	.036	1.47	-	-	.45	18.70	12.70	2.70							
7835	ALUM 38809	340041	4	.049	1.62	.024	.010	.55	17.10	13.50	2.46			78100	41000	70	OK	71.0
3	PM-CHECK	Tessop 38936	TR-42965	.049	1.64	.023	.011	.48	17.20	13.60	2.42			79250	(52 TESTS)	-	OK	(11-16-65)
7-9/4	WM-CHECK	Tessop 38936	TR-111965	.036	1.47	-	-	.45	18.70	12.70	2.70							
7835	ALUM 38809	340041	4	.049	1.62	.024	.010	.55	17.10	13.50	2.46			78100	41000	70	OK	71.0
4	PM-CHECK	Tessop 38936	TR-42950	.049	1.64	.023	.011	.48	17.20	13.60	2.42			77140	(52 TESTS)	-	OK	(11-16-65)
7-9/4	WM-CHECK	Tessop 38936	TR-111965	.045	1.60	-	-	.54	18.80	12.65	2.75							
7835	ALUM 38809	340041	4	.049	1.62	.024	.010	.50	17.10	13.50	2.46			78100	41000	70	OK	71.0
5	PM-CHECK	Tessop 38936	TR-42956	.049	1.64	.023	.011	.48	17.20	13.60	2.42			77140	(52 TESTS)	-	OK	(11-16-65)
7-9/4	WM-CHECK	Tessop 38936	TR-111965	.046	1.60	-	-	.54	18.80	12.65	2.75							

ALL LENGTHS DYE PENETRANT EXAMINED ON COMPLETED WELDS INSIDE AND OUTSIDE

ALL LENGTHS HAVE BEEN PASSIVATED INSIDE AND OUTSIDE

SANDBLASTED INSIDE AND OUTSIDE - NO HYDROSTATIC TEST - 100% X-RAYED

FERRITE - 5% ALL ITEMS

ABOVE DATA CERTIFIED CORRECT BY MANUFACTURER

National Annealing Box Co. BY *Gordon R. Kane*

DATE 11-22-

NATIONAL ANNALING BOX CO.

WASHINGTON, PENNA.

SHEET 1

MATERIAL RECORD
INSPECTIONPURCHASER: ILL. CO. DIVISIONTYPE EQUIPMENT: 352 (L-1 & GE. SPEC. 21A2103, REV #0)YEAR BUILT: 1965 (078411-4)DWG. NO. 116-2140-4 REV IIISERIAL NO. 7844-1 ETC.PUR. ORDER NO. W-7267 7359 NIAGARA-MOHAWKINSPECTED BY: G. WASE, ROBINSON, BARRY

LABORATORY TEST REPORT

KDJ

PART NO.	MANUFACTURER OF MATERIAL	HEAT TREATMENT SERIAL NO.	SEAB OR TEST NO.	CHEMICAL								PHYSICAL				
				C.	MN.	P.	S.	SIL.	CR	NI	MO	ULT. STRENGTH	EL. LIMIT	ELONG %	BEND °	RACTURE
7844	ALLUD 38809	29151	2	.049	1.63	.016	.017	.68	17.20	13.52	2.39	81900	39200	64	OK	69.3
-1-	PM CHECK	JESSOP 38936	42965	.048	1.60	.014	.016	.62	17.30	13.70	2.30	81580	(52 TESTS)	OK	12-28-65	
22-9"	WM	"	38936	.041	1.64	-	-	.64	18.80	12.35	2.78					
7844	ALLUD 38809	46580	1	.042	1.66	.018	.013	.45	17.62	13.40	2.77	82900	42700	56	OK	68.8
-2-	PM CHECK	JESSOP 38936	42965	.048	1.54	.021	.014	.43	17.80	13.75	2.46	79690	(52 TESTS)	OK	12-28-65	
22-9"	WM	"	40595	.057	1.56	-	-	.58	18.40	12.20	2.64					
7844	ALLUD 38809	46580	1	.042	1.66	.018	.013	.45	17.62	13.40	2.77	82900	42700	56	OK	68.8
-3-	PM CHECK	JESSOP 38936	42965	.048	1.54	.021	.014	.43	17.80	13.75	2.46	79690	(52 TESTS)	OK	12-28-65	
19-3"	WM	"	40595	.057	1.56	-	-	.58	18.40	12.20	2.64					
7844	ALLUD 38809	29151	2	.049	1.63	.016	.017	.68	17.20	13.52	2.39	81900	39200	64	OK	69.3
-4-	PM CHECK	JESSOP 38936	42965	.047	1.60	.013	.018	.62	17.40	13.65	2.26	81580	(52 TESTS)	OK	12-28-65	
15-9"	WM	"	38936	.041	1.64	-	-	.64	18.80	12.35	2.78					
7844	ALLUD 38809	34003	6	.055	1.60	.023	.010	.55	17.40	13.00	2.42	88400	42700	55	OK	69.4
-5-	PM CHECK	JESSOP 32934	42965	.047	1.52	.020	.011	.57	17.40	13.10	2.20	80580	(52 TESTS)	OK	12-28-65	
13-5 1/2"	WM	"	40595	.048	1.64	-	-	.60	18.80	12.15	2.78					
7844	ALLUD 38809	34003	7	.055	1.60	.023	.010	.55	17.40	13.00	2.42	88400	46000	52	OK	65.7
-6-	PM CHECK	JESSOP 38936	42965	.047	1.52	.020	.011	.57	17.40	13.10	2.20	80580	(52 TESTS)	OK	12-28-65	
13-5 1/2"	WM	"	40595	.048	1.64	-	-	.60	18.80	12.15	2.78					

ABOVE DATA CERTIFIED CORRECT BY MANUFACTURER

BY Gordon L. Hume

DATE 12-28-65

NATIONAL ANNALING BOX CO.

WASHINGTON, PENNA.

SHEET 2

MATERIAL RECORD INSPECTION

PURCHASER _____

TYPE EQUIPMENT _____

YEAR BUILT _____

DWG. NO. _____

SERIAL NO. _____

PUR. ORDER NO. W-7359 NIAGARA-MOHAWK

INSPECTED BY _____

LABORATORY TEST REPORT

PART NO.	MANUFACTURER OF MATERIAL	HEAT ANALYSIS SERIAL NO.	SAB OR. TEST NO.	CHEMICAL								PHYSICAL PER T. R. & A.				
				C.	MN.	P.	S.	SIL.	CR	NI	MO	ULT. STROTH.	EL. LIMIT	ELONG %	BEND °	FRACTURE
7844	ALLUD 38809	340039	7	.055	1.60	.023	.010	.55	17.40	13.00	2.42	88400	46000	52	17K	65.7
-7-	PM CHECK	JESSOP 38936	429.65	.047	1.52	.020	.011	.57	17.40	13.10	2.20	80580	(52 TESTS)	OK		12-22-65
13-5/8	WM	"	40595	.048	1.64	-	-	.60	18.80	12.15	2.78					
7844	ALLUD 38809	340039	6	.055	1.60	.023	.010	.55	17.40	13.00	2.42	88400	42900	55	OK	69.4
-8-	PM CHECK	JESSOP 38936	429.65	.047	1.52	.020	.011	.57	17.40	13.10	2.20	80580	(52 TESTS)	OK		12-22-65
13-5/8	WM	"	40595	.048	1.64	-	-	.60	18.80	12.15	2.78					
7844	ALLUD 38809	340041	3	.049	1.62	.014	.010	.55	17.10	13.50	2.46	82100	38900	65	OK	69.5
-9-	PM CHECK	JESSOP 38936	429.65	.049	1.62	.023	.014	.48	17.10	13.60	2.42	81870	(52 TESTS)	OK		12-25-65
12-9	WM	"	40595	.044	1.52	-	-	.64	18.80	12.25	2.62					
7844	ALLUD 38809	29151	3	.049	1.63	.016	.017	.68	17.20	13.52	2.39	83700	43400	61	OK	71.4
-10-	PM CHECK	JESSOP 38936	429.65	.047	1.60	.013	.018	.62	17.40	13.65	2.26	81580	(52 TESTS)	OK		12-22-65
12-1"	WM	"	38936	.041	1.64	-	-	.64	18.80	12.35	2.78					
7844	ALLUD 38809	29151	1	.049	1.63	.016	.017	.68	17.20	13.52	2.39	83700	43400	61	OK	71.4
-11-	PM CHECK	JESSOP 38936	429.65	.047	1.60	.013	.018	.62	17.40	13.65	2.26	81580	(52 TESTS)	OK		12-22-65
11-8 1/2	WM	"	38936	.041	1.64	-	-	.64	18.80	12.35	2.78					
7844	ALLUD 38809	340041	3	.049	1.62	.024	.010	.55	17.10	13.50	2.46	82100	38900	65	OK	69.5
-12-	PM CHECK	JESSOP 38936	429.65	.049	1.62	.023	.014	.48	17.10	13.60	2.42	81870	(52 TESTS)	OK		12-22-65
11-8 1/2	WM	"	40595	.044	1.52	-	-	.64	18.80	12.25	2.62					

ABOVE DATA CERTIFIED CORRECT BY MANUFACTURER National Annaling Box Co. BY Richard L. Hare Sr. DATE 12-28-65

NATIONAL ANV TAILING BOX CO.

WASHINGTON, PENNA.

SHEET 3

MATERIAL RECORD INSPECTION

PURCHASER _____

TYPE EQUIPMENT _____

YEAR BUILT _____

DWG. NO. _____

SERIAL NO. _____

PUR. ORDER NO. W-7359 NIAGARA-MOHAWK

INSPECTED BY _____

LABORATORY TEST REPORT

PART NO.	MANUFACTURER OF MATERIAL	MATERIAL SERIAL NO.	SIAB OR TEST NO.	CHEMICAL								PHYSICAL F&R TAP & A				
				C.	MN.	P.	S.	SIL.	CR	NI	MO	ULT. STRGHT.	EL. LIMIT	ELONG 8"	BEND °	FRACTURE
7844	ALLUD 38809	29151	1	.049	1.63	.016	.017	.68	17.20	13.52	2.39	83700	43400	61	OK	71.4
-13-	PM CHECK	JESSOP 38936	42965	.047	1.60	.013	.018	.62	17.40	13.65	2.26	81580	(52 TESTS)		OK	12-28-6
11-B $\frac{1}{2}$	WM	"	38936	.041	1.64	—	—	.64	18.80	12.35	2.78					
7844	ALLUD 38809	340041	3	.049	1.62	.024	.010	.55	17.10	13.50	2.46	82100	38900	65	OK	69.5
-14-	PM CHECK	JESSOP 38936	42965	.049	1.62	.023	.014	.48	17.10	13.60	2.42	81870	(52 TESTS)		OK	12-28-6
11-B $\frac{1}{2}$	WM	"	40595	.044	1.52	—	—	.64	18.80	12.25	2.62					
7844	ALLUD 38809	340041	3	.049	1.62	.024	.010	.55	17.10	13.50	2.46	82100	38900	65	OK	69.5
-15-	PM CHECK	JESSOP 38936	42965	.049	1.62	.023	.014	.48	17.10	13.60	2.42	81870	(52 TESTS)		OK	12-28-6
9-11 $\frac{1}{2}$	WM	"	40595	.044	1.52	—	—	.64	18.80	12.25	2.62					
7844	ALLUD 38809	29151	3	.049	1.63	.016	.017	.68	17.20	13.52	2.39	83700	43400	61	OK	71.4
-16-	PM CHECK	JESSOP 38936	42965	.047	1.60	.013	.018	.62	17.40	13.65	2.26	81580	(52 TESTS)		OK	12-28-6
9-B $\frac{1}{2}$	WM	"	38936	.041	1.64	—	—	.64	18.80	12.35	2.78					
7844	ALLUD 38809	340039	6	.055	1.60	.023	.010	.55	17.40	13.00	2.42	88400	42900	55	OK	60.4
-17-	PM CHECK	JESSOP 38936	42965	.047	1.52	.020	.011	.57	17.40	13.10	2.20	80580	(52 TESTS)		OK	12-28-6
3-3 $\frac{3}{4}$	WM	"	40595	.048	1.64	—	—	.60	18.80	12.15	2.78					
7844	ALLUD 38809	340039	7	.055	1.60	.023	.010	.55	17.40	13.00	2.42	88400	46000	52	OK	65.7
-18-	PM CHECK	JESSOP 38936	42965	.047	1.52	.020	.011	.57	17.40	13.10	2.20	80580	(52 TESTS)		OK	12-28-6
3-3 $\frac{3}{4}$	WM	"	40595	.048	1.64	—	—	.60	18.80	12.15	2.78					

ABOVE DATA CERTIFIED CORRECT BY MANUFACTURER National Anv Tailing Box Co. BY James L. House Jr. DATE 12-28-63 V

NATIONAL ANNALING BOX CO.

WASHINGTON, PENNA.

MATERIAL RECORD

INSPECTION

PURCHASER _____

TYPE EQUIPMENT _____

YEAR BUILT _____

DWG. NO. _____

SERIAL NO. _____

PUR. ORDER NO. W-7359 NIAGARA-MOHAWK

INSPECTED BY _____

LABORATORY TEST REPORT

PART NO.	MANUFACTURER OF MATERIAL	UPPER LEAD SERIAL NO.	SLAB OR. TEST NO.	CHEMICAL								PHYSICAL F & P % of A.				
				C.	MN.	P.	S.	SIL.	CR.	NI.	MO.	ULT. STRENGTH.	EL. LIMIT	ELONG%	BEND °	FRACTURE
7844	ALLUD 38809	340039	7	.055	1.60	.023	.010	.55	17.40	13.00	2.42	88400	46000	52	OK	65.7
-19- PM	CHECK	JESSOP 38936	42965	.047	1.52	.020	.011	.57	17.40	13.10	2.20	80580	(52 TESTS)	OK		12-28-65
3-3/4" WM	"	" 40595	121765	.048	1.64	-	-	.60	18.80	12.15	2.78					
7844	ALLUD 38809	340039	6	.055	1.60	.023	.010	.55	17.40	13.00	2.42	88400	42900	55	OK	69.4
-20- PM	CHECK	JESSOP 38936	42965	.047	1.52	.020	.011	.57	17.40	13.10	2.20	80580	(52 TESTS)	OK		12-28-65
3-3/4" WM	"	" 40595	121765	.048	1.64	-	-	.60	18.80	12.15	2.78					
7844	ALLUD 38809	29151	2	.049	1.63	.016	.017	.68	17.20	13.52	2.39	81900	39200	64	OK	69.3
-21- PM	CHECK	JESSOP 38936	42965	.047	1.60	.013	.018	.62	17.40	13.65	2.26	81580	(52 TESTS)	OK		12-28-65
3-3/4" WM	"	" 38936	111965	.041	1.64	-	-	.64	18.80	12.35	2.78					
7844	ALLUD 38809	340039	6	.055	1.60	.023	.010	.55	17.40	13.00	2.42	88400	42900	55	OK	69.4
-22- PM	CHECK	JESSOP 38936	42965	.047	1.52	.020	.011	.57	17.40	13.10	2.20	80580	(52 TESTS)	OK		12-28-65
1-4" WM	"	" 40595	121765	.048	1.64	-	-	.60	18.80	12.15	2.78					
7844	ALLUD 38809	340039	7	.055	1.60	.023	.010	.55	17.40	13.00	2.42	88400	46000	52	OK	65.7
-23- PM	CHECK	JESSOP 38936	42965	.047	1.52	.020	.011	.57	17.40	13.10	2.20	80580	(52 TESTS)	OK		12-28-65
1-4" WM	"	" 40595	121765	.048	1.64	-	-	.60	18.80	12.15	2.78					
7844	ALLUD 38809	340039	7	.055	1.60	.023	.010	.55	17.40	13.00	2.42	88400	46000	52	OK	65.7
-24- PM	CHECK	JESSOP 38936	42965	.047	1.52	.020	.011	.57	17.40	13.10	2.20	80580	(52 TESTS)	OK		12-28-65
1-4" WM	"	" 40595	121765	.048	1.64	-	-	.60	18.80	12.15	2.78					

ABOVE DATA CERTIFIED CORRECT BY MANUFACTURER

National Annaling Box Co. BY *James L. Hume Jr.*

DATE 12-28-65

MATERIAL RECORD

INSPECTION

PURCHASER _____

TYPE EQUIPMENT _____

YEAR BUILT _____

DWG. NO. _____

SERIAL NO. _____

PUR. ORDER NO. W-7359 NIAGARA-MOHAWK

INSPECTED BY _____

LABORATORY TEST REPORT

PART NO.	MANUFACTURER OF MATERIAL	HEAT NO. OR SERIAL NO.	SLAB OR. TEST NO.	CHEMICAL								PHYSICAL				
				C.	MN.	P.	S.	SIL.	CR	NI	MO	ULT. STRENGTH	EL. LIMIT	ELONG%	BEND	FRACTURE
7844	ALLCO 38809	340039	6	.055	1.60	.023	.010	.55	17.40	13.00	2.42	88400	42900	55	OK	69.4
25	PM CHECK	JESSOP 38936	42965	.047	1.52	.020	.011	.57	17.40	13.10	2.20	80570	(52 TESTS)		OK	12-28-65
1-4"	WM	"	40395	.048	1.64	—	—	.60	18.80	12.15	2.78					
7844	ALLCO 38809	46580	1	.042	1.66	.018	.013	.45	17.62	13.40	2.77	82900	42200	56	OK	68.8
26	PM CHECK	JESSOP 38936	42965	.048	1.54	.021	.014	.43	17.80	13.75	2.46	79690	(52 TESTS)		OK	12-28-65
1-4"	WM	"	JESSOP 40595	.057	1.56	—	—	.58	18.40	12.20	2.64					
HT #46580 - FERRITE 4 1/2 % HT #340039 - " 6 1/2 % HT #340041 - " 6 1/2 % HT #29151 - " 6 1/2 %																
ALL LENGTHS DYE PENETRANT EXAMINED ON COMPLETED WELDS INSIDE AND OUTSIDE ALL LENGTHS HAVE BEEN PASSIVATED INSIDE AND OUTSIDE ALL PIPE SANDBLASTED INSIDE AND OUTSIDE - NO HYDROSTATIC TEST - 100% X-RAYED																

 ABOVE DATA CERTIFIED CORRECT BY MANUFACTURER Structural Dynamics Corp. BY James R. Kane Jr. DATE 12-28-65

July 6, 1965

State of Missouri)
City of St. Louis) SS

James D. Hoey

R. E. Guerra

Chief Metallurgist

A-18

CHEMICAL ANALYSIS OF BASE METAL AND WELD METAL
TYPE 316 STAINLESS STEEL

Jersey Central
Manufacturing

ANALYSIS FOR BASE METAL

DATED 7-2-65
Page 1 of 2

	C	Mn	P	S	Si	Cr	Ni	Mo	Other
Mill Report - Heat No. 45015	.061	1.60	.026	.022	.49	17.13	13.37	2.50	
Check Analysis - Heat No. 45015	.065	1.62	.029	.026	.50	17.11	13.34	2.58	} 76° Ell
Mill Report - Heat No. 65122	.060	1.77	.025	.011	.52	17.32	12.76	2.39	
Check Analysis - Heat No. 65122	.059	1.79	.024	.014	.51	17.36	12.70	2.40	} Ell 76°
Mill Report - Heat No. 45109	.053	1.80	.025	.010	.59	17.26	13.02	2.29	
Check Analysis - Heat No. 45109	.055	1.78	.028	.012	.60	17.30	13.00	2.26	} Elbow 90°
Mill Report - Heat No. 44839	.057	1.53	.020	.021	.59	17.04	13.13	2.24	
Check Analysis - Heat No. 44839	.060	1.50	.020	.020	.60	17.08	13.10	2.30	} Elbow 90° 76°
Mill Report - Heat No. 44842	.057	1.70	.019	.010	.45	17.13	12.86	2.24	
Check Analysis - Heat No. 44842	.061	1.70	.020	.013	.47	17.10	12.80	2.19	} Elbow 90°
Mill Report - Heat No. 45012	.061	1.45	.020	.020	.51	16.90	12.96	2.57	
Check Analysis - Heat No. 45012	.060	1.45	.021	.020	.50	16.89	12.97	2.55	} Ell 76°
Mill Report - Heat No. 45110 ^{80°}	.060	1.48	.022	.016	.53	17.28	13.15	2.27	
Check Analysis - Heat No. 45110	.062	1.48	.020	.015	.50	17.30	13.13	2.25	} Elbow 90°
Mill Report - Heat No. 65120	.061	1.55	.022	.020	.64	16.88	13.44	2.45	
Check Analysis - Heat No. 65120	.063	1.59	.021	.020	.66	16.80	13.48	2.40	} Elbow 90° 76°
Mill Report - Heat No. 65121	.056	1.85	.022	.020	.61	17.17	13.09	2.20	
Check Analysis - Heat No. 65121	.060	1.80	.020	.024	.59	17.11	13.10	2.22	} Tee?
Mill Report - Heat No. 44840 ^{80°}	.051	1.57	.021	.021	.63	17.18	13.22	2.25	
Check Analysis - Heat No. 44840	.057	1.55	.022	.020	.59	17.17	13.18	2.20	} Elbow 90°
Mill Report - Heat No. 44838	.054	1.80	.022	.017	.62	17.32	12.88	2.30	
Check Analysis - Heat No. 44838	.060	1.81	.019	.021	.60	17.29	12.95	2.31	} Tee?
Mill Report - Heat No. 65123	.058	1.74	.024	.022	.53	17.27	13.00	2.23	
Check Analysis - Heat No. 65123	.061	1.70	.020	.020	.55	17.30	13.04	2.23	} Tee?

DIRECTIONAL ANALYSIS OF BASE METAL AND WELD METAL
Page 2 of 2

	C	Mn	P	S	Si	Cr	Ni	Mo	Other
Mill Report - Heat No. 65077	.052	1.55	.024	.013	.61	16.95	12.90	2.28	} E660-90
Check Analysis - Heat No. 65077	.050	1.58	.021	.012	.61	17.00	12.88	2.30	
Mill Report - Heat No. 45153	.059	1.64	.020	.013	.57	17.26	13.00	2.30	} Tee?
Check Analysis - Heat No. 45153	.060	1.65	.022	.014	.55	17.20	13.08	2.28	
Mill Report - Heat No. 45030	.055	1.65	.019	.011	.62	17.13	12.92	2.47	} Tee?
Check Analysis - Heat No. 45030	.066	1.64	.020	.010	.62	17.20	12.89	2.42	
Mill Report - Heat No. 45139 ^{22/86}	.060	1.70	.025	.028	.54	17.35	13.04	2.25	} Tee
Check Analysis - Heat No. 45139	.061	1.68	.020	.026	.55	17.30	13.01	2.24	
Mill Report - Heat No. 45157	.057	1.71	.025	.009	.47	17.35	13.06	2.27	} Tee?
Check Analysis - Heat No. 45157	.060	1.70	.021	.011	.50	17.33	13.07	2.30	
Mill Report - Heat No. 45043	.066	1.69	.024	.020	.45	17.69	12.97	2.30	} Tee?
Check Analysis - Heat No. 45043	.062	1.70	.020	.020	.46	17.60	12.99	2.30	
Mill Report - Heat No. 64788	.068	1.44	.020	.012	.63	17.25	12.91	2.01	} Tee?
Check Analysis - Heat No. 64788	.075	1.25	.008	.023	.52	16.47	13.43	2.04	

INDUSTRIAL PIPING LABORATORY
GRINNELL COMPANY, INC.
PROVIDENCE, R. I.

CHEMICAL ANALYSIS CERTIFICATE

DATE: June 30, 1967
CUSTOMER'S ORDER: P.O. 205-47538
OUR ORDER San Jose 76359-60

Material Grinnell Consumable Insert Rings

Size Ring I.D. 25.773", 25.821", 25.806", 12.476", 11.338", 5.734"

Grade 316

Alloy No. 316A1

Ferrite Content by Schaeffler Diagram 5%

Chemical Analysis: Carbon 0.028

Manganese 1.58

Silicon 0.48

Chromium 19.68

Nickel 13.42

Molybdenum 2.36


Phosphorus 0.021

Sulfur 0.019

Columbium

I certify that the above information is true and correct to
the best of my knowledge and belief.

GRINNELL COMPANY, INC.


Helmut Thielach
Metallurgical Engineer

Sworn to and subscribed

before me this 6

day of July, 1967



Notary Public

SUMMARY OF WELDING FILLER COMPOSITIONS AND CALCULATED FERRITE CONTENT

KINE HILL POINT PROJECT REQUISITION 302-20800

Weld Metal Supplier	Heat No.	C	Mn	P	S	Si	Cr	Ni	Mo	Ferrite H. Schaeffler	Ferrite Rp Long	
		.036	1.47	-	-	.45	18.70	12.70	2.70	-	8	0
		.045	1.60	-	-	.54	18.80	12.63	2.75	-	5	0
		.041	1.64	-	-	.64	18.80	12.35	2.78	-	6	0
		.057	1.56	-	-	.58	18.40	12.20	2.64	-	4	0
		.048	1.64	-	-	.60	18.80	12.15	2.78	-	6	0
		.044	1.52	-	-	.64	18.80	12.25	2.62	-	6	0
Arcos	C8936-T316 2-18-5B77	.053	1.24	.062	.016	.51	18.84	11.18	2.17	-	8	0
Arcos Chromend 316	4H105A	.028	2.16	.29	.008	.014	18.97	12.00	2.37	-	6	0
Chromenar	7778-316L	.011	1.88	.39	.011	.004	19.49	11.94	2.39	.048	9	8

*Not calculated since Nitrogen Analysis was not available.